Epigenetic Silencing of *RASSF1A* Promotes Tumourigenesis via Alternative Transcript Expression, SFK Activation and Exosome Secretion

Nikola Vitanov Vlahov

Trinity College

A Thesis submitted to the Medical Sciences Division of the University of Oxford in partial fulfilment of the requirements for the Degree of Doctor of Philosophy.

Trinity 2015

CRUK/MRC Oxford Institute for Radiation Oncology

Department of Oncology

University of Oxford

OXFORD INSTITUTE FOR RADIATION ONCOLOGY

`

Abstract

Epigenetic Silencing of *RASSF1A* Promotes Tumourigenesis via

Alternative Transcript Expression, SFK Activation and Exosome Secretion

Submitted for Degree of Doctor of Philosophy

Nikola Vitanov Vlahov, Trinity College, Trinity 2015

Loss of the tumour-suppressor gene *RASSF1A* upon promoter methylation is one of the most frequent events in sporadic human malignancies. Loss of RASSF1A is associated with progression and pathogenesis of solid tumours; and more aggressive clinical phenotype, leading to poor prognosis in breast, lung and colon cancers, amongst others. RASSF1A functions in a number of cellular processes, inducing apoptosis in response to DNA damage, cell cycle arrest and growth control. In tumours with *RASSF1* promoter methylation, an alternative isoform, *RASSF1C*, is expressed and we find is able to bind and activate SRC. We also identify a novel tumour-suppressor role for RASSF1A, associating with the kinase inactivation of SRC. RASSF1C expression promotes SRC-dependent phosphorylation and internalisation of adherens junctions, leading to loss of cell-cell contacts and subsequent increase in cell motility, growth and invasiveness, both *in vitro* and *in vivo*. RASSF1C, via active SRC, mediates the phosphorylation of β-catenin and YAP1, promoting their nuclear localisation and association with the transcription factors TEAD1 and TBX3, resulting in the upregulation of anti-apoptotic and pro-survival genes. We show that RASSF1C expression leads to differential packaging and secretion of exosomes, modulating the communication between cancer cells and increasing their tumourigenicity. Finally, we find that cells expressing RASSF1C undergo phenotypic and transcriptional changes associated with the generation of cancer stem cells. We conclude that RASSF1C is an oncogene that plays a variety of roles in cell adhesion, invasion, survival and extracellular communication, resulting in increased tumourigenesis. These functions are inhibited by the tumour suppressor RASSF1A. This work highlights the association of the epigenetic inactivation of the *RASSF1A* gene with the more aggressive, metastatic tumours, and its relation to increased cancer outcome and risk.

`

Acknowledgements

This D.Phil thesis is the product of four hard, but incredibly joyful years of research. None of this would have been true without my supervisor Dr. Eric O'Neill, who helped me in a time of need and made me the scientist I am today. For this, and for all his guidance, support and a truly invaluable sea of ideas, I am eternally grateful.

I would like to thank the previous and current members of the lab, who have made my life and work so much better. I would like to thank Dr. Dafni Pefani for all her support and for teaching me to always ask the right questions, in life and in research. I would like to thank Dr. Garth Hamilton for all his help and for teaching me never to fear the amount of work I have to do to achieve something. Special thanks to Dr. Karen Yee for the help, support and fun moments in and outside of the lab. I would like to thank Dr. Anna Grawenda, Dr. Angelos Papaspyropolous, and Dr. Daniela Pankova for all the help and support, especially in the last few months. Thank you, Dr. Aswin Abraham for all the great conversations we had and for all the advice you have given me about work, life and random medical conditions. A big thank you to Delia, Leanne and Maria for adding the 'joyful' element in my everyday life and for all the help when I really needed it.

A very big thank you to Dr. Simon Scrace for being such a great colleague and friend. I have learnt a lot from you and I appreciate all you have done for me. And thank you for placing the foundation, on which this project and thesis were based… and for reading it in the end!

Thank you, Selva, Monica, Daniel, Kasia, Joana, Neele for being there for me in the last four years. And big thank you to the people with whom I started my journey – Cindy, Armando, Gagan, Ben, Fevzi, Yasir, Maria.

To my friends from Trinity and Oxford, you have made my life so much better! Thank you, Stella, for being my friend in Oxford from my first day here. It has been incredible living with you and Jonathan, Ben, Malte, Nayab and Marc. A big thank you to Ventsislav, Vladimir, Deyan, Michaela and Yuliana for being such true friends and for all the wonderful moments we shared.

And I cannot thank enough the person, without who none of this would have happened – Atanas Iwanow, who believed in me and gave me the courage to apply to Oxford University. I appreciate everything you have done for me! Thank you my dear friend!

I would like to thank my wonderful family for all the support and love I have received from them and for helping me to always see the bigger picture in every aspect of life. Thank you Vitan, Yordanka and Elena, my beloved parents and grandmother, for absolutely everything. I owe it all to you! To my beloved girlfriend, Rocio Morin, thank you for always being there for me and making me smile.

And I would like to dedicate all I have done to my late grandparents Yordan, Lili and Nikola, who made me the person I am today. Thank you! I would have loved to share this with you!

Finally, I would like to acknowledge Cancer Research UK for all their financial support throughout my D.Phil. And I would like to thank Robert and Julia Hunt-Grubbe and Trinity College for the financial support while this thesis was being written.

`

Contents

Chapter 1 Introduction 1

1.1 Cancer 1

1.1.1 Oncogenes 1

1.1.2 Tumour-suppressor genes 3

1.2 The RASSF Family 5

1.3 RASSF1 7

1.4 RASSF1A 8

1.4.1 RASSF1A and the Hippo Pathway 10

1.4.2 RASSF1A Phosphorylation 12

1.4.3 RASSF1A Regulation by Domain Interaction 12

1.4.4 RASSF1A and the Cell Cycle 14

1.5 RASSF1C 17

1.6 Therapeutic Implications of RASSF1A Loss 20

1.6.1 *RASSF1A* Promoter Hypermethylation – A Prognostic Marker 21

1.6.2 Re-Expression of RASSF1A 22

1.7 Project Aims 23

Chapter 2 Materials and Methods 24

2.1 Materials 24

2.2 Cell Culture 24

2.3 Transfection 25
2.4 Quantitation of Cell Lysates 25
2.5 SDS-PAGE and Western Blot 26
2.6 Immunoprecipitation 27
2.7 Immunofluorescence 28
2.8 Cloning 29
2.9 Reverse-Transcriptase PCR (RT-PCR) 30
2.10 Quantitative Real-Time PCR 30
2.11 Retroviral Generation of Stable Cell Lines 31
2.12 Mammosphere Growth Assay 32
2.13 Proximity Ligation Assay 32
2.14 Real-Time Molecular Visualisation 33
2.15 Time Lapse Imaging 33
2.16 Fluorescent Recovery After Photobleaching (FRAP) 34
2.17 Calcium Switch Assay 34
2.18 Exosome Production and Isolation 35
2.19 Exosomes for SDS-PAGE and Western blot 35
2.20 Exosomes Treatment of Cells 36
2.21 Staining of Exosomes 36
2.22 Stem Cell Production 37
2.23 Flow Cytometry 37
2.23.1 Flow Cytometry for Cells Treated With Exosomes 37

2.23.2 Flow Cytometry for Stem Cells 38

2.24 Statistics 38

2.25 Tables 39

Chapter 3 RASSF1C-Dependent Activation of SFKs Promotes the Destabilisation of E-cadherin at Cell-Cell Junctions 44

3.1 Introduction 44

3.1.1 SRC Family Kinases 44

3.1.2 The Role of SRC in Migration and Invasion 46

3.1.3 The Adherens Junctions and E-cadherin 47

3.1.4 Aims 49

3.2 Both RASSF1A and RASSF1C Bind to SRC 50

3.3 RASSF1C Expression Leads to the Activation of SRC 52

3.4 SRC is Localised at the Plasma Membrane in RASSF1C-Expressing Cells 55

3.5 RASSF1C Expression Leads to the Internalisation of E-cadherin and Loss of Adherens Junctions 57

3.6 RASSF1C Leads to Changes in the Trafficking Mechanisms of 63

3.7 RASSF1C Expression Affects the Kinetics of Adherens Junctions 67

3.8 RASSF1C-Expressing Cells Obtain Partial EMT Traits 76

3.9 RASSF1C Expression Leads to Increased Cell Motility 78

3.10 RASSF1C Expression Leads to SRC-Dependent Tumourigenesis *in vitro* and *in vivo* 81

3.11 Discussion 85

`

Chapter 4 RASSF1C Promotes YAP1 and β-catenin-Dependent Transcription.....99

4.1 Introduction 99

4.1.1 The Hippo Pathway 99

4.1.2 YAP1 and RASSF1A 103

4.1.3 Aims 104

4.2 RASSF1C Expression Leads to E-cadherin Destabilisation and YAP1 Nuclear Localisation . 105

4.3 Loss of RASSF1A Mediates Nuclear Localisation of YAP1 107

4.4 The siRNA-Resistant RASSF1C Mutant Mediates Nuclear Localisation of YAP1 110

4.5 RASSF1C Expression Promotes pY357-YAP1 Phosphorylation 114

4.6 β-catenin is Localised to the Nucleus in RASSF1C Expressing Cells 117

4.7 RASSF1C Expression Promotes Upregulation of Anti-Apoptotic Genes 120

4.8 Discussion 125

Chapter 5 RASSF1C Expression Increases the Rates of Secretion and Alters the Proteins Packaged in Exosomes 135

5.1 Introduction 135

5.1.1 Exosomes 135

5.1.2 Exosomes in Cancer 137

5.1.3 Aims 139

5.2 Exosomal Marker Activity is Associated with RASSF1C-Expressing Cells 140

5.3 Cells Expressing RASSF1C Produce More Exosomes 143

5.4 Exosomes Secreted by RASSF1C Cells Vary in Their Protein Contents 146

5.5 The Changes in Exosome Cargo Do not Alter the Rates of Internalisation 150

5.6 Exosomes from RASSF1C Cells Increase the Growth of Mammospheres 153

5.7 Discussion 155

Chapter 6 RASSF1C Promotes a Cancer Stem Cell Phenotype 163

6.1 Introduction 163

6.1.1 Cancer Stem Cells 163

6.1.2 Cancer Stem Cells and Hippo Signalling 166

6.1.3 Aims 167

6.2 Expression of RASSF1C Leads to Changes in Cell Morphology 167

6.3 The Rounded RASSF1C-Expressing Cells are Functional and Not Dividing 169

6.4 RASSF1C Expressing Cells Remain in the Centre of the Mammospheres 172

6.5 RASSF1C Exosomes Induce the Upregulation of Vimentin 174

6.6 RASSF1C Exosomes Induce the Upregulation of Stem Cell Genes 176

6.7 Stem Cell Genes are Upregulated in RASSF1C-Expressing cells 178

6.8 RASSF1C Expression Induces a $CD44^{high}/CD24^{low}$ Phenotype 179

6.9 Discussion 181

Chapter 7 Discussion 189

Chapter 8 Appendix 205

8.1 CSK Binds to RASSF1A 205

8.2 Opposing Roles for SRC Regulation by RASSF1A and RASSF1C 206

8.3 RASSF1C Can Only Activate SRC in RASSF1A-Negative Cell Lines 206

8.4 RASSF1C Leads to SRC-Dependent Phosphorylation of E-cadherin 207

8.5 E-cadherin is not Accumulated in the Cell Organelles 208

8.6 RASSF1A Binds to RASSF1C 209

8.7 RASSF1C-Expressing Cells Accumulate in G1/S Phase 210

8.8 Analysis of Exosomes Treated with mTOR and PI3K Inhibitors 211

Chapter 9 References 214

`

Figures list

Chapter 1 Introduction

Figure 1.1	RASSF1 Gene Structure and the Splice Variants Produced	9
Figure 1.2	Cartoon Showing the Signalling Connection Made by RASSF1A and the Hippo Pathway to Regulate Apoptosis and Senescence	11

Chapter 2 Materials and Methods

Table 2.1	List of the Cell Lines Used in this Study	39
Table 2.2	siRNA Sequences Used During this Project	39
Table 2.3	Stable Cell Lines Produced and Used in the Project	40
Table 2.4	Antibodies Used During this Project	40
Table 2.5	Primers Used For Cloning, Site-Directed Mutagenesis and RT-PCR	42
Table 2.6	Common Buffers Used	43

Chapter 3 RASSF1C-Dependent Activation of SFKs Promotes the Destabilisation of E-cadherin at Cell-Cell Junctions

Figure 3.1	RASSF1A and RASSF1C Bind to SRC	51
Figure 3.2	RASSF1C, but not RASSF1A, Associates with Active SRC	54
Figure 3.3	RASSF1C Expression Promotes SRC Localisation to the Plasma Membrane	56
Figure 3.4	RASSF1C Leads to the Internalisation of Endogenous E-cadherin	58
Figure 3.5	RASSF1C Leads to Internalisation of E-cadherin-GFP	60

Figure 3.6	RASSF1C Expression Promotes SRC-Dependent Internalisation of E-cadherin and Destabilisation of Cell-Cell Junctions	62
Figure 3.7	RASSF1C Expression Leads to Impaired E-cadherin Trafficking	64
Figure 3.8	RASSF1C Fails to Affect the Trafficking of E-cadherin Y3F Mutant	66
Figure 3.9	FRAP Analysis of E-cadherin in the Presence of RASSF1C Shows SRC-Dependent Changes in the Stability of the E-Cadherin Molecules.	68
Figure 3.10	Calcium-Dependent Cell-Cell Contact Loss Occurs Within 90 Mins of Calcium Removal in MCF7 cells	70
Figure 3.11	Calcium-Dependent Cell-Cell Contact Loss is Accelerated in RASSF1C Expressing Cells	71
Figure 3.12	Calcium-Dependent Cell-Cell Contact Formation Occurs Within 90 Mins of Calcium Introduction in MCF7 Cells	73
Figure 3.13	Calcium-Dependent Cell-Cell Contact Formation is Disrupted by RASSF1C Expression	74
Figure 3.14	RASSF1C Expression Affects the Formation of Both Weak and Strong Junctions	75
Figure 3.15	Expression of RASSF1C Leads to Partial EMT Phenotype	77
Figure 3.16	MCF7 Cells, Expressing E-cadherin and DsRed-Empty Vector, are not Motile in a Live Cell 2D System	79
Figure 3.17	MCF7 Cells, Expressing E-cadherin and DsRed-RASSF1C, Show Increased Motility in a Live Cell 2D System	80
Figure 3.18	RASSF1C Expression Drives a More Aggressive Phenotype *In Vitro*	82
Figure 3.19	RASSF1C Promotes Invasive Spread and Tumourigenesis *In Vivo*	84
Figure 3.20	Cartoon Depicting the Hypothesis Generated from the Results in Chapter 3	98

`

Chapter 4 RASSF1C Promotes YAP1 and β-catenin-Dependent Transcription

Figure 4.1	The Hippo Pathway Network	101
Figure 4.2	RASSF1C Expression Leads to E-cadherin Destabilisation and YAP1 Nuclear Localisation	106
Figure 4.3	Loss of RASSF1A Mediates Nuclear Localisation of YAP1	108
Figure 4.4	RASSF1A Loss Leads to Increase in Nuclear Localisation of YAP1	110
Figure 4.5	The siRNA Resistant Forms of RASSF1C Mediate Nuclear Localisation of YAP1	112
Figure 4.6	RASSF1C Promotes Nuclear YAP1	113
Figure 4.7	Expression of RASSF1C Leads to Activation of YAP1 at pY357	115
Figure 4.8	RASSF1C Expression Leads to YAP1 Phosphorylation	117
Figure 4.9	RASSF1C Leads to β-catenin Nuclear Localisation	119
Figure 4.10	RASSF1C Expression, or RASSF1A loss, Promotes YAP1-β-catenin Dependent Transcription	121
Figure 4.11	RASSF1C Promotes YAP1-TEAD1-β-catenin-TBX3 Dependent Transcription	124
Figure 4.12	Cartoon Depicting the Hypothesis Generated from the Results in Chapter 4	134

Chapter 5 RASSF1C Expressions Leads to Increases the Rates of Secretion and Alters the Proteins Packaged in Exosomes

Figure 5.1	The Levels of ALIX, CD63 and CD81 Are Higher In RASSF1C-Expressing Cells	142
Figure 5.2	RASSF1C Cells Produce More Exosomes	145

Figure 5.3 RASSF1C Expression Leads to an Increase in Exosome Cargo 147

Figure 5.4 The Packaging of Proteins in Exosomes from RASSF1C Expressing Cells is Cell Line Dependent 149

Figure 5.5 The Exosomes Secreted by the Control or RASSF1C Cells are Able to Be Internalised 151

Figure 5.6 The Exosomes Secreted by the Control or RASSF1C Cells are Internalised by Equal Numbers of Naïve Cells 152

Figure 5.7 MDA-MB-231 Cells treated with Exosomes Derived from RASSF1C Cells Are More Invasive 154

Figure 5.8 Cartoon Depicting the Hypothesis Generated from the Work in Chapter 5 162

Chapter 6 RASSF1C Promotes a Cancer Stem Cell Phenotype

Figure 6.1 RASSF1C Expressing Cells Become Rounded 168

Figure 6.2 The Rounded RASSF1C-Expressing Cells Are Not in Mitosis 170

Figure 6.3 RASSF1C-Expressing Cells are Proliferative 171

Figure 6.4 RASSF1C-Expressing Cells are Not Apoptotic 171

Figure 6.5 RASSF1C-Expressing Cells Are Located in the Centre of the Mammospheres 173

Figure 6.6 Exosomes Derived From RASSF1C-Expressing Cells Induce Upregulation of Vimentin 175

Figure 6.7 Exosomes From RASSF1C-Expressing Cells Induce Upregulation of Stem Cell Genes 177

Figure 6.8 RASSF1C Expression Promotes the Upregulation of Stem Cell Genes 178

Figure 6.9 RASSF1C Expression Shifts Cell Population Towards CD44high/CD24low 180

CSC Phenotype

Figure 6.10 Cartoon Depicting Model Proposed From Data in Chapter 6 188

Chapter 7 Discussion

Figure 7.1 Cartoon Depicting the Model Generated from the Results in this Thesis 204

Chapter 8 Appendix

Figure 8.1 RASSF1A Binds to CSK and SRC 205

Figure 8.2 RASSF1A and RASSF1C Show Opposing Roles in SRC Activation 206

Figure 8.3 The Expression of RASSF1C Can Only Activate SRC in RASSF1A-Negative Cell Lines 206

Figure 8.4 RASSF1C Activation of SRC Leads to Tyrosine Phosphorylation of SRC Targets 207

Figure 8.5 RASSF1C Does Not Send E-cadherin to the Endosomes, Lysosomes or Golgi 208

Figure 8.6 RASSF1A Binds to RASSF1C 209

Figure 8.7 RASSF1C-Expressing Cells are Predominantly in G1 210

Figure 8.8 The Packaging of Proteins in Exosomes Depends on mTOR Activity in HCT116 Cells 211

Figure 8.9 The Packaging of Proteins in Exosomes Depends on mTOR Activity in Breast Cancer Cell Lines 212

Figure 8.10 Exosomes Derived From Cells Treated with mTOR Inhibitor Reduce the Growth of Mammospheres. 213

`

Abbreviations

AJ	Adherens junctions
AJC	Adhesion junction complex
AKT	RAC-alpha serine/threonine-protein kinase
AMOT	Angiomotin
APC	Adenomatous polyposis coli protein
APC/C	Anaphase promoting complex/cyclosome
aPKC	Atypical Protein kinase C
Arf	(e.g. ARF6) ADP-ribosylation factor 6
ASPP	Apoptosis-stimulating of p53 protein
ATCC	American Type Culture Collection
ATF2	Activating transcription factor 2
ATM	Ataxia telangiectasia mutated
ATP	Adenosine Triphosphate
ATR	Ataxia telangiectasia and Rad3-related protein
BCA	Bicinchoninic acid
Bcl-2	B-cell lymphoma 2
BH3	Bcl-2 homology domain 3
BIRC5	Baculoviral IAP Repeat Containing 5
BME	Beta mercaptoethanol
BPB	Bromophenol blue
β-PIX	PAK-interacting exchange factor beta
BRCA	Breast cancer susceptibility protein
BSA	Bovine serum albumin
CAFs	Cancer Associated Fibroblasts
Cas	Crk-associated substrate
cbl	Casitas B-lineage lymphoma proto-oncogene
CDC	Cell division control protein (e.g. cdc42, cdc20)
CDK	Cyclin-dependent kinase
cDNA	Complementary DNA
CHK	Checkpoint kinase
CHMP4	Charged multivesicular body protein 4a
CK1	Casein kinase 1

`

cm	Centimetre
CpG	Dinucleotide consisting of cytosine followed by guanine
CRUK	Cancer Research UK
CSC	Cancer Stem Cell
CSE1L	Cellular apoptosis susceptibility protein
CSK	C-terminal SRC kinase
CXCL12	C-X-C motif chemokine 12 (Stromal cell-derived factor 1 (SDF1))
CXCR4	C-X-C chemokine receptor type 4
DAG	Diacylglycerol
DAXX	Death Domain-associated protein
DDB1	DNA Damage Binding protein 1
DDR	DNA damage response
Dlg	Discs large
DMEM	Dulbecco's-Modified Eagles Medium
DMP	Dimethyl pimelimidate
DMSO	Dimethylsulfoxide
DNA	Deoxyribonucleic acid
DNA-PK$_{cs}$	DNA protein kinase catalytic subunit.
DOCK	Dedicator of cytokinesis protein 1
DSB	Double-stranded break
DsRed	*Discosoma sp*. red fluorescent protein
DTT	Dithiothreitol
DVL	Segment polarity protein dishevelled homolog
ECL	Enhanced chemiluminescence
ECM	Extracellular matrix
EDTA	Ethylenediaminetetraacetic acid
EEA1	Early Endosome Antigen 1
EFA6	Exchange factor for Arf6
EGF	Epidermal Growth Factor
EGFR	Epidermal growth factor receptor
EGR1	Early growth response protein 1
Emi1	Early mitotic inhibitor 1
EMT	Epithelial Mesenchymal transition
ERK	Extracellular signalling-regulated protein kinase

`

ESCRT	endosomal sorting complex required for transport
EWS	Ewing sarcoma breakpoint region 1 protein
FAK	Focal adhesion kinase
FBS	Fetal Bovine Serum
FGF2	Fibroblast growth factor 2
FLAG	An epitope tag of the sequence DYKDDDDK
FSG	Fish Skin Gelatin
GAP	GTPase activating protein
GDP	Guanosine Diphosphate
GEF	Guanine nucleotide exchange factor
Glu	Glutamine
GSK3	Glycogen synthase kinase-3
GTP	Guanosine Triphosphate
H_2O	Water
HA	An epitope tag of the sequence YPYDVPDYA
HAUSP	Herpes virus-associated ubiquitin-specific protease
HCl	Hydrogen Chloride
HDAC	Histone deacetylase
Hippo	*Drosophila* homolog of MST
hr	Hour
HSC70	Hear shock cognate 70 kDa
IC_{50}	Half maximal inhibitory concentration
IP	Immunoprecipitation
iPSC	Induced pluripotent stem cells
IR	Irradiation
JNK	c-jun N-terminal kinase
kb	Kilobase (DNA).
kDa	Kilodalton
KLF4	Krueppel-like factor 4
l	Litre
LATS	Large Tumour Suppressor
LB	Luria Broth
LDL	Low density lipoprotein
LFA-1	Lymphocyte function-associated antigen 1

`

Lgl	Lethal giant larvae
LIF	Leukaemia inhibitory factor
LOH	Loss of Heterozygosity
M	Molar
MAP1S	Microtubule-associated protein 1S
MAPK	Mitogen-activated protein kinase
MARK	MAP/Microtubule affinity-regulating kinase
MATS	Mob as a tumour suppressor
mDia	Diaphanous homolog
MDM2	Mouse double minute 2 protein
$MgCl_2$	Magnesium Chloride
MHC	Major histocompatibility complex
min	Minute
miRNA	MicroRNA
MLC	Myosin light chain
MLCK	Myosin light chain kinase
MMP	Matrix metalloprotease
MOAP1	Modulator of Apoptosis 1
MRE11	Meiotic recombination 11 protein
mRNA	Messenger RNA
MST	Mammalian Sterile 20-like Protein (Also called KRS)
MTOC	Microtubule organising centre
MVB	Multivesicular body
NaCl	Sodium chloride
NDR	Nuclear Dbf2-related kinase 1
NER	Nucleotide excision repair
NF-2	Neurofibromin-2 (Merlin)
NHERF	Na^+/H^+ exchange regulatory cofactor NHE-RF1
Nore1	Novel Ras Effector (RASSF5 (RASSF isoform 5))
NP40	Nonidet P-40
NTA	Nanotracker analysis
OCT4	Octamer-binding transcription factor 4
PAGE	Polyacrylamide gel electrophoresis
PAK	p21 Activating kinase

`

Par	Partitioning defective (e.g. Par3, Par6)
PBS	Phosphate buffered saline
PBST	PBS with the addition of 0.1% Tween 20
PCR	Polymerase chain reaction
PDCD6	Programmed cell death 6
PDCD6IP	Programmed cell death 6 Interacting protein
Pen/Strep	Penicillin/Streptomycin
PI3K	Phosphatidylinositide 3-Kinase
PIWIL	Piwi-like protein
PML	Promyelocytic leukaemia protein
pS	Phosphoserine residue
pT	Phosphothreonine residue
PTEN	Phosphatidylinositol 3,4,5-triphosphate 3-phosphatase and dual specificity protein phosphatase.
PTP	Protein tyrosine phosphatase
PUMA	p53 upregulated modulator of apoptosis
PVDF	Polyvinylidene fluoride
pY	Phosphotyrosine residue
RA	Ras Association (domain)
RACK1	Receptors for Activated C-Kinases
RASSF	Ras Association Domain Containing Family of Proteins
Rb (pRb)	Retinoblastoma protein
RNA	Ribonucleic acid
RNAi	RNA interference
ROCK	Rho kinase
RT	Room Temperature
RT-PCR	Reverse-transcriptase PCR.
SARAH	**Sa**v, **RA**SSF, **H**ippo
Sav	Salvador
SCF	SKP1-CUL1-F-box
SCID	Severe combined immunodeficiency
SDS	Sodium dodecyl sulphate
SEM	Standard Error of the Mean
SFK	SRC family kinases

`

siRNA	Small interfering RNA molecule.
Skp2	S-phase kinase-associated protein 2
SNARE	SNAP (Soluble NSF Attachment Protein) Receptor
SNP	Single Nucleotide Polymorphism
SOX2	SRY (sex determining region Y)-box 2
SRC	Proto-oncogene tyrosine-protein kinase SRC (v-SRC – viral SRC)
TAE	Tris-acetate-EDTA
TAZ	Transcriptional co-activator with PDZ-binding motif
TBS	Tris buffered saline
TBST	TBS with the addition of 0.1% Tween 20
TBX	T-Box
TCF/LEF	T-cell factor/Lymphoid Enhancer Factor
TEAD	TEA domain family member
TIAM	T-lymphoma invasion and metastasis-inducing protein
TNF	Tumour Necrosis Factor
TRAIL	TNF-related apoptosis-inducing ligand
TSG101	Tumor susceptibility gene 101
UV	Ultraviolet
v/v	Volume per volume
w/v	Weight per volume
WW45	45 kDa WW domain protein (Salvador/Sav1)
XP	Xeroderma pigmentosum (e.g. XPA - complementation group A)
YAP	Yes-associated protein
ZO-1	Zonula Occludens protein 1
ZsGreen	*Zoanthus* green fluorescent protein

`

Chapter 1 Introduction

1.1 Cancer

Cancer is a collection of neoplastic diseases, defined by a variety of alterations to normal cells which enables abnormal growth and metastatic dissemination. Fifteen years ago, these alterations, or hallmarks, were described as six distinctive and complementary capabilities: evading growth suppressors, sustaining proliferative signalling, enabling replicative immortality, resisting cell death, inducing angiogenesis and activating invasion and metastasis (Hanahan and Weinberg, 2000). Since then, the evasion of immune destruction and the deregulation of cellular energetics have emerged as further hallmarks. In addition, genome instability (resulting in the generation of random mutations) and tumour-promoting inflammation, have been described as additional cancer enabling characteristics (Hanahan and Weinberg, 2011). Together, these hallmarks complement each other to induce tumour progression from benign to malignant and finally metastatic. A succession of clonal expansions each developing from random mutations that gives a selective advantage has been suggested to be involved in tumour progression (Hanahan and Weinberg, 2011). This can be a result of inherited traits like a mutation, or via epigenetic mechanisms, such as DNA methylation.

1.1.1 Oncogenes

Oncogenes code for proteins that induce the transformation of normal cells into cancer cells when activated by structural alterations resulting from mutation or gene fusion, amplification or juxtaposition to enhancer elements. Many oncogenes are present in the genomes of normal cells as proto-oncogenes, but are converted into potent oncogenes such as *SRC*, *H-RAS* and *K-RAS* when activated by retroviruses, like the Rous sarcoma virus (Stehelin et al., 1976) and the Harvey and Kirsten sarcoma viruses (DeFeo et al., 1981), respectively. With the third member of the RAS-related

`

gene family, N-RAS, cloned from neuroblastoma and leukaemia cell lines, the RAS genes code for the founding members of a large superfamily of monomeric GTPases. The Ras GTPases regulate diverse cellular processes, including vesicular and nuclear transport, cell polarity and movement, actin cytoskeletal organisation, cell cycle progression and cell survival (Vigil et al., 2010). The Ras proteins, initially described to bind to guanine, function analogously to the heterotrimeric G proteins, which possess intrinsic GTP hydrolysis activity, shifting them between an inactive, GDP-bound state, and an active, GTP-bound state, in response to diverse cellular signals (Barbacid, 1987; Malumbres and Pellicer, 1998). The activation of Ras is regulated by upstream growth factor signals, which recruit Guanine-nucleotide exchange factors (GEFs), that convert Ras-GDP to Ras-GTP (Karnoub and Weinberg, 2008). GTPase activating proteins (GAPs) such as neurofibromin-1 (NF1) inactivate Ras by promoting the hydrolysis of GTP to GDP (Karnoub and Weinberg, 2008). The downstream signals of Ras are involved in a variety of biological functions, including: proliferation, apoptosis, differentiation, senescence and motility (Karnoub and Weinberg, 2008; Vigil et al., 2010). These signals are regulated by binding of effectors, including Raf kinases, phosphoinositide 3-kinase (PI3K) and RalGDS GEFs, to the active Ras-GTP form (Karnoub and Weinberg, 2008). These effectors contribute to oncogenic transformation by Ras. It has been shown that the oncogenic forms of Ras exhibit impaired GTPase activity and as a result remain in a constitutively active form. Mutations of K-Ras lead to the inhibition of GTPase activity and to a constitutively active Ras which lacks the requirement for upstream stimulation. The Ras mutant G12V is very frequently found in cancer, for example in more than 30% of colorectal tumours (Downward, 2003; Karnoub and Weinberg, 2008). In cancer cells, the loss of *K-RAS* expression has been linked to prevention of tumour initiation and decrease in growth (Gonzalez-Garcia et al., 2005). The cell viability was rescued by the transcriptional coactivator YAP1 (Shao et al., 2014). YAP1 participates in several transcriptional programs that regulate organ size and cell proliferation (Wang et al., 2009) and together with K-RAS lead to activation of the transcriptional program involved in the regulation of epithelial-mesenchymal transition (EMT) (Shao et al., 2014).

`

Interestingly, mutant K-Ras also appears to have a pro-apoptotic function, apart from its oncogenic one (Cox and Der, 2003). Also, loss of inducible Ras mutant G12V results in the regression of melanomas and high levels of tumour cell apoptosis (Chin et al., 1999). This phenomenon could be explained by the phosphorylation of oncogenic K-Ras by Protein Kinase C (PKC), promoting its translocation to the mitochondria and inducing apoptosis in a Bcl-X_L-dependent manner (Bivona et al., 2006). Or it could be due to the mammalian sterile 20-like kinase (MST2)-dependent activation of p53, through the interaction between K-Ras and the tumour suppressor protein, RASSF1A (Matallanas et al., 2011).

1.1.2 Tumour Suppressor Genes

Tumour suppressors are proteins that normally function to constrain or suppress cell proliferation and are often lost or inactivated in tumours. In addition to the mutation of growth-promoting oncogenes such as Ras or Raf, cancer cells must avoid the powerful programs that are involved in the negative regulation of cell proliferation. These programs depend on tumour suppressor genes which act as central control nodes within regulatory circuits that monitor the genomic integrity in cells and make the decision whether to proliferate or to activate senescence and apoptosis. The tumour suppressor p53 plays a central role in this process and is widely referred to as the 'guardian of the genome' (Lane, 1992).

A variety of mechanisms are linked to the inactivation of p53, including mutation in the DNA binding domain and deletion of the carboxy-terminal domain, leading to p53 loss of function in more than half of human tumours (Petitjean et al., 2007; Vogelstein et al., 2000). Some tumours retain wild-type (WT) p53, but its function is altered by DNA tumour viruses (Levine, 2009), or by upregulation of the E3 ubiquitin ligase, MDM2. MDM2, and its homolog MDMX, are a major regulator of p53 levels in unstressed cells, targeting p53 for degradation (Manfredi, 2010; Marine et al., 2007; Marine and Lozano, 2010; Poyurovsky and Prives, 2006). Cellular stresses like oncogene activation, DNA damage

`

and hypoxia can disrupt the MDM2/p53 complex leading to the activation of p53 (Vousden and Lu, 2002). Phosphorylation by the DNA damage kinases ATM, ATR, Chk1 and Chk2 activate p53 (Chao et al., 2000; Kurz and Lees-Miller, 2004; Saito et al., 2002; Siliciano et al., 1997). Activated p53 forms a tetramer, which acts as a sequence specific transcription factor that has been shown to regulate metabolic processes, inhibit cell cycle progression, promote senescence and induce apoptosis (Freed-Pastor and Prives, 2012). Inhibition of MDM2, by the promyelocytic leukaemia (PML) tumour suppressor protein (Bernardi et al., 2004) or by RASSF1A (Song et al., 2008b) can also result in p53 activation.

Mutation of p53 does not decrease its transcriptional activity (Levine et al., 1995), unlike other tumour suppressors such as Retinoblastoma (pRb) and Adenomatous polyposis coli (APC). On the contrary, due to the tetrameric nature of active p53, the mutant protein gains a dominant negative function. Mutation in one of the p53 alleles leads to inactivation of the transcription of WT p53 target genes by a dominant-negative mechanism, as well as an inactivation of the other members of the p53 family: p63 and p73. Mutant p53 can also induce genomic instability by binding to proteins such as the double-strand break repair protein MRE11 and promoting the expression of a number of genes that increase cell proliferation, such as *c-MYC*, *FOS* and *EGFR* (Epidermal growth factor receptor)(Freed-Pastor and Prives, 2012).

Although mutation is one of the mechanisms for the inactivation of tumour suppressors, they can also be inactivated by gene deletion, loss of heterozygosity (LOH), via epigenetic changes. Epigenetics is defined as heritable changes in the gene expression that do not require changes of the DNA sequence (Jones and Baylin, 2007). The main mechanisms that control epigenetic alterations are DNA methylation and histone modification. The majority of DNA epigenetic modifications occur as cytosine methylation within the context of CpG dinucleotides (Jones and Baylin, 2007). Methylations are not equally distributed thorough the genome, but instead occur in clusters on large repetitive sequences, such as retrotransposon elements and centromeric repeats (Bird, 2002; Takai and Jones,

`

2002). They can also occur in short CG-rich DNA stretches, known as 'CpG islands'. Methylation modifications occur predominantly in the promoter regions of genes. In normal cells the hypermethylation of one of two parental alleles act as an epigenetic regulator, that ensures monoallelic expression. The methylation of DNA also plays a role in chromosomal integrity, by preventing gene disruptions by transposable elements within the genome; and preventing chromosomal rearrangements and translocations (Bird, 2002; Eden et al., 2003; Esteller, 2007; Jones and Baylin, 2002).

The CpG islands at the promoter regions of 'housekeeping' genes are normally unmethylated, allowing the binding of transcription factors to these sites (Lopez et al., 2009). Methylation of these sites blocks transcription factor binding and also leads to the recruitment of methyl-binding domain proteins and histone deacetylases (HDACs) (Jones et al., 1998; Nan et al., 1998), which induces chromosome condensation and transcriptional inactivation of the targeted genes.

In human tumours, while a global loss of DNA methylation is seen, the hypermethylation of specific promoters has been observed (Chuang and Jones, 2007). DNA hypermethylation has been frequently shown to be associated with promoters of tumour suppressor genes. These include E-cadherin, RASSF1A and RASSF2A and members of the Hippo pathway (Donninger et al., 2007; Graff et al., 1995; Richter et al., 2009; Seidel et al., 2007; Takahashi et al., 2005).

1.2 The RASSF Family

The RASSF family of proteins is comprised of ten members, from RASSF1 to RASSF10, each with multiple splice variants, with the exception of RASSF9 and 10 (Richter et al., 2009; Volodko et al., 2014). The ten members are divided based on where the RA domain is located – either at the C-terminal for RASSF1 to RASSF6 (the classical RASSF proteins), or at the N-terminal, for RASSF7 to RASSF10.

`

The Ras-Association Domain Containing Family (RASSF) of proteins was originally discovered due to their sequence homology to domains that associate with Ras-like small GTP binding proteins. These domains, known as Ras association (RA) domains [RalGDS (Ral guanine nucleotide dissociation stimulator)/AF6 (ALL-1 fusion partner from chromosome 6)], are distinct from Ras binding domains (RBD), found on other molecules such as c-Raf-1 and Tiam1, which can bind an alternative set of Ras effectors (Ponting and Benjamin, 1996; Yamamoto et al., 1999). While originally suggested to associate with Ras (Vavvas et al., 1998), the RASSF family has a differential affinity for Ras-like GTPases, with NORE1 (Novel Ras/Rap effector 1 /RASSF5) displaying high affinity for the closely related Ras homolog, Rap1B (Wohlgemuth et al., 2005). Direct association with K-Ras has been observed for almost all of the members (Stieglitz et al., 2008; Volodko et al., 2014). The RA domain of RASSF1 binds preferentially to K-Ras, rather than to H-Ras or N-Ras (Matallanas et al., 2011). RASSF5 can bind to K-Ras GTP and regulate the proapoptotic activity of the MST1/2 (Khokhlatchev et al., 2002; Ortiz-Vega et al., 2002). RASSF1A has also been described to associate with Ran (Dallol et al., 2009).

The classical RASSF proteins also have a protein-protein interaction motif known as the SARAH domain, which is responsible for scaffolding and regulatory interactions (Hwang et al., 2007). This domain is a short coiled-coil region, located in the extreme C-terminus of genetically linked *Drosophila* proteins; Salvador (hSav1/WW45), dRASSF and Hippo (hMST1/2) (SARAH: **Sa**lvador, **Ra**ssf, **Hippo**). The SARAH domain mediates protein-protein interactions and facilitates the formation of both homo- and heterodimers of RASSF isoforms (Scheel and Hofmann, 2003). In the N-terminal RASSFs, there is no identifiable SARAH domain, although the SMART database predicts that RASSF7, 8 and 10 can dimerise due to their extensive coiled-coil regions (Grigoryan and Keating, 2008).

RASSF1A and RASSF5A also contain an N-terminal atypical diacylglycerol/phorbol ester-binding (DAG) domain. This domain is known as the protein kinase C conserved region (C1) domain and it contains a central Zinc Finger (Zinc binding domain) (Newton, 1995). This Zinc finger is considered 'atypical'

`

because it cannot bind to phorbol esters or DNA, due to the lack of the required critical residues. Nevertheless, it is involved in protein-protein interactions. Structural analyses indicate that the C1 domain of RASSF5A associates with the RA domain to occlude RAS association, which leads to activation of MST1 (Harjes et al., 2006). The N-terminal domain is responsible for the heterodimerisation of RASSF1A and RASSF5A, facilitating the association of RASSF1A with Ras-GTP and thus mediating the K-Ras regulation of RASSF1A (Ortiz-Vega et al., 2002). As none of the family members have any known enzymatic activity, they are thought to function by acting as scaffold/adaptor proteins which use various binding domains to bring target proteins together.

1.3 RASSF1

LOH has been detected at the 3p21.3 region in kidney, breast and lung tumours; with genetic instability at this locus being the earliest and most frequently detected deficiency in lung cancers (Hung et al., 1995; Kok et al., 1997; Sekido et al., 1998a; Sekido et al., 1998b; Sundaresan et al., 1992; Wistuba et al., 1999; Wistuba et al., 2000). This led the hypothesis that this particular locus was harbouring one or more tumour suppressors. This 120 kb region contains 8 genes, namely *ZMYND10/BLU, 101F6, PL6, CACNA2D2, NPRL2/G21, RASSF1/123F2, FUS1* and *MYAL2*. However, none of these candidate genes are frequently mutated in cancers (Lerman and Minna, 2000; Sekido et al., 1998a). During the LOH studies, RASSF1 was identified as an interacting partner of the DNA damage repair protein Xeroderma Pigmentosum Complementation Group A (XPA) (Dammann et al., 2000). The *RASSF1* gene consists of 8 exons spanning a region of about 11 kb (Figure 1.1). The C-terminal has high sequence homology with RASSF5 and contains an RA domain. Therefore the gene was named *RASSF1* for **R**as **Ass**ociation Domain **F**amily Member 1 (Dammann et al., 2000). Alternative splicing generates 8 isoforms (A-H) from promoters located within 2 CpG islands. The upstream CpG island partly overlaps the promoter regions of RASSF1A, D, E, F and G and methylation at this CpG island has been shown to be one of the most common events in human cancers

`

(Donninger et al., 2007; Hesson et al., 2007; Jones and Baylin, 2007). This methylation is due to the transcription factor HOXB3 (Homeobox B3)-driven overexpression of the DNA methyltransferase, *DNMT3B* (Palakurthy et al., 2009). The other promoter region of RASSF1 is located within the larger downstream CpG island and generates RASSF1B, C and H (van der Weyden and Adams, 2007). This CpG island usually remains unmethylated in cancers, so cells retain expression of these isoforms (Donninger et al., 2007). RASSF1A and RASSF1C are the major transcripts of the *RASSF1* gene and are expressed ubiquitously in normal tissues (Richter et al., 2009).

In *Drosophila*, there is only one RASSF member, dRASSF, which shares the RA and SARAH domain with its mammalian counterparts, but does not contain a C1 domain. Instead, the N-terminal contains a cysteine and histidine rich, zinc-coordinating domain composed of two tandemly repeated zinc fingers LIM domain, which shares some similarities with the C1 domain. dRASSF has been observed to inhibit, not activate the Hippo pathway (discussed in Section 1.4.1) (Polesello et al., 2006; Ribeiro et al., 2010).

1.4 RASSF1A

Numerous studies have shown that *RASSF1A* is a prominent and epigenetically silenced tumour suppressor (Donninger et al., 2007; Grawenda and O'Neill, 2015). Exogenous expression of *RASSF1A* has been shown to reduce colony formation in soft agar and reduced tumourigenicity in nude mice (Burbee et al., 2001; Dammann et al., 2000; Dreijerink et al., 2001; Kuzmin et al., 2002). Similarly, the use of demethyltransferase inhibitors such as Zebularine and 5-aza-2'-deoxycytidine has led to the re-expression of *RASSF1A*, and subsequently, significant growth arrest in ovarian cancer cell lines (Balch et al., 2005). Reciprocally, *Rassf1A* knockout mice develop spontaneous tumours, particularly in combination with a knock-out of p53, demonstrating the role of the loss of Rassf1A in tumour development (Tommasi et al., 2011a; Tommasi et al., 2005; van der Weyden et al., 2005).

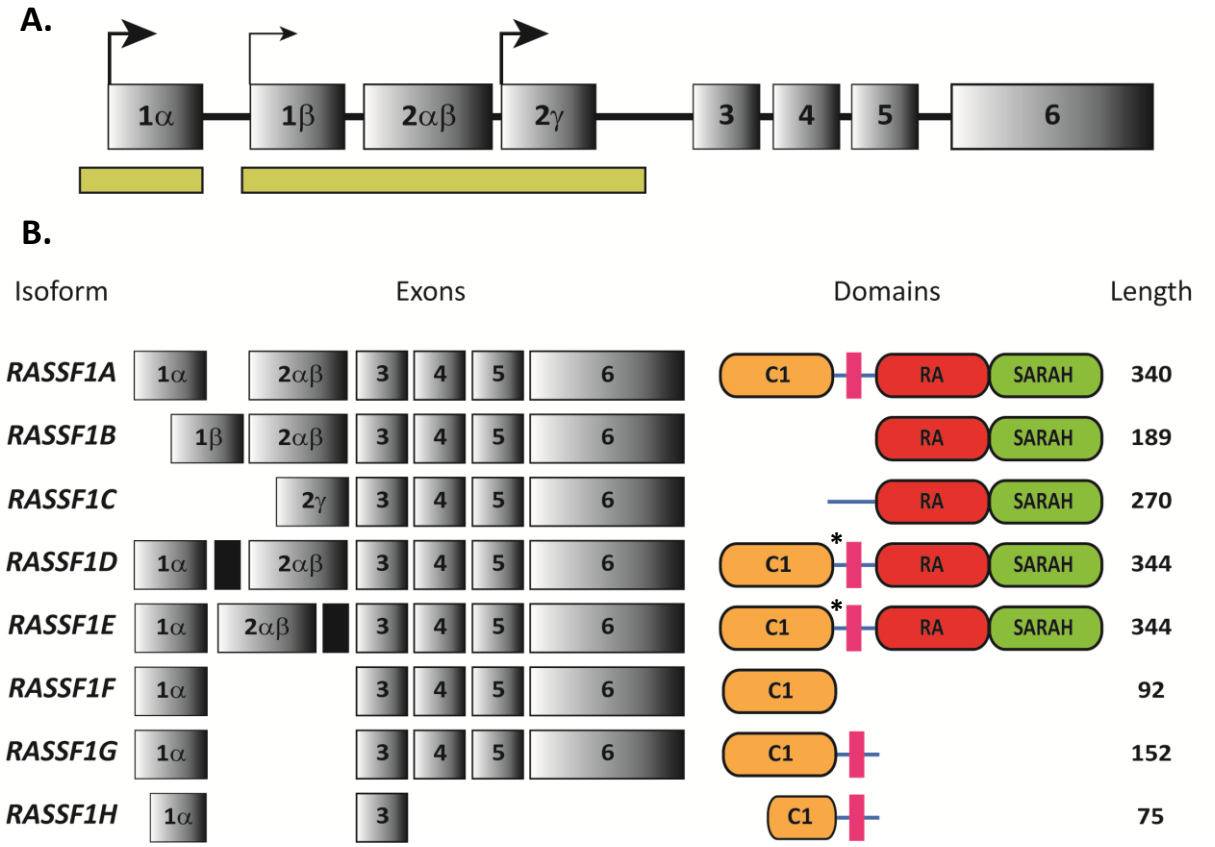


Figure 1.1. RASSF1 Gene Structure and the Splice Variants Produced. **A.** Diagram depicting the exons of the *RASSF1* gene (grey boxes), the two promoters (green boxes) and the start sites used to produce the eight isoforms of RASSF1 (arrows). **B.** Arrangement of the exons present in each of the isoforms of RASSF1 (A-H), the domains present in each of the isoforms and the amino acid length of each polypeptide chain. Black boxes seen in exons of RASSF1D and RASSF1E represent 4 amino acids added to these transcripts that are not present in RASSF1A. Their position in the protein structure is represented by an asterisk. Figure is adapted from (van der Weyden and Adams, 2007).

In addition, these *Rassf1A*$^{-/-}$, *p53*$^{-/-}$ mice revealed an important role for RASSF1A in maintaining genomic integrity, as high levels of cell aneuploidy/tetraploidy were observed. RASSF1A is also involved in cell cycle control, microtubule organisation, promotion of apoptosis and the DNA damage response (Donninger et al., 2007; Hamilton et al., 2009; van der Weyden and Adams, 2007). These will be discussed in more detail in the following sections.

`

1.4.1 RASSF1A and the Hippo Pathway

Studies on the *Drosophila* homologs of MST1/2 and LATS, Hippo and Warts respectively, have revealed a pathway responsible for controlling proliferation and apoptosis, which is conserved in both vertebrates and invertebrates. Mutations in key members of the pathway such as Hippo (MST1/2), Warts (LATS1/2), Salvador (WW45) or Mats (Mob1 as a tumour suppressor) result in significant tissue overgrowth. Dysfunctional Hippo pathway is associated with lack of inhibition of the downstream target Yorkie (YAP1), a non-DNA binding transcriptional co-activator that binds the transcription factor Scalloped (TEAD1-4), leading to the upregulation of proteins that promote cell division and inhibit apoptosis, such as Cyclin E and Diap-1. When the Hippo pathway is active, Hippo phosphorylates Warts, leading to phosphorylation of Yorkie, creating a site for 14-3-3 protein binding which sequesters Yorkie in the cytoplasm, preventing its interaction with Scalloped and thus inhibits its oncogenic activity (Zhao et al., 2007). However, in mammals, RASSF1A and DNA damage lead to phosphorylation of YAP1 by LATS, resulting in a pool of YAP1, that remains in the nucleus, switching from being a binding partner in the anti-apoptotic, YAP1-TEAD complex to a pro-apoptotic YAP1-p73 complex (Figure 1.2) (Yee and O'Neill, 2010). The interaction between YAP1 and p73 stabilises p73 by preventing its nuclear export and subsequent degradation (Basu et al., 2003; Dobbelstein et al., 2005; Melino et al., 2004). This complex leads to an upregulation of p73 responsive genes, such as the pro-apoptotic BH3 only Bcl-2 family member, PUMA (Matallanas et al., 2007; Strano et al., 2005).

In *Drosophila* dRASSF and Salvador are known to compete for MST binding. Salvador acts as an adaptor and brings Hippo and Warts together to activate the Hippo pathway, which is antagonised by dRASSF (Polesello et al., 2006). In mammals however, RASSF1A, using different regions from the SARAH domain, can bind to both MST1/2 and Salvador at the same time. Using an L308P mutant of RASSF1A, able to bind to Salvador, but not MST1, it has been shown that the RASSF1A-Salvador interaction can activate p73 in an MST-independent manner (Donninger et al., 2011).

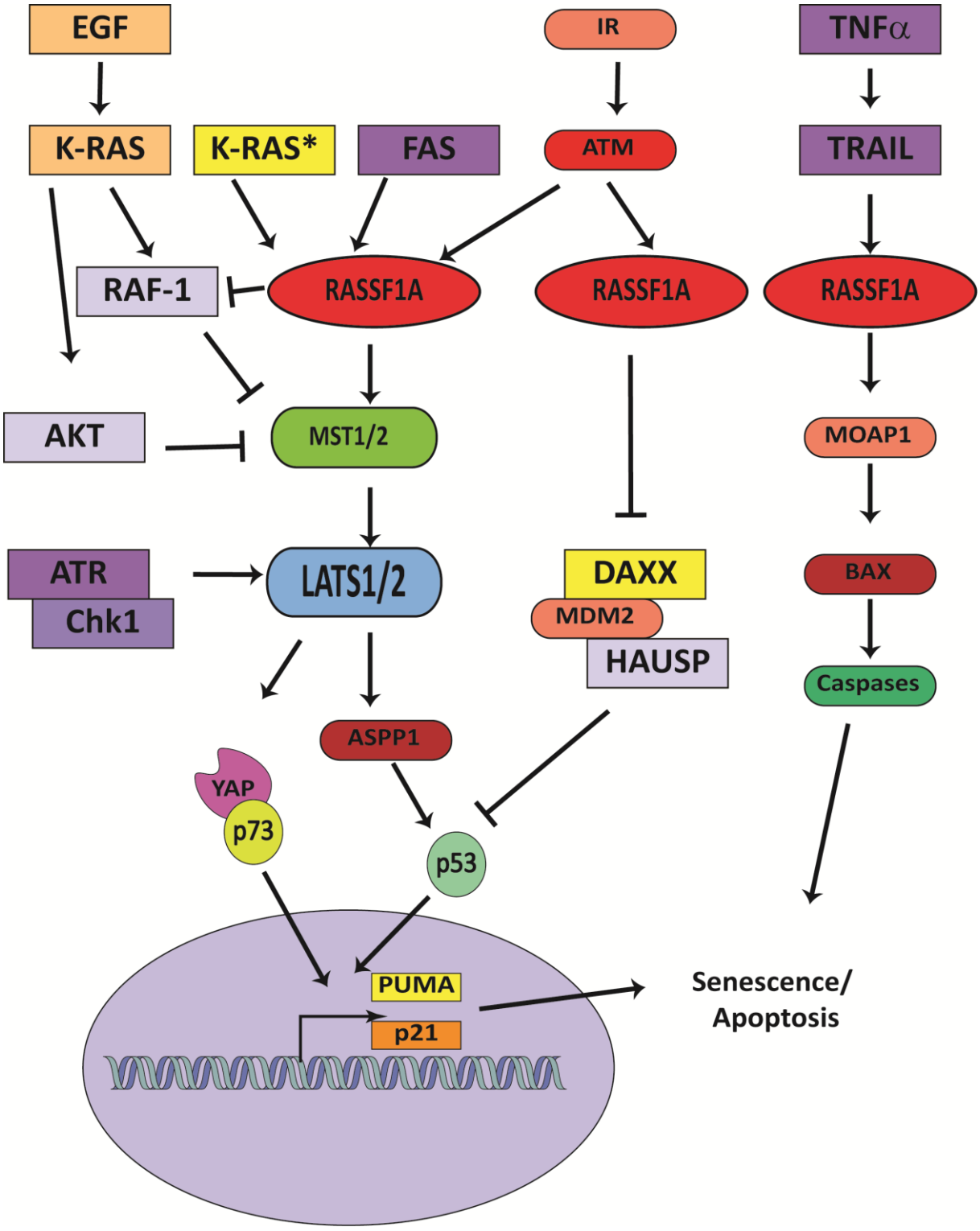


Figure 1.1. Cartoon Showing the Signalling Connections Made by RASSF1A and the Hippo Pathway to Regulate Apoptosis and Senescence. RASSF1A is activated by a number of upstream signalling pathways in response to cellular stresses. Oncogenic K-Ras (K-Ras*), DNA damage and Fas signalling promote Hippo pathway activation by RASSF1A, leading to p53 and p73 stabilisation and activation. RASSF1A can also directly stabilise p53 in response to DNA damage through the sequestration of MDM2 away from the deubiquitinating protein HAUSP. TNFα stimulation of TRAIL also activates RASSF1A, stimulating apoptosis through MOAP1 and BAX. WT EGF can inhibit RASSF1A activation of p53 through the inhibition of MST2 by AKT and Raf kinases.

`

1.4.2 RASSF1A Phosphorylation

The Phosphatidylinositol 3-related kinase, ATM (Ataxia Telangiectasia Mutated), ATR (ATM- and Rad3-Related) and DNA-PKcs (DNA-Dependent Protein Kinase catalytic subunit) are the initial kinases that are activated in the response to DNA breaks and the consequent repairs (Durocher and Jackson, 2001). During the DNA damage response, ATM phosphorylates RASSF1A on Serine 131 (S131), a site conserved in vertebrates and unique amongst the RASSF family members (Hamilton et al., 2009; Kim et al., 1999). Inactivating mutations of this site, particularly S131F, removed the ability of RASSF1A to induce cell cycle arrest and block cell proliferation (Shivakumar et al., 2002), as well as the ability to respond to various DNA damaging agents (Hamilton et al., 2009). Mutations occurring near the ATM target phosphorylation sequence have been shown to inhibit phosphorylation at this site. One of these is the non-synonymous single nucleotide polymorphism (SNP) (rs2073498) which predicts the conversion of alanine to serine at residue 133 of RASSF1A (p.Ala133Ser), which, through a minor allele, has significant frequencies in human populations. It is suggested that individuals carrying this polymorphism may have a defective cellular response to DNA damage due to decreased ability to activate the MST2/LATS pathway (required for YAP1/p73-mediated apoptosis), as well as p53. Indeed, individuals which are homozygous for the minor allele of the RASSF1A-p.133Ser polymorphism have been linked to early onset of tumours (Endoh et al., 2003; Gao et al., 2008) and male soft tissue sarcoma patients carrying the polymorphism exhibited poorer tumour-specific survival and earlier age of onset of cancer (Yee et al., 2012).

1.4.3 RASSF1A Regulation by Domain Interaction

As mentioned earlier, RASSF1A is thought to act as a scaffold protein, mediating its tumour suppressor activity through its protein interaction domains. The two most important domains are the C1 domain and the SARAH domain.

`

1.4.3.1 RASSF1A and Apoptosis

The most significant binding partners identified to interact with the C1 domain are the TNF-R1/TRAIL-R1 - Modulator of Apoptosis-1 (MOAP-1) complexes and the MDM2/DAXX/HAUSP/p53 complex (Figure 1.2)(Foley et al., 2008; Song et al., 2008b). MOAP-1 and RASSF1A are recruited to either TNF-R1 or TRAIL-R1 in response to TNFα stimulation. RASSF1A binds to and activates MOAP-1, which in turn binds to the pro-apoptotic Bcl-2 family member BAX, creating a pore in the outer mitochondrial membrane and leading to the release of cytochrome C and induction of caspase-dependent apoptotic signalling pathways (Baksh et al., 2005; Foley et al., 2008; Law et al., 2015). It has also been shown that following DNA damage, RASSF1A disrupts a complex, consisting of MDM2, DAXX (death-domain associated protein) and HAUSP1 (a deubiquitinating enzyme). RASSF1A can then sequester MDM2 away from p53, in an ATM-dependent manner (Song et al., 2008b). Release of DAXX from the complex is thought to allow its re -localisation to the plasma membrane where it can bind the death receptor Fas and activate c-Jun NH_2-terminal kinase (JNK), leading to apoptosis (Yang et al., 1997). The RASSF1 promoter is also a target for p53 (Tian et al., 2011). Interestingly, p53 can downregulate the transcription of RASSF1A and negatively regulate itself in addition to the upregulation of MDM2.

1.4.3.2 RASSF1A and DNA Damage Response

The SARAH domain of RASSF1A makes two significant interactions: with MST1/2 and with the scaffold protein Salvador. The interaction of RASSF1A with MST1/2 leads to its trans-phosphorylation and auto-activation (Glantschnig et al., 2002) and to the further stabilisation of kinase activity by preventing its dephosphorylation (Guo et al., 2011). Upon DNA damage, RASSF1A is phosphorylated by ATM on S131, leading to activation of MST2 (Colombani et al., 2006; Hamilton et al., 2009; Wen et al., 2010) and the consequent activation of LATS1 and LATS2 (Guo et al., 2007; O'Neill et al., 2005). Pefani et al. (2014) have also shown that ATR is also able to activate RASSF1A-mediated LATS1

`

activation and that the loss of RASSF1A-LATS1 signalling compromises the stability of DNA replication forks, leading to chromosomal aberrations and genomic instability (Pefani et al., 2014).

LATS2 has been shown to activate p53 both indirectly by driving the nuclear accumulation of ASPP1 (Apoptosis-Stimulating Protein of p53); and directly, by binding to and inhibiting MDM2 (Aylon et al., 2010; Aylon et al., 2009). RASSF1A activates LATS1/2 in response to DNA damage. This could potentially induce ASPP1-dependent activation of p53 and contribute to the overall p53 response. Interestingly the *Drosophila* ASPP protein (dASPP) has also been shown to interact with dRASSF8 to regulate C-terminal SRC kinase (dCsk) and adherens junctions (Langton et al., 2009); a site key to the regulation of the core Hippo pathway (Pan, 2010).

In early studies, Fas was shown to activate the pathway from RASSF1A to YAP1 (Matallanas et al., 2007). Recently, activation of MST2 and LATS1 by RASSF1A was shown to be mediated by oncogenic K-Ras (Matallanas et al., 2011). Activation of MST2 led to sequestration of MDM2 and the activation of p53, but not of p73 (Matallanas et al., 2011). The activation of MST2 by RASSF1A was shown to be blocked by wildtype K-Ras activation of AKT, which can phosphorylate MST2 (Matallanas et al., 2011). Phosphorylated MST2 by AKT fails to form an active complex with RASSF1A and leads to formation of a complex between MST2 and Raf-1, promoting MST2 inhibition (Romano et al., 2010). Interestingly, caspase cleaved, constitutively active MST1 was shown to inhibit AKT, possibly promoting a potential positive feedback loop, further activating MST1 and inducing apoptosis (Cinar et al., 2007).

1.4.4 RASSF1A and the Cell Cycle

Overexpression of RASSF1A has been shown to induce a cell cycle arrest at the G1-S checkpoint (Shivakumar et al., 2002). RASSF1A suppresses JNK activity and interacts with Ewing sarcoma breakpoint protein (EWS) (Whang et al., 2005; Whitehurst et al., 2008) to regulate this checkpoint by the inhibition of cyclin D1 activity (Shivakumar et al., 2002). JNK is a stress-activated mitogen-

`

activated protein kinase that is activated by exposure of cells to extracellular stresses, leading to diverse outcomes such as cell survival, tumour development and apoptosis (Davis, 2000; Liu et al., 1996; Vivo et al., 2003). RASSF1A expression leads to a downregulation of JNK signalling, by ablation of phospho-JNK and its target proteins such as the transcription factors c-jun and Activating transcription factor-2 (ATF-2) (Derijard et al., 1994; Gupta et al., 1995). Since cyclin D1 is induced by ectopic expression of c-jun, inhibition of JNK activity by RASSF1A will reduce cyclin D1 transcription. EWS is a transcription factor which forms a fusion protein with the transcription factor Friend leukaemia integration 1 (FLI1) to cause Ewing's sarcoma by acting as dominant oncoproteins (Arvand and Denny, 2001). EWS was found to interact with RASSF1A through its C1 domain following a yeast 2-hybrid library screening (Whitehurst et al., 2008). Interaction between RASSF1A and EWS was observed to prevent the accumulation of cyclin D1, leading to cell cycle arrest. A possible reason could be that the inhibition of EWS prevents it from positively regulating c-fos, which like c-jun can upregulate cyclin D1 (Kim et al., 2006). Alternatively, EWS could play an active role in translation of cyclin D1, which is inhibited by RASSF1A expression (Shivakumar et al., 2002).

The levels of RASSF1A vary during the different stages of the cell cycle. RASSF1A protein levels increase from mitosis until the G1-S checkpoint, followed by a sudden decrease which is attributed to ubiquitination-mediated degradation of RASSF1A by the Skp2-Cul1-F-box (SCF) ubiquitin ligase complex (Song et al., 2008a). The ubiquitination and degradation of RASSF1A is dependent on phosphorylation of RASSF1A on Serine 203 by the CDK4-Cyclin D1, creating a phospho-degron to which the oncogenic subunit of the Skp1–Cul1–F–box ubiquitin ligase complex, SKP2, binds (Song et al., 2008a). Loss of RASSF1A appears to impair entry into S-phase as demonstrated by BrdU labelling (Whitehurst et al., 2008).

Unidirectional progression of the cell through mitosis requires the timed destruction of the proteins by the APC/C. Such proteins include: cyclin A, targeted for degradation in prometaphase after it has promoted nuclear envelope breakdown; cyclin B, which is targeted for degradation in anaphase; and

`

securin, targeted for degradation once the spindle checkpoint has been overcome to allow chromosome segregation (den Elzen and Pines, 2001; Geley et al., 2001; Hagting et al., 2002). The APC/C controls such events by forming a complex with either of two WD40 domain-containing proteins: CDH1 and CDC20. CDC20 activates APC/C in early mitosis and CDH activates APC/C in late mitosis and throughout the G1-phase of the cell cycle (Jaspersen et al., 1999; Kramer et al., 2000; Pines, 2006). Inhibiting the interaction between APC/C and either CDC20 or CDH1 can cause cell cycle arrest during mitosis, a method used by a number of proteins, including RASSF1A and the spindle checkpoint proteins BUBR1 and MAD2 to promote cell cycle arrest (Fang et al., 1998; Millband and Hardwick, 2002; Sudakin et al., 2001; Tang et al., 2004).

One of the first identified functions of RASSF1A was its ability to associate with and stabilise microtubules (Rong et al., 2004). This interaction is particularly strong at the centrosomes and on the spindles during mitosis. The interaction between RASSF1A and the microtubules requires the RA domain, which seems important for its tumour suppressor function during pro-metaphase. Initially, it was shown that, bound to microtubules, RASSF1A induces a pro-metaphase arrest by sequestering CDC20, in association with C19ORF5 (Dallol et al., 2004; Song et al., 2005; Song et al., 2004). This would prevent CDC20 from associating with the APC/C and therefore CDC20 would remain inactive. The RASSF1A-CDC20 interaction is inhibited by the binding of the transcriptional repressor Id-1, allowing CDC20 to bind to the APC/C to form an active APC/C^{CDC20} complex leading to cyclin B1 and securin degradation and premature mitosis (Wang et al., 2008). However, a publication by Liu et al. (2007) showed that RASSF1A failed to interact with CDC20 and instead suggested a role for RASSF1A in the completion of cytokinesis (Liu et al., 2007).

In early mitosis RASSF1A binds to and is upregulated by Aurora A, enabling Aurora A to act as a RASSF1A kinase, phosphorylating RASSF1A on Threonine 202 and/or Serine 203 (Liu et al., 2008; Rong et al., 2007; Song et al., 2009b). This phosphorylation can lower the affinity and lead to disassociation of RASSF1A from CDC20 (Song et al., 2009b), followed by dissociation of RASSF1A from

`

the microtubules (Rong et al., 2007; Song et al., 2009b). Aurora A phosphorylation of RASSF1A converts it from a repressor of APC/C^{CDC20} to a target of it, inducing the ubiquitination and degradation RASSF1A, driving the APC/C^{CDC20} –dependent partial ubiquitination of Cyclin A in the presence of spindle checkpoint, leading to the initiation of anaphase (Chow et al., 2012). Aurora B has also been shown to phosphorylate RASSF1A in late mitosis (Song et al., 2009a; Song et al., 2009b), but this phosphorylation occurs in telophase when RASSF1A is located at the midbody. This promotes RASSF1A binding to the t-SNARE Syntaxin 16. The interaction occurs though the C-terminal of RASSF1A and has been shown to be required for successful cytokinesis (Song et al., 2009a).

During mitosis, RASSF1A plays an important role in the maintenance of genomic stability by acting as an integrity checkpoint factor. RASSF1A targets MST1/2 kinase activity towards the Ran-GEF (GTP Exchange Factor) RCC1, inhibiting its functions and resulting in elevated Ran-GTP near the metaphase plate (Dallol et al., 2009). This promotes the formation of a Ran-GTP gradient between spindle poles and the metaphase plate, stabilising the mitotic spindle and allowing successful completion of mitosis.

1.5 RASSF1C

RASSF1C is the second isoform of the *RASSF1* gene that is ubiquitously expressed. In contrast with RASSF1A, hypermethylation of the RASSF1C promoter region was not observed in almost all paediatric, breast, lung and pancreatic endocrine tumours and tumour cell lines tested (Burbee et al., 2001; Dammann et al., 2000; Harada et al., 2002; Malpeli et al., 2011). However, no RASSF1C was detected in the KRC/Y renal cell carcinoma cell line (Li et al., 2004), suggesting a tissue-specific effect of expression. Like RASSF1A, RASSF1C contains an ATM consensus sequence at Serine 61, and has been shown to associate with K-Ras (Vos et al., 2000). The sequence of the ATM phosphorylation site is identical between RASSF1A and RASSF1C, but it remains unclear if RASSF1C is also phosphorylated

`

and activated by ATM. In the embryonic kidney cell line 293T and human lung tumour cell line NCI-H1299, overexpression of wildtype RASSF1C, but not of the Serine 61 to phenylalanine (S61F) mutant of RASSF1C, was able to block the genomic destabilising effects of overexpressed Ras mutant G12V, which was ablated by overexpression of wildtype RASSF1C (Vos et al., 2004). This data suggests that similar to the involvement of RASSF1A-S131 in DNA damage response, the phosphorylation of RASSF1C S61 site might be required for the activation of RASSF1C during DNA damage. RASSF1C has been implicated in a DNA damage response pathway involving DAXX and JNK (Kitagawa et al., 2006). In unstressed cells, RASSF1C is able to form a complex with DAXX in the nucleus, which can be resolved by nuclear magnetic resonance spectroscopy (Escobar-Cabrera et al., 2010). Upon ultraviolet radiation or Methyl methanesulfonate (MMS)-induced DNA damage, this interaction is lost. This leads to RASSF1C localisation to the cytoplasm where it aids the activation of SAPK/JNK signalling, leading to apoptosis (Kitagawa et al., 2006). DAXX, however, remains in the nucleus concentrated at PML bodies. The signal for the release of RASSF1C from DAXX remains unknown.

In addition, RASSF1A and RASSF1C levels are thought to be regulated by the oncogenic protein CSE1L via a methylation independent mechanism. In *RASSF1A*-negative cells, loss of CSE1L leads to the upregulation of RASSF1C. This sensitises cells to cisplatin treatment, promoting apoptosis (Lorenzato et al., 2012). Conversely, another study has shown that RASSF1C is targeted for degradation under stress conditions. Treatment of cells with doxorubicin or exposure to UV radiation leads to RASSF1C phosphorylation by GSK3β creating a phosphodegron at S19/23 which is recognised by the E3 ubiquitin ligase $SCF^{\beta\text{-}TRCP}$, thereby targeting RASSF1C for degradation (Zhou et al., 2011). The phosphorylation and degradation of RASSF1C was GSK3β-dependent. The GSK3 activity was inhibited by the known GSK3 regulator PI3K/AKT pathway, leading to upregulation of RASSF1C protein levels (Zhou et al., 2011). Since AKT activity can induce RASSF1C upregulation, it suggests that RASSF1C could function as an oncogene. This is in accordance with several recent reports showing that overexpression of RASSF1C was able to increase cell proliferation in osteoblast cells and lung cancer; and migration in breast cancer cell lines (Amaar et al., 2006a; Reeves et al., 2012; Reeves et

`

al., 2010). It has been suggested that the pro-proliferative effect of RASSF1C is mediated through the upregulation of Extracellular-signal-regulated kinase 1/2 (ERK1/2), potentially through an interaction with Insulin growth factor binding partner -2 (IGFBP-2) (Amaar et al., 2006a; Amaar et al., 2006b; Reeves et al., 2012; Reeves et al., 2010). The variety of downstream genes, upregulated upon RASSF1C overexpression also suggest an oncogenic role for the protein. For example, overexpression of RASSF1C in breast cancer cell lines, leads to CXCR4 upregulation, which enhances cell proliferation and metastasis (Reeves et al., 2010); whereas, in lung cancer cell lines, upon RASSF1C expression, the stem cell renewal factor PIWIL1 was shown to be upregulated (Reeves et al., 2012). Recent studies have shown that the interaction of Insulin-like growth factor binding protein 5 (IGFBP-5) with RASSF1C is able to inhibit the RASSF1C association with and upregulation of PIWIL1. This inhibition of the association between RASSF1C and PIWIL1 negatively regulates β-catenin expression and consequently, lung cancer growth and progression (Reeves et al., 2014).

RASSF1C is a target for $SCF^{\beta\text{-TRCP}}$ -mediated degradation. RASSF1C was also shown to bind and inhibit the receptor subunit of the $SCF^{\beta\text{-TRCP}}$, β-TRCP, re-localising it from the nucleus to the cytoplasm, reducing its stability (Estrabaud et al., 2007). This RASSF1C-dependent β-TRCP inhibition has been associated with an increase in β-catenin nuclear accumulation and transcriptional transactivation, (Estrabaud et al., 2007). β-catenin is an integral structural component of cadherin-based adherens junctions, the key nuclear effector of canonical Wnt signalling and often results in deregulated growth leading to cancer and metastasis (Valenta et al., 2012).

A number of clinical studies support the role of RASSF1C as an oncogene. Multiple groups have shown that RASSF1C expression is upregulated in a variety of human cancers, including pancreatic endocrine tumours, large cell neuroendocrine carcinomas and small cell lung carcinomas (da Costa Prando et al., 2011; Malpeli et al., 2011; Pelosi et al., 2010). RASSF1C expression was also shown to be an adverse prognostic factor in lung cancers (Pelosi et al., 2010).

`

1.6 Therapeutic Implications of RASSF1A Loss

One of the most common and frequent events to occur in sporadic human malignancies is the loss of RASSF1A expression (Donninger et al., 2007; Hesson et al., 2007; van der Weyden and Adams, 2007). This loss is due to hypermethylation of the upstream CpG island in the promoter region of the *RASSF1* gene (Burbee et al., 2001; Dammann et al., 2000). Methylation of the *RASSF1* gene has been reported in over 37 tumour types (Dammann et al., 2005; Hesson et al., 2007).

The incidence of epigenetically driven loss of *RASSF1A* correlates well with the increasing grade of the tumour, with frequency ranging up to 99% methylation in tumours compared with 0% in normal surrounding tissue (Donninger et al., 2007; Grawenda and O'Neill, 2015). Hypermethylation of *RASSF1A* has been linked to advanced stage and high grade tumours of bladder (Gao et al., 2012; Jarmalaite et al., 2008; Kim et al., 2012b; Maruyama et al., 2001), cervix (Neyaz et al., 2008), endometrium (Jo et al., 2006; Liao et al., 2008; Pallares et al., 2008), head and neck (Fendri et al., 2009; Li et al., 2005; Yang et al., 2014; Zhang et al., 2014a), kidney (Kawai et al., 2010), melanoma (Tanemura et al., 2009), and brain tumours, such as glioma (Hesson et al., 2004), neuroblastoma (Stutterheim et al., 2012) and pituitary adenomas (Qian et al., 2005). Tumours with methylated *RASSF1A*, such as bladder (Jarmalaite et al., 2008; Maruyama et al., 2001; Meng et al., 2012), endometrium (Jo et al., 2006) and head and neck are associated with local and distant metastases. In other tumours like neuroblastomas (Stutterheim et al., 2012), kidney (Kawai et al., 2010; Ohshima et al., 2012), bladder (Kim et al., 2012b), head and neck (Fendri et al., 2009; Li et al., 2005) and cervical tumours (Mitra et al., 2012), loss of RASSF1A is associated with shorter overall survival. The hypermethylation of *RASSF1A* gene promoter has been used as a prognostic marker in sarcomas, where it has been linked to poor disease outcome (Danielsen et al., 2014; Seidel et al., 2005). The increase in the invasive characteristics of prostate cancer tumours has also been linked to *RASSF1A* promoter methylation in independent studies (Jeronimo et al., 2004; Kawamoto et al., 2007; Liu et al., 2011b; Liu et al., 2002; Maruyama et al., 2002) and meta-analysis of 1123 cases (Ge et al., 2014).

`

Meta-analysis of data from patients with a number of different cancers including breast, non-small cell lung cancer and colorectal carcinoma have now been done, each supporting the significance of *RASSF1A* methylation as a prognostic marker. In lung tumours, the methylation of *RASSF1A* has been shown to correlate with poor differentiation, advanced disease stage and local recurrence (Buckingham et al., 2010; Endoh et al., 2003; Kubo et al., 2009; Lee et al., 2012; Tomizawa et al., 2002; Wang et al., 2007).

1.6.1 *RASSF1A* Promoter Hypermethylation – A Prognostic Marker

The clinical significance of *RASSF1A* methylation has been best studied in breast cancer, where it has been shown to be a better prognostic marker than standard prognostic parameters (Muller et al., 2003). A recent meta-analysis of data from 1795 patients from 8 studies used multivariate analysis to investigate disease free survival and overall survival in breast cancer patients with methylated *RASSF1A*, and showed a significant correlation between these parameters (Jiang et al., 2012). A variety of reports lend strong support to the involvement of RASSF1A promoter hypermethylation in the tumourigenesis of breast cancer, including increased cancer risk, poor prognosis, adverse cancer outcome, higher risk of recurrence, advanced stage, lymph node metastasis. It has also been shown to negatively affect the progression-free survival and the overall survival. These studies are comprehensively reviewed in (Grawenda and O'Neill, 2015).

Colorectal carcinogenesis is often associated with constitutive activation of Ras or downstream pathway members B-Raf and PI3K (De Roock et al., 2011; Velho et al., 2010). The methylation of the *RASSF1A* gene promoter in colorectal cancers varies from 12 % (Yoon et al., 2001), to 81 % (Sakamoto et al., 2004). A number of these studies have shown that *RASSF1A* methylation rarely occurs together with K-Ras mutations (Fernandes et al., 2012). In order to counter the tumour-suppressor functions of RASSF1A, cancer cells inhibit the apoptotic signal downstream of RASSF1A, by K-Ras-dependent downregulation of MST2 via AKT activation (Matallanas et al., 2011). Another study

`

showed that methylation of *RASSF1A* was associated with increased genomic instability and an accumulation of mutation in *KRAS* and *BRAF* genes (Oliveira et al., 2005).

A number of studies have shown that *RASSF1A* promoter methylation status can be determined from the cell-free circulating tumour DNA (Chan et al., 2008a; Gobel et al., 2011; Ponomaryova et al., 2013; Wang et al., 2007). This method offers an alternative for diagnostic material for clinical use as it is easier and faster than conventional biopsy. Together, these studies support the utility of *RASSF1A* hypermethylation as a prognostic marker of poor outcome and cancer progression.

1.6.2 Re-Expression of RASSF1A

RASSF1A methylation has also been shown to correlate with a decreased responsiveness to DNA damaging therapies (Catto et al., 2005; Dote et al., 2005; Honda et al., 2008). The DNA methyltransferase (DNMT) inhibitor Zebularine has been used to effectively re-express *RASSF1A* in cancer cells, resulting in increased sensitivity to radiation-induced damage *in vitro* and *in vivo* (Dote et al., 2005) as well as to cisplatin (Balch et al., 2005). A 48 hrs treatment with Zebularine, which corresponded to the maximum re-expression of *RASSF1A*, increased the radiosensitivity of DU145,U251 and PaCa pancreatic cancer cell lines by 1.5 times and delayed tumour progression in U251 xenograft models in mice (Dote et al., 2005). A 48 hrs treatment with Zebularine had a similar effect, increasing the sensitivity of ovarian cancer cells to DNA damage and the reduction in IC_{50} of cisplatin in resistant ovarian cancer cells (Balch et al., 2005). Another DNMT inhibitor, 5-aza-2'-deoxycytidine, currently in clinical trials, increased the sensitivity of testicular germ cell tumours to cisplatin (Beyrouthy et al., 2009).The effectiveness of the 5-aza-2'-deoxycytidine treatment was dependent on the level of DNMT3B levels with greater effects seen with higher DNMT3B levels. As one of the most significant target genes for DNMT3B was shown to be RASSF1A, the observed increased sensitivity to cisplatin with 5-aza-2'-deoxycytidine treatment could be due to the re-expression of *RASSF1A*. The increase in the sensitivity to chemotherapeutics such as fluorouracil,

`

mitomycin as well as cisplatin of hepatocellular carcinoma cell line, SMMC-7721, was also shown to be attributed to the re-expression of *RASSF1A* due to 5-aza-2'-deoxycytidine (Zhao and Dou, 2007). Together these results support a clinically relevant role for RASSF1A in the DNA damage response, supported by phase I and II clinical trials in myelodysplasia and leukaemia, where 5-aza-2'-deoxycytidine was shown to be effective both alone and in combination with the histone deacetylase (HDAC) inhibitor valproic acid (Garcia-Manero et al., 2006; Ruter et al., 2006). Therapeutic failure upon RASSF1A loss can also be counteracted by targeting the downstream DNA damage responsive signalling pathway. Direct activation of BAX via the BH3 mimetic ABT-737 has recently been put forward as a potential treatment for medulloblastoma which have lost *RASSF1A* due to hypermethylation (Levesley et al., 2011).

1.7 Project Aims

The aims of this project are to investigate the role of RASSF1C as a potential oncogene in human cancer cell lines and the mechanisms through which these roles are achieved in order to better understand how loss of RASSF1A and consequent expression of RASSF1C contributes to tumourigenesis. I shall fulfil these aims by identifying novel functions of RASSF1C in regulating cell adhesion and invasion. A previously undescribed association of RASSF1C in the translocation and activation of transcription factors will be assessed and the consequences of this will be analysed in the context of RASSF1A loss. A new role for RASSF1C-dependent production of exosomes and generation of cancer stem cells will be investigated. The data generated in this project will provide new evidence to explain why patients that have lost one isoform of the *RASSF1* gene, but not the other, have worse prognosis and why expression of RASSF1C in cancers is associated with a more malignant, metastatic phenotype.

`

Chapter 2 Materials and Methods

2.1 Materials

Unless stated otherwise, all chemicals were purchased from either Sigma – Aldrich or Fisher Scientific and used according to manufacturer's guidelines. Tissue culture plastic was purchased from Sarstedt and Corning. Glassware was purchased from Fisher and VWR.

2.2 Cell Culture

Unless stated otherwise, all cell lines (Table 2.1) were maintained in complete Dulbecco's Modified Eagle Medium (DMEM) supplemented with 10 % (v/v) Fetal Bovine Serum (FBS), 2 mM Glutamine and 100 U/ml Penicillin/Streptomycin (Pen/Strep)). All media and supplements were purchased from Gibco® (Life Technologies). Cells were maintained at 37 ^{o}C, with 5 % CO_2 in a humidified incubator.

From frozen, cells were defrosted rapidly in a water bath at 37 ^{o}C. Once thawed, cells were diluted in complete media and centrifuged at 500 x g for 5 min. Cell pellets were resuspended in 10 ml of complete media and seeded into a T75 flask (Sarstedt).

Upon reaching confluency, cells were washed in Phosphate Buffered Saline (PBS) and trypsinised using 0.25 % Trypsin-EDTA solution (Life Technologies). Media was then added to the trypsinised cells and a proportion of them reseeded into a new flask containing fresh complete media.

Cells were routinely frozen down in freezing media containing 90 % (v/v) FBS, 10 % (v/v) Dimethyl sulfoxide (DMSO). Cells were trypsinised, resuspended in complete media, centrifuged at 500 x g for 5 min and the pellets resuspended in freezing media and aliquoted into 1.5 ml cryovials (Thermo Scientific). Cryovials were placed into a Nalgene® Mr Frosty containing 200 ml isopropanol at room temperature (RT), and placed at -80 ^{o}C for 24 hrs prior to long term storage in liquid Nitrogen.

`

2.3 Transfection

All cells undergoing transfection were plated in the presence of complete DMEM (Life Technologies), but without antibiotics. All transfections, either with plasmid DNA or siRNA, were done using the Lipofectamine 2000 transfection reagent (Life Technologies) and following the manufacturer's guidelines. This was done at a ratio of 1 μg siRNA to 1 μl of Lipofectamine 2000 or 1 μg plasmid DNA to 1 μl of Lipofectamine 2000. All cells were transfected with 50 nM siRNA.

Appropriate for each experiment volumes of siRNA or plasmid DNA and Lipofectamine 2000 were diluted in separate tubes in OptiMEM (Life Technologies) and incubated at room temperature for 5 min. Then the contents of the two tubes were mixed together and left at room temperature for 25 min. After the incubation the mixture was added in a dropwise manner to the cells. After 6 hrs the media containing the mixture of siRNA or plasmid DNA and Lipofectamine 2000 was aspirated and was changed to fresh complete media, in which, unless stated otherwise, the cells were kept until harvesting.

2.4 Quantitation of Cell Lysates

Cells were washed once with PBS and lysed directly in the plate by the addition of appropriate amounts of laemmli lysis buffer (Table 2.6), supplemented with 1 X protease inhibitor cocktail (Roche). Cells were scraped off the plate using a rubber cell scraper (Sarstedt) and the lysates transferred to a 1.5 ml universal tube. The lysates were then boiled at 100 ^{o}C for 10 min and stored at -20 ^{o}C until needed.

The protein concentration of cell lysates was determined using Bradford assay. For the generation of a standard curve, Bovine Serum Albumin (BSA) (Thermo Scientific) was used at concentrations ranging from 0 – 2000 μg/ml. Lysates were diluted 1/10 with water and of this solution, 5 μl were added to the wells of a 96 well plate. To each well 250 μl of Bradford reagent (Thermo Scientific) was

`

added. The absorbance of each well was measured at wavelength of 595 nm using a plate reader (BMG POLARstar Omega). The standard curve was used to calculate the actual concentration of each sample in μg/μl and to normalise and equalise each of the samples with Laemmli lysis buffer, so that equal loading per experiment was achieved. To each sample an appropriate volume of 4 x SDS-PAGE sample buffer (Table 2.6) was added. Samples were boiled for 5 min, 100 ^{o}C before loading onto an SDS-PAGE gel for electrophoresis or stored until needed at -20^{o}C.

2.5 SDS-PAGE and Western Blot

Protein samples were loaded onto a gel and separated by SDS-PAGE. NuPAGE® pre-cast gels (10 % or 4-12 %) (Life Technologies) were loaded into a Novex® mini gel tank, filled with 1 X NuPAGE® MOPS SDS running buffer (Life Technologies). Self-cast gels made with 10 % resolving gel (10 % final concentration of 30 % (v/v) acrylamide: 0.8 % (v/v) Bis solution, 375 mM Tris pH 8.8, 0.1 % (w/v) SDS, 0.1 % (w/v) APS, 0.01 % (v/v) TEMED) and a 4 % stacking gel (4 % final concentration of 30 % (v/v) acrylamide: 0.8 % (v/v) Bis solution, 125 mM Tris pH 6.8, 0.1 % (w/v) SDS, 0.1 % (w/v) APS, 0.01 % (v/v) TEMED) (Laemmli, 1970) and were loaded into Bio-Rad Mini Protean® TetraCell gel tanks filled with SDS-PAGE running buffer (Table 2.6). Samples were loaded using gel loading tips (Starlabs), along with See Blue® plus 2 Pre-stained protein standard (Life Technologies) for the NuPAGE® pre-cast gels and Fermentas PageRuler™ prestained protein ladder (Thermo Scientific) for the self-cast gels. Gels were run at a constant voltage of 120 V using PowerPac^{TM} HC High-current power supply (Bio-Rad). The protein samples were separated by gel electrophoresis and were transferred from the gel onto an Amersham Protran 0.45 Nitrocellulose membrane (GE Healthcare). The membrane was activated using transfer buffer (Table 2.6) before the transfer was performed using the BioRad mini gel blotting system, in which the gel and membrane were sandwiched between two sheets of Whatman paper and compacted using sponges. The transfer was performed in transfer buffer (Table

`

2.6) at a voltage of 100 V for between 90 min using PowerPac™ HC High-current power supply (Bio-Rad).

Following transfer, Nitrocellulose membranes were blocked for 1 hr on a SSL4 See-saw rocker (Stuart) at room temperature in 5 % skimmed milk (w/v) in PBS-T (Table 2.6). After blocking, the primary antibody was added to the membrane at a concentration of 1:1000 (v/v) in 5 % skimmed milk (w/v) in PBS-T. All primary antibodies were incubated with the membrane overnight at 4 ^{o}C.

Following primary antibody incubation, membranes were washed (3 x 5 min) in PBS-T on a See-saw rocker before being incubated with secondary HRP-conjugated antibody (Table 2.4). Membranes were incubated at room temperature for 1 hr prior to being washed (3 x 5 min) in PBS-T. The nitrocellulose membranes were then exposed to either Enhanced chemiluminescence (ECL) solution (Thermo Scientific) for normal exposure or ECL advance (GE Healthcare) for low abundance proteins according to manufacturer's protocol. Membranes were exposed to FujiFilm X-ray film RX (Fuji) and developed using a XoGraph processor (XoGraph Imaging Systems) before being scanned onto a computer.

In order to allow membranes to be probed with multiple primary antibodies, membranes were stripped for 10 min at RT on a See-saw rocker, using Restore™ western blot stripping buffer (Thermo Scientific). Membranes were washed three times with PBS-T before re-blocking and incubating with primary antibody.

2.6 Immunoprecipitation

Cells were washed two times with PBS before lysis with immunoprecipitation lysis buffer (Table 2.6) supplemented with protease inhibitor cocktail (Roche) and 50 mM sodium fluoride, 10 mM β-glycerophosphate and 0.5 mM sodium orthovanidate. Cells were scraped from the dish and collected into a 1.5 ml microfuge tube and incubated end over end at 4 ^{o}C for 10 min. Lysates were then

`

cleared by centrifugation (20817 x g, 10 min, 4 ^{o}C). The protein concentration of the lysates was then determined by Bradford assay, so that an equal amount of protein was loaded into each immunoprecipitation.

Protein A agarose (Millipore) and protein G metallic (Millipore) beads were used during this project. All beads were washed 3 times in immunoprecipitation lysis buffer before being aliquoted into 1.5 ml microfuge tubes. 1-2 μg antibody or corresponding amounts of IgG (Mouse or Rabbit, (Cell Signalling)) were added per 10 μl of the protein A agarose or protein G metallic beads before lysate was added to the tubes and incubated end over end at 4 ^{o}C for 3 hrs. Samples containing protein A agarose beads were washed three times by collecting the beads by centrifugation (2150 x g, 4 ^{o}C, 2 min) before aspirating the supernatant and resuspending the beads. Protein G metallic beads were washed three times by immobilising the beads using a magnet, aspirating the supernatant and resuspending the beads. Protein was removed from the antibody by boiling at 100 ^{o}C for 5 min in 1 x SDS-PAGE sample buffer (Table 2.6). An equal volume of each sample was then loaded onto a gel for electrophoresis and western blot analysis (Section 2.5).

2.7 Immunofluorescence

Cells, plated onto glass coverslips (Fisher), were washed twice with PBS and fixed in 4 % (v/v) Paraformaldehyde solution (16 % (v/v) Paraformaldehyde diluted in PBS) for 15 min at RT, protected from light. Coverslips were washed twice with PBS before the cells were permeabilised with 0.2 % (v/v) Triton-X solution (in PBS) for 5 min at RT. Cells were washed with PBS and blocked with 0.2 % (v/v) Fish Skin Gelatin (FSG) (Sigma – Aldrich) (in PBS) for 1 hr at RT. Cells were then incubated overnight at 4 ^{o}C with primary antibody (Table 2.4). Coverslips were washed 3 times with PBS for 5 min before the secondary antibody was added (Table 2.4) and the cells incubated for a further 1 hr at RT. Coverslips were washed with PBS (3 x 5 min) and mounted onto microscope slides (Fisher) using Prolong® Gold antifade reagent with DAPI (Life Technologies). Slides were sealed with clear nail

`

varnish and analysed by microscopy. Light microscopy was done using a Nikon 90i or a Nikon 2000TE microscope using the NIS elements software, versions 4.2 and 3.8, respectively. Confocal microscopy was done using a Zeiss LSM710 or Zeiss LSM780 with Zeiss Zen program, version 2010 and 2011, respectively.

2.8 Cloning

The constructs in Table 2.3 were made using standard cloning techniques. All sequences of interest were amplified by PCR using Platinum *Pfx* (Life Technologies). Each PCR mix contained dsDNA template (0.4 ng/ml), Forward primer (0.3 ng/ml), Reverse primer (0.3 ng/ml), Reaction buffer (1 X), dNTP mix (0.3 mM), $MgSO_4$ (1 mM), Platinum *Pfx* enzyme (1 unit) and Nuclease-free water (Qiagen). The samples were then transferred to a thermal cycler (My Cycler, Bio-Rad) and ran following the manufacturer's instructions: Denaturation (1 cycle at 94 ^{o}C for 60 sec), Amplification (30 cycles of 94 ^{o}C for 30 sec, 55 ^{o}C for 30 sec and 68 ^{o}C for 60 sec per 1 kb of DNA) and final extension of 68 ^{o}C for 300 sec. The amplified DNA was ran on 0.8 % (w/v) agarose gel and purified using agarose gel purification kit (Qiagen Gel purification kit) following manufacturer's protocol.

Restriction endonucleases, purchased from Roche, were used to digest the purified PCR product and the vector into which the PCR product was to be ligated following manufacturer's instructions. The vector was then dephosphorylated and the insert and vector ligated using the rAPid DNA dephosphorylation and ligation kit (Roche). Ligated DNA was transformed by heat shock (42 ^{o}C, 30 sec) into DH5α *E.coli* (Life Technologies) and plated onto agar plates with the appropriate antibiotic selection agent, either Kanamycin or Ampicilin (Sigma – Aldrich). Single clones were picked and amplified overnight. The DNA was then purified using a mini-prep kit (Qiagen). Correct insertion of the PCR product into the vector was tested by double restriction digest, to show reconstitution of the

`

cut sites, and also by Sanger sequencing (Source Biosciences). Large scale DNA purification was done by Maxi-prep (Qiagen).

Site-directed mutagenesis was carried out using Agilent QuickChange II Site-directed Mutagenesis Kit following the manufacturer's protocol. The primers used were generated following the manufacturer's guidelines. Positive clones were confirmed by Sanger sequencing for the presence of the introduced mutation.

2.9 Reverse-Transcriptase PCR (RT-PCR)

The Reverse-Transcriptase PCR was prepared using the Power SYBR Green Cells-to-Ct Kit (Life Technologies) protocol. Cells (2 x 10^5/well) were plated onto 6 well plates. Cells were washed, counted and 5 x 10^4 cells were used for cell lysis and cDNA preparation. Cells were centrifuged at 500 x g for 5 min, washed with ice-cold PBS and the pellet was lysed in 25 μl lysis buffer, in the presence of DNase I, for 5 min. The reaction was stopped by the addition of 2.5 μl Stop Solution from the kit. For the RT-PCR, each tube of the reaction mix consisted of 5 μl RNA, 25 μl of 2 X SYBR RT Buffer, 2.5 μl of 20 X RT Enzyme Mix and 17.5 μl of Nuclease- free water. The tubes were then transferred to a thermal cycler (My Cycler, Bio-Rad) following the suggested protocol of 37 ^{o}C for 60 min and 95 ^{o}C for 5 min, for the inactivation of the RT enzyme. The samples were then stored at -20 ^{o}C.

2.10 Quantitative Real-Time PCR

The Quantitative Real-Time PCR was done according to the Power SYBR Green Cells-to-Ct Kit (Life Technologies) protocol. The cDNA used was diluter 4 times in Nuclease-free water. The PCR mix for each sample included 5 μl of Power SYBR Green PCR Master Mix, 0.2 μl of Forward and Reverse primer mix (10 μM stock concentrations) and 0.8 μl of Nuclease-free water. The PCR mix and 4 μl of

`

the cDNA/water mixture were added to a well of 96-well plate (Life Technologies) and the plate was sealed with a plastic film (VWR) and ran in Applied Biosystems 7500 Fast real-time thermal cycler (Applied Biosystems). The protocol used was Holding Step (1 X cycle: 95 ^{o}C 10 min), Cycling Step (50 X cycle: 95 ^{o}C 15 sec, 60 ^{o}C 1 min) and Melt Curve Step (1 X cycle: 95 ^{o}C 15 sec, 60 ^{o}C 1 min, 95 ^{o}C 30 sec, 60 ^{o}C 15 sec). The expression of 18S was used as an internal control for all the experiments. The calculation of the $\Delta\Delta$Ct was done on Microsoft Excel.

2.11 Retroviral Generation of Stable Cell Lines

For the generation of stable cell lines, expressing either control (ZsGreen) or ZsGreen-RASSF1C, retroviral infection was used by cloning the sequences of interest onto the retroviral vector pQCXIP (Clontech). To that end, 4 days prior to infection, HEK293T cells (5 x 10^6/flask) were seeded into T75 flasks (Sarstedt). The following day the cells were transfected with the retroviral plasmid. This was done as follows: 10 μg of the plasmid of interest (pQCXIP-ZsGreen or pQCXIP-ZsGreen-RASSF1C), 10 μg of the packaging plasmid pVSV-G (Clontech), 10 μg of GAG/POL -containing plasmid, 100 μl of 2.5 M $CaCl_2$ and up to 1 ml of sterile water were added and mixed in a 30 ml multipurpose container (Greiner Bio-One). While bubbling, 1 ml of 2 X HBS buffer (pH 7.08) was added dropwise to the plasmid/ $CaCl_2$ mixture. The combined solution was then incubated at RT for 1 min. Prior to the addition of the mixture, Chloroquine was added to each flask of cells at 25 μM final concentration. The mixture was then added dropwise to the cells. The media was aspirated 24 hrs later and fresh complete media was added to the 293T. The same day MDA-MB-231 or MCF7 cells were plated (2 x 10^5 cells/condition) into T75 flasks in complete media. The following day, the media from the 293T cells was removed and filtered using a 10 ml syringe (Terumo) and 0.45 μm filters (Millipore). The filtered media was then added to the MDA-MB-231 or MCF7 cells with the addition of Polybrene (Sigma – Aldrich, 8 mg/ml) at 1/1000 dilution. This process of filtration and infection of the MDA-MB-

`

231 or MCF7 was repeated 3 times, every 24 hrs. The cells were then selected for 3 days using appropriate for each cell line amounts of Puromycin.

2.12 Mammosphere Growth Assay

Matrigel (Corning) was thawed overnight on ice at 4 ^{o}C and mixed in a ratio of 1:1 with ice cold DMEM without FBS on ice using pipettes and pipette tips stored at -20 ^{o}C overnight. Of the mixture, 300 μl were then pipetted into each well of a pre-cooled 24 well plate. Matrigel was then allowed to solidify by incubating at 37 ^{o}C for 30 min. During the incubation, MDA-MB-231 cells were trypsinised, counted and a solution of 5000 cells/ml was made in complete DMEM. From the solution, 500 μl were added to each well of solidified Matrigel. Plates were incubated at 37 ^{o}C, 5 % CO_2 in a humidified incubator to allow mammosphere growth. The media was changed every 3 days for 10 days at which point images were taken using a Nikon TE2000 Eclipse microscope at 20 X or 10 X magnification, depending on the size of the mammosphere. The image analysis was done with Nikon NIS Elements 4.0, by measuring the area and the perimeter of each mammosphere. The aggressiveness was assessed by counting the number of projections per mammosphere. An aggressive mammosphere was defined as one with greater than five projections into the surrounding matrigel.

2.13 Proximity Ligation Assay

Performed as previously described using the Duolink Starter Kit (Sigma – Aldrich) (Soderberg et al., 2006). H1299 cells were transfected and treated as per instructions before overnight incubation with primary antibodies (SRC, SRC pY416, SRC pY527 (Cell Signalling); ZsGreen (Clontech); RASSF1A (Epitomics); RASSF1C (Abcam); Flag -tag (Sigma – Aldrich); HA tag (Milipore)) and secondary antibodies for 1 hr. Hybridisation was performed for 30 minutes in a humidified chamber, ligation

`

reactions for 30 minutes, amplification for 100 minutes and DAPI was used for cell detection. The dot-like structures were imaged using Zeiss LSM780 microscope using a 63 X (NA 1.4) objective. For each cell 5 Z-stack images were taken and analysed with BlobFinder V3.2 (Uppsala University) (Allalou and Wahlby, 2009). The average values, SEM and significance were calculated using Prism 6.0 (Graphpad) software.

2.14 Real-Time Molecular Visualisation

MCF7 cells (2 x 10^5 cells/condition) on glass bottom plates (Ibidi, Germany) were transfected with GFP-E-cadherin and DsRed or DsRed-RASSF1C plasmids. Cells were grown in complete media until imaging, when media was changed to complete DMEM/F-12 media without phenol red and supplemented with 10 % (v/v) FBS, 2 mM Glutamine and 100 U/ml Pen/Strep. Cells were imaged using Zeiss LSM780 confocal microscope using a 63 X objective, for the time lapse 1 image per second for a total of 200 seconds. Tracking of internalized E-cadherin was achieved using Imaris 7.71 software (Bitplane, ANDOR). Threshold was determined for each video and varied between 0.4-0.6 um in size. The average distance travelled was set at a threshold of 1 μm. A Quality filter was applied and the threshold set at 15. The data was extracted using the Vantage feature and average values, SEM and significance were calculated using Prism 6.0 (Graphpad) software. On average, 5 cells and 700 vesicles each were counted per experiment and the data shown represents 3 independent experiments.

2.15 Time Lapse Imaging

MCF7 cells (3 x 10^5 cells/well) were plated onto 12 well plate. Cells were incubated for 24 hrs before media was changed to complete DMEM/F-12 media without phenol red. The cells were then imaged for up to 8 hrs at a rate of 1 picture every 15 min, using a Nikon TE2000 inverted microscope at 20 x

`

magnification at 37 ^{o}C and 5 % CO_2. The collected pictures and videos were analysed using Nikon NIS Elements 4.0 program.

2.16 Fluorescent Recovery After Photobleaching (FRAP)

MCF7 cells (2 x 10^5 cells/condition) were plated on 35 mm glass bottom plates (Ibidi, Germany). Cells were grown in complete media until imaging, when media was changed to complete DMEM/F-12 media without phenol red. Cells were imaged using Zeiss LSM780 confocal microscope using a 63 X (NA 1.4) objective. Each bleach was done at full laser power and 2 pulses were used in order to achieve 60 % bleach per region of interest. Images were taken every 2 seconds for 5 minutes after the bleach. Data was analysed using easyFRAP software (Rapsomaniki et al., 2012). The immobile and mobile fractions were calculated using double exponential formula (Intensity (I) = IE – I1 x e(-t/T1) – I2 x e(-t/T2)).

2.17 Calcium Switch Assay

MCF7 cells were grown at high density (3 x 10^5 cells/condition) on cover slips in calcium containing complete DMEM. With the exception of 'Control', cells were washed twice with PBS before being incubated overnight in calcium-free media (DMEM supplemented with 2 mM Glutamine and 100 U/ml Penicillin/Streptomycin (Pen/Strep), (Life Technologies)) supplemented with calcium-depleted 10 % (v/v) FBS (Life Technologies) using Chelex® 100 (Bio-Rad Laboratories). The cells were then washed in PBS and complete media was added for up to 180 min. Coverslips were collected at the indicated time points. The coverslips were then stained using the immunofluorescence protocol. Images were taken using Zeiss LSM780 using a 63 X (NA 1.4) objective and analysed using ZEN2011 software. Cells expressing GFP-empty vector or GFP-RASSF1C were utilised for single cell analysis. Total contacts were calculated as the percentage of junctions formed vs the total number of cells in

`

contact with the cell being analysed. Weak contacts were defined as being diffuse or interrupted staining at the site of cell-cell junction. Strong contacts were defined as robust, well defined staining at site of the cell-cell junction.

2.18 Exosome Production and Isolation

Cells were plated at high density (5 x 10^6 cells/condition) on two T175 flasks (Sarstedt) per condition. Where indicated, cells were transfected following the previously discussed method. For the production of the conditioned media, cells were washed twice with PBS and incubated for three days with DMEM supplemented with 0.1 % (v/v) FBS (depleted of bovine exosomes by overnight centrifugation at 100 000 x g), 2 mM Glutamine and 100 U/ml Pen/Strep (exosome free DMEM). The conditioned media (40 ml/condition) was then collected and exosomes were isolated as previously described by (Thery et al., 2006) by sequential ultracentrifugation at 2000 x g for 30 min, 10 000 x g for 40 min, 100 000 x g for 14 – 18 hrs in a Optima XPN-80 (Beckman Coulter) ultracentrifuge using UltraClear Thinwall tubes. The pellet was then resuspended in 1 ml of PBS, transferred to a 1.5 ml universal tube and purified by centrifugation at 100 000 x g for 80 min in an Optima MAX-XP Ultracenrifuge (Beckman Coulter). After the centrifugation the PBS was removed and the exosomes used for analysis or further treatment of cells.

2.19 Exosomes for SDS-PAGE and Western blot

Collected and washed exosomes were kept in a 1.5 ml universal tube and lysed in 50 μl Radioimmunoprecipitation assay buffer (RIPA buffer, (Cell Signalling)) containing 20 mM Tris-HCl (pH 7.5), 150 mM NaCl, 1 mM Na_2EDTA, 1 mM EGTA, 1 % NP-40, 1 % sodium deoxycholate, 2.5 mM sodium pyrophosphate, 1 mM β-glycerophosphate, 1 mM Na_3VO_4, 1 μg/ml leupeptin. The samples were then boiled at 100 ^oC for 10 min and 5 μl of each sample was used for protein quantitation

`

using the Micro BCA assay (Thermo Scientific) following the manufacturer's protocol. In brief, a standard curve was generated using Bovine Serum Albumin (BSA) (Thermo Scientific) at concentrations ranging from 0 – 200 μg/ml. Of each sample 5 μl were put in wells of 96 well plate and 150 μl of the mixture of the three provided reagents from the assay kit was added. The mixture contained 25 parts of Micro BCA reagent MA, 24 parts of reagent MB and 1 part of reagent MC. The plate was then sealed with a plastic film (VWR) and incubated at 37 ^{o}C for 2 hrs. The absorbance was then measured at wavelength of 562 nm using a plate reader (BMG POLARstar Omega). The standard curve was then used to calculate the actual concentration of each sample in μg/μl and to normalise and equalise each of the samples with RIPA lysis buffer (Cell Signaling), so that equal loading per experiment was achieved. To each sample an appropriate volume of 4 x SDS-PAGE sample buffer, without 2-mercaptoethanol (Table 2.6) was added. Samples were then boiled for 5 min at 100 ^{o}C before being loaded onto an SDS-PAGE gel for electrophoresis or stored until needed at -20^{o}C.

2.20 Exosomes Treatment of Cells

Cells (2 x 10^5 cells/well) were plated on 6 well plates and kept in complete media for 24 hrs prior to treatment with exosomes. Exosomes were collected and washed as previously stated. The collected pellet was then resuspended in 1 ml of exosome free DMEM. The exosomes and the DMEM were then added to the cells for 18 hrs until the cells were trypsinised, counted and collected for SDS-PAGE or RT-PCR.

2.21 Staining of Exosomes

All staining of exosomes was done using the PKH67 Green Fluorescent Cell Linker Mini Kit (Sigma – Aldrich) following manufacturer's protocol. In brief, exosomes were collected and washed as previously stated. Each exosomal pellet was resuspended in 250 μl of Diluent C in a universal tube. At

`

the same time 1 μl of the 2 X fluorescent dye solution was added to 250 μl of Diluent C in another universal tube. The exosome solution was then quickly added to the dye solution and mixed immediately by pipetting. The cell/dye suspension was then incubated for 5 min with periodic mixing every minute. After the incubation, 500 ml of complete DMEM supplemented with 10 % (v/v) FBS (depleted of bovine exosomes) was added to stop the staining and incubated for 1 min. The universal tube was then centrifuged at 100 000 x g for 80 min. After the centrifugation the solution was aspirated, the pellet washed in 1 ml PBS, transferred to another 1.5 universal tube and centrifuged again at 100 000 x *g* for 80 min. The collected pellet was then resuspended in complere DMEM supplemented with 0.1 % (v/v) FBS (depleted of bovine exosomes) and the solution added to cells as previously stated.

2.22 Stem Cell Production

Cells (2 x 10^5 cells/well) were plated in 6 well plates and, 24 hrs later, transfected as described above. The following day the cells were trypsinised, counted and plated as single cell suspensions (1000 cells/cm^2) on ultra-low attachment plates (Costar). Spheroids were left to form for 5 days, then trypsinised, counted and plated onto a new ultra-low attachment plate at 1000 cells/cm^2 for a second round of spheroid formation. This was repeated once more in order to achieve tertiary spheroids, at which point the cells were collected and analysed by flow cytometry.

2.23 Flow Cytometry

2.23.1 Flow Cytometry for Cells Treated With Exosomes

Cells (3 x 10^5/well) were plated onto 6 well plates in complete media and left overnight. Exosomes were produced, harvested, washed and stained as described above. Cells were then treated with the

`

exosomes in the presence of exosome free DMEM and incubated for 18 hrs. The cells were then washed once with PBS and trypsinised. The trypsin was inactivated with 5 ml of complete media and the cells were centrifuged at 500 x g for 5 min. The media was then aspirated and the cells were resuspended in PBS, transferred to a 1.5 ml universal tube and centrifuged again at 500 x g for 5 min. The PBS was aspirated and the cells were resuspended in 500 μl of 2 % (w/v) BSA in PBS. The cells were immediately transferred to a round-bottom, polystyrene FACS tubes (BD Biosciences) and analysed by flow cytometry on a FACS-Calibur instrument, integrated with Cell-Quest software (BD Biosciences). Untreated cells were used as control for the set up and the definition of the fluorescence threshold. For each sample 10 000 events were counted and analysed.

2.23.2 Flow Cytometry for Stem Cells

Tertiary spheroids were grown on ultra-low attachment plates as described above. Both the media and the PBS from the wash were collected into the same tube. Cells were detached from the plates using TrypLE (Life Technologies) for 5 min and collected. The tubes were centrifuged at 500 x g for 5 min and the cells were transferred to a 1.5 ml universal tube, washed once in PBS and blocked for 30 min at RT in 2 % (w/v) BSA in PBS. To the blocking solution, 100 μl of either anti-human CD44 (clone G44-26, APC-conjugated, BD Biosciences) or anti-human CD24 (clone ML5, PE-conjugated, BD Biosciences) or both were added and incubated for 1 hr at RT. Cells were then centrifuged at 500 x g for 5 min, the buffer aspirated and the cells washed with PBS. This was done 3 times before the cells were resuspended in the blocking buffer and analysed by flow cytometry on a FACS-Calibur instrument, integrated with Cell-Quest software (BD Biosciences). Unstained cells were used as control for the set up and the definition of the fluorescence threshold. For each sample 10 000 events were counted and analysed.

2.24 Statistics

For all *in vitro* experiments, statistical analysis was carried out using a Student's T-test, calculated on Microsoft Excel or Prism 6.0 (Graphpad). The Standard Error Mean (SEM), used for error bars, was

`

calculated by the division of the standard deviation by the square root of the number of measurements made. Tumor areas were compared by analysis of variance (ANOVA) followed by post-doc Newman-Keuls T-tests.

2.25 Tables

Name	Type	Source
293T	Human Embryonic Kidney	Madalena Tarsounas
CaCo2	Colorectal adenocarcinoma	Xin Lu
H1299	Non-small cell lung carcinoma	CRUK
HeLa	Cervix adenocarcinoma	CRUK
MCF7	Breast adenocarcinoma	CRUK
MDA-MB-231	Breast adenocarcinoma	ATCC
SW480	Colorectal adenocarcinoma	ATCC
U2OS	Osteosarcoma	ATCC

Table 2.1. List of the Cell Lines Used in this Study. Table indicates the cell line, the tissue of origin and where they were acquired from.

Target Gene	siRNA target sequence	Purchased from
siRASSF1 (siGenomeSMARTpool)	ACGCACAAGGGCACGUGAA CAAGGACGGUUCUUACACA GCAAGAAGCCACCCUCCUU CUACAUAACUUCCUACGUA	Thermo (Dharmacon)
siRASSF1A	GACCUCUGUGGCGACUUC	Eurofins MWG
siRASSF1_1	ACGCACAAGGGCACGUGAA	Eurofins MWG OPERON
siRASSF1_2	CAAGGACGGUUCUUACACA	Eurofins MWG OPERON
siSRC (6714) (siGenome)	GAGAACCUGGUGUGCAAAG	Thermo (Dharmacon)
siRASSF1_1	ACGCACAAGGGCACGUGAA	Eurofins MWG
siRASSF1_2	CAAGGACGGUUCUUACACA	Eurofins MWG
siYAP1	CUGGUCAGAGAUACUUCUUtt	
siCTNNB1 (siGenome SMARTpool) (β-catenin)	GCUGAAACAUGCAGUUGUA GAUAAAGGCUACUGUUGGA CCACUAAUGUCCAGCGUUU ACAAGUAGCUGAUAUUGAU	Thermo (Dharmacon)
siTEAD1 (siGenome SMARTpool)	Cat no. GS7003	Qiagen
siTEAD2 (siGenome SMARTpool)	GGAAGACCCGAACUCGAAA GGAAUGAACUGAUCGCCCG	Thermo (Dharmacon)

`

	GCAGUUGAUUCUUACCAGA CGAAGGAAAUCAAGGGAAA	
siTBX2	GUUUCACAACUCCCGCUGGUU	Colin Goding
siTBX3	CAGCTCACCCTGCAGTCCA	Ambion
siNT siGenome sequence No. 2	siGenome sequence No. 2	Thermo(Dharmacon)

Table 2.2. siRNA Sequences Used During this Project. Table indicates the siRNA sequence and where were they acquired from.

Cell Line	Expression	Vector	Selection agent
MDA-MB-231	ZsGreen1	pQXCIP	Puromycin (0.6 μg/ml)
MDA-MB-231	ZsGreen-RASSF1C	pQXCIP	Puromycin (0.6 μg/ml)

Table 2.3. Stable Cell Lines Produced and Used in the Project. MDA-MB-231 cells were retrovirally infected with the indicated plasmids. The pQXCIP was purchased from Clontech.

Antibody	Company	Catalogue No.	Use (Dilution)
Primary Antibodies			
RASSF1	Santa Cruz Biotechnology	Sc-58470	WB (1/500) IP (1/250)
AIF (D39D2) XP®	Cell Signalling Technology	#5318	IF (1/100)
ALIX (3A9)	Cell Signalling Technology	2171s	WB (1/1000)
Anti-phosphotyrosine (4G10)	Millipore	05-1050	IP (1/250)
APC-CD44	BD	559942	FC (1/500)
β-catenin	Santa Cruz Biotechnology	Sc-7199	WB (1/1000), IF (1/100)
Caveolin	Cell Signalling Technology	#3238	WB (1/1000), IF (1/100)
CD63	University of Iowa	H5C6	WB (1/1000), IF (1/100)
CD63 (H-193)	Santa Cruz Biotechnology	sc-15363	WB (1/1000)
Cd81(B-11)	Santa Cruz Biotechnology	sc-166029	WB (1/1000), IF (1/100)
Csk (C-20)	Santa Cruz Biotechnology	Sc-286	WB (1/1000)
DYKDDDK Tag (FLAG)	Cell Signalling Technology	#2368	WB (1/2000)
E-Cadherin	Cell Signalling Technology	#4065	WB (1/1000),IP (1/250),IF (1/100)
EEA1 (C45B10)	Cell Signalling Technology	#3288	IF (1/100)
Fibrilarin	Abcam	ab5821	WB(1/1000)
FLAG M2	Agilent	200472-21	WB (1/2000), IF (1/100)
GAPDH (14C10)	Cell Signalling Technology	#2118	WB (1/5000)
GM130	Abcam	Ab52649	IF (1/100)
HA Tag	Millipore	05-904	WB (1/1000), IP (1/250)
Ki-67	Millipore	AB9260	WB (1/1000), IF (1/100)
LAMP1 (D2D11) XP®	Cell Signalling Technology	#9091	IF (1/100)
LATS1	BETHYL	A300-477A	WB(1/1000)
LFA-1	Abcam	ab3981	WB (1/1000)
MST2 (N-term)	Epitomics	1943-1	WB (1/2000)
MYC Tag	Millipore	05-724	WB (1/1000), IP (1/250)

`

PDCD6 (ALG2) (EP3259)	Abcam	ab109181	WB (1/1000), IF (1/100)
PE-CD24	BD	555428	FC (1/500)
Phospho-LATS1 (Ser909)	Cell Signalling Technology	#9157S	WB(1/1000)
Phospho-LATS1 (Thr1079)	Cell Signalling Technology	#8654S	WB(1/1000)
Phospho-MST1 (T183)/MST2 (T180)	Cell Signalling Technology	3681s	WB (1/1000)
Phospho-MST1 Thr183 MST2 Thr180	Cell Signalling Technology	#3681	WB (1/1000)
phospho-S6 ribosomal protein (S235/236)	Cell Signalling Technology	2211s	WB (1/1000)
Phospho-SRC Family Tyr416	Cell Signalling Technology	#2101	WB (1/1000), IF (1/50)
Phospho-SRC Family Tyr527	Cell Signalling Technology	#2105s	WB(1/1000), IF (1/100)
Phospho-Tyr (PY99)	Santa Cruz Biotechnology	sc-7020	WB(1/1000)
phospho-YAP1 Y357	Abcam	ab62751	WB (1/1000) IF (1/100)
Phospho-YAP1 Ser127	Cell Signalling Technology	#4911s	WB(1/1000), IF (1/100)
RASSF1C	Abcam	Ab24419	WB (1/1000)
S6 Ribosomal protein (54D2)	Cell Signalling Technology	2317s	WB (1/1000)
Scrib (C-6)	Santa Cruz Biotechnology	sc-55543	WB (1/1000), IF (1/100)
SRC (L4A1)	Cell Signalling Technology	#2110	WB (1/1000)
TBX2 (62-2)	Coling Goding	In house	WB (1/1000)
TBX3 (A-20)	Santa Cruz Biotechnology	sc-17871	WB (1/1000)
TSG101	Cell Signalling Technology	sc-7964	WB (1/1000)
YAP1	Santa Cruz Biotechnology	sc-15407	WB(1/1000), IF (1/100)
ZO-1	Invitrogen	339100	IF (1/100)
ZsGreen	Clontech	632474	WB (1/1000), IF (1/100)
Secondary Antibodies			
Alexa fluor® goat anti-mouse 488 nm	Invitrogen, Life Technologies	A-11001	IF (1/500)
Alexa fluor® goat anti-mouse 568 nm	Invitrogen, Life Technologies	A-21422	IF (1/500)
Alexa fluor® goat anti-mouse 594 nm	Invitrogen, Life Technologies	A-11005	IF (1/500)
Alexa fluor® goat anti-rabbit 488 nm	Invitrogen, Life Technologies	A-11008	IF (1/500)
Alexa fluor® goat anti-rabbit 594 nm	Invitrogen, Life Technologies	A-11012	IF (1/500)
Alexa fluor® goat anti-rabbit 633 nm	Invitrogen, Life Technologies	A-31576	IF (1/500)
HRP conjugated anti-Mouse	Jackson ImmunoResearch	315-035-048	WB (1/5000)
HRP conjugated anti-Rabbit	Jackson ImmunoResearch	711-035-152	WB (1/5000)

Table 2.4. Antibodies Used During This Project. Table indicates the technique the antibody was used for and the dilution of the antibody used for each technique. WB: western blot, IP: immunoprecipitation, IF: immunofluorescence, FC: flow cytometry.

Primer Name	Sequence	Construct
Cloning Primers		

`

RASSF1A_F	AATAATAAGCTTCGATGTCGGGGGAGCCTGAGC TC	pDsRed-Express2-C1 and pZsGreen-C1
RASSF1A_R	AATAATGGATCCTCACCCAAGGGGGCAGGCGTG C	pDsRed-Express2-C1 and pZsGreen-C1
RASSF1C_F	AATAATAAGCTTCGATGGGCGAGGCGGAGGCGC CTTC	pDsRed-Express2-C1 and pZsGreen-C1
RASSF1C_R	AATAATGGATCCTCACCCAAGGGGGCAGGCGTG C	pDsRed-Express2-C1 and pZsGreen-C1
ZsGreen-RASSF1A_F	AATAATGAATTCATGTCGGGGGAGCCTGAGCTC	pQCXIP (Clontech)
ZsGreen-RASSF1A_R	AATAATGAATTCGGATCCTCACCCAAGGGGGCA GGCGTGC	pQCXIP (Clontech)
ZsGreen-RASSF1C_F	AATAATGAATTCATGTCGGGGGAGCCTGAGCTC	pQCXIP (Clontech)
ZsGreen-RASSF1C_R	AATAATGAATTCGGATCCTCACCCAAGGGGGCA GGCGTGC	pQCXIP (Clontech)
ZsGreen_F	AATAATGAATTCATGGCCCAGTCCAAGCACGGCC TG	pQCXIP (Clontech)
ZsGreen_R	AATAATGAATTCGGATCCTGAGTCCGGAGGGCA AGGCGGAG	pQCXIP (Clontech)
Site-Directed Mutagenesis		
E-cadherin (Y3F) Y753F, Y754F, Y755F Forward	GCCTCCTTCTTCATCAAAGAAAAAAACG TTGTCCCGGGTGTCATC	pcDNA3-E-cadherin-GFP (Anderson *et al.* 2009)
E-cadherin (Y3F) Y753F, Y754F, Y755F Reverse	GATGACACCCGGGACAACGTTTTTTTCT TTGATGAAGAAGGAGGC	pcDNA3-E-cadherin-GFP (Anderson *et al.* 2009)
RT-PCR primers		
Target Gene	**Forward Primer**	**Reverse Primer**
18S	AGTCCCTGCCCTTTGTACACA	GATCCGAGGGCCTCACTAAAC
BCL2L1	ACTCTTCCGGGATGGGGTAA	ACAAAAGTATCCCAGCCGCC
BIRC5	TGACGACCCCATAGAGGAACA	CGCACTTTCTCCGCAGTTTC
CLAUDIN1	TTTACTCCTATGCCGGCGAC	TTGCTTGCAATGTGCTGCTC
C-MYC	CCTACCCTCTCAACGACAGC	CTTGTTCCTCCTCAGAGTCGC
CTGF	CACCCGGGTTACCAATGACA	GGATGCACTTTTTGCCCTTCTTA
DESMOPLAKIN	GAGGAGAGGACGAAGCGAAG	TAGATGCCTCTAAAGCCTGC
E-CADHERIN	GGTGCTCTTCCAGGAACCTC	GAAACTCTCTCGGTCCAGCC
FIBRONECTIN	ATACCATCATCCCAGAGGTGC	TGGTGGAAGAGTTTAGCGGG
INTEGRIN 5α	AGCAAGAGCCGGATAGAGGA	CTGCTCCCCAAACACTTCCA
NANOG	GGTGTGACGCAGAAGGCCTCA	CCCAGTCGGGTTCACCAGGCA
OCCLUDIN	GAATTGGTCACCGAGGGAGG	AACCAATCTGCTGCGTCCTA
OCT4	GGCTCGAGAAGGATGTGGTCCG	GGGCTCCCATAGCCTGGGGT
RASSF1A	AGTGCGCGCATTGCAAGTT	AAAGGTCAGGTGTCTCCCAC
RASSF1C	CTGCAGCCAAGAGGACTCGG	GGGTGGCTTCTTGCTGGAGGG
SNAIL 1	CCAGTGCCTCGACCACTATG	CTGCTGGAAGGTAAACTCTGG
SNAIL 2	TCGGACCCACACATTACCTTG	AAAAAGGCTTCTCCCCCGT
SOX2	GGGGGAAAGTAGTTTGCTGCCTCT	TGCCGCCGCCGATGATTGTT
VIMENTIN	GGCTCGTCACCTTCGTGAAT	GAGAAATCCTGCTCTCCTCGC
ZEB 1	GATGACCTGCCAACAGACCA	GCCCTTCCTTTCCTGTGTCA

Table 2.5. Primers Used For Cloning, Site-Directed Mutagenesis and RT-PCR. Table shows the name of primer, the primer sequence and the construct generated using the primer.

`

Buffer Name	Contents	For 1 l
4 X DNA Loading Buffer	50 % (v/v) Glycerol 1 X TAE Orange G	500 ml Glycerol 500 ml 1 x TAE Orange G to colour.
2 % Flow cytometry Blocking Buffer	2 % (w/v) Bovine Serum Albumin 1 X PBS	20 g BSA 1 l PBS
4 x SDS-PAGE Sample Buffer	40 % (v/v) Glycerol 250 mM Tris-HCl pH 6.8 8 % SDS 11.56 mM Bromophenol Blue 8 % (v/v) 2-mercaptoethanol	400 ml Glycerol 250 ml Tris-HCl pH 6.8 80 g SDS 2.5 g Bromophenol Blue 80 ml 2-mercaptoethanol
5 % skimmed Milk blocking Solution	5 % (w/v) skimmed milk powder in 1 x PBS-T	50 g skimmed milk powder 1 l PBS-T
Immunoprecipitation lysis buffer	150 mM NaCl 0.5 % (v/v) NP40 20 mM Hepes pH7.5	30 ml of 5 M NaCl 50 ml of 10 % (v/v) NP40 50 ml of 1 M Hepes pH7.5
Laemmli Lysis Buffer	50 mM Tris-HCl pH 6.8 2 % (w/v) SDS 1 x Protease inhibitor cocktail	20 ml Tris-HCl pH 6.8 20 g SDS
LB Broth	2 % (w/v) LB broth	20 g LB broth
PBS (Phosphate-buffered Saline)	137 mM NaCl 2.7 mM KCl 10 mM Na_2HPO_4 1.76 mM KH_2PO_4 pH7.4	8.01 g NaCl 0.2 g KCl 1.78 g Na_2HPO_4 0.27 g KH_2PO_4
PBS-T (PBS Tween)	PBS as above 0.1 % (v/v) Tween 20	1 ml Tween per l of PBS
SDS-PAGE Running Buffer	25 mM Tris 190 mM Glycine 0.1 % (w/v) SDS	3.03 g Tris 14.4 g Glycine 1 g SDS
SDS-PAGE Sample Buffer	10 % (v/v) Glycerol 62.5 mM Tris-HCl pH 6.8 2 % (w/v) SDS 2.89 mM Bromophenol Blue 2 % (v/v) 2-mercaptoethanol	100 ml Glycerol 62.5 ml Tris-HCl pH 6.8 20 g SDS 0.625 g Bromophenol blue 20 ml 2-mercaptoethanol
TAE Buffer	40 mM Tris 18 mM Glacial acetic acid 1 mM EDTA pH 8.0	4.48 g Tris 1.14 ml Glacial acetic acid 2 ml 0.5 M EDTA pH 8
Western Blot Transfer Buffer	25 mM Tris 190 mM Glycine 20 % (v/v) Methanol	3.03 g Tris 14.4 g Glycine 200 ml Methanol

Table 2.6. Common Buffers Used During This Project. Unless stated, all solutions are diluted in water.

`

Chapter 3 RASSF1C-Dependent Activation of SFKs Promotes the Destabilisation of E-cadherin at Cell-Cell Junctions

3.1 Introduction

RASSF1A is a tumour suppressor that has been linked to the regulation of various cellular functions from genomic stability (Hamilton et al., 2009; Pefani et al., 2014) to control of migration (Donninger et al., 2007). RASSF1A phosphorylation at serine 131 by ATM leads to MST2 activation, stabilisation of a transcription factor complex that includes YAP1 and p73, and upregulation of the proapoptotic gene *PUMA* (Hamilton et al., 2009). RASSF1A has also been linked to the activation of p53 by the sequestration of MDM2 (Song et al., 2008b). The other ubiquitously expressed isoform of the *RASSF1* gene, *RASSF1C*, has been suggested to have certain tumour suppressor functions in ovarian, prostate and renal cancer cells (Kitagawa et al., 2006; Li et al., 2004; Vos et al., 2000; Vos et al., 2004), but recently reports have shown RASSF1C may function as an oncogene. It has been demonstrated that RASSF1C promotes breast and lung cancer proliferation (Amaar et al., 2005; Amaar et al., 2006a; Reeves et al., 2010) and accumulation of β-catenin, leading to increased transcriptional activity (Estrabaud et al., 2007). Previous work in the lab had shown that both RASSF1A and RASSF1C can interact with SRC.

3.1.1 SRC Family Kinases

The SRC Family Kinases are non-receptor tyrosine kinases. The first oncogene to be discovered was v-SRC, the viral counterpart of the cellular proto-oncogene c-SRC. The gene sequence and the signalling properties of SRC were identified in 1970s and in the 1990s the discovery of the 3D structure of c-SRC

`

allowed the true understanding of its biological functions (Kim et al., 2009; Xu et al., 1997). Of the nine members of the SRC family kinases, three are ubiquitously expressed (SRC, FYN and YES). The other six have a more-restricted expression (Thomas and Brugge, 1997).

SRC family kinases have a variety of biological functions, all of which are important in cancer progression: regulation of cell adhesion complex assembly and turnover, motility, proliferation and survival. Elevated expression and/or activity of SRC is associated with the development of tumours, particularly colon and breast (Cartwright et al., 1989; Verbeek et al., 1996) and correlates with advanced stage and metastatic potential of disease (Cartwright et al., 1990; Irby et al., 1999), similar to the epigenetic loss of RASSF1A (Fendri et al., 2009; Tommasi et al., 2011b). These factors make SRC an attractive target for therapy. In 2010 a number of SRC inhibitors were in phase I, II and III clinical trials (Aleshin and Finn, 2010; Kim et al., 2009).

The structure of SRC family kinases consists of six functional domains: an SH4 domain, containing an amino-terminal myristylation site; SH3 and SH2 domains; a SH1 kinase domain, with an autophosphorylation site at Y416; and a regulatory C-terminal, which contains an inhibitory phosphorylation site at Y527 (Sandilands and Frame, 2008). Phosphorylation of Y527 by C-terminal SRC kinase (CSK) causes a conformational change, leading to the SH2 domain to recognise and bind to the phosphorylated Y527 residue, producing a 'closed' state that prevents the phosphorylation of the Y416 site, rendering the kinase inactive (Xu et al., 1997). Dephosphorylation of Y527 by protein tyrosine phosphatase alpha (PTPα) reverses this process. Overexpression of PTPα or loss of the C-terminal regulatory region has been associated with cell transformation and tumourigenesis (Zheng et al., 1992).

In addition to the structural regulation, SRC family kinases are also spatially regulated within cells. Two pools of v-SRC have been identified in the cell: an inactive perinuclear pool and an active plasma membrane associated pool (Courtneidge et al., 1980; Rohrschneider, 1979; Welham and Wyke, 1988). c-SRC activity was found to be regulated in the same way. The majority of wildtype c-SRC was

`

associated with the microtubule organising centre (MTOC) in the perinuclear region and co-localized with endosomal markers (Kaplan et al., 1992). Active c-SRC was found at the cell periphery, associated with focal adhesions (Kaplan et al., 1994). Rho-GTPases, endosomal trafficking and actin polymerisation regulate the translocation of SRC from the perinuclear region to the plasma membrane (Gasman et al., 2003b; Kaplan et al., 1992; Sandilands et al., 2007; Sandilands et al., 2004; Sandilands and Frame, 2008; Timpson et al., 2001).

3.1.2 The Role of SRC in Migration and Invasion

Active SRC plays a critical role in the control of cell adhesion, invasion and metastasis by regulating both focal adhesions (Ren et al., 2000) and adherens junctions (Daniel and Reynolds, 1997). Focal adhesions attach the cell to the extracellular matrix via integrins. They are associated with the actin cytoskeleton and are regulated by the focal adhesion kinase (FAK) (Kornberg et al., 1992). SRC has been linked to the disruption of focal adhesions by suppressing integrin attachment to the extracellular matrix (Datta et al., 2002; Sakai et al., 2001); interruption of RhoA function, that has a role in actin filament assembly (Arthur and Burridge, 2001); and the activation of FAK via its phosphorylation (Schaller et al., 1992; Schaller et al., 1994). The promotion of a migratory phenotype by active SRC is dependent on the loss of adherens junctions and requires FAK phosphorylation at β_1 integrin-dependent protrusions (Avizienyte et al., 2002). Through the regulation of the actin cytoskeleton, FAK-dependent SRC signalling results in a change of the cell adhesion type from cadherin-based to integrin-based, promoting a more motile phenotype. The loss of focal adhesions has been shown to be important for cell motility (Brunton et al., 2004).

At the leading edge of a migrating cell SRC activates Rac1. This is done through the recruitment of Rac-GEFs: Pak-interacting exchange factor-beta (ten Klooster et al., 2006), Dock180 (Brugnera et al., 2002; Kiyokawa et al., 1998), and Vav2 (Marcoux and Vuori, 2003; Marignani and Carpenter, 2001). Rac1 activity induces membrane protrusions through the rearrangement of actin (Machesky and Hall,

`

1997; Ridley et al., 1992). RhoA-ROCK activity promotes actomyosin contractility at the back of a migrating cell. This function is suppressed at the front of the cell by mutual inhibition by Rac1 which upregulates the Rho-GAP p190RhoGAP. However, the RhoA effector protein mDia1 is active at the leading edge of the cell, responsible for the production of long straight Actin fibres, which are required for membrane protrusions (Huveneers and Danen, 2009). Therefore the directionality of movement depends on the differential activation of Rac and Rho.

An important factor in the development of distant metastatic sites is the invasion of cells through matrix barriers, including basement membranes and tissue compartments, vessels, perineural spaces and organ boundaries (Guarino, 2010). There are two types of invasion. The Rac-mediated mesenchymal-type combines migration and pericellular ECM breakdown. This is mediated by matrix-degrading proteases at the leading edge, creating a path through which the cell can move. The second one is the amoeboid-type, where rounded cells move through the matrix by a Rho-ROCK-mediated actomyosin-dependent mechanism (Carragher et al., 2006; Price et al., 2004). SRC is thought to regulate mesenchymal invasion, by activating Rac (Hsia et al., 2003; Van Slambrouck et al., 2009). Interestingly, SRC phosphorylation of Caspase 8 switches its function from pro-apoptotic to pro-migratory. This dual function protects cells from apoptosis. By inhibiting Caspase 8 activation it enables Caspase 8 to interact with PI3K and stimulate the subsequent activation of Rac1, ERK and Calpain (Frisch, 2008).

3.1.3 The Adherens Junctions and E-cadherin

Signalling by the tyrosine kinase SRC plays a major role in the expression, function and trafficking of the junctional component E-cadherin. SRC phosphorylates the E-cadherin-catenin complex leading to the disruption of cell-cell adhesion (Daniel and Reynolds, 1997). The tyrosine phosphorylation of E-cadherin leads to the recruitment of the c-Cbl-like E3ubiquitin ligase Hakai, which binds to tyrosine residues in the juxtamembrane tail domain of E-cadherin. Hakai then ubiquitinates E-cadherin and

`

induces its endocytosis and degradation, a process linked to facilitation of cell motility (Fujita et al., 2002).

A defining feature of all epithelial sheets is the presence of apical adherens junctions (Fristrom, 1988). The adherens junction functions to connect the actin cytoskeleton of neighbouring cells (Hartsock and Nelson, 2008). The adherens junctions, together with the tight junctions, desmosomes, hemidesmosomes and gap junctions, form the epithelial cell-cell contacts that maintain normal tissue architecture. The adherens junction involves interactions between transmembrane glycoproteins, such as epithelial cadherin (E-cadherin) and the catenin family members – α-catenin, β-catenin and p120-catenin which control their formation, maintenance and function (Ozawa et al., 1989; Reynolds et al., 1994). E-cadherin is characterised by long ectodomain, comprising five extracellular cadherin repeats, that form Ca^{2+}-dependent, homophilic interactions between neighbouring cells (Gumbiner et al., 1988; Takeichi, 1977). The cytoplasmic domain associates with a variety of intracellular proteins linking the cell adhesion domain to the actin-myosin network, vesicle transport and cell polarity. One of these intracellular linking proteins is the Armadillo repeat protein β-catenin, which links to the actin cytoskeleton via an interaction with α-catenin. The interaction between β-catenin and α-catenin allows E-cadherin to interact and change the actin filament organisation in order to stabilise the intercellular junctions (Baum and Perrimon, 2001; Perez-Moreno et al., 2003). The Rho family GTPases (Rac1, RhoA and Cdc42), along with their accessory proteins are involved in the control and the stability of E-cadherin attachment to actin (Adams et al., 1998; Braga et al., 1997). In addition, changes in cell-cell contacts can lead to signals being generated at the site of cell-cell junctions and transduced, via the cytoplasmic domain of E-cadherin, to the nucleus, in order to affect gene expression and control cell proliferation, preventing tumourigenesis (Okada et al., 2007).

The adherens junctions are continually formed and disassembled, making them highly dynamic (Cavey et al., 2008; de Beco et al., 2009; Fujita et al., 2002; Pilot et al., 2006). The fast turnover of E-

`

cadherin allows rapid transitions between epithelial and mesenchymal states (Baum et al., 2008). The internalisation and recycling of E-cadherin has been shown to be dependent on endocytosis regulated by clathrin (Le et al., 1999), dynamin and actin (Georgiou et al., 2008; Leibfried et al., 2008). Also, the loss of the GTPases Rab5 and the ADP-ribosylation factor (ARF) 6 has been shown to inhibit the endocytosis of E-cadherin (Kamei et al., 1999; Palacios et al., 2002; Paterson et al., 2003). The dynamics of E-cadherin internalisation and recycling are also important in the epithelial-to-mesenchymal transition (EMT) during development (Miller and McClay, 1997), or through the transcription factor Snail, in metastasis (Cano et al., 2000). E-cadherin plays an important role in cancer. During their progression towards metastasis, epithelial tumours lose E-cadherin (Strumane et al., 2004) either through loss of heterozygosity (Cleton-Jansen et al., 2001), DNA methylation (Yoshiura et al., 1995) or tyrosine kinase phosphorylation.

3.1.4 Aims

Both RASSF1A and RASSF1C have previously been linked to cell migration. Previous report has shown that RASSF1A could inhibit cell migration by inhibiting PI3K and preventing the activation of Rac1 (Dallol et al., 2005). RASSF1C has been linked to the upregulation of the chemokine receptor CXCR4 via the Ras-Raf-MEK-MAP kinase pathway. In RASSF1C-expressing breast cancer cells, the increase in CXCR4 has been shown to lead to more efficient migration towards a CXCL12 (CXRC4 ligand) gradient (Reeves et al., 2010). It has been demonstrated in previous studies that active SRC translocates to the plasma membrane where it leads to phosphorylation of the E-cadherin-catenin complex and sequential loss of adherens junctions and degradation of E-cadherin. The destruction of the junctions is important in cell motility and EMT. Previous work from the lab has shown an association between the RASSF1 isoforms and SRC (Scrace and University of Oxford). In this chapter we study the oncogenic role of RASSF1C in the activation of SRC and its regulation and disruption of adherens junctions, potentially leading to more invasive and aggressive tumours.

`

3.2 Both RASSF1A and RASSF1C Bind to SRC

A mass spectrometry screen was previously carried out in the lab in order to identify novel binding partners of RASSF1A and RASSF1C. One of the hits from the screen was SRC (Vlahov et al., 2015). In order to validate this, we transiently transfected 293T, RASSF1A null, cells with MYC –tagged SRC and either HA-RASSF1A or HA-RASSF1C. Since SRC can be activated by a variety of growth factors, including EGF and HGF, cells were cultured in 0.1 % FBS containing medium overnight to remove the exogenous stimuli of SRC, before proteins were immunoprecipitated with an anti-HA tag antibody. Samples were then analysed by SDS-PAGE gel and western blot for MYC-SRC and HA-tag (RASSF1A, or RASSF1C). We found that both RASSF1 isoforms bind to SRC, but that RASSF1A has a greater affinity towards SRC (Figure 3.1A*). Previous work from the lab has also shown that RASSF1A and RASSF1C bind to the other members of the SFK: FYN and YES (Vlahov et al., 2015). Also, only RASSF1A was able to bind to the inhibitory SRC kinase CSK (Figure 8.1). This interaction suggests that RASSF1A could act as an inactivator of SRC, in keeping with its role as a tumour suppressor.

In order to further investigate the interaction of endogenous SRC with the RASSF1 isoforms we performed a Proximity Ligation Assay (PLA). This technique allows the detection of two proteins, which are in close proximity (40 nm) to be identified. Here, two antibodies conjugated with a short DNA strand bind to the primary antibodies. When the two proteins are in close proximity, the DNA strands interact, forming oligonucleotides, which are amplified using polymerase, increasing the signal by 700 fold (Soderberg et al., 2006). H1299 cells, not expressing RASSF1A, were transiently transfected with ZsGreen control, ZsGreen-RASSF1A or ZsGreen-RASSF1C plasmids. Cells were cultured in 0.1 % FBS containing medium overnight, before they were fixed and incubated with anti-ZsGreen or anti-SRC antibodies (Figure 3.1B). We observed that both RASSF1 isoforms trigger the PLA reaction with SRC, meaning that the proteins are in close proximity. The generated data validates the hit from the mass spectrometry, showing that RASSF1A and RASSF1C can interact with SRC. Therefore, we sought to further investigate the functionality of this interaction.

* This experiment was carried out by Simon Scrace, a DPhil student in the laboratory.

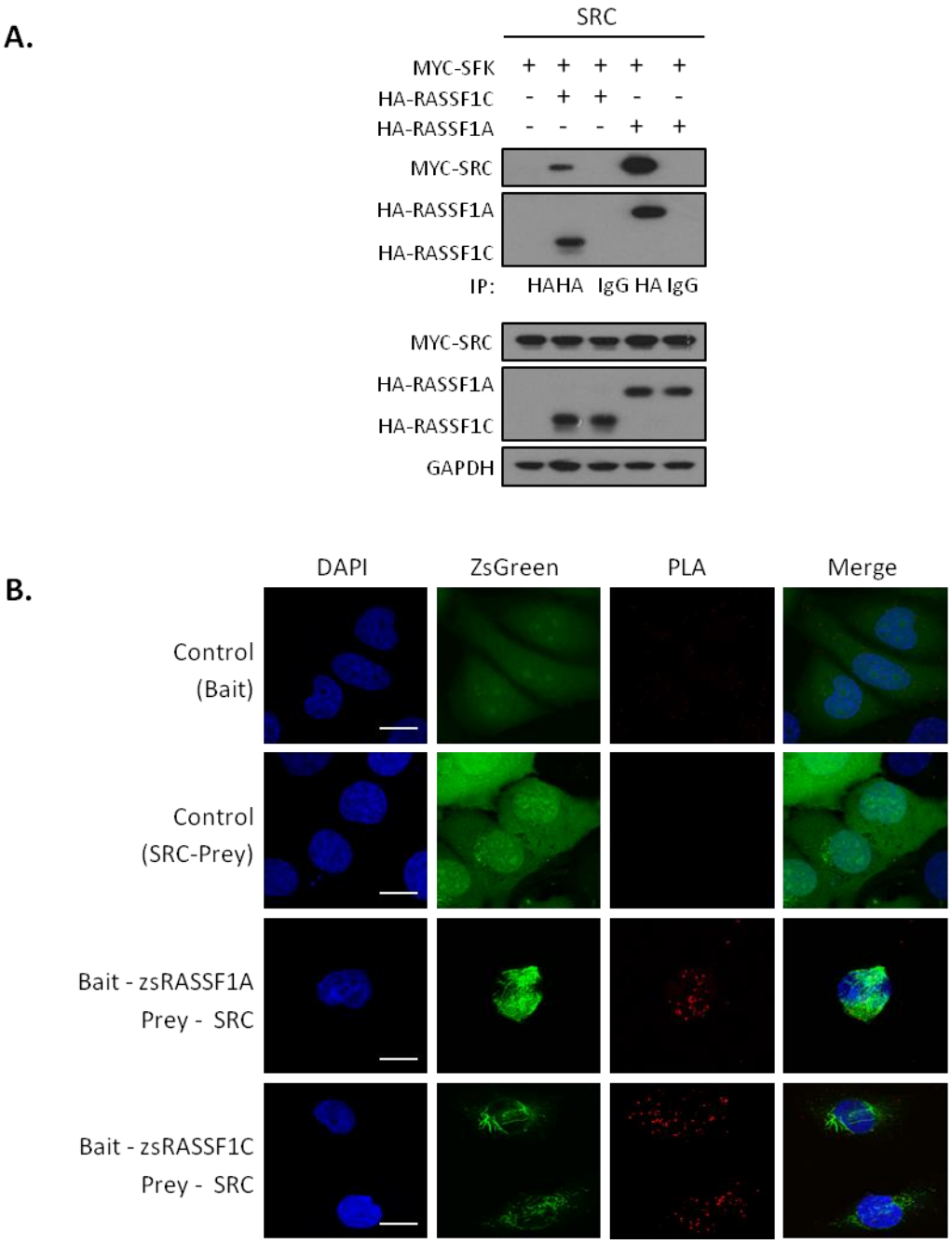


Figure 3.1. RASSF1A and RASSF1C Bind to SRC. A. 293T cells (1 x 10^6cells/plate) were transfected with MYC-SRC and either HA-RASSF1A or HA-RASSF1C. Cells were lysed by scraping into 0.5 % NP40, 150 mM NaCl lysis buffer supplemented with protease and phosphatase inhibitors. Cells were immunoprecipitated for 4 hrs with anti-MYC or anti-HA antibodies. Protein was recovered from the beads by boiling into 1 x loading buffer for 5 mins. Samples were analysed by SDS-PAGE and western blot for MYC and HA. SRC binds to both RASSF1A and RASSF1C, but binds more strongly to RASSF1A. **B**. H1299 cells (1 x 10^4 cells/well) were plated on 16-well chamber slide (Thermo Scientific) and transfected with either ZsGreen-empty vector, ZsGreen-RASSF1A or ZsGreen-RASSF1C. Wells were and treated with the Duolink PLA assay kit as per instructions, before overnight incubation with anti-ZsGreen (bait) and anti-SRC (prey) primary antibodies and the provided probes-conjugated secondary antibodies for 1 hr, followed by hybridisation for 30 minutes in a humidified chamber, ligation reactions for 30 minutes and amplification for 100 minutes. DAPI was used for cell nucleus detection. The PLA reaction occurs only if two proteins are in close proximity (40nm). Scale bars represent 20 μm. Both RASSF1A and RASSF1C bind to SRC.

`

3.3 RASSF1C Expression Leads to the Activation of SRC

RASSF1C has been shown to drive proliferation and migration in breast and lung cancer cells (Amaar et al., 2006a; Reeves et al., 2010), two biological functions also associated with SRC activity (Masaki et al., 2003; Sanchez-Bailon et al., 2012). In addition, we have observed that RASSF1A binds to the inhibitor of SRC, CSK (Figure 8.1). Once we had confirmed that both isoforms of RASSF1 were able to bind to SRC, and that only RASSF1A bound CSK, we wanted to further investigate the role that RASSF1A and RASSF1C play in the activation or deactivation of SRC by looking at the phosphorylation of the tyrosine sites Y416 and Y527, respectively (Cartwright et al., 1987; Xu et al., 1997). In order to do that we carried out a PLA assay in H1299 cells, transiently transfected with ZsGreen control, ZsGreen-RASSF1A or ZsGreen-RASSF1C plasmids. Cells were cultured in 0.1 % FBS containing medium overnight, before they were fixed and probed with anti-ZsGreen or antibodies against phospho-SRC Y416 or phospho-SRC Y527 (Figure 3.2A). The PLA showed that while both isoforms are in close proximity to SRC, however, RASSF1C associated with the active SRC pY416, whereas RASSF1A associated with the inactive, CSK phosphorylated, SRC pY527. Quantification of the interactions was shown to be highly significant (Figure 3.2B). This led us to believe that RASSF1C leads to the phosphorylation of SRC at Y416, but RASSF1A, in an opposing manner, would phosphorylate the inhibitory Y527 site. Further experiments confirmed that this was indeed the case. Expression of RASSF1C led to increase in the SRC pY416 (Figure 8.2 A), whereas RASSF1A was able to increase the levels of SRC pY527 (Figure 8.2 B).

Interestingly, RASSF1C expression can activate SRC only when RASSF1A is absent from the cells. Transiently transfected FLAG-RASSF1C into RASSF1A-expressing (U2OS, SW480, and HeLa), or RASSF1A null (MCF7 and MDA-MB-231) cells was only able to phosphorylate SRC pY416 in the RASSF1A null cell lines (Figure 8.3). Taken together these results indicate a new role for RASSF1A and RASSF1C, regulating SRC. RASSF1C expression leads to active SRC, whereas RASSF1A phosphorylates SRC at Y527, keeping it ‘closed’ and inactive. These results suggest a novel mechanism for SRC

`

activation in cancers where the tumour suppressor RASSF1A is lost due to hypermethylation. Given the role of SRC in cancer and that the promoter of RASSF1C remains unmethylated in cancers, we decided to concentrate on the effects that this isoform had in SRC regulation.

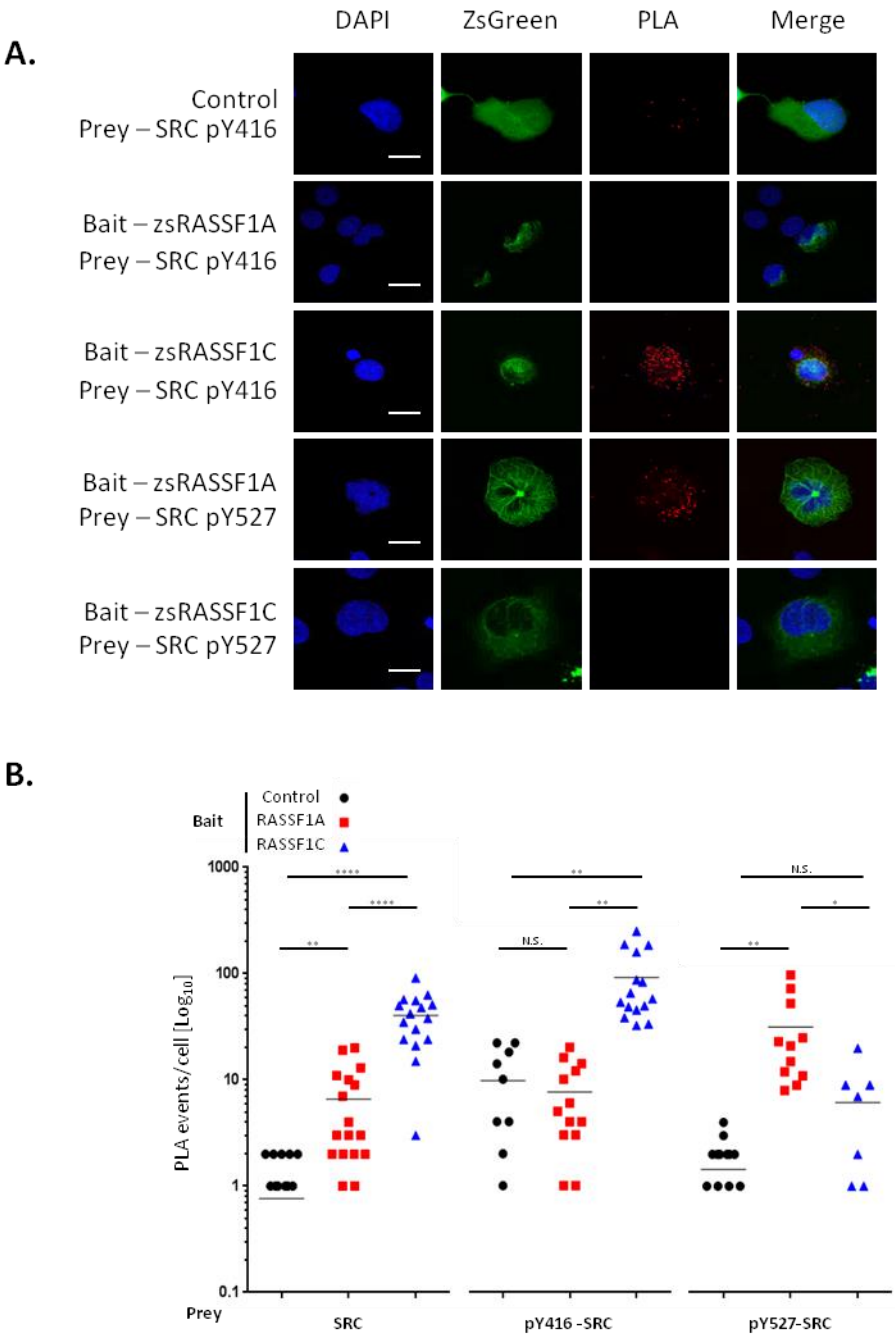


Figure 3.2. RASSF1C, but not RASSF1A, Associates with Active SRC. A. H1299 cells (1 x 10^4 cells/well) were plated on 16-well chamber slide (Thermo Scientific) and transfected with either ZsGreen-empty vector, ZsGreen-RASSF1A or ZsGreen-RASSF1C. Cells were then treated with the Duolink PLA assay kit as per instructions, before overnight incubation with primary anti-ZsGreen (bait) and anti-SRC pY416 (active SRC) or anti-SRC pY527 (inactive SRC) (prey) primary antibodies and the provided probes-conjugated secondary antibodies for 1 h, followed by hybridisation for 30 minutes in a humidified chamber, ligation reactions for 30 minutes and amplification for 100 minutes. DAPI was used for cell nucleus detection. Scale bars represent 20 µm.RASSF1C colocalises with SRC pY416,SRC activation, whereas RASSF1A colocalised with SRC pY527, Inactive SRC. **B**. Quantification of the events per cell for the Duolink PLA assay experiment. For each cell 5 Z-stack images were taken and analysed with BlobFinder V3.2. The average values, SEM and significance were calculated using Prism 6.0 (Graphpad) software. N.S $p > 0.05$, * $p \leq 0.05$, ** $p \leq 0.01$, *** $p \leq 0.001$, **** $p \leq 0.0001$.

`

3.4 SRC is Localised at the Plasma Membrane in RASSF1C-Expressing Cells

Having shown that RASSF1C associated with active SRC, we wanted to investigate the physiological role this active SRC plays. Active SRC controls cell adhesion, invasion and metastasis by regulating both focal adhesions (Ren et al., 2000) and adherens junctions (Daniel and Reynolds, 1997). Therefore, we decided to test whether SRC, accumulated at the plasma membrane, is able to translocate and phosphorylate the junctions in cells expressing RASSF1C. H1299 cells were seeded onto glass cover slips before being transiently transfected with eGFP-SRC and either DsRed control or DsRed-RASSF1C. Cells were kept in 0.1 % FBS for 18 hrs before cells were collected, fixed and probed with anti-phosphotyrosine 416 antibody in order to investigate if SRC remains active at the plasma membrane. We were able to visualise total SRC and SRC pY416 at the plasma membrane in control cells (Figure 3.3A), however, the amount of active SRC increased when RASSF1C was exogenously expressed (Figure 3.3B, C). The total levels of SRC and pY416 in the cytoplasm remained unchanged for both the control and the RASSF1C-expressing cells (Figure 3.3D).

These results confirm our hypothesis that RASSF1C plays a role in the activation of SRC and that this leads to translocation of SRC to the plasma membrane. Therefore we wanted to investigate whether SRC was also affecting cell adhesion.

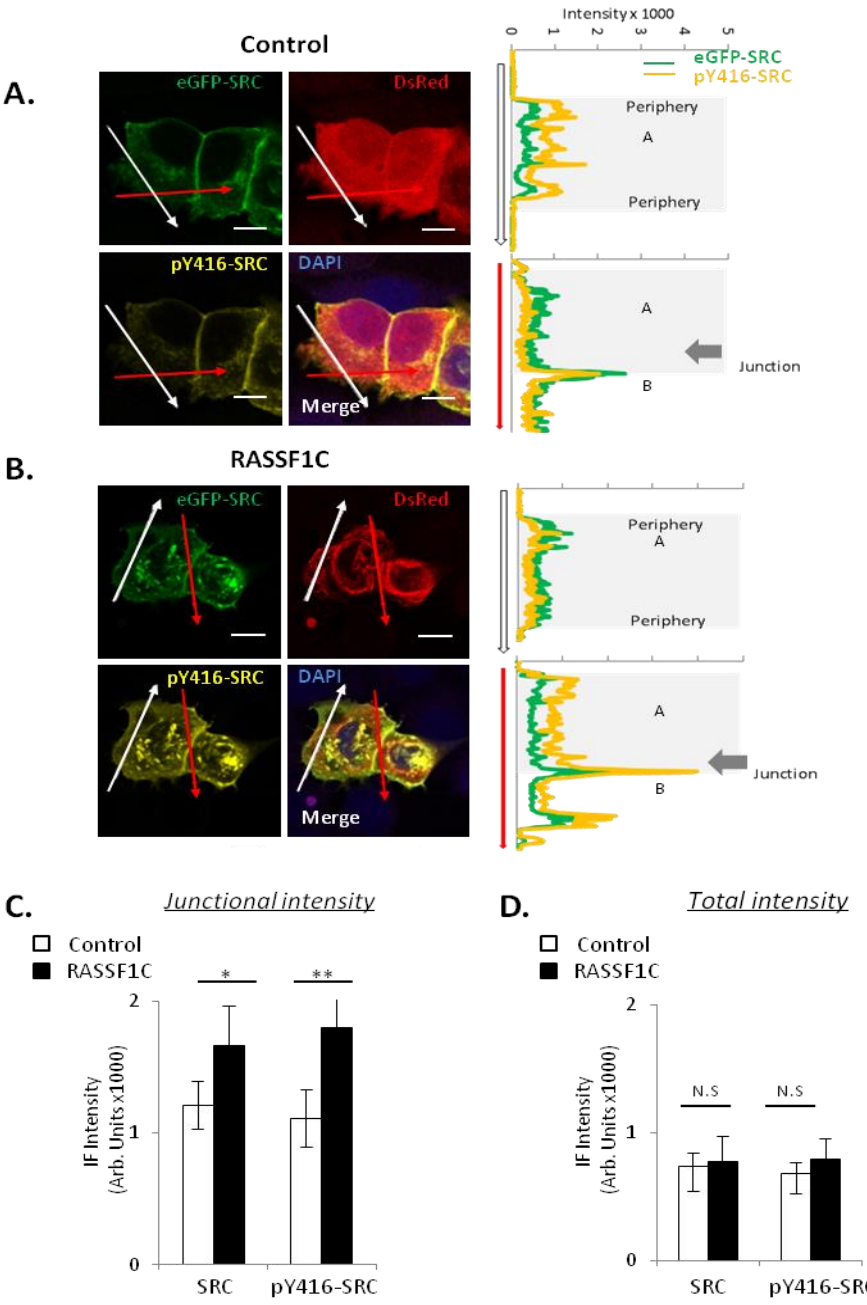


Figure 3.3. RASSF1C Expression Promotes SRC Localisation to the Plasma Membrane. H1299 cells (3 x 10^5 cells/condition) were plated onto glass cover slips and transfected with eGFP-SRC and (**A**) DsRed-empty vector or (**B**) DsRed-RASSF1C. Cells were fixed for 15 mins with 4 % PFA, permeabilised for 5 mins with 0.2 % Triton X solution and blocked for 30 mins with 0.2 % Fish Skin Gelatin (FSG). Cells were probed with anti-SRC pY416 and Alexa-fluor 633 nm. Cover slips were mounted onto slides using mounting media containing DAPI. Images were taken using a Zeiss LSM 780 microscope at 63 x magnification. Scale bars represent 10 µm. Intensity was measured using Zeiss Zen 2011 software. Histograms represent the measurements acquired using the arrows – white arrow represent a section across a part of the cell that does not include the junction, and red arrow represents a section that passes across the junction. **C**. Graph representing the measured intensity of SRC and SRC pY416 at the junctions. * $p < 0.05$, ** $p < 0.01$.. **D**. Graph representing the measured intensity of SRC and SRC pY416 throughout the entire cell. N.S. $p > 0.05$. Data is representative of three independent experiments. In cells expressing RASSF1C there is a significantly higher association of both SRC and SRC pY416 with the site of cell-cell junctions.

`

3.5 RASSF1C Expression Leads to the Internalisation of E-cadherin and Loss of Adherens Junctions

It has been shown that SRC binds and phosphorylates the E-cadherin, β-catenin, p120-catenin complex (Behrens et al., 1993). The phosphorylation of E-cadherin leads to HAKAI-dependent ubiquitination and degradation (Fujita et al., 2002). This phosphorylation has been shown to be modulated by SRC-binding scaffold proteins, such as RACK1 (Swaminathan and Cartwright, 2012). Since RASSF1C is a scaffold protein that can bind directly to SRC (Figure 3.1), we wanted to further investigate whether the expression of RASSF1C could be involved in the phosphorylation and targeted degradation of E-cadherin. These experiments were done in MCF7 cells, because they are methylated for RASSF1A, but maintain an E-cadherin expression, thus allowing the verification of potential regulatory effect of RASSF1C, independently of RASSF1A. Previous work in the lab has shown that RASSF1C expression leads to increased phosphorylation of E-cadherin and β-catenin, but not p120-catnein or FAK (Figure 8.4). Interestingly, the phosphorylation of E-cadherin and β-catenin was reduced in cells where RASSF1A was expressed alone or in combination with RASSF1C (Data not shown).

The activation of SRC promotes the internalisation of E-cadherin into the cytoplasm, depleting it from the sites of cell-cell contact. Therefore, we wanted to examine whether expression of RASSF1C, which binds to and activates SRC, leads to the internalisation of E-cadherin. MCF7 cells were seeded onto glass cover slips before being transiently transfected with either DsRed control or DsRed-RASSF1C plasmids. The cells were then probed with anti-E-cadherin antibody (Figure 3.4). In the presence of RASSF1C, endogenous E-cadherin is being depleted from the adherens junctions accumulating in the cytoplasm.

`

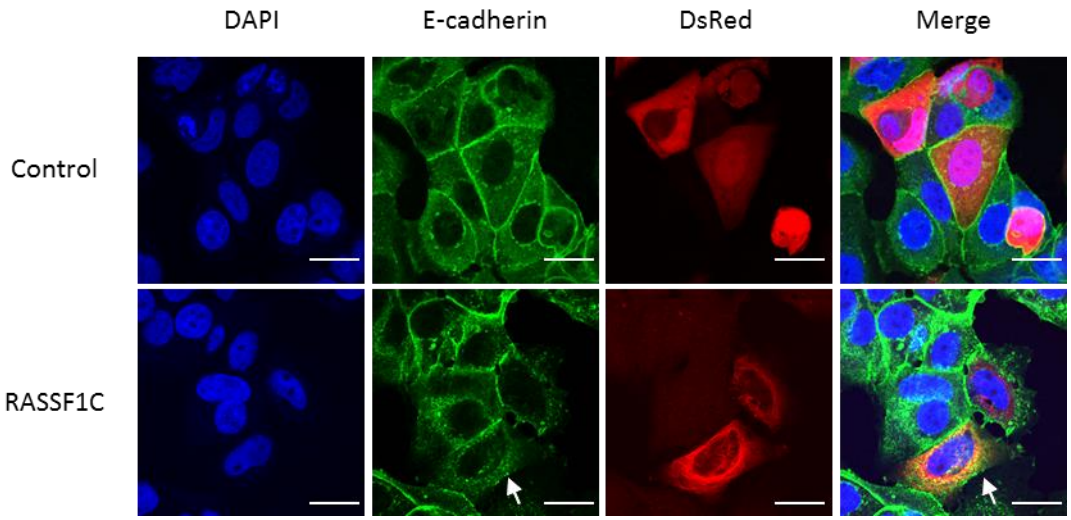


Figure 3.4. RASSF1C Leads to the Internalisation of Endogenous E-cadherin. MCF7 cells (3 x 10^5 cells/condition) were plated onto glass cover slips and transfected with DsRed-empty vector or DsRed-RASSF1C. Cells were fixed for 15 mins with 4 % PFA, permeabilised for 5 mins with 0.2 % Triton X solution and blocked for 30 mins with 0.2 % FSG. Cells were probed with the anti-E-cadherin antibody. Secondary antibody was Alexa-fluor 488 nm. Cover slips were mounted onto slides using mounting media containing DAPI. Images were taken using a Zeiss LSM 780 microscope at 63 x magnification. Scale bars represent 10 μm. Endogenous E-cadherin is internalised and aggregated in RASSF1C-expressing cells (arrows).

`

In order to further investigate the internalisation of E-cadherin, we used an E-cadherin-GFP construct (Miranda et al., 2001), which we transiently co-transfected into MCF7 cells, with DsRed control or DsRed-RASSF1C. The cells were grown on 35 mm glass bottom plates and imaged live using a confocal microscope. Again, we observed that when RASSF1C was expressed, E-cadherin-GFP was internalised and aggregated in the cytoplasm, compared to cells transfected with GFP-control (Figure 3.5A) or compared to control cells expressing E-cadherin-GFP (Figure 3.5B).

So far we have identified that RASSF1C is able to bind and activate SRC, and that in these cells E-cadherin is being internalized. Active SRC is known to phosphorylate two of three consecutive tyrosines (Y753 and 754) on E-cadherin and these sites are known to be recognition sites for HAKAI (Fujita et al., 2002). We therefore decided to generate a triple mutant where all three tyrosines (Y753, Y754 and Y755) are mutated to phenylalanines using site-directed mutagenesis (Figure 3.5D). This E-cadherin mutant (Y3F) cannot be phosphorylated by SRC and also fails to bind to HAKAI (Mukherjee et al., 2012). When transfected into MCF7 cells, E-cadherin Y3F was not internalised as much as the WT construct in cells expressing RASSF1C (Figure 3.5C). This suggests that RASSF1C plays an important role in the regulation of E-cadherin at the adherens junctions, and that RASSF1C expression promotes its internalisation.

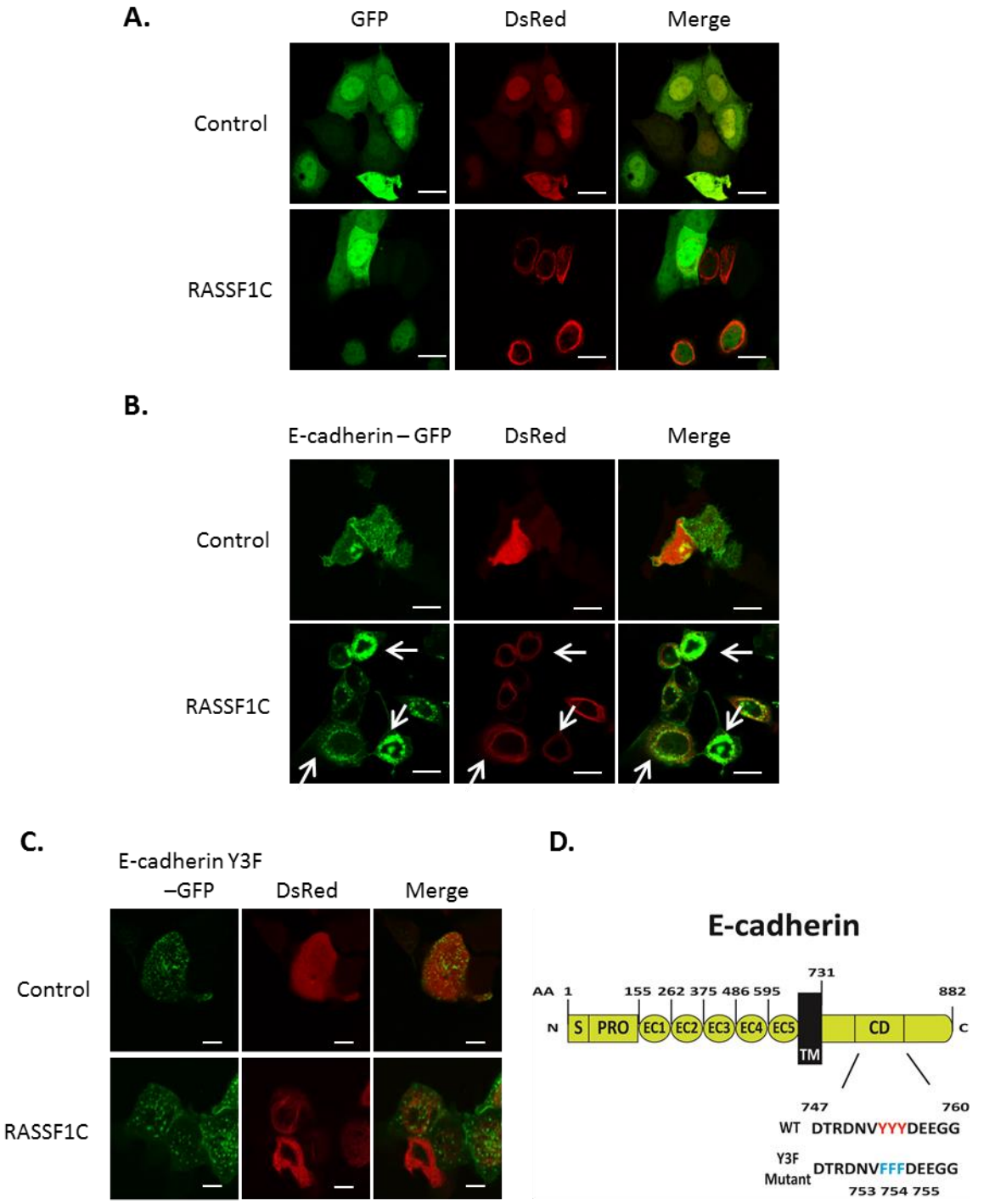


Figure 3.5. RASSF1C Leads to Internalisation of E-cadherin-GFP. MCF7 cells (2 x 10^5 cells/condition) were plated onto 35 mm glass bottom plate and transfected with either GFP-empty vector (**A.**), E-cadherin-GFP (**B.**) or E-cadherin Y3F (**C.**) and DsRed or DsRed-RASSF1C. Cells were imaged 24 hrs later with a Zeiss LSM 780 microscope at 63 x magnification, at 37 ^{o}C and 5 % CO_2. RASSF1C expression does not lead to accumulation of GFP-empty vector in the cytoplasm (**A.**). The expression of RASSF1C leads to internalisation and accumulation of E-cadherin-GFP inside the cells (arrows) (**B.**), but not of the mutated E-cadherin Y3F-GFP (**C.**). Data is representative of three independent experiments. Scale bars represent 20 μm. **D.** Graphical representation of the E-cadherin protein with the amino acids (AA) that were mutated. N, amino-terminal end; S, signal peptide; PRO, propeptide; EC, extracellular cadherin repeat; TM, transmembrane region; CD, cytoplasmic domain; C, carboxy-terminal end.

`

Having shown that RASSF1C expression drives the E-cadherin internalisation, we wished to investigate to what extent the expression of RASSF1C depletes E-cadherin from adherens junctions. In order to do this MCF7 cells were plated onto 35 mm glass bottom plates and were transiently transfected with DsRed control or DsRed-RASSF1C in combination with E-cadherin-GFP or E-cadherin Y3F – GFP. Cells were then imaged and the fluorescence intensity of E-cadherin at the sites of cell-cell junctions was measured. E-cadherin intensity was significantly decreased at cell-cell junctions, aggregating in the cytoplasm in cells expressing RASSF1C (Figure 3.6A and B). In cells transfected with the E-cadherin Y3F – GFP the junctional intensity remained unchanged between control and RASSF1C-expressing cells (Figure 3.6C and D), once again suggesting that RASSF1C drives a SRC-dependent internalisation of E-cadherin. Taken together, these data suggest that RASSF1C expression activates SRC, targeting it to the cell-cell junctions where it phosphorylates E-cadherin leading to its internalisation, which in turn leads to the loss of adherens junctions.

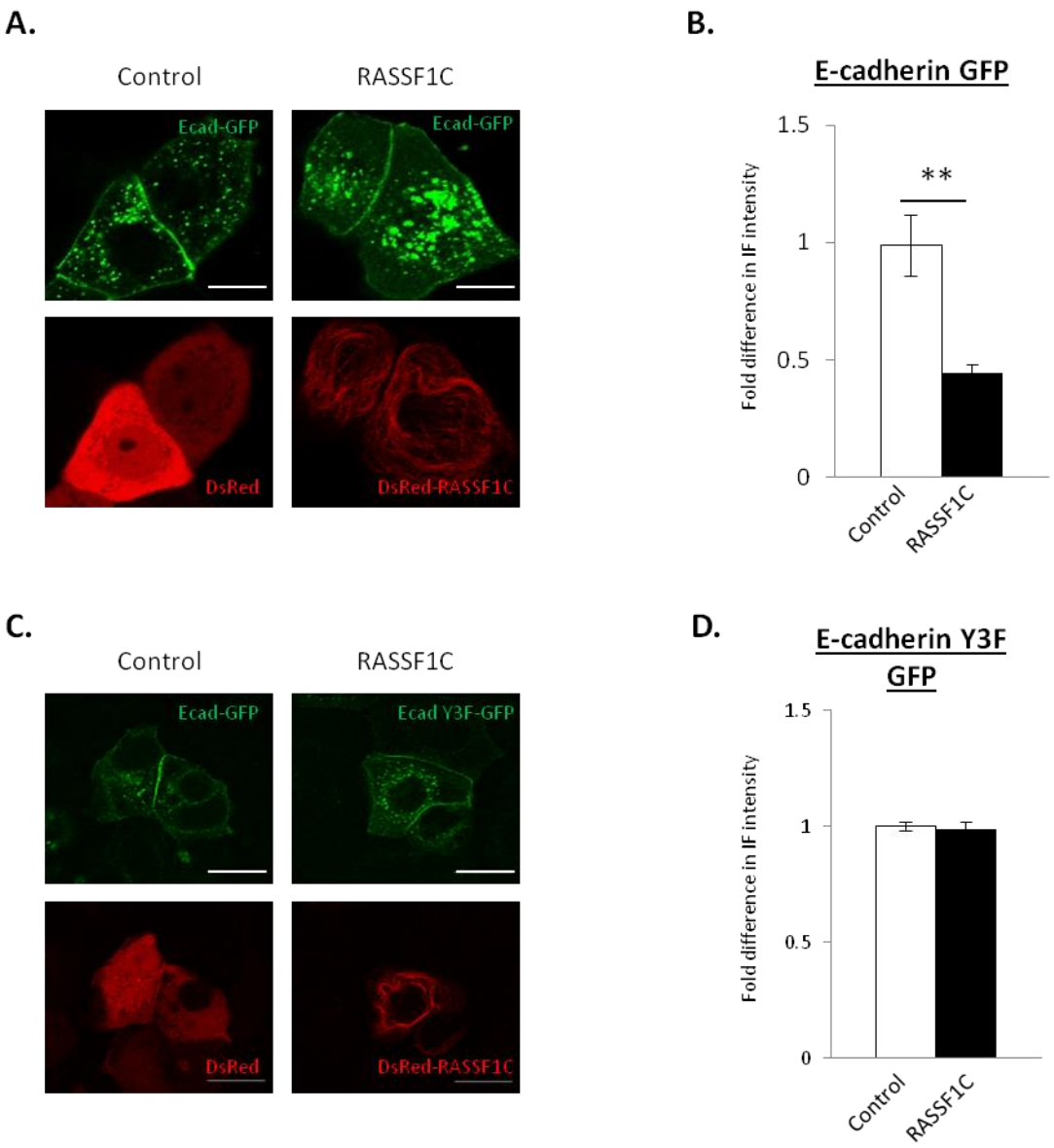


Figure 3.6. RASSF1C Expression Promotes SRC-Dependent Internalisation of E-cadherin and Destabilisation of Cell-Cell Junctions. MCF7 cells (2 x 10^5 cells/condition) were plated onto 35 mm glass bottom plate and transfected with E-cadherin-GFP, E-cadherin Y3F-GFP and DsRed-empty vector, or DsRed-RASSF1C. Cells were imaged 24 hrs post transfection with a Zeiss LSM 780 microscope at 63 x magnification, at 37 ^{o}C and 5 % CO_2. **A.** Representative images showing the adherens junctions that are established in Control and RASSF1C-expressing cells. RASSF1C leads to increased accumulation of E-cadherin-GFP inside the cells, and decreased GFP-E-cadherin at the cell-cell junctions. **B**. Cells were analysed and the intensity of the junctions quantified using Zeiss Zen 2011 programme. RASSF1C-expressing cells have significantly lower levels of E-cadherin at the sites of cell-cell junctions. ** $p < 0.01$. Error bars represent 1 x SEM. **C.** Representative images showing the adherens junctions that are established in Control and RASSF1C-expressing cells in the presence of E-cadherin Y3F. RASSF1C expression fails to increase the internalisation E-cadherin inside the cell and (**D**) the junctional intensity remains unchanged vs. the Control**.** All data is representative of three independent experiments, 10 images of cells with established cell-cell junctions were analysed per experiment.

`

3.6 RASSF1C Leads to Changes in the Trafficking Mechanisms of E-cadherin

Having shown that RASSF1C expression drives the loss of adherens junctions and the internalisation of E-cadherin, we next asked whether RASSF1C was involved in the trafficking of E-cadherin to the cytoplasm, when removed from the junctions. It has been known that E-cadherin is actively internalised and then recycled back to the plasma membrane in order to regulate junction formation in development, tissue remodelling and tumourigenesis (Le et al., 1999). We have previously shown that in RASSF1C-expressing cells, E-cadherin is accumulated at high levels in the cytoplasm. In order to further investigate whether RASSF1C is regulating E-cadherin recycling we imaged live MCF7 cells, plated onto 35 mm glass bottom plates and transiently transfected with E-cadherin-GFP and DsRed control or DsRed-RASSF1C. We observed that in control cells, the internalised E-cadherin was highly mobile within the cytoplasm, coming out from, or replenishing the adherens junctions (Figure 3.7A). When RASSF1C was present, we observed that the aggregated E-cadherin was static, or had limited mobility. Also, E-cadherin was observed to move away from the junctions (Figure 3.7A). In order to accurately measure these observations we used Imaris 8.0 analysis software. We tracked and measured the movements of the internalised E-cadherin in the control and RASSF1C cells. We measured the speed of the E-cadherin vesicles (Figure 3.7B) as well as the total distance travelled (Figure 3.7C). The analysis showed that, in cells expressing RASSF1C, the internalised E-cadherin vesicles move significantly slower compared to the control (Figure 3.7D) and that the distance they travel is also significantly reduced due to the RASSF1C expression (Figure 3.7E).

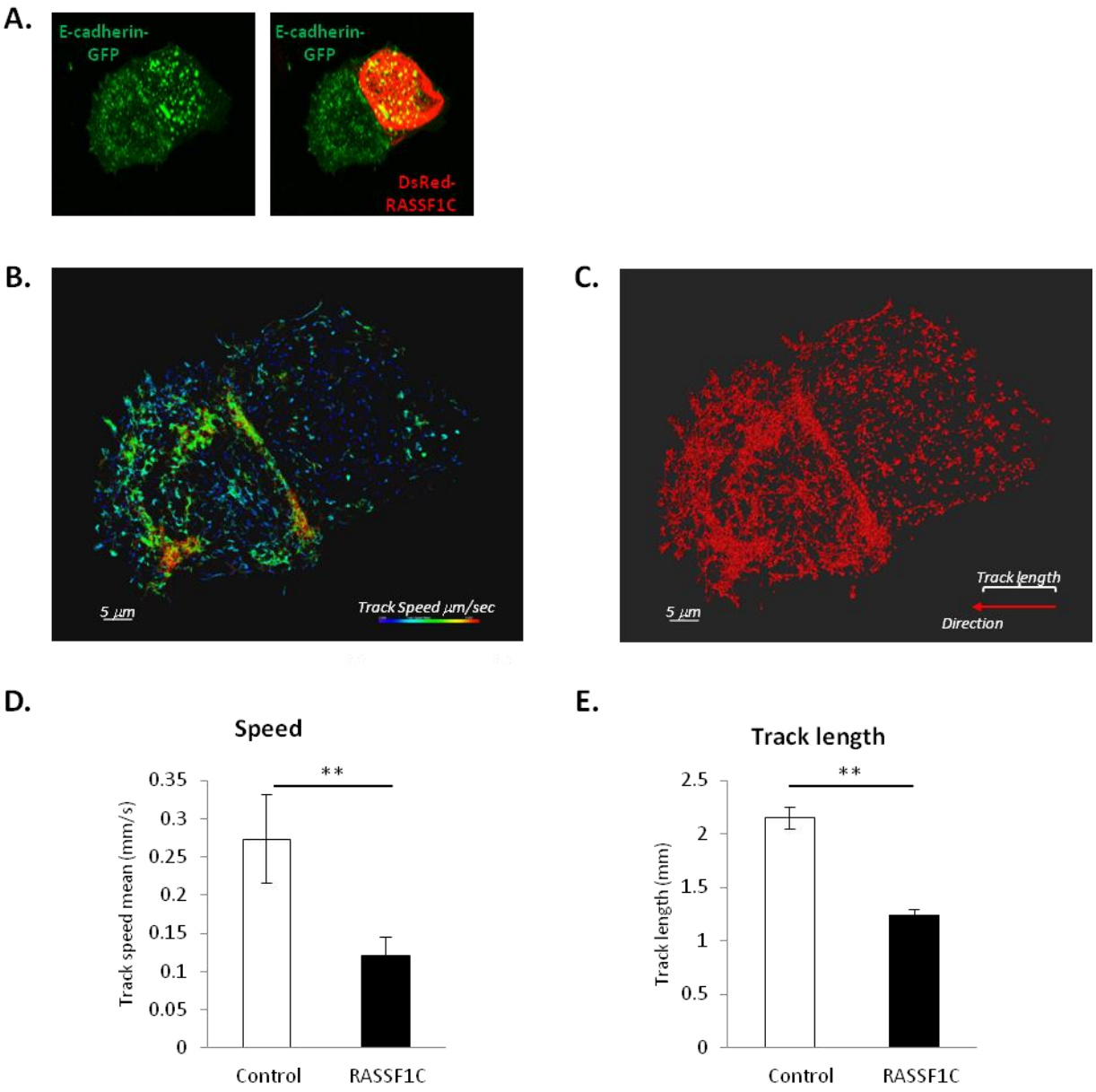


Figure 3.7. RASSF1C Expression Leads to Impaired E-cadherin Trafficking. **A**. MCF7 cells (2 x 10^5 cells/condition) were plated onto 35 mm glass bottom plate and transfected with E-cadherin-GFP and DsRed-empty vector, or DsRed-RASSF1C. Cells were imaged 24 hrs post transfection with a Zeiss LSM 780 microscope at 63 x magnification, at 37 ^{o}C and 5 % CO_2. In total 200 images were taken at 1 image/second. The expression of RASSF1C leads to the internalisation and accumulation of E-cadherin-GFP inside the cells. **B**. Of the pictures, 100 were used for measurement by Imaris 8.0 (Bitplane) of the speed and distance travelled by the internalised E-cadherin. The average aggregate size was varied between 0.4-0.6 μm. The average distance travelled was set at a threshold of 1 μm. On average, 10 cells and 700 detected vesicles were tracked per experiment. The speed of movement for the cytoplasmic E-cadherin is lower in cells expressing RASSF1C, compared to control. **C**. Vesicles were analysed as in **B** and the length of each track was measured. Internalised E-cadherin vesicles from RASSF1C-expressing cells travel a shorter distance, compared to the vesicles in the control cells. **D**. The cells and vesicles were analysed as in **B**, and the results were plotted using the Vantage function of the Imaris 8.0 to visually represent the data on the actual cell. Average values, SEM and significance were calculated using Prism 6.0 (Graphpad) software. Control E-cadherin vesicles move significantly faster and over greater distance, **E**, compared to vesicles when RASSF1C is expressed. Data is representative of three independent experiments. ** $p \leq 0.01$, *** $p \leq 0.001$. Error bars represent 1 x SEM.

`

We next investigated whether the phosphorylation of SRC plays a role in the trafficking and movement of internalised E-cadherin. To do this we measured the movement of vesicles in cells expressing E-cadherin Y3F–GFP in the presence or absence of DsRed-RASSF1C. We observed no difference in the amount of internalised E-cadherin Y3F in the control (Figure 3.8A) and the RASSF1C-expressing cells (Figure 3.8C). Furthermore, there was no difference in the speed or the distance travelled by the vesicles in the cytoplasm (Figure 3.8 B, D, quantified in 3.8 E and F).

Taken together these data suggest that RASSF1C not only disrupts adherens junctions by promoting the internalisation of E-cadherin, but also impairs the physical trafficking of E-cadherin back to cell-cell contacts through a process that is SRC-dependent.

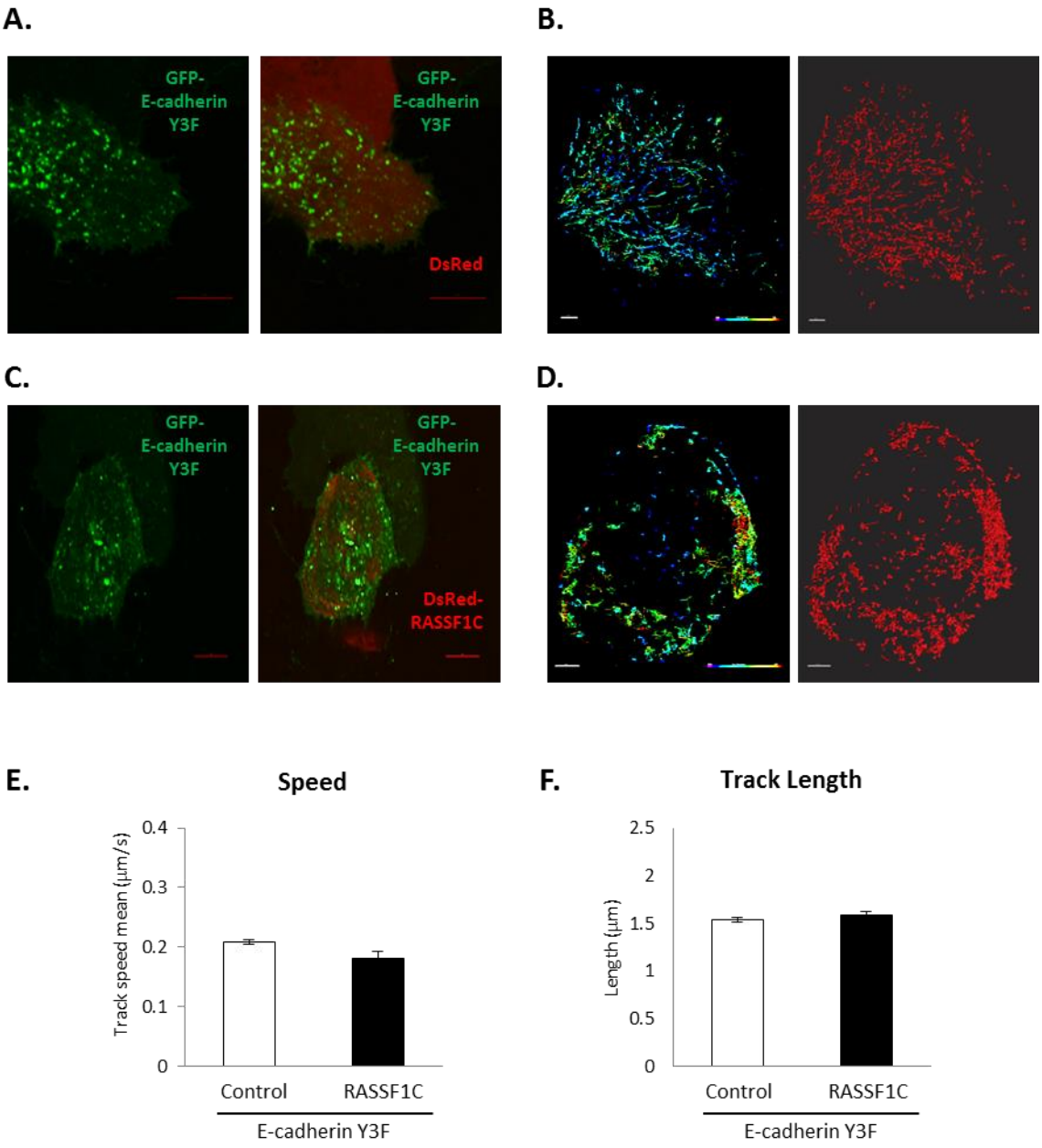


Figure 3.8. RASSF1C Fails to Affect the Trafficking of E-cadherin Y3F Mutant. MCF7 cells (2 x 10^5 cells/condition) were plated onto 35 mm glass bottom plate and transfected with E-cadherin Y3F-GFP and DsRed-empty vector, or DsRed-RASSF1C. Cells were imaged 24 hrs post transfection with a Zeiss LSM 780 microscope at 63 x magnification, at 37 ^{o}C and 5 % CO_2. In total 200 images were taken at 1 image/second. Of them, 100 were used for measurement by Imaris 8.0 (Bitplane) of the speed and distance travelled by the internalised E-cadherin. The average aggregate size was varied between 0.4-0.6 μm. The average distance travelled was set at a threshold of 1 μm. On average, 10 cells and 700 detected vesicles were tracked per experiment. Average values, SEM and significance were calculated using Prism 6.0 (Graphpad). **A, C.** When SRC cannot phosphorylate E-cadherin, RASSF1C expression does not increase the accumulation of E-cadherin in the cytoplasm. The rate of travel and the distance travelled of the vesicles of cytoplasmic E-cadherin Y3F remain unchanged between the cells expressing the mutant. **(B.)** vs RASSF1C-expressing cells **(D.)**. **E, F.** The distance and speed of the internalised E-cadherin Y3F vesicles from RASSF1C cells are unchanged vs. those from control cells. Data is representative of three independent experiments. Error bars represent 1 x SEM.

`

3.7 RASSF1C Expression Affects the Kinetics of Adherens Junctions

Having shown that expression of RASSF1C leads to the internalisation of E-cadherin and impairs its trafficking back to the adherens junctions, we wanted to investigate how RASSF1C expression affects the strength and stability of the junctions. In order to do this we performed Fluorescence Recovery After Photobleaching (FRAP) analysis on E-cadherin-GFP containing junctions (Serrels et al., 2009) in control and RASSF1C-expressing cells. The FRAP analysis is a technique that uses a laser to photobleach the fluorescent molecules of an area of the cell and then measure the rate of return of fluorescent molecules from an unbleached surrounding area (Figure 3.9A). We transfected MCF7 cells with E-cadherin-GFP and DsRed control or DsRed-RASSF1C and performed FRAP analysis on the E-cadherin-GFP at the plasma membrane. We measured the mobile fraction, i.e. the fraction of free, unbound and unstable fluorescent molecules that can participate in the FRAP exchange, and found that it was significantly higher for the RASSF1C-expressing cells compared to the control (Figure 3.9 B). This suggested that in the presence of RASSF1C, the association between each E-cadherin molecule was reduced, thus decreasing the stability of the junctions. By measuring the time it took for the molecules to return to the site of the bleach, we were able to conclude that the E-cadherin molecules were less stable in the RASSF1C-expressing cells, compared to the control (Figure 3.9C). These processes were shown to be SRC-dependent, since the addition of the SRC inhibitor Dasatinib was able to rescue the phenotype (Figure 3.9 B, C).

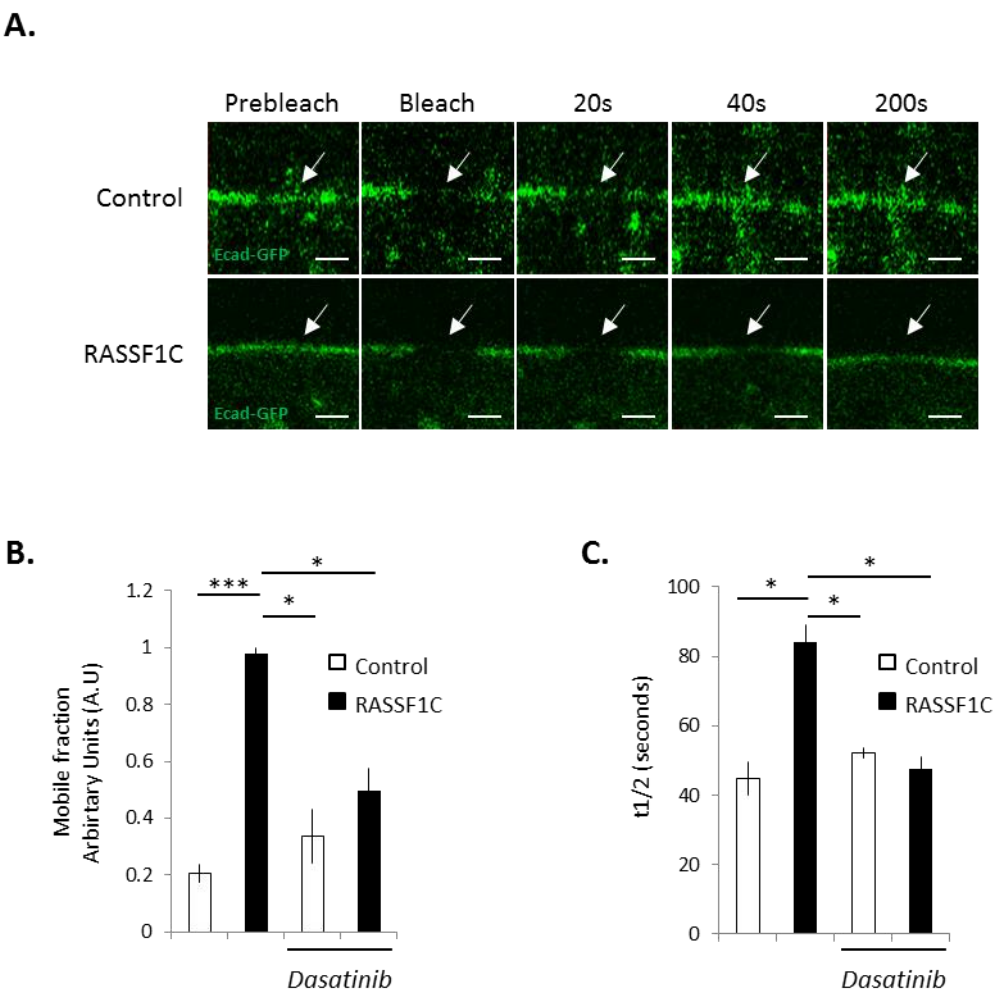


Figure 3.9. FRAP Analysis of E-cadherin in the Presence of RASSF1C Shows SRC-Dependent Changes in the Stability of the E-Cadherin Molecules. MCF7 cells (2 x 10^5 cells/condition) were plated on 35mm glass bottom plates and transfected with E-cadherin-GFP and DsRed-empty vector or DsRed-RASSF1C. Cells were imaged 24 hrs post transfection with a Zeiss LSM 780 microscope at 63 x magnification, at 37 ^{o}C and 5 % CO_2. Each bleach was done at full laser power and 2 pulses were used in order to achieve 60 % bleach per region of interest. Images were taken every 2 seconds for 5 minutes after the bleach. **A**. Representative immunofluorescent images showing the site of bleach (Arrow) and the rate or E-cadherin return at various time points for cells expressing DsRed-empty vector or DsRed-RASSF1C. E-cadherin molecules take longer to repopulate the site of bleach when RASSF1C is expressed. Scale bar represent 2μm. **B**. The mobile fraction of E-cadherin-GFP at the sites of the photobleach is higher when RASSF1C is expressed and this phenotype is SRC-dependent. **C.** The half-time of the return of E-cadherin-GFP at the sites of photobleach is higher in RASSF1C-expressing cells and is SRC-dependent. All the collected images were analysed using easyFRAP software. The immobile and mobile fractions were calculated using double exponential formula (Intensity (I) = IE – I1 x e(-t/T1) – I2 x e(-t/T2)). Data is representative of four independent experiments, 10 individual FRAP analysis per experiment. * $p < 0.05$, *** $p \leq 0.001$. Error bars represent 1 x SEM.

`

Having seen that the E-cadherin molecules were less stable at the site of adherens junctions when RASSF1C was expressed, we wanted to see whether RASSF1C increases the rate of junctional loss under conditions in which junctions are depleted. E-cadherin can dimerize and form calcium-dependent homophilic interactions and cadherin clusters with E-cadherin molecules on neighbouring cells (Takeichi, 1977). Therefore, removal of calcium (Ca^{2+}) leads to loss of the E-cadherin contacts and in turn, adherens junctions. We therefore decided to measure the time it takes the RASSF1C-expressing cells to completely lose their junctions when Ca^{2+} is depleted from the cell culture. For this, MCF7 cells were grown on coverslips and transfected with GFP or GFP-RASSF1C. Cells were grown to high density in Ca^{2+} containing media, before the media was changed to media without Ca^{2+}. Cells were fixed every 15 minutes for 60 mins and a final time point was taken at 90 mins. The RASSF1C-expressing cells (Figure 3.11) lose their adherens junctions within 45 min, significantly faster than the control cells (Figure 3.10), which retain their junctions until 60 mins. The disruption of the adherens junction also affected the stability of the tight (ZO-1-containing) junctions. These were also lost more rapidly when RASSF1C was expressed.

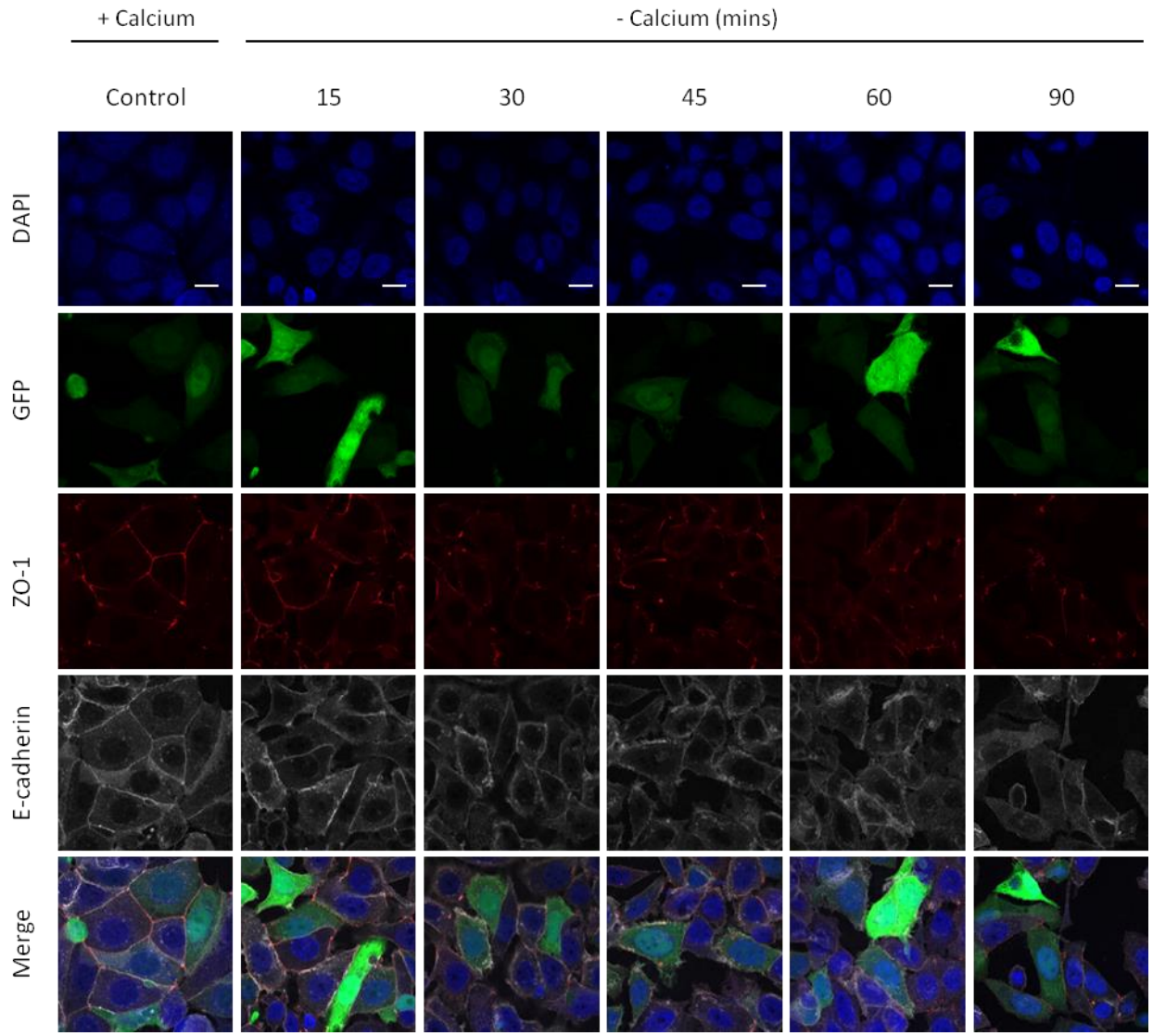


Figure 3.10. Calcium-Dependent Cell-Cell Contact Loss Occurs Within 90 Mins of Calcium Removal in MCF7 cells. MCF7 cells (3 x 10^5 cells/condition) were plated onto glass cover slips and transfected with GFP empty vector. Cells were incubated for 48 hrs before the media was changed to calcium free media for the indicated time period to disrupt calcium-dependent cell-cell junctions (with the exception of the slides for the images marked 'control' that were maintained in calcium containing media). When calcium was removed from the media, cells were fixed for 15 mins with 4 % PFA every 15 mins for up to 90 mins. Cells were permeabilised for 5 mins with 0.2 % Triton X solution and blocked for 30 mins with 0.2 % fish skin gelatin before being probed with anti-ZO-1 and anti-E-cadherin antibodies. Secondary antibodies were Alexa-fluor 566 nm for ZO-1 and Alexa-fluor 633 nm for E-cadherin. Cover slips were mounted onto slides using mounting medium containing DAPI. Images were taken with a Zeiss LSM 780 confocal microscope at 63 x magnification. Cell junctions are being lost at 90 min post calcium removal and cells start to display a rounded phenotype. Scale bars represent 10 μm.

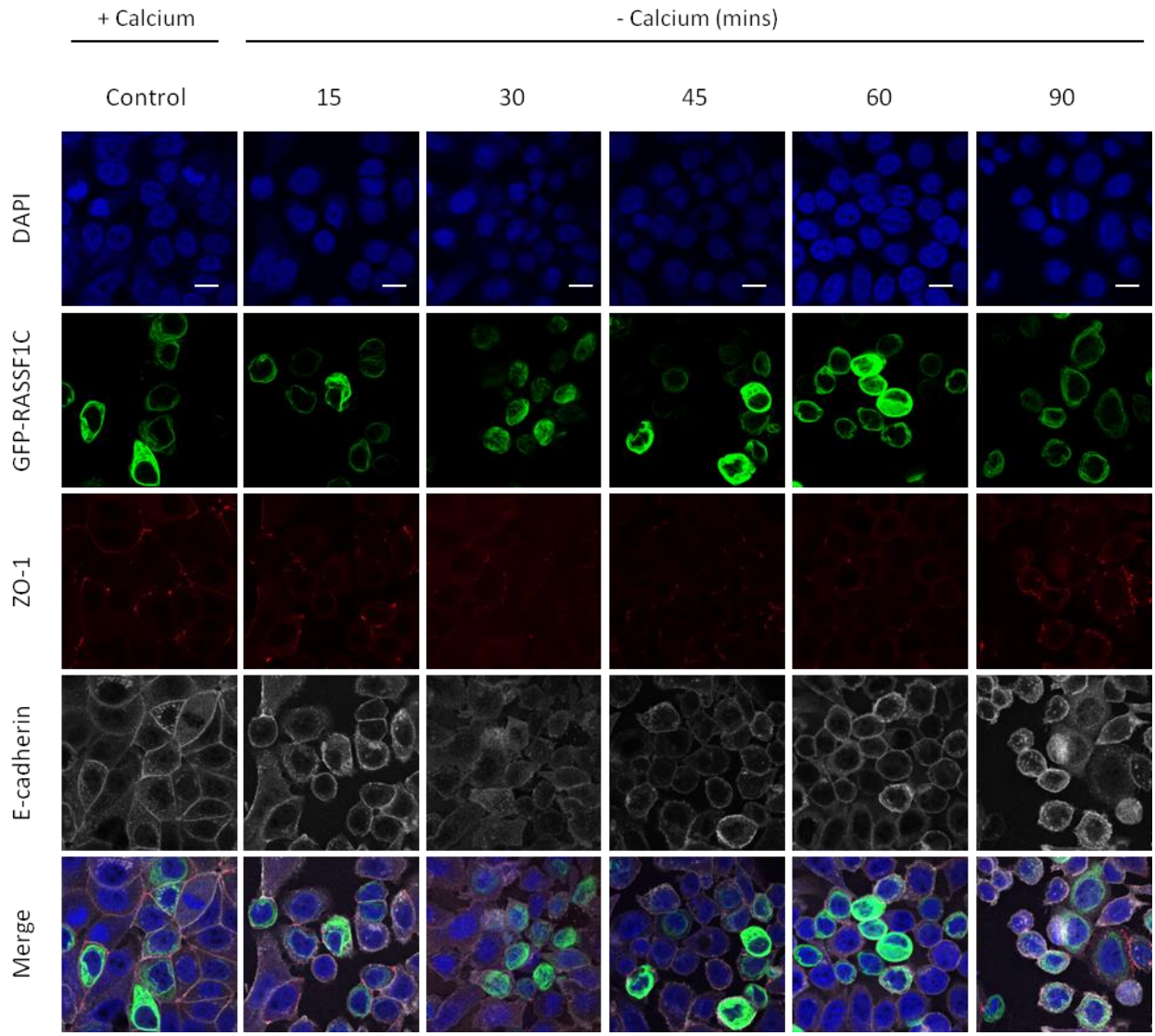


Figure 3.11. Calcium-Dependent Cell-Cell Contact Loss is Accelerated in RASSF1C-Expressing Cells. MCF7 cells (3 x 10^5 cells/condition) were plated onto glass cover slips and transfected with GFP-RASSF1C vector. Cells were incubated for 48 hrs before the media was changed to calcium free media for the indicated time to disrupt calcium-dependent cell-cell junctions (with the exception of the slides for the images marked 'control' that were maintained in calcium containing media). When calcium was removed from the media, cells were fixed for 15 mins with 4 % PFA every 15 mins for up to 90 mins. Cells were permeabilised for 5 mins with 0.2 % Triton X solution and blocked for 30 mins with 0.2 % fish skin gelatin before being probed with anti-ZO-1 and anti-E-cadherin antibodies. Secondary antibodies were Alexa-fluor 566 nm for ZO-1 and Alexa-fluor 633 nm for E-cadherin. Cover slips were mounted onto slides using mounting medium containing DAPI. Images were taken with a Zeiss LSM 780 confocal microscope at 63 x magnification. When RASSF1C is expressed, cell junctions are being lost at 45 min post calcium removal and cells begin to display a rounded phenotype earlier than the control. Scale bars represent 10 μm.

`

Having observed that RASSF1C-expression leads to more rapid loss of adherens junctions and impaired trafficking of E-cadherin (Figure 3.7), we wanted to investigate whether RASSF1C expression also affects the rate at which the junctions can be re-formed. Here, we used Ca^{2+}-depleted media to disrupt the adherens junctions. We then re-introduced Ca^{2+} and followed the re-formation of the adherens junctions. MCF7 cells were transfected with GFP control or GFP-RASSF1C before putting the cells into Ca^{2+} free media. Upon complete loss of the adherens junctions, complete media with Ca^{2+} was added to the cells. Cells were fixed every 30 min for 150 min. We observed that the adherens junctions were re-established in cells transfected with the control plasmid within 30 min and appeared to have formed strong adherens (E-cadherin) and tight (ZO-1) junctions by 90 min (Figure 3.12). By contrast, RASSF1C-expressing cells showed slower reformation of the junctions, taking up to 150 min before the cells began to re-establish the contacts (Figure 3.13). By measuring the intensity of the junctions at the different time points, we were able to conclude that it took longer for the RASSF1C-expressing cells to form the adherens junctions (Figure 3.14A), and that the junctions formed were predominantly weakly stained (Figure 3.14B). RASSF1C-expressing cells also failed to re-establish strongly stained junctions after the Ca^{2+} depletion (Figure 3.14C).

Interestingly, work in the lab has indicated that RASSF1C expression also decreases the physical strength of the junctions. This was measured by Dispase assay (Canel et al., 2010) and showed that RASSF1C expression weakened cellular cohesion in a SRC-dependent manner (Vlahov et al., 2015).

Taken together, these data suggest that RASSF1C plays an important role not only in the trafficking of E-cadherin, but in the mechanism of formation of adherens junctions and their general stability.

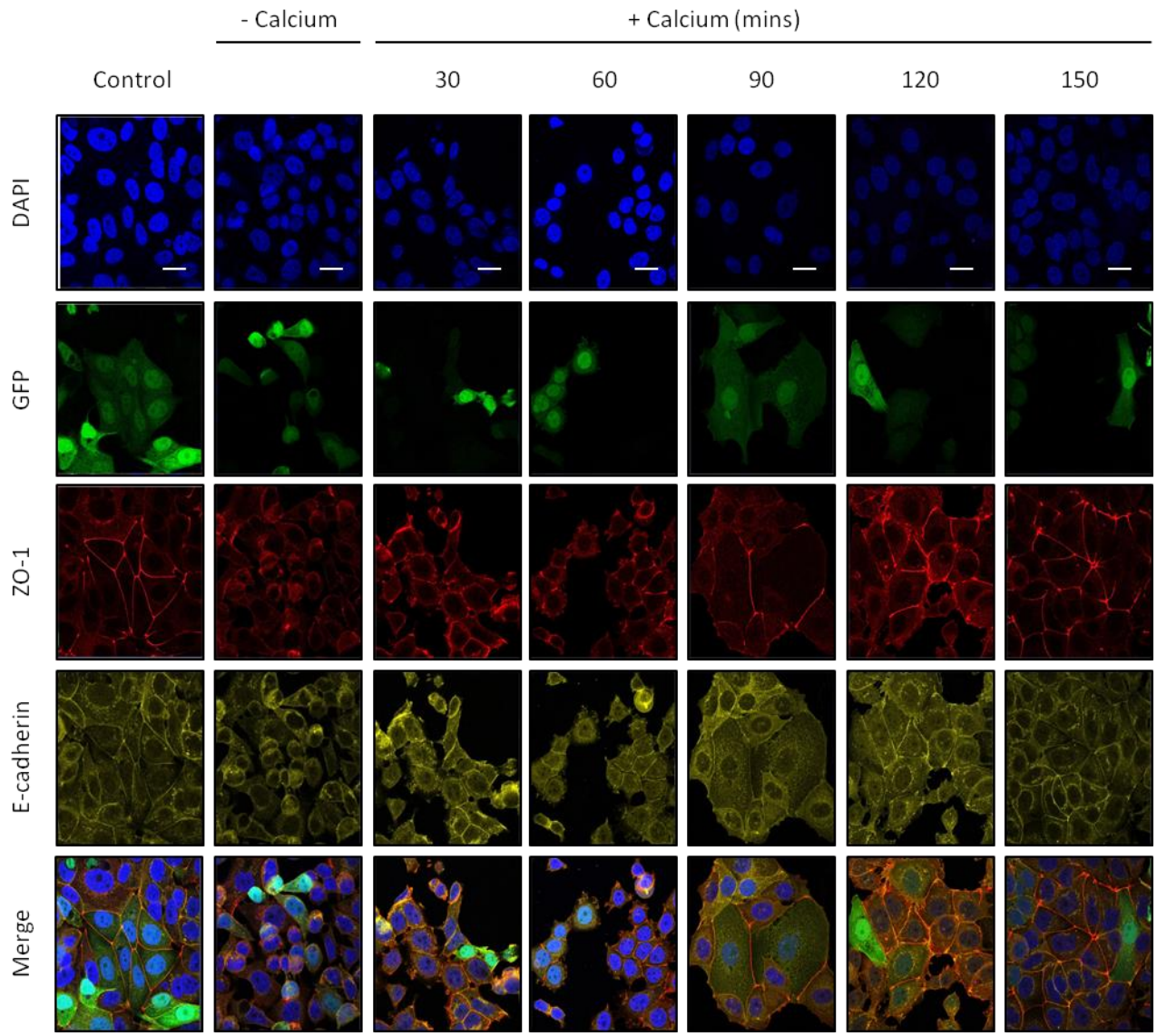


Figure 3.12. Calcium-Dependent Cell-Cell Contact Formation Occurs Within 90 Mins of Calcium Introduction in MCF7 Cells. MCF7 cells (3 x 10^5 cells/condition) were plated onto glass cover slips and transfected with GFP empty vector. Cells were incubated for 48 hrs before the media was changed to calcium free media for 16 hrs to disrupt calcium-dependent cell-cell junctions (with the exception of the slides for the images marked 'control' that were maintained in calcium containing media). Calcium was then re-added to the media and cells were fixed for 15 mins with 4 % PFA every 30 mins for 150 mins. Cells were permeabilised for 5 mins with 0.2 % Triton X solution and blocked for 30 mins with 0.2 % fish skin gelatin before being probed with anti-ZO-1 and anti-E-cadherin antibodies. Secondary antibodies were Alexa-fluor 566 nm for ZO-1 and Alexa-fluor 633 nm for E-cadherin. Cover slips were mounted onto slides using mounting medium containing DAPI. Images were taken with a Zeiss LSM710 confocal microscope at 63 x magnification. Cell junctions are lost and cells have a rounded phenotype upon withdrawal of calcium. Cell-cell junctions begin to reform 30 mins after re-addition of calcium forming strong mature junctions by 90 mins. Scale bars represent 10 μm.

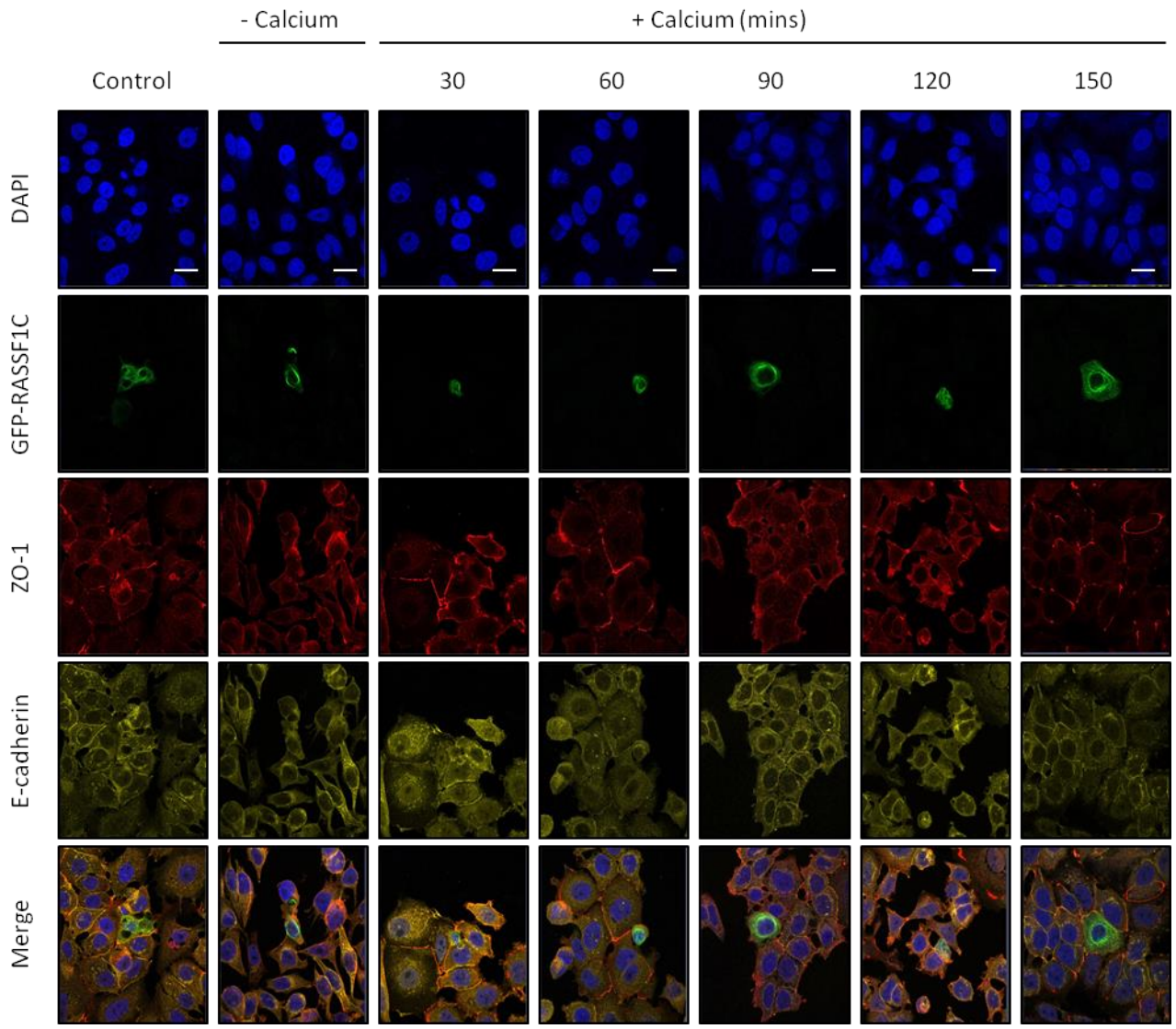


Figure 3.13. Calcium-Dependent Cell-Cell Contact Formation is Disrupted by RASSF1C Expression. MCF7 cells (3 x 10^5 cells/condition) were plated onto glass cover slips and transfected with GFP-RASSF1C. Cells were incubated for 48 hrs before the media was changed to calcium free media for 16 hrs to disrupt calcium-dependent cell-cell junctions (with the exception of the slides for the images marked 'control' that were maintained in calcium containing media). Calcium was then re-added to the media and cells were fixed for 15 mins with 4 % PFA every 30 mins for 150 mins. Cells were permeabilised for 5 mins with 0.2 % Triton X solution and blocked for 30 mins with 0.2 % fish skin gelatin before being probed with anti-ZO-1 and anti-E-cadherin antibodies. Secondary antibodies were Alexa-fluor 566 nm for ZO-1 and Alexa-fluor 633 nm for E-cadherin. Cover slips were mounted onto slides using mounting medium containing DAPI. Images were taken with a Zeiss LSM710 confocal microscope at 63 x magnification. It can be seen that the junctions are already weakened in the RASSF1C-expressing cells before the removal of calcium, but like the control cells junctions are completely lost and the cells form a rounded phenotype with the removal of calcium from the media. Unlike control cells, RASSF1C-expressing cells do not form strong, mature junctions by 90 mins. This is delayed and can be seen to begin to occur at only 150 mins post re-addition of calcium. Scale bars represent 10 μm.

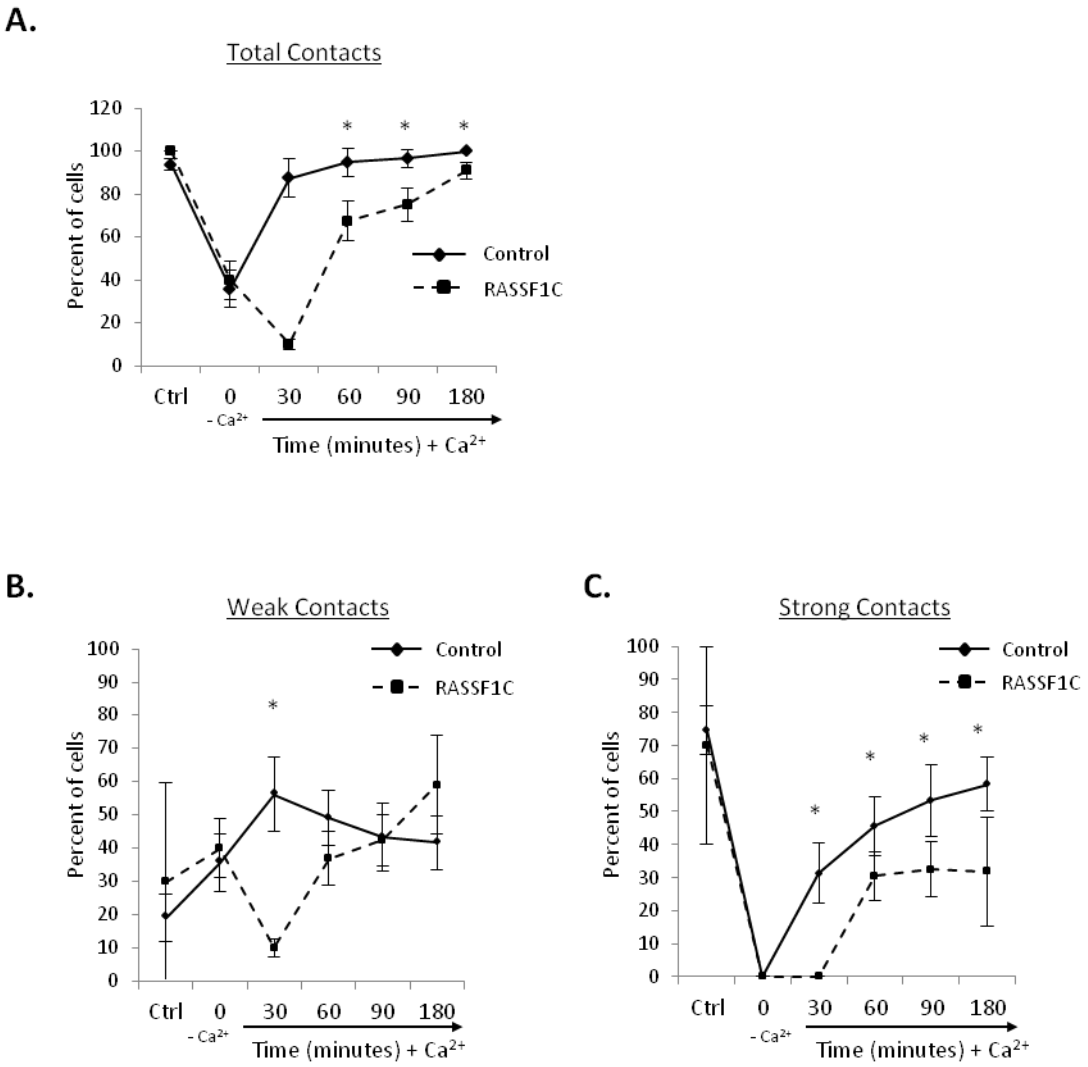


Figure 3.14. RASSF1C Expression Affects the Formation of Both Weak and Strong Junctions. MCF7 cells (3 x 10^5 cells/condition) were plated onto glass cover slips and transfected with GFP-RASSF1C. Cells were incubated for 48 hrs before the media was changed to calcium free media for 16 hrs to disrupt calcium-dependent cell-cell junctions (with the exception of the slides for the images marked 'Control' that were maintained in calcium containing media). Calcium was then re-added to the media and cells were fixed for 15 mins with 4 % PFA every 30 mins for 150 mins. Cover slips were treated as in Figure 3.12 and 3.13. Cover slips were mounted onto slides using mounting medium containing DAPI. Images were taken with a Zeiss LSM710 confocal microscope at 63 x magnification. Cells expressing GFP-empty vector or GFP-RASSF1C were utilised for single cell analysis. **A**. Total contacts were calculated as the percentage of junctions formed vs the total number of cells in contact with cell being analysed. **B**. Weak contacts were defined as being diffuse or interrupted staining at the cell-cell junction. **C**. Strong contacts were defined as robust, well defined staining at the cell-cell junction. Upon re-addition of calcium, RASSF1C-expressing cells took longer to reform both types of junctions and the levels of strong contacts remain lower than the control ones throughout the whole duration of the experiment. Data is representative of three independent experiments. * $p < 0.05$. Error bars represent 1 x SEM.

`

3.8 RASSF1C-Expressing Cells Obtain Partial EMT Traits

During epithelial to mesenchymal transition, epithelial cells are converted to more migratory and invasive ones. The process of EMT includes the downregulation of epithelial cell traits, such as E-cadherin (Huber et al., 2005; Kalluri and Neilson, 2003). However, in many instances, the distinction between an epithelial versus mesenchymal state can be relatively fluid and a partial EMT/MET frequently occurs, especially in development (Tsai and Yang, 2013). Change in the expression of E-cadherin has been associated with EMT in cancer, tissue fibrosis and embryonic development (Hay and Zuk, 1995). Since RASSF1C expression plays a role in the localisation and stability of E-cadherin, we sought to investigate whether RASSF1C affects its transcription, since the protein levels of E-cadherin do not vary (Figure 8.4). We investigated whether expression of RASSF1C could induce a phenotype similar to EMT. In order to do this we transiently transfected MCF7 cells with pcDNA3 control or FLAG-RASSF1C. The cells were then collected and processed for qRT-PCR. We used a panel of genes previously shown to be associated with an EMT phenotype (Ocana et al., 2012). We observed that of all the genes tested, only Vimentin was upregulated in cells expressing RASSF1C compared to the control cells (Figure 3.15). Interestingly, although we have shown that RASSF1C expression affected the localisation and trafficking of E-cadherin, we did not observe any changes to E-cadherin expression in RASSF1C cells. Therefore we concluded that RASSF1C expression does not lead to a canonical EMT, but to an intermediate, partial one.

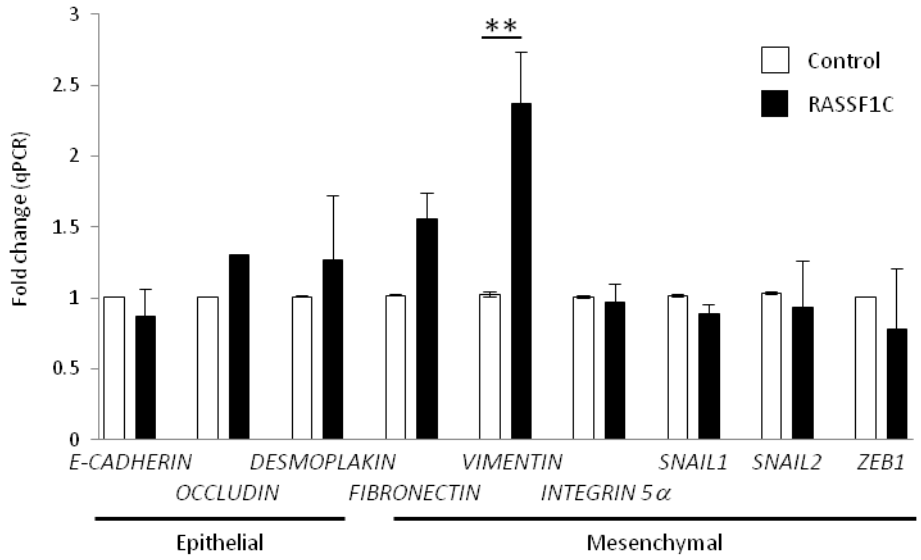


Figure 3.15. Expression of RASSF1C Leads to Partial EMT Phenotype. MCF7 cells (2 x 10^5 cells/well) were plated onto 2 wells of 6 well plate and transfected with either pcDNA3 or FLAG-RASSF1C. After 48 hrs the cells were collected and 50,000 cells were lysed and cDNA prepared and qPCR was performed on an Applied Biosystems 7500 Fast Real Time PCR system. Expression of 18S was used as an internal control. From all the epithelial and mesenchymal genes, only Vimentin is upregulated when cells express RASSF1C. Data is representative of three independent experiments. ** $p \leq 0.01$. Error bars represent 1 x SEM.

`

3.9 RASSF1C Expression Leads to Increased Cell Motility

So far I have shown that RASSF1C expression activates SRC, deregulating E-cadherin at cell-cell junctions and upregulates Vimentin expression. Loss of E-cadherin has been linked to an increase in cancer cell motility and invasiveness (Frixen et al., 1991; Vleminckx et al., 1991). Additionally, both SRC activity and Vimentin expression have been linked to EMT, increased invasiveness and metastasis (Boyer et al., 1989; Fujita et al., 2002; Raymond and Leong, 1989; Shimizu et al., 2003). Previous work in the lab has shown that RASSF1C increases the motility of cells in a scratch wound assay, and transmembrane motility assay. To confirm these data we decided to examine the real time motility of RASSF1C-expressing cells. MCF7 cells were transiently transfected with E-cadherin-GFP and either DsRed control or DsRed-RASSF1C and observed for 8 hrs in order to understand their behaviour. We found that cells expressing DsRed control showed little movement, remaining static for the duration of the experiment (Figure 3.16). In contrast, when RASSF1C was expressed, the cells left the monolayer and demonstrated increased motility (Figure 3.17). Interestingly, we observed that over the time course, the level of RASSF1C expression and IF intensity increased, we observed a corresponding accumulation of E-cadherin in the cytoplasm confirming our previous experiments. The detached, mobile cell, expressing RASSF1C also left behind extracellular membranous vesicles containing E-cadherin (Figure 3.17, Arrows). The nature of these vesicles is investigated further in Chapter 5.

`

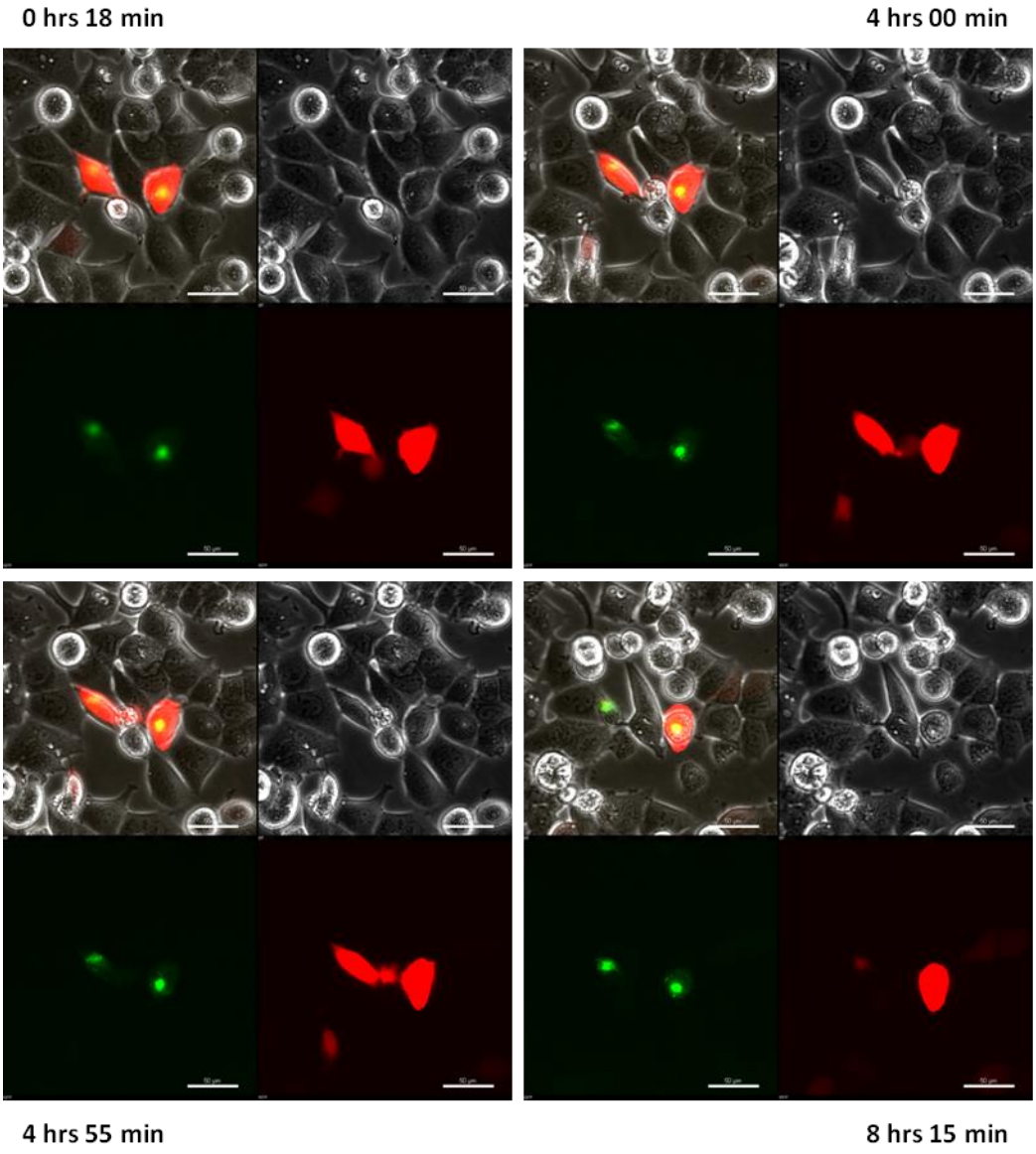


Figure 3.16. MCF7 Cells, Expressing E-cadherin and DsRed-Empty Vector, are not Motile in a Live Cell 2D System. MCF7 cells (3 x 10^5 cells/well) were plated into a 12 well plate and transfected with E-cadherin-GFP and DsRed-empty vector. Cells were incubated for 24 hrs before imaged for 8 hrs at a rate of 1 picture every 15 min, using a Nikon TE2000 inverted microscope at 20 x magnification. Scale bars represent 50 μm. Cells expressing both E-cadherin-GFP and DsRed-empty vector do not show signs of increased motility in a 2D system.

`

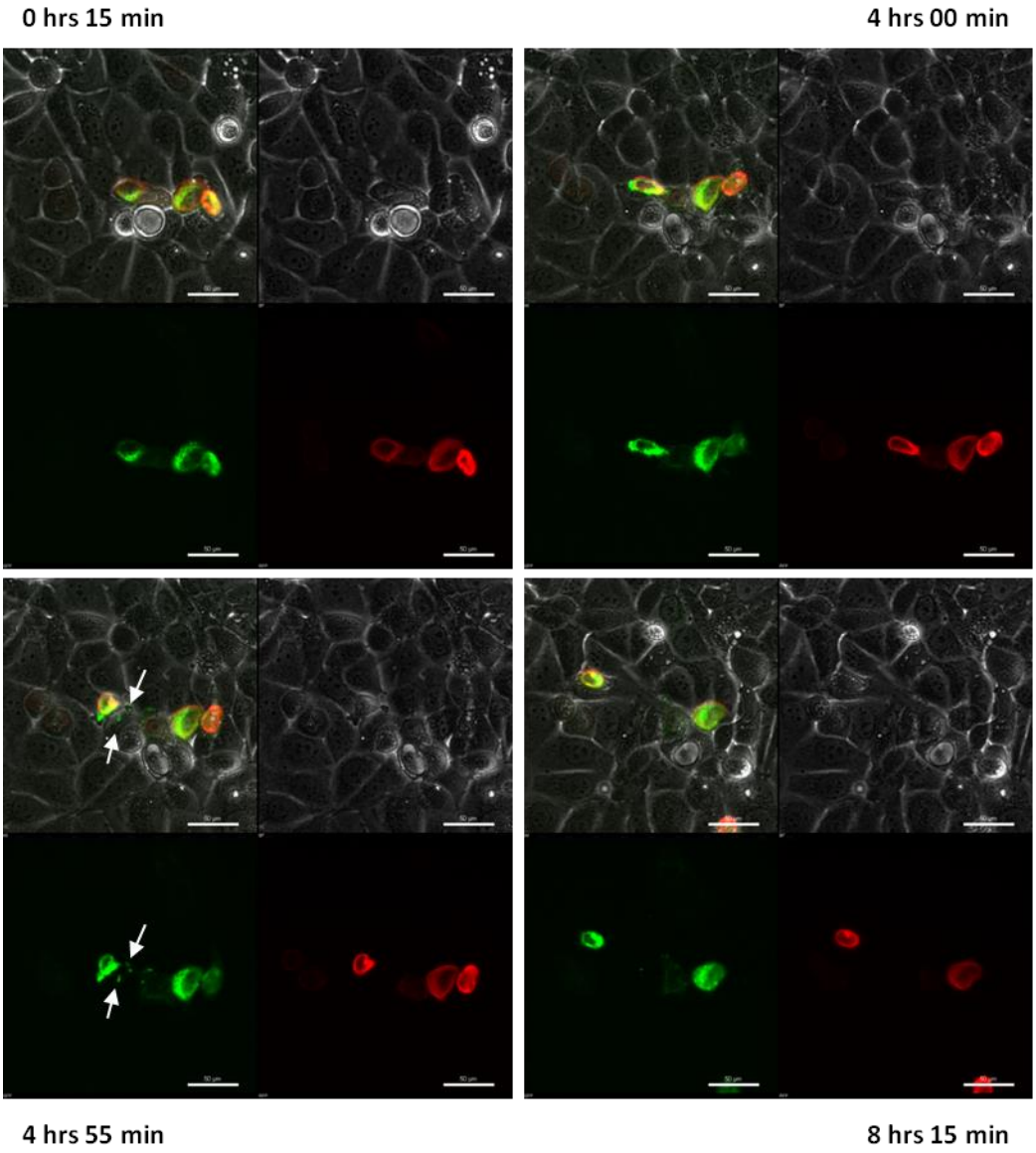


Figure 3.17. MCF7 Cells, Expressing E-cadherin and DsRed-RASSF1C, Show Increased Motility in a Live Cell 2D System. MCF7 cells (3 x 10^5 cells/well) were plated into a 12 well plate and transfected with E-cadherin-GFP and DsRed-RASSF1C. Cells were incubated for 24 hrs before imaged for 8 hrs at a rate of 1 picture every 15 min, using a Nikon TE2000 inverted microscope at 20 x magnification. Scale bars represent 50 μm. Cells expressing both E-cadherin-GFP and DsRed-RASSF1C show signs of increased motility in a 2D system. This phenotype is triggered by the build-up of both RASSF1C and E-cadherin in the cell cytoplasm. The motile RASSF1C cell also secretes membranous vesicles containing E-cadherin as the movement occurs (white arrows).

`

3.10 RASSF1C Expression Leads to SRC-Dependent Tumourigenesis *in vitro* and *in vivo*

In this chapter we have shown that RASSF1C behaves as an oncogene that can activate SRC, alter E-cadherin localisation and function at the adherens junctions and increase its motility in a 2D system. We therefore decided to investigate whether RASSF1C expression also promotes tumourigenicity of cancer cells in a 3D matrigel system. We generated MDA-MB-231 cells stably expressing either empty vector or MYC-RASSF1C. MDA-MB-231 cells were selected because they are weakly metastatic and can provide a good model for motility and invasion (Minn et al., 2005). In order to test the tumourigenicity, we plated the stable cell lines onto matrigel. In 10 days the cells formed mammospheres which were imaged and quantified, measuring their size and number of mammospheres with an aggressive phenotype, defined by the number of protrusions coming out of the mammosphere. Mammospheres with 5 or more projections were considered aggressive. The growth in matrigel is anchorage independent, so in order to form the mammospheres, the cells must invade into the matrigel. More aggressive cells will invade into the matrigel with higher efficiency, having more invasive protrusions, and will proliferate faster, resulting in larger mammospheres. We observed that both control and RASSF1C-expressing cells were able to form mammospheres in matrigel (Figure 3.18A), but the mammospheres stably expressing RASSF1C were significantly larger (Figure 3.18B). We also found that a higher proportion of the RASSF1C-expressing cells had an aggressive phenotype compared to control (Figure 3.18C). Since we have seen that RASSF1C leads to activation of SRC, previously linked with invasiveness and tumourigenesis, we wanted to determine whether the aggressive phenotype seen, was SRC dependent. When the mammospheres, stably expressing RASSF1C, were treated every three days with a low dose of SRC inhibitors, Dasatinib and AZD0530, we observed that we were able to reverse the formation of large (Figure 3.18A and B), aggressive (Figure 3.18C) mammospheres back to that observed for the control cells, suggesting that the RASSF1C-dependent tumourigenesis was SRC dependent.

`

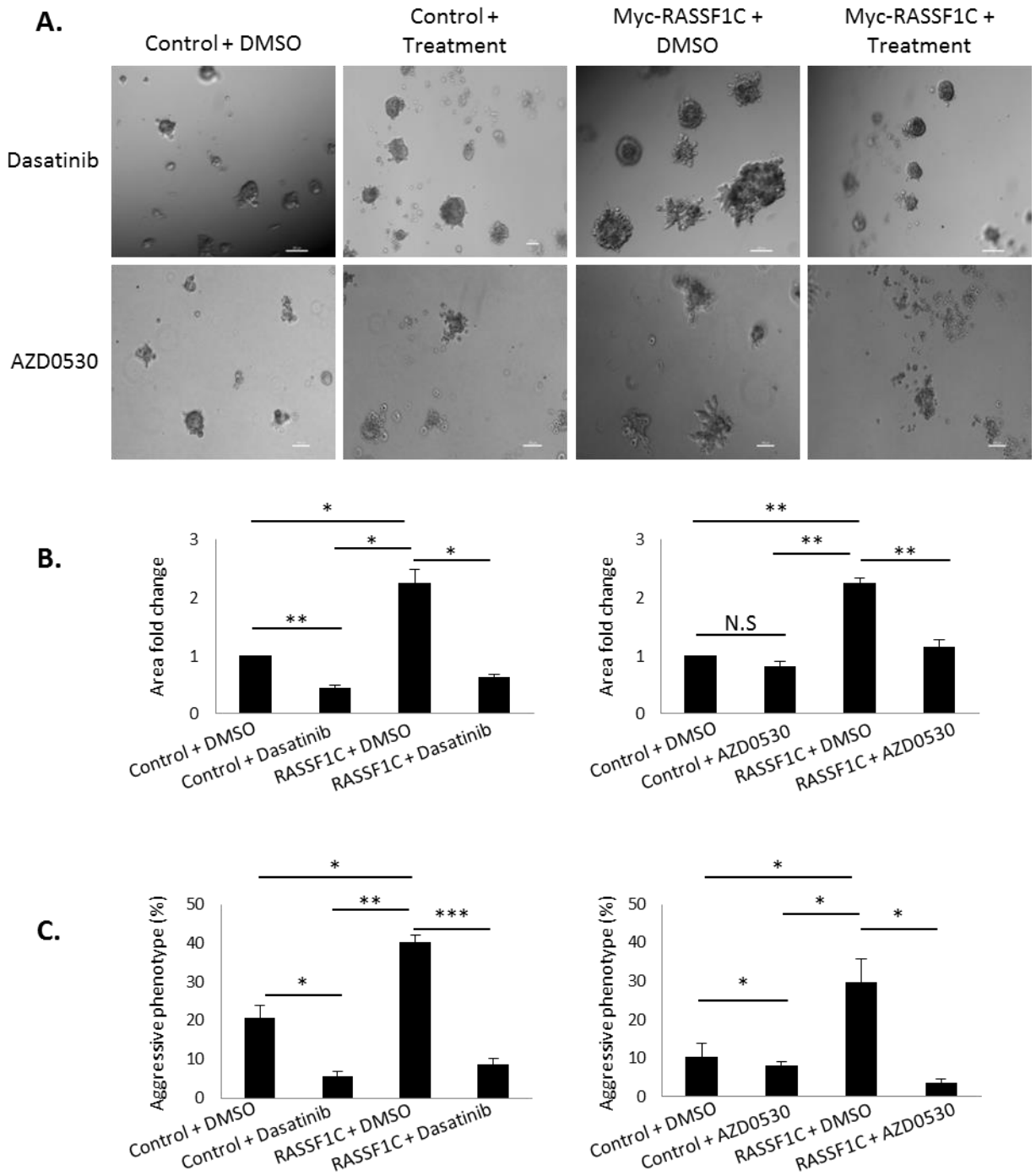


Figure 3.18. RASSF1C Expression Drives a More Aggressive Phenotype *In Vitro*. MDA-MB-231 cells stably expressing empty vector (control) or MYC-RASSF1C were seeded onto matrigel and cultured for 10 days, changing media every 3 days to allow mammospheres formation. A low concentration of Dasatinib (10 nM) of AZD0530 (1.25 μM) were added to the Myc-RASSF1C on days 3, 6 and 9. Images were taken at 4 x magnification using a Nikon TE2000 Eclipse microscope. **A.** Representative images of mammospheres of Dasatinib treated (top panel or AZD0530 treated (bottom panel) control or MYC-RASSF1C cells. Scale bars represent 200 μm. **B.** Five mammospheres were chosen at random in each of the 60 images taken per sample and the area was measured using Image J. RASSF1C induced a SRC-depended formation of bigger mammospheres. **C.** Mammospheres were graded as aggressive if they had greater than, or equal to, five projections from the main mammosphere body into the surrounding matrigel. RASSF1C-expressing cells formed significantly more aggressive mammospheres than the control cells. N.S $p > 0.05$, * $p \leq 0.05$, ** $p \leq 0.01$, *** $p \leq 0.001$. Error bars represent 1 x SEM.

`

So far I have shown that RASSF1C expression leads to an increase in the motility, invasiveness and aggressiveness of the cancer cells. In order to confirm the role of RASSF1C in tumourigenesis, we decided to measure the growth of the RASSF1C cancer cells in an *in vivo* system. Given that we have shown that RASSF1A and RASSF1C appear to have opposite effects on SRC activity, we decided to see if RASSF1C expression may also affect brain metastasis (Marzese et al., 2014). To directly address the tumourigenesis and invasive spread we used a brain seeding model, which allows spread of human cells to be readily traced. We therefore injected naïve MDA-MB-231 cell, or either control or RASSF1C stably expressing MDA-MB-231 cells, into the left striatum of Severe Combined Immunodeficiency (SCID) mice. After 21 days the mice were sacrificed and the brains were analysed by measuring the size of the tumour growth. Human Vimentin was used as identify that the cells are of human origin (Figure 3.19A*). We saw that the RASSF1C –expressing cells formed significantly larger, more aggressive tumours, than either naïve or empty vector controls (Figure 3.19 B, C*).

Taken together, these data show that RASSF1C plays a role in the invasiveness and aggressiveness of cancer cells both *in vitro* and *in vivo*.

*This experiment was carried out by Manuel Sarimento Soto, a postdoctoral researcher in Nicola Sibson's laboratory, as part of an ongoing collaboration.

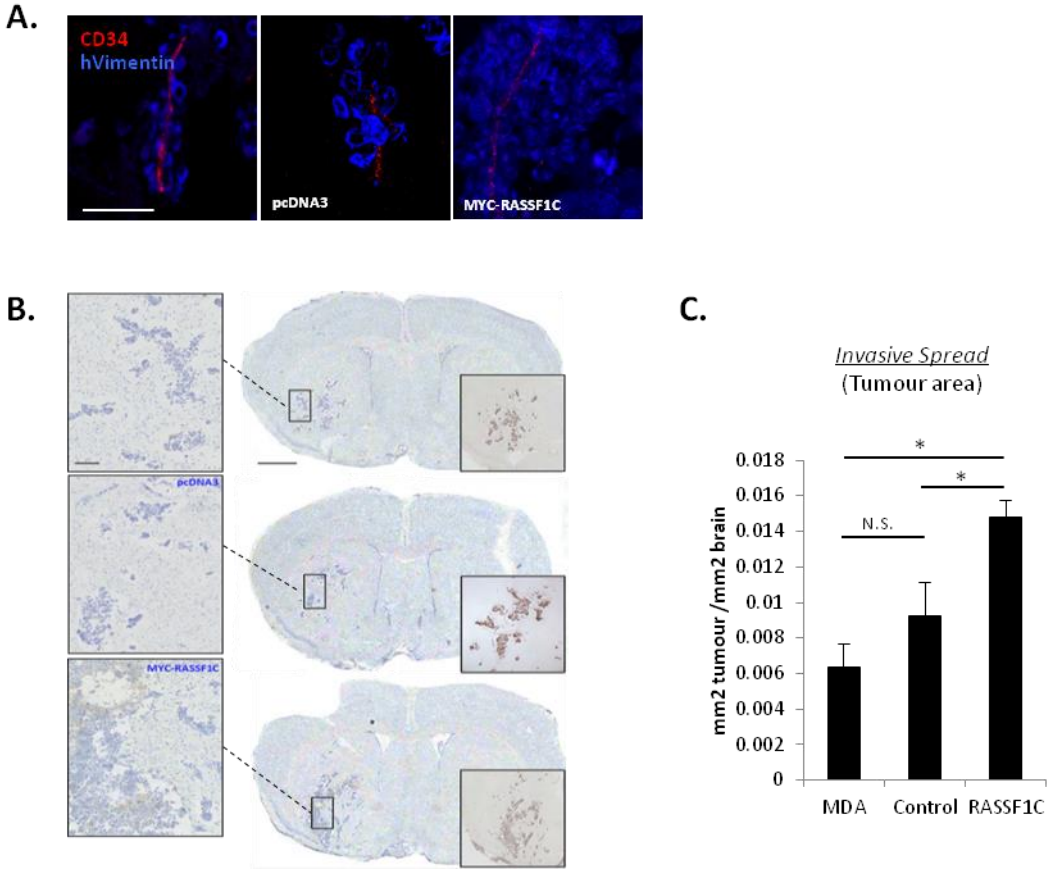


Figure 3.19. RASSF1C Promotes Invasive Spread and Tumourigenesis *in vivo.* Female SCID mice, 7-8 weeks old, were anaesthetised with 2-3 % isoflurane in 70 % N_2O: 30 % O_2, placed in a stereotaxic frame (Stoetling Co., USA) and subsequently maintained with 1 % isoflurane. The skull was exposed and a burr-hole drilled. Three different groups of animals were focally injected with either 5 x 10^3 MDA-MB-231 tumour cells, MDA-MB-231 stably expressing empty vector (pCDNA3) or MYC-RASSF1C, in 0.5 µl PBS in the left striatum (coordinates relative to Bregma; anterior +0.5 mm, lateral 1.5 mm, depth 2.5 mm) using a 75 mm-tipped glass microcapillary (Clark Electromedical Instruments, UK). At day 21 after intracerebral tumour cell injection all animals were transcardially perfusion-fixed under terminal anaesthesia (n = 4 per group) with 0.9 % heparinised saline followed by 200 ml of periodate lysine paraformaldehyde (PLP) containing only 0.025 % glutaraldehyde (PLP*light*). The brains were post-fixed, cryoprotected, embedded and frozen in isopentane at -40 ^{o}C. **A.** For immunofluorescence, sections were quenched with 1 % hydrogen peroxide in PBS, streptavidin and biotin-blocked (SP-2002, Vector Laboratories) and then incubated with Tris-NaCl blocking buffer (TNB, PerkinElmer). Sections were subsequently incubated for 16 hrs at 4 ^{o}C with anti-CD34 primary antibody (Abcam, UK, brain vessels) and anti-Vimentin antibody (VectorLabs, tumour cells), rinsed with PBS and incubated with the appropriate secondary antibody (biotinylated anti-Rat and anti-Rabbit antibodies respectively) in TNB for 30 min. Sections were then washed with PBS, incubated with streptavidin-HRP (PerkinElmer) in TNB for 30 min, washed and incubated for 8 min in the dark with TSA-biotin (PerkinElmer) in amplification buffer (PerkinElmer). Slides were washed and incubated with a streptavidin-Cy3 fluorophore (Invitrogen) for 30 min. To detect the other fluorophore, the AMCA-conjugated secondary antibody was added at the same time as streptavidin-Cy3. Slides were cover-slipped using Vectashield mounting medium (Vector Laboratories). **B**. For immunohistochemical detection of tumour cells, 10 µm sections were collected onto gelatinised slides, washed in phosphate-buffered saline (PBS; Thermo Fisher Scientific, UK; pH 7.4) and counterstained 5 min in cresyl violet. Slides were mounted and coverslipped using DPX mounting solution (Thermo Fisher Scientific, UK). **C**. To assess areas of tumour colonisation, photomicrographs of each brain section were obtained using ScanScope CS slide scanner (Aperio, Vista, CA, USA) and analysed using ImageScope (Aperio). Mice injected with MDA-MB-231 cells, stably expressing RASSF1C, grow significantly bigger tumours. Error bars depict 1 x SEM. * $p < 0.05$.

`

3.11 Discussion

In this chapter I have demonstrated that both RASSF1A and RASSF1C bind to SRC and that RASSF1A associates with CSK, leading to the inhibitory phosphorylation of SRC at Y527. We have shown that RASSF1C associates with the active SRC phosphorylation at Y416 site, leading to the phosphorylation and internalisation of E-cadherin, causing the loss of adherens junctions. The trafficking of E-cadherin was shown to be impaired, leading to its accumulation in the cytoplasm. Finally, the expression of RASSF1C was shown to increase motility and tumourigenesis both *in vitro* and *in vivo*.

Previous work in the lab has shown that SRC could not be activated by RASSF1C in cells expressing RASSF1A (Figure 8.3) and that knockdown of expression of both RASSF1A and RASSF1C prevents the activation of SRC by growth factors (Vlahov et al., 2015). RASSF1A is well characterised as a tumour suppressor and is involved in a range of cellular functions from maintenance of cell cycle checkpoints to control of migration (Balch et al., 2005; Burbee et al., 2001; Dammann et al., 2000; Dreijerink et al., 2001; Kuzmin et al., 2002; Tommasi et al., 2011a; Tommasi et al., 2005; van der Weyden et al., 2005). Conversely, RASSF1C has been shown to have both tumour suppressive and oncogenic properties (Amaar et al., 2006a; Reeves et al., 2012; Reeves et al., 2013; Reeves et al., 2014). Therefore, we wanted to identify targets of RASSF1A and RASSF1C that would identify novel pathways through which they perform their respective tumour suppressive and oncogenic activities.

In a mass spectrometry screen, we identified that SRC was bound to both RASSF1A and RASSF1C. We confirmed these interactions and, interestingly, found that RASSF1A bound with higher affinity. Given that we have shown that RASSF1C activates SRC and RASSF1A appears to inactivate it, it would be interesting to investigate whether the two RASSF1 isoforms compete for SRC binding. This could be addressed by an immunoprecipitation, using purified proteins for SRC, RASSF1A and RASSF1C. We would expect that, in accordance with its inhibitory properties towards SRC, RASSF1A would be able to prevent RASSF1C from associating with SRC, or to sequester RASSF1C from the active SRC pY416.

`

SRC activity is controlled by phosphorylation of an activatory and an inhibitory tyrosine residue, Y416 (Xu et al., 1997) and Y527 (Cartwright et al., 1987), respectively. Activation of SRC by phosphorylation of the Y416 residue by the kinase domain can only occur when the inhibitory C-terminal tyrosine site Y527 is not phosphorylated by CSK (Okada and Nakagawa, 1989). Therefore, we hypothesised that, given that RASSF1A is a tumour suppressor and RASSF1C an oncogene, we wanted to investigate whether their interaction with SRC led to changes in these phosphorylation sites. We used Proximity Ligation Assay (PLA) in order to confirm the previous findings in the lab that showed that RASSF1C expression increased pY416, whereas RASSF1A expression increases pY527 (Figure 8.2A and B). The PLA assay added to our previous work by generating spatial data. This is because signal can only be generated when the two target proteins are within 40nm of each other (Figure 3.2). From this we were able to identify a novel tumour suppressor function for RASSF1A in regulating SRC activity through promoting the phosphorylation of Y527. This data, plus that from work previously done in the lab, allowed us to conclude that when RASSF1A expression is lost due to methylation, observed in many cancers, the remaining isoform, RASSF1C, is able to activate SRC by promoting phosphorylation of Y416.

From the PLA data showing that RASSF1A expression was associated with increased SRC pY527, we hypothesised that RASSF1A may bind CSK, scaffolding it with SRC. Immunoprecipitation was used to show that RASSF1A did indeed interact with CSK, but that RASSF1C did not (Figure 8.1A). This interaction was further validated using purified proteins of RASSF1A, CSK and SRC. We identified that RASSF1A, CSK and SRC could all be found as part of one complex (Figure 8.1B). However, we have so far been unable to detect the interaction between RASSF1A and CSK using the PLA system. We could attribute that to the quality of the antibodies used, or this could be due to the presence of another scaffold protein facilitating the interaction between RASSF1A and CSK in cell systems, increasing the distance between these two proteins beyond the limits of detection for the PLA assay. Protein Kinase A (PKA) phosphorylates CSK at S364 increasing its kinase activity (Yaqub et al., 2003). PKA also binds to and phosphorylates RASSF1A at S203 and affects the apoptotic signalling of RASSF1A (Richter et

`

al., 2010). In RASSF1A$^{-/-}$ cardiomyocytes, PKA activity is significantly reduced following TNF-α induction (Mohamed et al., 2014). Therefore, it would be interesting to see if RASSF1A activates CSK through an interaction with PKA.

Inactive SRC remains in the perinuclear region until its activation when SRC translocates to the periphery of the cell (Courtneidge et al., 1980; Kaplan et al., 1994; Rohrschneider, 1979; Welham and Wyke, 1988). Given that RASF1C can bind and lead to SRC activation, we hypothesised that in the presence of RASSF1C, SRC would be phosphorylated at Y416, and predominantly at the periphery of the cell. Indeed, RASSF1C expression led to a significant increase in the localisation of SRC and SRC pY416 at the plasma membrane (Figure 3.3). We have not addressed the mechanism through which SRC is translocated to the plasma membrane, but several possible ones exist.

One such mechanism through which RASSF1C could promote translocation to the plasma membrane is through the endosomal trafficking system. Endosomal trafficking regulates the translocation of SRC to the plasma membrane (Sandilands and Frame, 2008). Endosomal trafficking is a complex and dynamic process during which proteins and lipids are internalised from the cell membrane before being either recycled back to the PM, or targeted for degradation. The regulation of endosomal trafficking involves many different proteins, for example, the Rab GTPases (Ceresa, 2006), soluble N-ethylmaleimide-sensitive factor attachment protein receptors (SNAREs) (Cai et al., 2007), ubiquitin (Hoeller et al., 2006), calmodulin and protein kinase C (PKC) (Llado et al., 2008). Rho GTPases such as RhoA, RhoD and RhoB also regulate aspects of the endosomal trafficking (Ellis and Mellor, 2000). There are over 60 Rab proteins, among which Rab5, associated with early endosomes (Bucci et al., 1992; Gorvel et al., 1991; McLauchlan et al., 1998), and Rab11, associated with recycling endosomes (Ullrich et al., 1996), have been studied the most. Another GTPase that plays a role in membrane transport and early endosomes is ARF6 (Franco et al., 1999; Londono et al., 1999). Both the Rab and Arf proteins are members of the Ras superfamily (Wennerberg et al., 2005) binding specific effectors in a GTP-dependent manner. GTP exchange factors (GEFs) activate the GTPases by promoting the

`

dissociation of GDP and by the uptake of GTP. GTPase-activating proteins (GAPs) inactivate the GTPase by promoting the cleavage of GTP back to GDP (Karnoub and Weinberg, 2008). GTPases interact with, and activate, specific target proteins when in the GTP bound state. One example of this is Ras-GTP that binds to and activates Raf. Both RASSF1A and RASSF1C have an RA (Ral Guanosine nucleotide-exchange factor (Ral GDS) and the ALL-1 fusion partner from chromosome 6 (AF6)) domain (Ponting and Benjamin, 1996; Yamamoto et al., 1999). It has previously been shown that RASSF1A uses its RA domain to interacts with K-Ras (Matallanas et al., 2011). This would suggest that both RASSF1A and RASSF1C could interact with other GTPases, such as members of the Rab or Arf families, and through this to regulate the recruitment of SRC to the plasma membrane.

Other Rho GTPase proteins might also play a role in the membrane trafficking of SRC, such as RhoD and RhoB. RhoD has been shown to co-localise with SRC in early endosomes in HeLa cells (Gasman et al., 2003a), but active SRC has been mostly associated with RhoB-containing endosomes (Sandilands et al., 2004). The connector enhancer of KSR (CNK1) has been shown to interact with Rho and to be necessary for Rho activation of transcription (Jaffe et al., 2004). KSR is known to bind directly to RASSF1A and RASSF1C (Rabizadeh et al., 2004). Therefore, RASSF1C could regulate the trafficking of SRC through Rho GTPases and KSR.

SRC translocation to the periphery is also Actin dependent (Gasman et al., 2003b; Kaplan et al., 1994; Kaplan et al., 1992; Sandilands et al., 2004). mDia, a RhoD binding partner was shown to modulate cytoskeleton organisation, recruit Actin and activate c-SRC in HeLa cells (Gasman et al., 2003b). Previous work in the lab has shown a link between RASSF1C and proteins linked with Actin stability. It would be interesting to look for an association between RASSF1C and mDia or the Rho GTPases as this may highlight a mechanism through which RASSF1C promotes the translocation of SRC to the plasma membrane.

E-cadherin is a tumour suppressor that mediates calcium-dependent cell adhesion through homophilic interactions. E-cadherin, along with its binding partners, the catenin proteins, has been

`

shown to regulate contact inhibition through the activation of the Hippo pathway (Kim et al., 2011). Through this mechanism the E-cadherin-catenin complex blocks epithelial tumour progression. Consequently, in tumours, E-cadherin is often downregulated. This can be via mutation of the E-cadherin gene, downregulation of expression, or mislocalisation of E-cadherin protein, each resulting in destabilisation of cell-cell adhesion, and consequently promoting EMT (Berx and van Roy, 2009; Gumbiner, 2005; Hartsock and Nelson, 2008; Jeanes et al., 2008). SRC family kinases can phosphorylate both E-cadherin and the catenin proteins on tyrosine residues, which leads to the destabilisation of the cadherin-catenin complex. The SRC-dependent phosphorylation of E-cadherin leads to its ubiquitination by the E3 ubiquitin ligase HAKAI, which promotes the internalisation and degradation of E-cadherin in the lysosomes (Behrens et al., 1993; Fujita et al., 2002; Palacios et al., 2005). Here, we have shown that RASSF1C acts as an adapter protein that can lead to the phosphorylation and activation of SRC. In addition, previous studies in the lab have shown that cells expressing RASSF1C have increased SRC kinase activity towards its target proteins, E-cadherin and β-catenin (Figure 8.3). From this, we hypothesised that the RASSF1C-driven, SRC-dependent phosphorylation of E-cadherin would lead to its destabilisation and internalisation from the plasma membrane. Through a series of IF experiments we were able to show that both endogenous and overexpressed E-cadherin was internalised from the plasma membrane in cells expressing RASSF1C (Figures 3.4 and 3.5).

One unanswered question, however, is whether RASSF1C actively promotes the degradation of E-cadherin or only increases the rate at which E-cadherin is internalised. Previous work in the lab has suggested that in the presence of RASSF1C, HAKAI forms a complex with E-cadherin, which would indicate that RASSF1C promotes E-cadherin degradation (Fujita et al., 2002; Palacios et al., 2005), however, expression of RASSF1C did not alter the protein levels of E-cadherin (Figure 8.4). One possible explanation for this could be that the E-cadherin degradation occurs at a later stage, going beyond the 24-48 hrs after transfection, during which we observe the highest RASSF1C activity.

`

Therefore, the protein levels of E-cadherin could be measured beyond 48 hrs of RASSF1C expression, in order to answer this question.

Another possible explanation for the internalised, but not degraded E-cadherin, could be that RASSF1C expression promotes the internalisation and accumulation of E-cadherin in a cellular compartment that is normally associated with E-cadherin trafficking and recycling. Binding of E-cadherin to p120-catenin stabilises the cadherin complex at the site of the adherens junction and regulates E-cadherin recycling via the endosome recycling pathway (Miyashita and Ozawa, 2007; Yap et al., 1998). SRC binds to and phosphorylates E-cadherin and p120-catenin (Behrens et al., 1993; Mariner et al., 2001), leading to uncoupling of E-cadherin from p120-catenin and promoting E-cadherin internalisation and accumulation in the early endosomes (Miyashita and Ozawa, 2007). From here, E-cadherin can be sent to the lysosomes for destruction. The translocation to the lysosome involves the Rab5 and Rab7 GTPases, which direct E-cadherin through various endosomal compartments to the lysosome in a SRC-dependent manner (Palacios et al., 2005). Since RASSF1C expression promotes the activation of SRC, we hypothesised that E-cadherin could be internalised and located either in the endosomes, or in the lysosomes. We have so far failed to see E-cadherin overlapping with the early endosomal marker EEA1 (Figure 8.5A), or the lysosomal marker LAMP-1 (Figure 8.5B). One way we could further address this is by density centrifugation, using sucrose gradients, which would indicate if E-cadherin is targeted towards these cellular compartments. This would allow us to indicate towards which compartment E-cadherin is being targeted.

Internalised E-cadherin could be accumulated at the Golgi complex. After Epithelial Growth Factor (EGF) stimulation, E-cadherin is recycled from the cell membrane by sorting nexin (SNX1) (Bryant et al., 2007). The sorting nexins play a role in cargo sorting and are required for retromer-mediated retrieval of cargo to the Golgi complex (Carlton et al., 2005). Conversely, E-cadherin is packaged in the Golgi complex by golgin-97-dependent tubulovesicular carriers that fuse with the recycling endosomes on route to the plasma membrane (Kucia et al., 2005). The loss of the polarity protein

`

Scribble (Scrb), which normally regulates E-cadherin-dependent cell-cell adhesion (Qin et al., 2005), weakens the E-cadherin-p120 catenin interaction, promoting the internalisation and accumulation of E-cadherin in the Golgi (Lohia et al., 2012). RASSF1A has been shown to have regulatory effects on the Golgi organisation, by stabilising microtubules which act as a scaffold for Golgi assembly (Arnette et al., 2014). Since RASSF1C can also bind to the microtubules (Dallol et al., 2004), we investigated whether RASSF1C expression led to accumulation of E-cadherin in the Golgi complex. However, we failed to see any association of internalised E-cadherin with the Golgi (Figure 8.5C). As previously discussed, the localisation of the internalised E-cadherin can be addressed by density gradient centrifugation or by using an electron microscope, which would show the actual structure of these aggregates.

As with SRC, both ARF6 and the Rab GTPases play a role in the trafficking and dynamics of E-cadherin. The adherens junction disassembly has been linked to the ARF6 GTPase (Palacios et al., 2001), which interacts with, and promotes the Nm23-H1-dependent E-cadherin sequestration from the junctions by activating the membrane-remodelling GTPase Dynamin (Palacios et al., 2002). This interaction has also been linked to the downregulation of Rac1 activity, which also facilitates the loss of the junctions (Otsuki et al., 2001). Rac1 plays an important role in cadherin and catenin maintenance at the adherens junctions by regulating their translocation to sites of cell-cell contact and stabilising them through recruitment of Actin filaments (Hordijk et al., 1997). A Rac1-GEF, Tiam1 stimulates cadherin adhesion through the activation of Rac1 (Hordijk et al., 1997; Sander et al., 1999). Tiam1 is phosphorylated by SRC on Y384 and this leads to activation of ERK1/2, leading to the destruction of Tiam1 by activation of the protease Calpain (Woodcock et al., 2009). RASSF1C has previously been shown to indirectly activate ERK1/2 (Reeves et al., 2010). Our data would suggest that RASSF1C activation of SRC could promote ERK1/2 activation by phosphorylating Tiam1, leading to Tiam1 destruction. This would result in loss of Rac1 activity and destabilisation of E-cadherin. Therefore, through activation of SRC, RASSF1C could destabilise E-cadherin both directly by phosphorylation and indirectly, through downregulation of Rac1.

`

The extracellular domains of E-cadherin allow it to interact in a *trans* (engaged state) with the cadherins on neighbouring cells or in *cis* with laterally situated cadherins on the same membrane (Leckband and Sivasankar, 2000). The organisation of E-cadherin through *cis-trans* cluster formation could account for the range of junctional strength between low molecular affinities and strong adhesion. Mature junctions appear 24 hrs after the onset of cell-cell contact, due to the formation of high-affinity adhesive *trans* dimers, resulting in strong adhesion (Klingelhofer et al., 2002). Since Dynamin controls the endocytosis of E-cadherin, in mature junctions the chemical inhibition of Dynamin leads to loss of endocytosis and failure of E-cadherin to return to the site of photobleach (FRAP analysis) (de Beco et al., 2009). We have observed that in RASSF1C-expressing cells the return of the E-cadherin molecules to the site of photobleach is impaired (Figure 3.9). As mentioned before, Arf6 regulates the SRC-induced endocytosis of E-cadherin via the recruitment of the dynamin-regulating kinase Nm23-H1. Activation of ARF6 recruits Nm23-H1 to the sites of cell-cell contact, activating dynamin and also downregulating Tiam1 and Rac1 activation (Palacios et al., 2002). We would hypothesise that RASSF1C may inhibit Dynamin via SRC and ARF6, preventing the formation of strong, mature junctions. In order to investigate the ability of RASSF1C to affect the formation of junctions, we analysed the dynamics of E-cadherin cell-cell adhesion, using Ca^{2+}-depletion (Figures 3.10 and 3.11) and Ca^{2+}-re-addition assays (Figures 3.12 and 3.13). We have found that the disruption of the junctions in RASSF1C-expressing cells leads to failure to re-form strong, mature junctions (Figure 3.14). Given that the formation of strong adhesive *trans* dimers takes 24 hrs to fully understand the possible impairment on junction formation in RASSF1C-expressing cells we may have to follow their formation beyond the 24 hrs we have so far examined. Nevertheless, control cells initiate strong junctional formation earlier than the RASSF1C cells (Figure 3.14C). Further experiments will be required to understand if Dynamin levels are regulated by RASSF1C expression.

The initiation of primary tumours of epithelial origin is characterised by excessive cell proliferation and angiogenesis (Hanahan and Weinberg, 2000). Subsequently, cells acquire invasive properties leading initially to the invasion through the basement membrane, and eventually, through a

`

multistep process to metastatic dissemination, with life-threatening consequences. The multi-step process from epithelial-like cells to invasive mesenchymal-like cells is known as EMT. EMT has been proposed as the critical mechanism for the acquisition of malignant phenotypes by epithelial cancer cells (Thiery, 2002). The connection between the loss of E-cadherin expression and the transition through an EMT has been well established (Edelman et al., 1983; Tepass et al., 2000). Interestingly, re-expression of the full length, or even just the cytoplasmic domain of E-cadherin are thought to revert the cells that have undergone EMT back to an epithelial phenotype (Eger et al., 2000; Reichmann et al., 1992). This suggests that members of the adherens junctions complex, such as β-catenin, that are sequestered by E-cadherin at the plasma membrane, are able to translocate to the nucleus to promote EMT upon loss of E-cadherin, but that re-expression of E-cadherin is able to sequester β-catenin and other oncogenes, back to the plasma membrane reversing the EMT process. In the nucleus, β-catenin forms a complex with the transcription factor, T-cell factor (TCF)/lymphoid enhancer factor 1(LEF) and upregulates genes that promote the acquisition of an invasive phenotype (Gottardi et al., 2001; Kim et al., 2002; Stockinger et al., 2001; Thiery, 2002). Interestingly, SRC has been linked with the induction of EMT (Behrens et al., 1993; Takeda et al., 1995). In order to investigate whether the expression of RASSF1C and sequential activation of SRC was promoting an EMT transcriptional profile through the deregulation of E-cadherin localisation we tested whether RASSF1C expression regulated a panel of genes previously implicated in the process of EMT (Ocana et al., 2012). Of the 9 genes tested, we only found that *VIMENTIN* to be significantly upregulated (Figure 3.17). Vimentin is a type III intermediate filament, found in mesenchymal cells during the developmental stages of various tissues types (Coulombe and Wong, 2004). Vimentin has also been associated with cancer invasion and poor prognosis (Satelli and Li, 2011). Nuclear localisation of β-catenin has been linked to the increase in expression of Vimentin (Gilles et al., 2003). We hypothesised that RASSF1C expression may lead to the relocalisation of β-catenin from the sites of cell-cell junctions to the nucleus. This will be further investigated in Chapter 4. It is also interesting to note that RASSF1C expression does not affect the expression any of the other EMT markers, including

`

E-cadherin. This suggests that RASSF1C is regulating the internalisation and arrest of the E-cadherin already present in the cell, rather than the *de novo* transcription of E-cadherin. The functional hallmark of the EMT program is to allow stationary epithelial cells to gain the ability to migrate (Boyer and Thiery, 1993). Higher levels of Vimentin have been associated with invasion and circulating tumour cells (Bonnomet et al., 2012; Livasy et al., 2006; Sorlie et al., 2001). In combination with Snail1, Slug and Twist1, Vimentin has been associated with partial EMT (Grande et al., 2015; Tsai et al., 2012). The increased expression of Vimentin, but not the other EMT markers, suggests that RASSF1C expression could induce a partial EMT phenotype (Kalluri and Weinberg, 2009). It remains unclear whether the other genes associated with partial EMT will be upregulated at a later stage, since RASSF1C-dependent Vimentin upregulation could represent the initial step towards the cells becoming mesenchymal. This question will be addressed in the future using a longer time course or by the generation of stable cells lines which would retain the expression of RASSF1C for longer periods.

In Figures 3.16 and 3.17 we showed that RASSF1C-expressing cells are more motile and have increased invasive capabilities. SRC can promote motility through the activation of Rac1 leading to the formation of lamellipodia at the front, and activation of Rho, promoting actomyosin contraction at the back of the cell (Huveneers and Danen, 2009). Many of the pathways that stimulate Rac and Rho activity rely on signalling through FAK and β_1-integrins (Avizienyte et al., 2002; Gimond et al., 1999). One of these pathways acts through the integrin/FAK activation of MEK, which leads to ERK1/2 activation (Avizienyte et al., 2004). ERK1/2 is able to activate Myosin Light Chain Kinase (MLCK) leading to the peripheral accumulation of phospho-MLC which generates cellular protrusions through the formation of focal complexes and the promotion of lamellipodial spreading (Brahmbhatt and Klemke, 2003; Giannone et al., 2004; Webb et al., 2004). RASSF1C expression has previously been shown to activate ERK (Reeves et al., 2010). Additionally, SRC has been shown to activate PI3-K, which, through the recruitment of FAK and activation of Rac1, promotes motility (Cantley, 2002; Yip et al., 2007). Given that we have observed that RASSF1C expression can activate SRC and promote

`

motility it would be interesting to see whether RASSF1C expression affects motility through increase in ROCK activity and MLC phosphorylation.

Since we had shown that RASSF1C could promote motility and given that SRC has been implicated in promoting EMT and invasion, we decided to investigate the role that RASSF1C played in invasion. This was done using a mammosphere assay in matrigel. This assay showed that RASSF1C expression promoted tumourigenesis, since RASSF1C-expressing cells produced larger, more aggressive mammospheres than controls (Figure 3.18). This was also shown to be SRC dependent as both the SRC inhibitor Dasatinib and AZD0530 were able to revert this phenotype. Surprisingly, we also observed a significant reduction in the size and percentage of mammospheres with an aggressive phenotype in control cells treated with Dasatinib (Figure 3.18B and C). This could be explained with the variety of reported off-target effects of Dasatinib (Chan et al., 2012). Therefore, the more specific SRC inhibitor, AZD0530, was used to confirm our findings (Nam et al., 2013)(Figure 3.18).

Metastasis occurs through a set of steps termed the invasion-metastasis cascade (Fidler, 2003; Talmadge and Fidler, 2010). In order for the cancer cells to establish themselves at the site of distant metastasis, the cells have to pass through several matrix barriers: basement membranes, tissue compartments, vessels, perineural spaces and organ boundaries (Guarino, 2010). There are two types of invasion; mesenchymal-type, and amoeboid-type (Carragher et al., 2006; Price et al., 2004). The activation of Rac1 at the leading edge of the cell is crucial to the mesenchymal-type invasion. Rac1 can be activated by SRC and FAK, CAS or Paxillin. Rac1 driven remodelling of the cytoskeleton activates JNK signalling, which leads to the upregulation of matrix metalloproteases (MMPs) 2 and 9 which breakdown the ECM at the leading edge (Hsia et al., 2003; Van Slambrouck et al., 2009). The cell can move by breaking down the ECM creating a space into which to invade. SRC could also promote amoeboid-type invasion through the activation of Rho. This could occur through the loss of cell-cell junctions, recruitment of Par3 and Par6 and the activation of p190RhoGAP, which together with upregulation of RhoE inhibit Rho-dependent actomyosin contractility and lead to collective cell

`

migration (Hidalgo-Carcedo et al., 2011). If E-cadherin is lost due to RASSF1C expression and SRC activity, then there could be a rise in the activity of Rho, which would promote amoeboid invasion. It would be interesting to investigate the exact pathway through which RASSF1C cells invade. This could also depend on the surrounding matrix geometry (Tozluoglu et al., 2013).

In order to further support our *in vitro* data, which showed that RASSF1C expression increases tumourigenesis, we used an *in vivo* mouse model to assess the tumour formation in the brain. We saw significantly larger tumours in MDA-MB-231 cells stably expressing RASSF1C (Figure 3.19). One unanswered question is whether this increased tumourigenesis *in vivo* is SRC-dependent. This will be addressed in the future by treatment of the animals with either Dasatinib or AZD0530 post cell implantation. Given the results from the mammosphere assay, we would hypothesise that inhibition of SRC will impair the tumourigenic potential of the RASSF1C-expressing MDA-MB-231 cells. Previous work from the lab has shown that RASSF1C-expressing cells are more prone to undergo transendothelial migration, which requires disruption of junctions between adjacent cells, in order to squeeze between them (Data not shown). Therefore further *in vivo* experiments might be required to better understand the potential of RASSF1C-expressing cells to invade and populate sites of distant metastasis. One method to investigate the role of RASSF1C in metastasis would be to use cells, stably expressing RASSF1C, which are also prone to metastasise to particular organs, such as the bone (Myoui et al., 2003). By injecting these cells into a distant site, we can measure the potential of the cells to form metastasis into the bone, but also their potential for extravasation and metastatic site tissue remodelling.

Together the work presented in this chapter (summarised in Figure 3.20) shows that both RASSF1A RASSF1C can bind to SRC. In normal conditions RASSF1A and CSK can inactivate SRC; however, in cells where RASSF1A is lost due to promoter methylation, RASSF1C promotes SRC activation, targeting it to the plasma membrane. There, active SRC leads to disruption of the adherens junctions and E-

`

cadherin internalisation. Accumulated cytoplasmic E-cadherin is not recycled back to the sites of cell junctions, which promotes cell motility, invasion and tumourigenesis, both *in vitro* and *in vivo*.

Following on from this we aim to look at the other roles of RASSF1C in the induction of tumourigenicity and the supporting gene transcription.

`

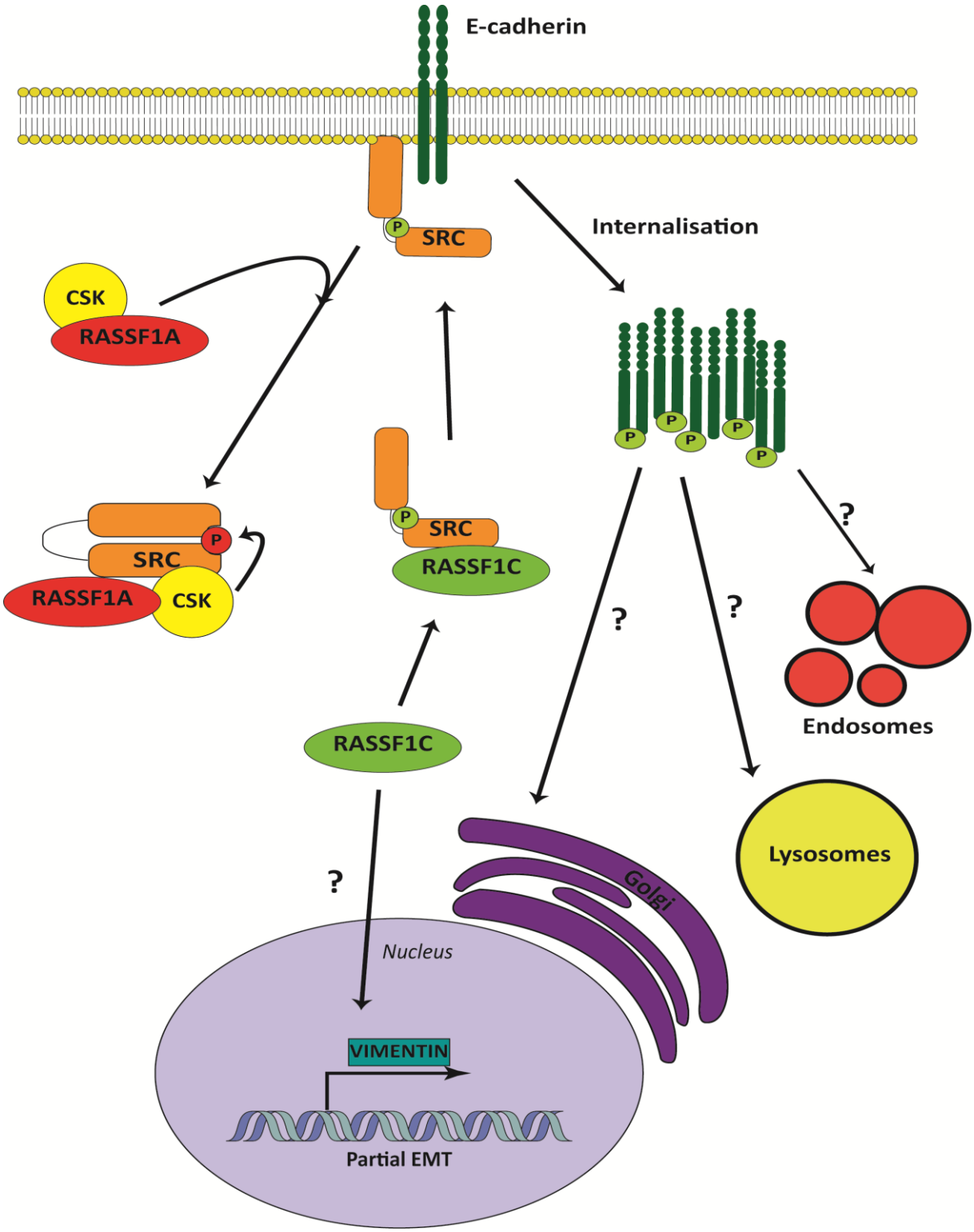


Figure 3.20. Cartoon Depicting the Hypothesis Generated from the Results in Chapter 3. SRC family kinases are activated in the perinuclear region by the binding of RASSF1C, promoting their translocation to the plasma membrane and subsequent activation by phosphorylation of the Y416 site. RASSF1A interacts with CSK and recruits CSK to SRC, promoting its inactivation by phosphorylation of Y527. At the plasma membrane, active SRC phosphorylates and disrupts E-cadherin, leading to E-cadherin internalisation and loss of cell-cell junctions. E-cadherin remains arrested in the cytoplasm, from where it can be further processed by association with the Golgi complex, endosomes or degraded in the lysosomes. In addition to loss of junctions, RASSF1C-expressing cells initiate partial EMT profile by upregulating Vimentin gene expression.

`

Chapter 4 RASSF1C Promotes YAP1 and β-catenin-Dependent Transcription

4.1 Introduction

In Chapter 3 we analysed the role RASSF1C plays in the destabilisation of junctional E-cadherin. It was found that RASSF1C, but not RASSF1A, was responsible for the activation of SRC, which consequently led to internalisation of E-cadherin and the increase in cell motility and tumourigenesis. We now move on to look at the consequences of this and its role in cancer development.

4.1.1 The Hippo Pathway

The core Hippo pathway was originally identified in genetic screens in *Drosophila melanogaster* for tumour suppressor genes. In *Drosophila*, the classical Hippo pathway is defined as a serine-threonine kinase cascade, consisting of the core kinases Hippo and Warts; the adaptors, Salvador and Mats; a number of upstream modulators such as Expanded, Merlin, Fat and Dachsous; and a transcriptional module made up from Yorkie and Scalloped, that regulate the expression of genes that control growth, such *diap1, cyclin E* and the miRNA *bantam* (Genevet and Tapon, 2011). Each of the components of the *Drosophila* pathway is represented by mammalian orthologues. Hippo is represented by Mammalian Sterile 20-like kinase 1 (MST1, also known as STK4) and Mammalian Sterile 20-like kinase 2 (MST2, also known as STK3); Warts, by Large Tumour Suppressor 1 (LATS1) and Large Tumour Suppressor 2 (LATS2); Yorkie by two closely related paralogues YES-associated protein (YAP1) and the Transcriptional co-activator with PDZ-binding motif (TAZ, also known as WWTR1) (Oka et al., 2008; Zhao et al., 2007). YAP1 and TAZ are transcriptional co-activators, which

`

are not able to bind directly to DNA. Instead, they form complexes with the sequence specific transcription factors TEA Domain-containing family members (TEAD1 to TEAD4)(Scalloped in *Drosophila*) as their main partners (Goulev, 2008; Vassilev et al., 2001; Wu et al., 2008a; Zhang, 2008; Zhao, 2008). YAP1 and TAZ can also bind to other transcription factors to regulate gene expression such as p73, RUNT-related transcription factor 1 (RUNX1) and RUNX2, T-box transcription factor 5 (TBX5) and SMADs (Johnson and Halder, 2014; Moroishi et al., 2015).

The activation of the Hippo pathway is associated with the activation of the MST and LATS kinases. In complex with SAV1 (*Drosophila* Salvador), the MST1/2 kinases can phosphorylate and activate the LATS1/2 kinases and MOB1 (*Drosophila* Mats) cofactors (Callus et al., 2006; Chan, 2005; Praskova et al., 2008; Wei et al., 2007; Wu et al., 2003). In turn, LATS1/2 and MOB1 phosphorylate the downstream targets YAP1 (at S127) and TAZ (at S89), resulting in their nuclear export, cytoplasmic retention and β-TRCP (β-transducin repeat-containing E3 ubiquitin protein ligase)-dependent degradation by the proteasome (Dong et al., 2007; Hao et al., 2008; Huang et al., 2005; Lei, 2008; Liu, 2010; Oh and Irvine, 2008; Oka et al., 2008; Ren et al., 2009; Zhao et al., 2010; Zhao et al., 2007). Therefore, when the Hippo pathway is activated, YAP1 and TAZ activity is inhibited, leading to a suppression of YAP1- and TAZ-driven gene expression. Conversely, when the Hippo pathway is inactive, YAP1 and TAZ accumulate in the nucleus, where they form complexes with transcription factors and drive gene expression.

In mammals, the Hippo pathway is regulated by four main interconnected upstream branches that include: regulators that act upstream of MST kinases; the Crumbs (CRB) complex; the actin cytoskeleton; and the adherens junctions (Figure 4.1). The upstream kinases and regulators that modulate the activity of MST kinases include the TAO (Thousand And One amino acid protein) kinases; the MAP/microtubule affinity-regulating kinase 1 (MARK1; also known as PAR1), a cell polarity kinase that directly phosphorylates MST (Boggiano et al., 2011; Huang, 2013; Poon et al., 2011); and the adaptor protein KIBRA (Kidney and Brain protein, WWC1)(Genevet et al., 2010).

`



Figure 4.1. The Hippo Pathway Network. The Hippo pathway network as described in Chapter 4. Components of the pathway that promote the activity of Yes-associated protein (YAP) and transcriptional co-activator with PDZ-binding motif (TAZ) are shown in green. The components that inhibit YAP and TAZ activity are shown in red. Pointed and blunt arrowheads indicate activating and inhibitory interactions, respectively. AMOT, angiomotin; β-TRCP, β-transducin repeat-containing E3 ubiquitin protein ligase; CRB, Crumbs homolog; GPCR, G protein-coupled receptor; KIBRA, kidney and brain protein; LATS, large tumour suppressor homolog; MARK, MAP/microtubule affinity-regulating kinase; MASK, multiple ankyrin repeats single KH domain-containing protein; MOB1A, MOB kinase activator 1A; MST, mammalian STE20-like protein kinase; NF2, neurofibromin 2 (also known as Merlin); PATJ, PALS1-associated tight junction protein; RASSF, RAS association domain-containing family protein; SAV1, Salvador homolog 1; TAO, thousand and one amino acid protein kinase; TEAD, TEA domain-containing sequence-specific transcription factor; ZO, zona occludens protein. Figure is adapted from (Johnson and Halder, 2014).

`

In *Drosophila*, Kibra regulates Hippo signalling in conjunction with Expanded and Merlin (Hamaratoglu, 2006; Yu, 2010).

A second branch is the CRB complex, containing apically localised transmembrane proteins, which assemble multiprotein complexes that function in cell polarity and regulate the Hippo pathway (Chen, 2010; Robinson et al., 2010; Varelas, 2010). This regulation is achieved by the recruitment of members of the angiomotin (AMOT) family of adaptor proteins that bind directly to components of the Hippo pathway. Initially, AMOT was thought to bind directly to YAP1 and to lead to its LATS-dependent phosphorylation and nuclear exclusion (Paramasivam et al., 2011; Wang et al., 2011b; Yi, 2011; Zhao, 2011), but recently it has been shown to promote nuclear localisation of YAP1, TEAD-dependent gene expression, and *in vivo*, a YAP1-dependent overgrowth of Neurofibromin 2(Nf2, *Drosophila* Merlin)-mutant mouse livers (Yi, 2013).

The third branch of the Hippo pathway involves a signalling mechanism, mediated by the actin cytoskeleton, where the cell matrix attachment and the mechanical properties of the extracellular matrix regulate the activity and localisation of YAP1 and TAZ, through a process that requires F-actin (Dupont et al., 2011; Sansores-Garcia et al., 2011; Wada et al., 2011). This process is also present in *Drosophila* (Fernandez, 2011). F-actin acts downstream of the MST kinases, but the exact mechanism is unclear and may involve LATS-dependent and –independent regulation of YAP1 and TAZ (Aragona et al., 2013; Zhao et al., 2012). In addition, extracellular cues such as lysophosphatidic acid and sphingosine-1, which act via G protein-coupled receptors and Rho GTPases, can modulate the actin cytoskeleton and YAP1/TAZ activity (Miller, 2012; Mo et al., 2012; Yu, 2012).

The fourth branch involves the adherens junctions. The nuclear localisation and activity of YAP1 is suppressed, via MST, by E-cadherin at the adherens junctions (Kim et al., 2011). Also, the E-cadherin-associated protein α-catenin regulates YAP1 directly, sequestering YAP1-14-3-3 complexes to the cytoplasm (Schlegelmilch et al., 2011; Silvis et al., 2011). Members of Ajuba, a junction-associated protein family, directly inhibit LATS kinase activity (Das Thakur, 2010). However, it remains unclear whether these junction-associated regulators of the Hippo pathway function independently or

`

coordinately of each other. Interestingly, crosstalk between the different regulatory branches exist, since CRB and the adherens junctions regulate the actin cytoskeleton and polarity proteins (Muthuswamy and Xue, 2012; Twiss and de Rooij, 2013).

In addition to the four branches of upstream Hippo regulators, there are other proteins, most of which conserved in *Drosophila*, that modulate the activity of the pathway. These include direct interactors with YAP1 and TAZ, such as β-TRCP, casein kinase 1, 14-3-3 protein, WW domain-containing protein (WBP2), multiple ankyrin repeats single KH domain-containing protein (MASK), zona occludens protein (ZO1), ZO2 and casein kinase 1 (CSNK1) (Johnson and Halder, 2014). WNT pathway stimulation can also induce YAP1/TAZ signalling by reducing the association of the β-catenin destruction complex with YAP1/TAZ, which stabilises β-catenin and promotes the nuclear accumulation of YAP1/TAZ (Azzolin et al., 2014). Other proteins that interact with upstream Hippo kinase complexes include: protein phosphatase 2A (PP2A)(Ribeiro et al., 2010), Scribble, the Scribble-associated proteins discs large (Dlg) and lethal giant larvae (Lgl)(Chen et al., 2012a; Cordenonsi et al., 2011) and the RAS association domain-containing family proteins (RASSFs) (Polesello et al., 2006; Praskova et al., 2004).

4.1.2 YAP1 and RASSF1A

In *Drosophila*, dRASSF (homologous to RASSF6 in mammals) inhibits Hippo in two ways: by competing with the positive regulator of Hippo, Salvador; and by bringing Hippo into close proximity with the dSTRIPAK-PP2A complex leading to dephosphorylation and inactivation of Hippo (Polesello et al., 2006; Ribeiro et al., 2010). In mammals, RASSF1A makes two significant interactions through its SARAH domain: with MST1/2 and with SAV1. Unlike in *Drosophila*, RASSF1A interaction with MST1/2 results in MST trans-phosphorylation and auto-activation (Glantschnig et al., 2002). The interaction also prevents dephosphorylation of MST1/2 (Guo et al., 2011). Following DNA damage, signalling through RASSF1A-MST leads to activation of the LATS1/2 (Guo et al., 2007; O'Neill et al., 2005) and

`

phosphorylation of YAP1. However, unlike when stimulated by canonical pathway signals, RASSF1A-dependent phosho-YAP1 maintains in the nucleus, switching binding partner from the anti-apoptotic, YAP1-TEAD complex to a pro-apoptotic YAP1-p73 complex (Hamilton et al., 2009; Matallanas et al., 2007; Yee and O'Neill, 2010). The interaction between YAP1 and p73 stabilises p73, preventing its nuclear export and subsequent degradation, and promoting its interaction with PUMA (Basu et al., 2003; Dobbelstein et al., 2005; Hamilton et al., 2009; Melino et al., 2004).

It has been well recognised that deregulation of the Hippo pathway and especially YAP1/TAZ activation can lead to the development of neoplasia and cancer (Harvey et al., 2013; Moroishi et al., 2015). Active YAP1 has been linked to K-RAS tumourigenicity (Hong et al., 2014; Kapoor et al., 2014; Shao et al., 2014; Zhang et al., 2014b; Zhang et al., 2014c), EMT (Chen et al., 2012b; Shao et al., 2014), resistance to anoikis (Zhao et al., 2012), and metastasis (Lamar et al., 2012). The pathway from RASSF1A to YAP1, originally shown to be activated by Fas signalling (Matallanas et al., 2007), has now also been linked to upstream activation through oncogenic K-Ras (Matallanas et al., 2011). The activation of MST2 by RASSF1A was shown to be blocked by wildtype K-Ras activation of AKT, which can phosphorylate MST2 (Matallanas et al., 2011). This phosphorylation limits MST2 activity by inhibiting its formation of an active complex with RASSF1A and promoting the formation of an inhibitory complex with Raf-1 (Romano et al., 2010). Thus, YAP1 can act as an oncogene and a tumour suppressor in a RASSF1A context-dependent manner.

4.1.3 Aims

The work in Chapter 3 highlighted a novel role for RASSF1A and RASSF1C in the regulation of SRC, leading to changes in the stability of E-cadherin and the adherens junctions. E-cadherin can regulate the Hippo pathway activation and inhibition of YAP1 (Kim et al., 2011). Also, YAP1 is known to be sequestered to the sites of cell-cell junctions by α-catenin and Angiomotin (Chan, 2011; Schlegelmilch et al., 2011; Zhao, 2011). RASSF1A has been shown to regulate the functions of YAP1,

`

but the role of RASSF1C in this process remains unclear. Therefore, the work shown in this chapter aims to uncover whether RASSF1C expression, and the consequent disruption of E-cadherin, leads to an increase in YAP1 activity and transcription.

4.2 RASSF1C Expression Leads to E-cadherin Destabilisation and YAP1 Nuclear Localisation

RASSF1A is an important upstream regulator of YAP1 signalling, promoting the switch of YAP1 from binding oncogenic proteins, such as TEAD, to binding tumour suppressor proteins, such as p73 (Matallanas et al., 2007; van der Weyden et al., 2012). In Chapter 3 I showed that RASSF1C expression promoted E-cadherin destabilisation. It has been previously shown that loss of junctional components like E-cadherin (Kim et al., 2011) or α-catenin (Schlegelmilch et al., 2011; Silvis et al., 2011) lead to the destabilisation of adherens junctions which in turn results in the relocalisation of the transcriptional activator YAP1. Given that RASSF1C is an oncogene that is able to destabilise E-cadherin through activation of SRC, we sought to investigate whether RASSF1C expression would also promote nuclear accumulation of YAP1. In order to test this we transiently transfected MCF7 cells with either E-cadherin, or E-cadherin mutant for the three tyrosine sites that active SRC phosphorylates (Y3F) and either DsRed-control, or DsRed-RASSF1C before staining cells for YAP1 localisation. In cells expressing the control plasmid, both GFP-E-cadherin and GFP-E-cadherin Y3F are localised to the membrane and YAP1 appears cytoplasmic. However, in cells expressing RASSF1C and GFP-E-cadherin, where the GFP-E-cadherin is destabilised and re-localised to the cytoplasm, as we have previously observed in Chapter 3, we observe an increase in YAP1 nuclear localisation (Figure 4.2). However, when RASSF1C is coexpressed with GFP-E-cadherin Y3F, which is not destabilised and relocalised to the cytoplasm, we do not observe increased nuclear YAP1 localisation. This indicates that RASSF1C expression activates SRC, leading to the destabilisation of E-cadherin at the junctions. This destabilisation releases oncogenes, such as YAP1, which are sequestered at the junctions,

`

allowing them to move to the nucleus. This led us to investigate the role that RASSF1C plays in YAP1 activity as an oncogene.

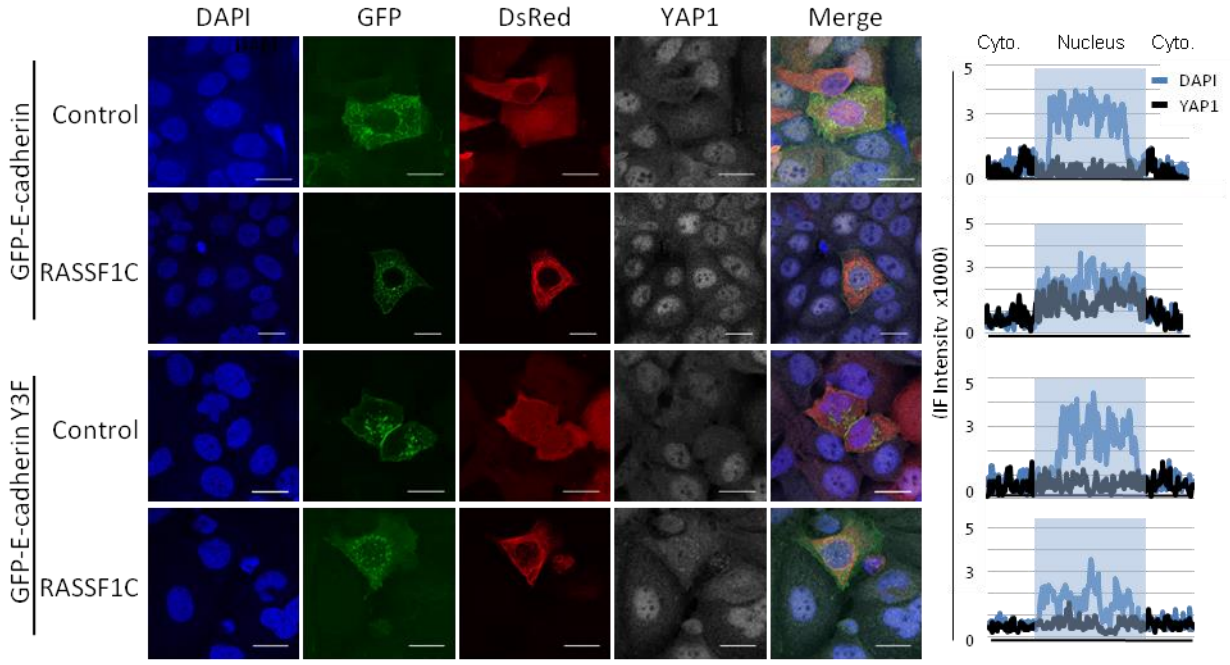


Figure 4.2. RASSF1C Expression Leads to E-cadherin Destabilisation and YAP1 Nuclear Localisation. Left: Representative images showing the localisation of E-cadherin and YAP1 in MCF7 cells (3 x 10^5 cells/condition), which were plated onto glass cover slips and transfected with DsRed-empty vector, or DsRed-RASSF1C plasmids and either GFP-E-cadherin, or GFP-E-cadherin mutant. Cells were fixed for 15 mins with 4 % PFA, permeabilised for 5 mins with 0.2 % Triton X solution and blocked for 30 mins with 0.2 % FSG. Cells were probed with anti-YAP1 antibody. Secondary antibody was Alexa-fluor 633 nm. Cover slips were mounted onto slides using mounting media containing DAPI. Images were taken using a Zeiss LSM 780 microscope at 63 x magnification. Scale bars represent 20 μm. Right: Representative distribution of DAPI (blue) and YAP1 (black) across equatorial cell vector, determined by immunofluorescence and measured using Zeiss Zen 2010. Cells expressing RASSF1C and GFP-E-cadherin show destabilized, internalized E-cadherin and nuclear accumulation of YAP1. Cells expressing RASSF1C and GFP-E-cadherin Y3F mutant do not show destabilisation of E-cadherin, which remains at the cell-cell junctions and YAP1 remains in the cytoplasm.

`

4.3 Loss of RASSF1A Mediates Nuclear Localisation of YAP1

Having shown that expression of RASSF1C leads to YAP1 nuclear localisation in cells that do not express RASSF1A and the previously discussed functions of RASSF1A in the inhibition of YAP1, we decided to investigate how the localisation of YAP1 is regulated when we alter RASSF1A and RASSF1C expression levels in cells that express both isoforms. The activation of the Hippo pathway in mammals leads to the phosphorylation of YAP1 at the pS127 site and its cytoplasmic localisation (Dong et al., 2007). We have previously observed a significant correlation between the loss of the *RASSF1A* gene due to hypermethylation and the low levels of pS127-YAP1 in clinical samples from Glioma, Bladder and Breast cancer cohorts from The Cancer Genome Project (TCGA) (Vlahov et al., 2015). This suggested that YAP1 could be active and nuclear in cells that have lost RASSF1A. In order to test this hypothesis we used siRNA to downregulate the expression of RASSF1A in U2OS cells, which unlike many cancer cell lines retain the expression of both RASSF1A and RASSF1C. We transiently transfected U2OS cells with either non-targeting siRNA (siNT), or siRNA targeting all the RASSF1 isoforms (siRASSF1); or siRNA that specifically targets the RASSF1A isoform (siRASSF1A). Cells were incubated for 48 hrs post transfection, after which they were collected and stained for pS127-YAP1 and total YAP1. The RASSF1C isoform is susceptible to siRASSF1, since it targets the shared C-terminal end. There was no difference in the levels of pS127-YAP1 and nuclear YAP1 in cells transfected with siRASSF1, compared to control (Figure 4.3A). However, the specific ablation of the RASSF1A isoform appeared to increase nuclear localisation of YAP1, and a decrease in the cytoplasmic levels of pS127-YAP1. Quantification of the images confirmed nuclear YAP1 was increased in cells specifically ablated for RASSF1A (Figure 4.3B and C). Taken together, the data suggests that in cells that have lost RASSF1A, but retain the expression of RASSF1C, YAP1 is localised into the nucleus.

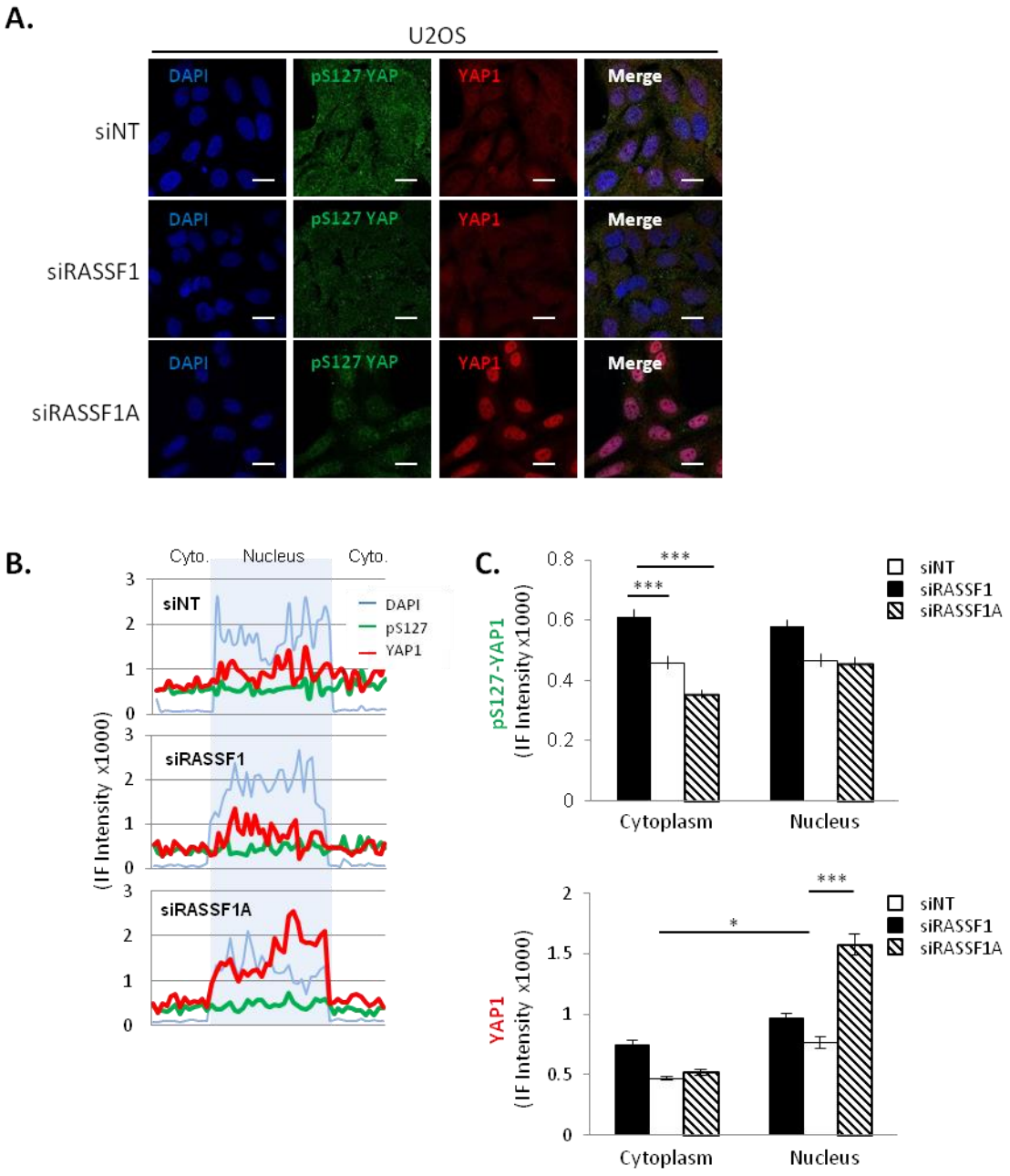


Figure 4.3. Loss of RASSF1A Mediates Nuclear Localisation of YAP1. A. Representative images showing the localisation of pS127-YAP1 and total YAP1 levels in U2OS cells (3 x 10^5 cells/condition), which were plated onto glass cover slips and transfected with either siNT, siRASSF1 or siRASSF1A and incubated for 48 hrs. Cells were fixed for 15 mins with 4 % PFA, permeabilised for 5 mins with 0.2 % Triton X solution and blocked for 30 mins with 0.2 % FSG. Cells were probed with the anti-YAP1 or anti pS127-YAP1 antibodies. Secondary antibodies were Alexa-fluor 488 nm and Alexa-fluor 594 nm. Cover slips were mounted onto slides using mounting media containing DAPI. Images were taken using a Zeiss LSM 780 microscope at 63 x magnification. Scale bars represent 10 μm. **B**. Representative distribution of DAPI (blue), pS127-YAP1 (green) and YAP1 (red) across equatorial cell vector, determined by immunofluorescence and measured using Zeiss Zen 2010. **C.** Graphs representing the intensity of pS127-YAP1 (Top) and YAP1 (Bottom) in the nucleus and the cytoplasm. The intensity was measured by using 2 separate equatorial vectors per cell. Data is representative of three independent experiments. * $p < 0.05$, *** $p < 0.001$. Error bars represent 1 x SEM. In cells with RASSF1A, but not both RASSF1A and RASSF1C knock down, YAP1 is localised at the nucleus. Knockdown of both RASSF1A and RASSF1C (siRASSF1) or RASSF1A alone led to decrease in the cytoplasmic pS127-YAP1.

`

In order to further evaluate the localisation of YAP1 in the U2OS cells, we transiently transfected the cells with siNT, siRASSF1 and siRASSF1A before performing a nuclear-cytoplasmic fractionation of the cells. In agreement with the immunofluorescence data (Figure 4.3A), the levels of YAP1 in the nuclear fraction of the cells transfected with siRASSF1A were higher than for cells transfected with either siNT, or siRASSF1 (Figure 4.4A). We also observed that when RASSF1A and RASSF1C (siRASSF1), or RASSF1A alone were lost, there was a reduction in the total pS127-YAP1 levels, which also agrees with the immunofluorescence data (Figure 4.4A). This suggests that RASSF1C could reduce the levels of pS127-YAP1 due to the loss of RASSF1A-dependent regulation of the Hippo pathway. Given that loss of RASSF1A and RASSF1C led to increased nuclear localisation, but loss of RASSF1A alone did not, when both conditions led to a reduction of pS127-YAP1, we hypothesized that reduced pS127-YAP1 is required, but insufficient for nuclear YAP1 localisation in cells expressing RASSF1C.

In order to test this hypothesis, we expressed RASSF1C in MDA-MB-231 and H1299 cells, which do not express RASSF1A, and looked for changes in pS127-YAP1. We found that in these cell lines the overexpression of RASSF1C did not affect the levels of pS127-YAP1 (Figure 4.4B), suggesting that although overexpression of RASSF1C is able to change the localisation of YAP1 and loss of RASSF1A and RASSF1C lead to loss of pS127-YAP1, RASSF1C loss alone does not affect the phosphorylation of pS127. Therefore, in agreement with the TCGA data, loss of RASSF1A must be responsible for the effects we observed on pS127-YAP1. We next wanted to investigate whether RASSF1C was able to promote nuclear YAP1.

`

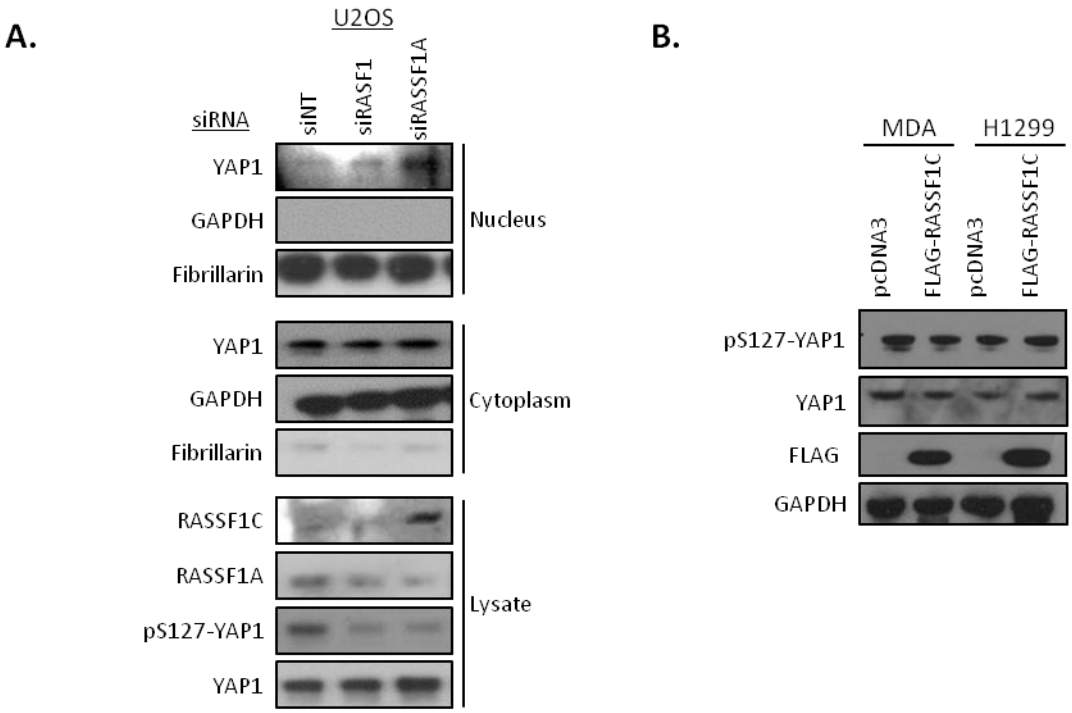


Figure 4.4. RASSF1A Loss Leads to Increase in Nuclear Localisation of YAP1. A. Nuclear/cytoplasmic fractionation of U2OS cells (2 x 10^6cells/plate), which were transfected with siNT, siRASSF1 or siRASSF1A. Cells were trypsinised and washed twice with ice cold PBS and collected by centrifugation (500 x g, 5 min). Cells were then kept on ice and processed using NE-PER^{TM} Nuclear and Cytoplasmic Extraction kit (Thermo Scientific), following manufacturer's instructions. Samples were analysed by SDS-PAGE and western blot for the indicated antibodies. YAP1 is localised to the nucleus when RASSF1A, but not when RASSF1A and RASSF1C, are depleted from the cells. **B**. Western blot showing the total levels of YAP1 and pS127-YAP1 in MDA-MB-231 and H1299 cells (2.5 x 10^5 cells/well), transfected with either control vector or FLAG-RASSF1C . Cells were lysed with laemmli lysis buffer and analysed by SDS-PAGE and western blot with the indicated antibodies. The expression of RASSF1C does not lead to increase in the total levels of YAP1 and pS127-YAP1.

4.4 The siRNA-Resistant RASSF1C Mutant Mediates Nuclear Localisation of YAP1

Having shown that loss of RASSF1A, but not loss of both RASSF1A and RASSF1C, leads to nuclear localisation of YAP1, we decided to further investigate the role RASSF1C plays in this process. We therefore generated mutated derivatives of RASSF1A and RASSF1C, designed to be resistant to two of the four sequences that make up the SMARTpool siRNA used thus far (known from now on as siRASSF1_1 and siRASSF1_2) (Scrace and University of Oxford). Each mutation made the construct resistant to one siRNA sequence from the SMARTpool. We transiently transfected U2OS cells with

`

either siNT or siRASSF1_1 or siRASSF1_2. The cells were also transfected with either pcDNA3 or the resistant forms of FLAG-RASSF1A (FLAG-RASSF1A Resist 1 and FLAG-RASSF1A Resist 2) and FLAG-RASSF1C (FLAG-RASSF1C Resist 1 and FLAG-RASSF1C Resist 2). The cells were collected after 48 hrs and stained for pS127-YAP1 and total YAP1. We hypothesised that the overexpression of the resistant forms of RASSF1C would promote nuclear localisation of YAP1, both when treated with siNT or the two siRASSF1 sequences from the siRASSF1 SMARTpool. As before, loss of RASSF1 did not alter the nuclear localisation of YAP1 vs siNT and the re-expression of RASSF1A into the cells, treated with siRASSF1, also had no effect. In agreement with our hypothesis, expression of the siRNA resistant RASSF1C construct led to an increase in nuclear YAP1 (Figure 4.5A and B). When quantified, the difference was shown to be significant (Figure 4.6A). Interestingly, the expression of RASSF1C did not affect the pS127-YAP1 levels. These data show that the translocation of YAP1 away from the nucleus when both RASSF1A and RASSF1C were depleted was due to loss of RASSF1C, as re-expression under conditions where both isoforms were lost, gave the same result as when only RASSF1A was lost.

The expression of the two siRNA resistant isoforms of RASSF1C (Figure 4.6A) was associated with an increase in the nuclear YAP1, however, the RASSF1C_Resist_2 construct showed decreased effectiveness in resisting downregulation by the siRASSF1_2. Therefore, we focused on the RASSF1C_Resist_1 in order to further validate the observed increase in YAP1 localisation into the nucleus after RASSF1C expression. We performed a nuclear/cytoplasmic fractionation of the U2OS cells, expressing the resistant forms of the RASSF1A and RASSF1C. In agreement with the immunofluorescence data, we saw that RASSF1C expression restored nuclear YAP1 in the siRASSF1_1 transfected cells, compared to siNT or the cells transfected with either pcDNA3 or RASSF1A_Resist_1 (Figure 4.6B). Given these data we concluded that RASSF1C expression promotes the accumulation of YAP1 in the nucleus.

`

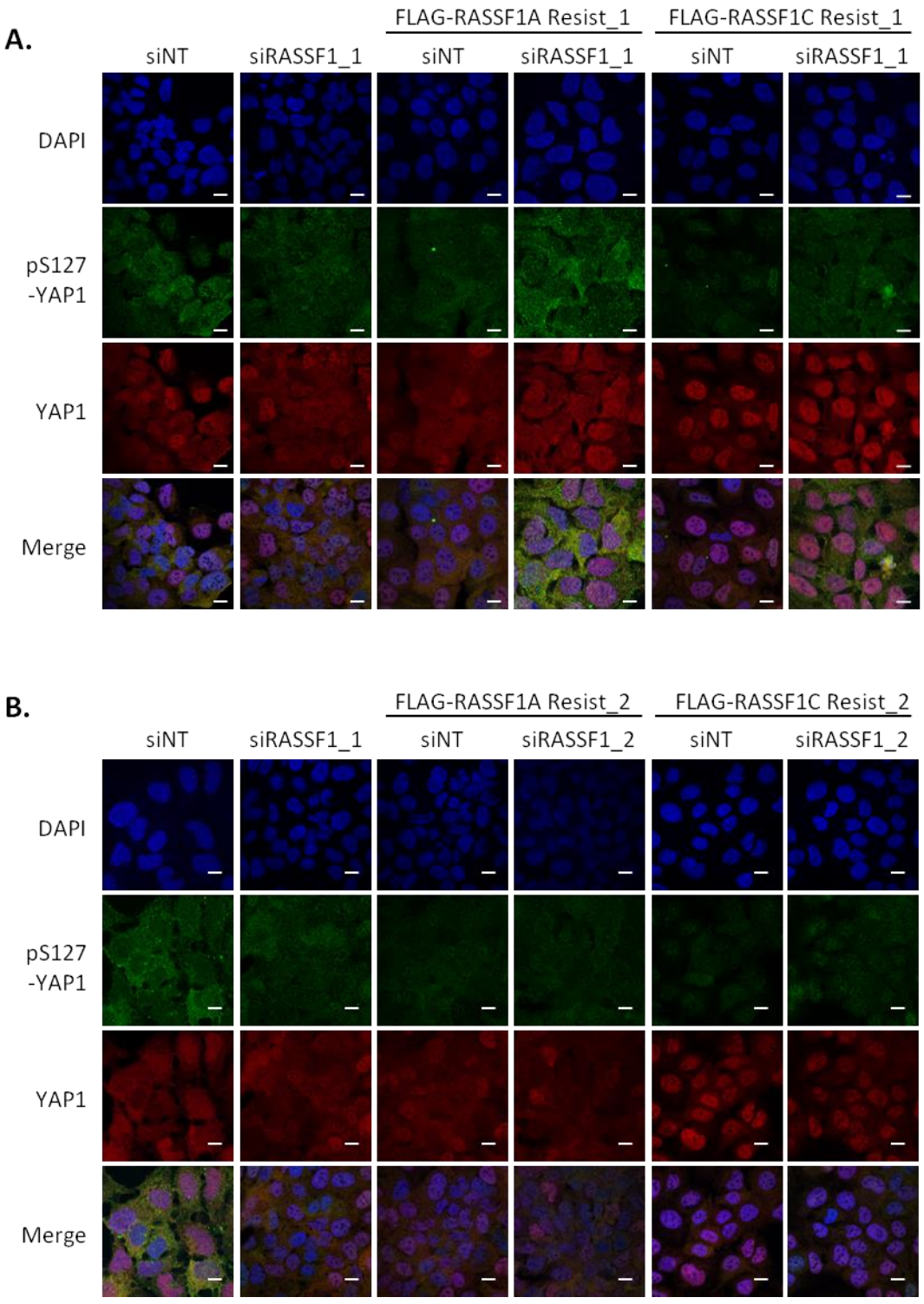


Figure 4.5. The siRNA Resistant Forms of RASSF1C Mediate Nuclear Localisation of YAP1. Representative images showing the localisation of pS127-YAP1 and total YAP1 levels in U2OS cells (3 x 10^5 cells/condition), which were plated onto glass cover slips and transfected with (**A.)** siNT, siRASSF1 sequence 1 (from SMARTpool siRASSF1) and pcDNA3, FLAG-RASSF1A or FLAG-RASSF1C, resistant to siRASSF1 sequence 1; or (**B.)** siNT, siRASSF1 sequence 2 (from SMARTpool siRASSF1) and pcDNA3, FLAG-RASSF1A or FLAG-RASSF1C, resistant to siRASSF1 sequence 2. Cells were probed with the anti-YAP1 or anti p127-YAP1 antibodies. Images were taken using a Zeiss LSM 780 microscope at 63 x magnification. Scale bars represent 10 μm. Overexpression of siRASSF1-resistant form of RASSF1C, but not of RASSF1A, leads to nuclear localisation of YAP1.

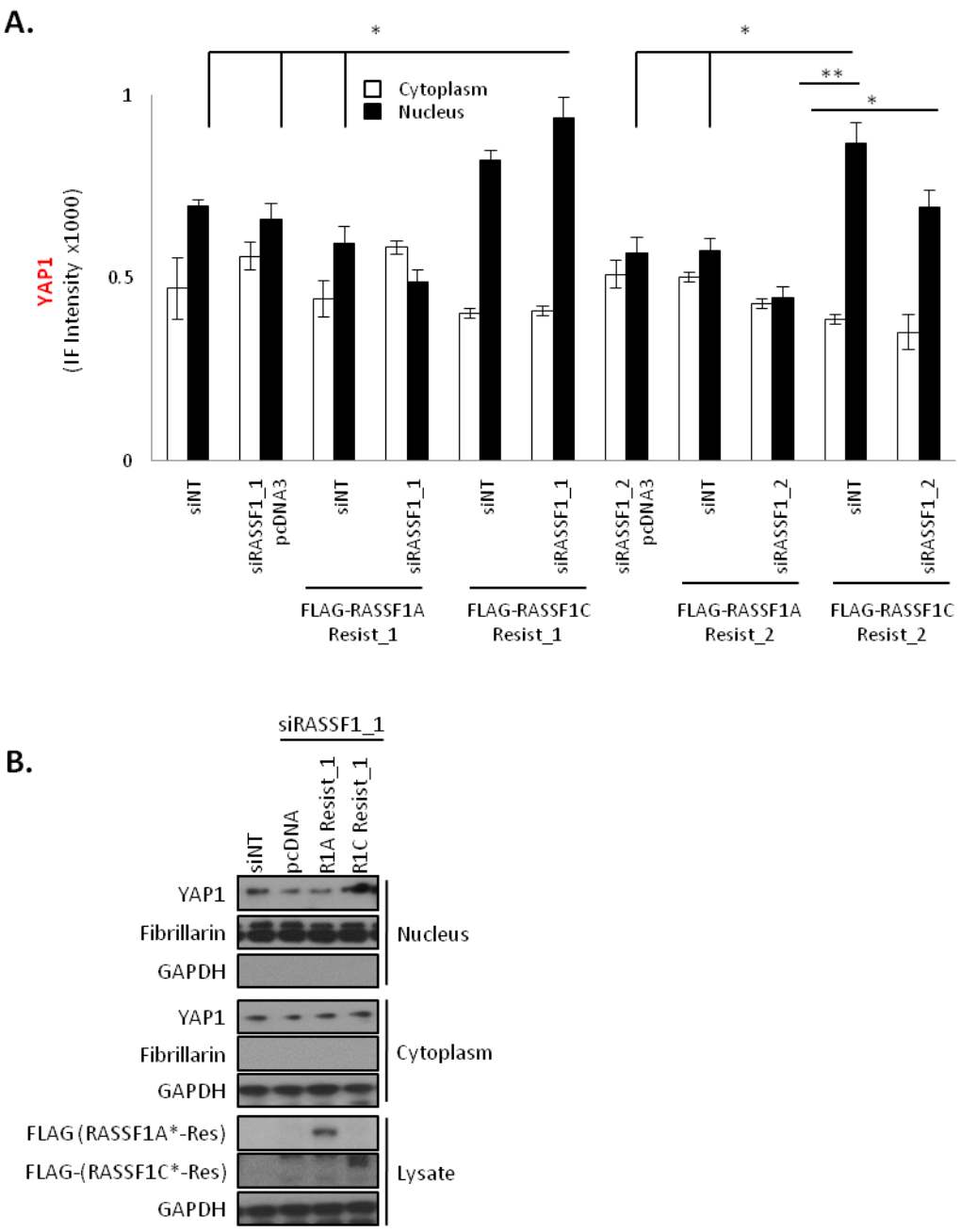


Figure 4.6. RASSF1C Promotes Nuclear YAP1. A. Bar graphs showing the intensity distribution of YAP1 in the cytoplasm and nucleus. U2OS cells (3 x 10^5 cells/condition), were plated onto glass cover slips and transfected with siNT, siRASSF1 sequence 1 (from SMARTpool siRASSF1) and pcDNA3, FLAG-RASSF1A or FLAG-RASSF1C, resistant to siRASSF1 sequence 1; or siRASSF1 sequence 2 (from SMARTpool siRASSF1) and pcDNA3, FLAG-RASSF1A or FLAG-RASSF1C, resistant to siRASSF1 sequence 2. Cells were probed with the anti-YAP1 or anti p127-YAP1 antibodies. Images were taken using a Zeiss LSM 780 microscope at 63 x magnification. Immunofluorescence intensity was measured by using 2 separate equatorial cell vectors. Data is representative of three independent experiments. * $p \leq 0.05$, ** $p \leq 0.01$. Error bars represent 1 x SEM. Overexpression of siRASSF1-resistant form of RASSF1C leads to nuclear localisation of YAP1. **B.** Nuclear/cytoplasmic fractionation of U2OS cells (2 x 10^6 cells/plate), which were transfected with either siNT or siRASSF1_1 and either pcDNA3 or siRASSF1_1-resistant forms of FLAG-RASSF1A and FLAG-RASSF1C. Cells were processed using NE-PER™ Nuclear and Cytoplasmic Extraction kit (Thermo Scientific), following manufacturer's instructions. Samples were analysed by SDS-PAGE and western blot for the indicated antibodies. YAP1 is localised to the nucleus when the siRASSF1-resistant form of RASSF1C is expressed.

`

4.5 RASSF1C Expression Promotes pY357-YAP1 Phosphorylation

We have previously identified that RASSF1C can bind to the SFKs- SRC, FYN and YES. We have shown that RASSF1C expression leads to SRC activation, which promotes loss of cell-cell junctions and leads to YAP1 nuclear localisation. YAP1 was originally identified as YES-Associated Protein (Sudol et al., 1995). YAP1 has been shown to bind to YES and SRC (Zaidi et al., 2004) and to be phosphorylated by the SFK in embryonic stem cells (Tamm et al., 2011). YES was recently shown to phosphorylate YAP1 at tyrosine 357 (Levy et al., 2008; Rosenbluh et al., 2012). Given these points, we hypothesised that RASSF1C expression could lead to phosphorylation of YAP1 at Y357 via its activation of SFKs. In order to test this we exogenously expressed pcDNA3 or FLAG-RASSF1C in U2OS cells. After 48 hrs the cells were collected and tyrosine phosphorylated proteins were immunoprecipitated with an anti-phospho-tyrosine antibody. Samples were then analysed by SDS-PAGE gel and western blot for YAP1. As predicted, RASSF1C expression led to an increased phosphorylation of tyrosine YAP1 (Figure 4.7A), which we hypothesised to be at the Y357 site. In order to test this further, we investigated the localisation of pY357-YAP1 in U2OS cells, transiently transfected with siNT, siRASSF1 or siRASSF1A by immunofluorescence. The immunofluorescence images show that the loss of RASSF1A, unlike loss of both RASSF1 isoforms, leads to nuclear localisation of YAP1, which overlaps with the staining for pY357-YAP1 (Figure 4.7B). We further confirmed the increase in nuclear localisation of YAP1 and pY357-YAP1 in the U2OS cells transfected with siRASSF1A by nuclear/cytoplasmic fractionation (Figure 4.7C). Combined, these data suggest that loss of RASSF1A and subsequent activation of RASSF1C leads to the accumulation of YAP1 in the nucleus and that is phosphorylated at Y357.

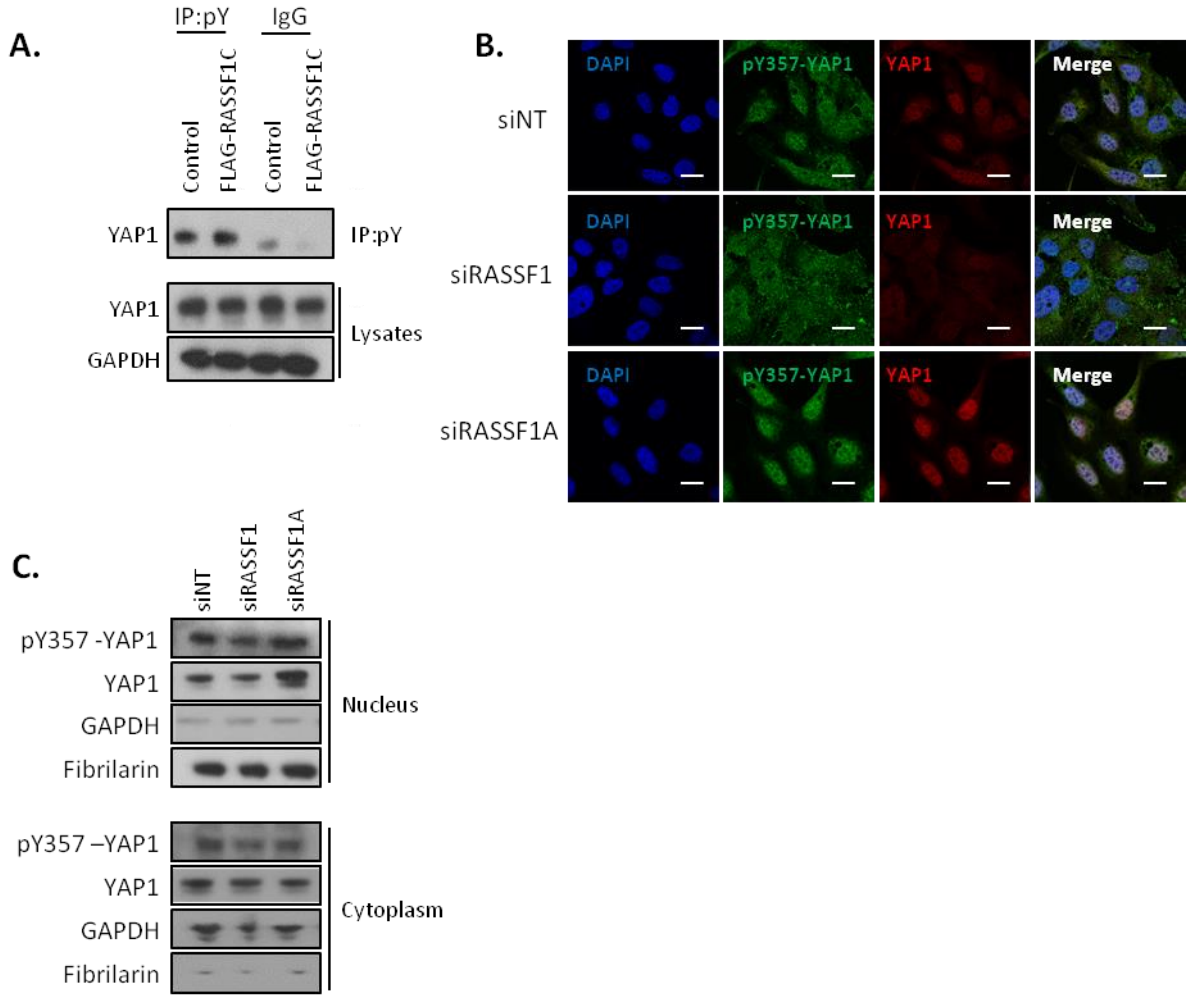


Figure 4.7. Expression of RASSF1C Leads to Activation of YAP1 at pY357. A. Immunoprecipitation of U2OS cells (2 x 10^5 cells/plate) transfected with either pcDNA3 or FLAG-RASSF1C. Cells were lysed by scraping into 0.5 % NP40, 150 mM NaCl lysis buffer supplemented with protease and phosphatase inhibitors. Lysates were immunoprecipitated for 3 hrs with anti-phosphotyrosine antibody. Proteins were recovered from the beads by boiling for 5 mins in 1 x loading buffer and samples were analysed by SDS-PAGE and western blot for YAP1. Cells expressing RASSF1C have higher levels of tyrosine phosphorylated YAP1, compared to controls. **B.** Representative images showing the localisation of YAP1 and pY357-YAP1 in U2OS cells (1 x 10^5 cells/well), transfected with either siNT, siRASSF1 or siRASSF1A. Cells were fixed for 15 mins with 4 % PFA, permeabilised for 5 mins with 0.2 % Triton X solution and blocked for 30 mins with 0.2 % FSG. Cells were probed with anti-YAP1 and anti-pY357-YAP1 antibodies. Cover slips were mounted onto slides using mounting media containing DAPI. Images were taken using a Zeiss LSM 780 microscope at 63 x magnification. Scale bars represent 20 μm. Loss of RASSF1A, but not of both RASSF1A and RASSF1C, lead to the localisation of pY357-YAP1 in the nucleus. **C.** Nuclear/cytoplasmic fractionation of U2OS cells (2 x 10^6 cells/plate), which were transfected with siNT, siRASSF1 or siRASSF1A. Cells were processed using NE-PER™ Nuclear and Cytoplasmic Extraction kit (Thermo Scientific), following manufacturer's instructions. Samples were analysed by SDS-PAGE and western blot for the indicated antibodies. Increase in nuclear YAP1 and pY357-YAP1 occurs only when both RASSF1A and RASSF1C, but not RASSF1A alone, are lost.

`

Given that RASSF1A loss led to nuclear localisation of YAP1 and an increase in the levels of pY357-YAP1, we hypothesised that expression of RASSF1C should have the same effect. In order to test this, we imaged MDA-MB-231 cells, stably expressing either Control or MYC-RASSF1C, stained with anti-YAP1 and anti-pY357-YAP1 antibodies. In agreement with our hypothesis and previous experimental data (Figure 4.5 and 4.6), RASSF1C expression led to YAP1 localisation to the nucleus and increased staining for pY357-YAP1 (Figure 4.8A). We also wanted to examine the role of SFK in the phosphorylation of YAP1 in our system. We hypothesised that, given the increase of SRC activity in RASSF1C-expressing cells and the previously reported phosphorylation of Y357-YAP1 by SRC and YES (Rosenbluh et al., 2012), that RASSF1C expression would lead to SRC and YES activation and an increase in the pY357-YAP1 levels. Therefore, we transiently transfected H1299 cells with pcDNA3 or FLAG-RASSF1C with either ZsGreen-YES or ZsGreen-SRC before the cells were lysed and we analysed by SDS-PAGE gel and western blot for pY357-YAP1 and pY416-SRC. Firstly, the data showed that the expression of RASSF1C led to the activation of both YES and SRC. Secondly, in accordance with our hypothesis, we showed that RASSF1C expression with SRC, or YES, resulted in phosphorylation of YAP1 at Y357 (Figure 4.8B). Together, these data show that RASSF1C leads SFK-dependent phosphorylation of Y357-YAP1 and YAP1 nuclear localisation.

`

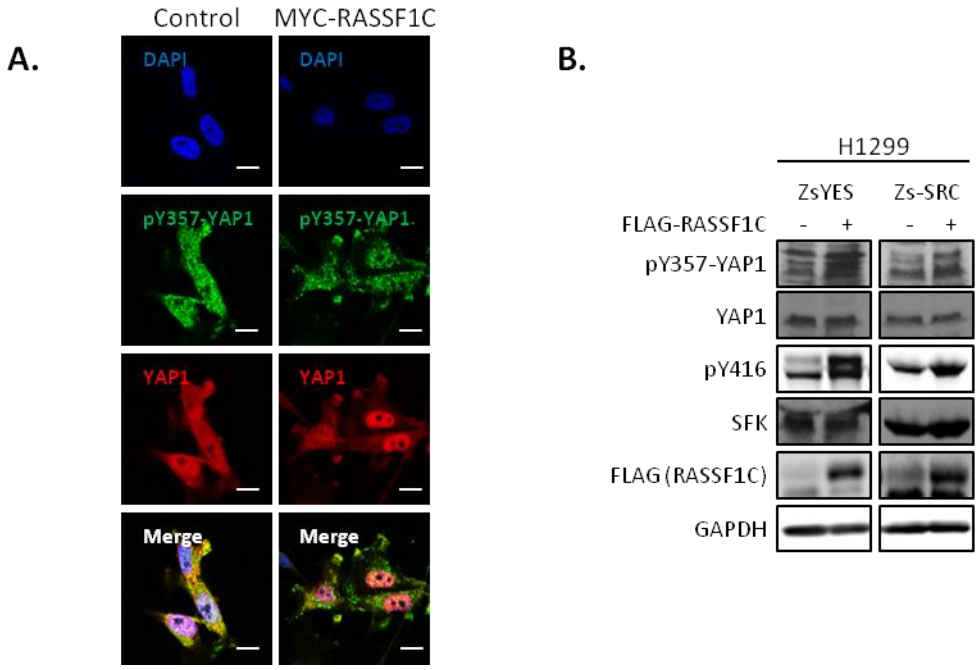


Figure 4.8. RASSF1C Expression Leads to YAP1 Phosphorylation. A. Representative images showing the localisation of YAP1 and pY357-YAP1 in MDA-MB-231 cells (1 x 10^5 cells/well), stably expressing either pcDNA3 or MYC-RASSF1C, plated onto glass cover slips. Cells were fixed for 15 mins with 4 % PFA, permeabilised for 5 mins with 0.2 % Triton X solution and blocked for 30 mins with 0.2 % FSG. Cells were probed with anti-YAP1 and anti-pY357-YAP1 antibodies. Cover slips were mounted onto slides using mounting media containing DAPI. Images were taken using a Zeiss LSM 780 microscope at 63 x magnification. Scale bars represent 20 μm. Overexpression of RASSF1C promotes the accumulation of YAP1 and pY357-YAP1 in the nucleus. **B.** Immunoprecipitation of H1299 cells (2 x 10^5 cells/plate) transfected with either pcDNA3 or FLAG-RASSF1C and ZsGreen-YES or ZsGreen-SRC plasmids. Cells were cultured for a total of 48 hrs and lysed with laemmli lysis buffer and analysed by SDS-PAGE and western blot with the indicated antibodies. The expression RASSF1C leads to SRC and YES activation and the consequent phosphorylation of YAP1 at the pY357 site.

4.6 β-catenin is Localised to the Nucleus in RASSF1C-Expressing Cells

In Chapter 3 we saw that RASSF1C expression leads to changes in the cell membrane dynamics. It has been shown that strong E-Cadherin contacts require β-catenin, which is protected from degradation through its interaction with E-cadherin (Estrabaud et al., 2007). We have seen that RASSF1C expression promotes the phosphorylation of E-cadherin and β-catenin (Figure 8.3). SRC phosphorylation of β-catenin decreases its affinity for E-cadherin, leading to its dissociation from the membrane (Coluccia et al., 2006; Roura et al., 1999). This allows β-catenin to enter the nucleus and

`

upregulate the transcription of target genes. These target genes include TCF4 (Korinek et al., 1997; Morin et al., 1997), HIF-1 (Kaidi et al., 2007) and androgen receptor (Mulholland et al., 2002). Furthermore, β-catenin was shown to bind to YAP1 in the nucleus, where they would drive a YES-dependent pro-tumorigenic program via the upregulation of anti-apoptotic genes (Rosenbluh et al., 2012). YAP1 and β-catenin have also been shown to co-regulate essential genes for cardiac development (Heallen et al., 2011). Having shown that RASSF1C expression leads to phosphorylation of β-catenin (Figure 8.4) we were interested in determining whether RASSF1C expression would promote β-catenin accumulation into the nucleus, where it is able to bind YAP1 (Rosenbluh et al., 2012). We transiently transfected H1299 cells with either pcDNA3, FLAG-RASSF1A, FLAG-RASSF1C or both FLAG-RASSF1A and FLAG-RASSF1C. The localisation of β-catenin was then analysed by nuclear/cytoplasmic fractionation. Cells expressing RASSF1A did not show any increase in nuclear β-catenin levels, compared to the control cells. However, expression of RASSF1C led to an increase in the nuclear β-catenin levels. Previous work done in the lab has shown that RASSF1A binds to and inhibits RASSF1C (Figure 8.6 and Data not shown). In agreement with these findings, cells co-expressing both RASSF1A and RASSF1C demonstrated similar levels of nuclear β-catenin to those expressing just RASSF1A or control plasmid. This suggests that RASSF1A expression inhibited the RASSF1C-dependent nuclear accumulation of β-catenin (Figure 4.9A). Immunofluorescence of H1299 cells transiently transfected with pcDNA3 or FLAG-RASSF1C was used to confirm that RASSF1C expression promoted nuclear accumulation of β-catenin (Figure 4.9B). Interestingly we saw that β-catenin was also lost from the sites of cell-cell junctions. Taken together, these data suggest that RASSF1C, through its activation of SRC and disruption of junctions, leads to the nuclear accumulation of β-catenin and that RASSF1A co-expression inhibits this process, in agreement with its inhibitory role on SRC and potentially RASSF1C.

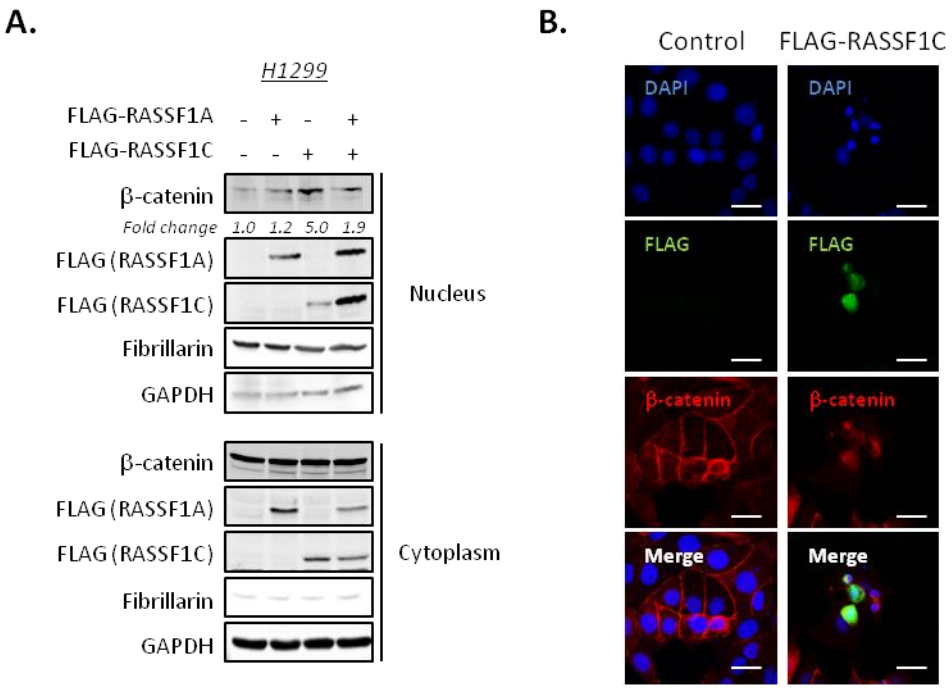


Figure 4.9. RASSF1C Leads to β-catenin Nuclear Localisation. A. Nuclear/cytoplasmic fractionation of H1299 cells (2 x 10^5 cells/plate) transfected with either pcDNA3, FLAG-RASSF1A, FLAG-RASSF1C or both. Cells were trypsinised and washed twice with ice cold PBS and collected by centrifugation (500 x g, 5 min). Cells were then kept on ice and processed using NE-PER™ Nuclear and Cytoplasmic Extraction kit (Thermo Scientific), following manufacturer's instructions. Samples were analysed by SDS-PAGE and western blot with the indicated antibodies. Blots are representative of three independent experiments which have been quantified using ImageJ software for β-catenin expression (values under β-catenin blot). RASSF1C expression, but not RASSF1A, leads to the nuclear localisation of β-catenin. Dual expression of both RASSF1A and RASSF1C led to a decrease in nuclear β-catenin. **B**. Representative images showing the localisation of β-catenin in H1299 cells (1 x 10^5 cells/well) plated onto glass cover slips and transfected with pcDNA3 or FLAG-RASSF1C. Cells were fixed for 15 mins with 4 % PFA, permeabilised for 5 mins with 0.2 % Triton X solution and blocked for 30 mins with 0.2 % FSG. Cells were probed with anti-FLAG and anti-β-catenin antibody. Cover slips were mounted onto slides using mounting media containing DAPI. Images were taken using a Zeiss LSM 780 microscope at 63 x magnification. Scale bars represent 20 μm. RASSF1C expression promotes the nuclear accumulation of β-catenin.

`

4.7 RASSF1C Expression Promotes Upregulation of Anti-Apoptotic Genes

Rosenbluh *et al.* recently showed that YAP1 and β-catenin both interact with (Murakami et al., 2005) and bind to the T-box transcription factor (TBX5) (Rosenbluh et al., 2012). Given that we have observed that RASSF1C drives YAP1 and β-catenin nuclear localisation, we sought to investigate whether RASSF1C expression was also driving a YAP1-β-catenin-dependent transcriptional response (Kaidi et al., 2007; Zhao et al., 2008). Together, YAP1 and β-catenin were shown to drive a YES-dependent pro-tumorigenic program via the upregulation of the anti-apoptotic genes *BIRC5* and *BCL2L1* (Rosenbluh et al., 2012). Once in the nucleus, β-catenin has been shown to bind to the transcription factors T-cell factor (TCF)/Lymphoid enhancer-binding factor (LEF) to promote transcription of WNT/β-catenin target genes, such as *cyclinD1* and *c-MYC* (He et al., 1998; Teuliere et al., 2005; Valenta et al., 2012). Given that YAP1 has been shown to induce the transcription of *c-MYC* (Dong et al., 2007), we hypothesised that in our system, where expression of RASSF1C promotes the nuclear localisation of both YAP1 and β-catenin, RASSF1C could also lead to the upregulation of *BIRC5* and *BCL2L1* and *c-MYC*.

First we decided to drive nuclear localisation in U2OS cells through the knockdown of RASSF1A. U2OS cells were transfected with siNT, siRASSF1 or siRASSF1A before cells were collected and processed for qRT-PCR. In agreement with our previous observations, transfection of cells with siNT or siRASSF1, which do not affect YAP1 or β-catenin localisation, did not result in any change in the expression of *BIRC5*, *BCL2L1* and *c-MYC* (Figure 4.10A). However, in accordance with our hypothesis, loss of RASSF1A, which promotes the accumulation of YAP1 and β-catenin in the nucleus, led to the upregulation of *BIRC5*, *BCL2L1* and *c-MYC.* In order to confirm that RASSF1C was driving the upregulation of these YAP1-β-catenin target genes and to determine the role of SFKs in the process, we transfected MCF7 cells with either pcDNA3 or FLAG-RASSF1C before treating them with either DMSO, or the SRC inhibitors Dasatinib or AZD0530 for 18 hrs before being processed for qRT-PCR.

`

The expression of RASSF1C, treated with DMSO, led to the upregulation of all three genes. However, the inhibition of SFK leads to a reduction in the levels of *BIRC5*, *BCL2L1* and *c-MYC*, in accordance with previously published data (Figure 4.10B) (Gomez-Casares et al., 2013; Rosenbluh et al., 2012).

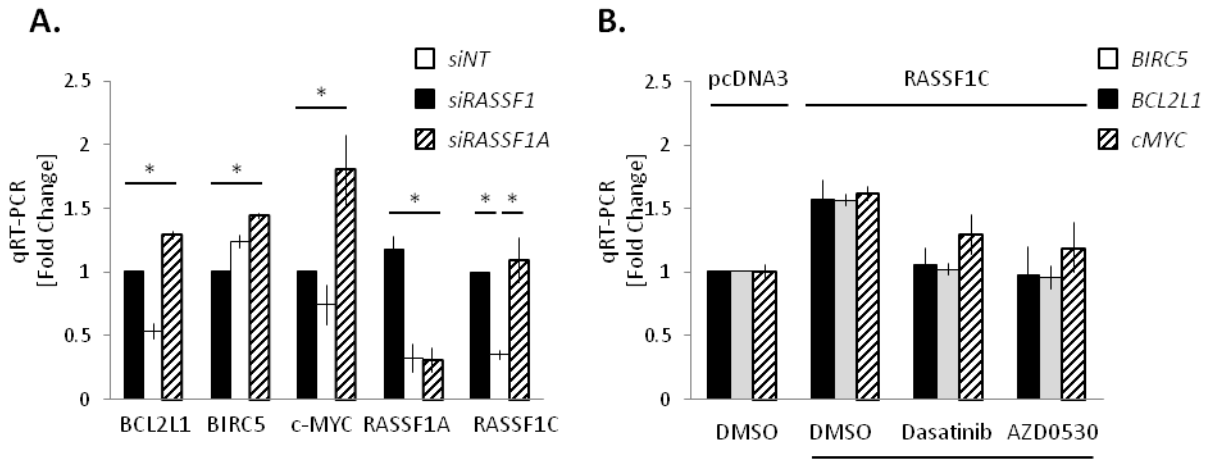


Figure 4.10. RASSF1C Expression, or RASSF1A Loss, Promotes YAP1-β-catenin Dependent Transcription. A. Quantification of qRT-PCR for the β-catenin-YAP- target genes *BCL2L1*, *BIRC5*, and *c-MYC* as well as RASSF1A and RASSF1C expression in U2OS cells (2 x 10^5cells/well). transfected with siNT, siRASSF1 or siRASSF1A. After 48 hrs the cells were collected and 50,000 cells were lysed and cDNA prepared. qPCR was performed on an Applied Biosystems 7500 Fast Real Time PCR system. Expression of *18S* was used as an internal control. Loss of RASSF1A, but not both RASSF1A and RASSF1C leads to upregulation of *BCL2L1*, *BIRC5*, and *c-MYC.* Data is representative of three independent experiments. * $p \leq 0.05$. Error bars represent 1 x SEM. **B**. Quantification of qRT-PCR for *BCL2L1*, *BIRC5* and *c-MYC* genes in MCF7 cells transfected with empty vector or FLAG-RASSF1C and treated with either Dasatinib (50 nM, 18 hrs) or AZD0530 (2.5 mM, 18 hrs). RASSF1C expression promotes the upregulation of *BCL2L1*, *BIRC5* and *c-MYC*. Treatment of RASSF1C-expressing cells with the SRC inhibitors, Dasatinib, or AZD0530, reverses this upregulation back to baseline levels. Data is representative of two biological repeats, each composed of three technical repeats. Error bars represent 1 x SD.

`

Traditionally, YAP1 induces transcription by associating with the sequence specific transcription factors TEAD1 or TEAD2 (Vassilev et al., 2001; Wu et al., 2008a; Zhao, 2008) and β-catenin binds to the TCF/LEF transcription factors to trigger WNT-mediated transcription (Valenta et al., 2012). However, Rosenbluh *et al.* have shown that *BIRC5* and *BCL2L1* are transcriptional targets of the β-catenin-YAP1 binding to the transcription factor TBX5 (Rosenbluh et al., 2012). We therefore wanted to investigate whether the transcription factor TBX5 had any role in breast cancer cells. siRNA depletion of TBX5 did not drive downregulation of the *BIRC5* and *BCL2L1* gene expression (Data not shown). Two homologs of TBX5, TBX2 and TBX3, which share DNA binding consensus with TBX5, have been associated with cancer (Jacobs et al., 2000; Peters et al., 2013) and invasive cellular behaviour (Mowla et al., 2011; Peres and Prince, 2013; Stephens et al., 2012). We sought to investigate whether the RASSF1C-dependent upregulation of *BIRC5*, *BCL2L1* and *c-MYC* was due to YAP1/β-catenin association with TBX2 and/or TBX3. We were also interested in whether the RASSF1C-dependent gene upregulation was due to YAP1/β-catenin binding to either of the downstream YAP1 transcription factors, TEAD1 and/or TEAD2. To test this transfected MCF7 cells with either pcDNA3 or FLAG-RASSF1C and then treated them with siRNAs against YAP1, TEAD1, TEAD2, TBX2, TBX3 and β-catenin. In accordance with our hypothesis that the expression of *BCL2L1*, *BIRC5* and *c-MYC* was driven by YAP1 and β-catenin, knockdown of either YAP1 or β-catenin led to decrease in gene expression in cells expressing RASSF1C. We found that RASSF1C increased the expression of BLC2L1 BIRC5 and c-MYC in a YAP1 and β-catenin dependent manner. We also identified that knockdown of TEAD1 and TBX3, but not TEAD2 or TBX2 led to the reduction in *BCL2L1*, *BIRC5* and *c-MYC* gene expression in RASSF1C-expressing cells (Figure 4.11A). The levels of expression of CTGF, the traditional YAP-TEAD target, required for cell growth and increased oncogenic functions (Zhao et al., 2008) remained unchanged. This suggests that a complex exists between YAP1-TEAD1-β-catenin-TBX3 which drives the upregulation of *BCL2L1*, *BIRC5* and *c-MYC* in response to RASSF1C expression. The western blot analysis of the cell samples showed that all genes were knocked down successfully

`

(Figure 4.11B). This showed us that the lack of effect we observed in the expression of *BCL2L1*, *BIRC5* and *c-MYC*, was not due to failure to knock down TEAD2 and TBX2.

Together, these data show that RASSF1C expression leads to SRC activation, which destabilises the cell-cell junctions. SRC-driven loss of β-catenin from the junctions, together with the phosphorylation of YAP1 at pY357, lead to accumulation of a β-catenin/YAP1 complex in the nucleus. This complex binds to TEAD1 and TBX3 transcription factors, inducing the expression of the anti-apoptotic and pro-invasiveness genes *BCL2L1*, *BIRC5* and *c-MYC*, suggesting a potential cascade of events that start with the hypermethylation of the *RASSF1A* gene in tumours.

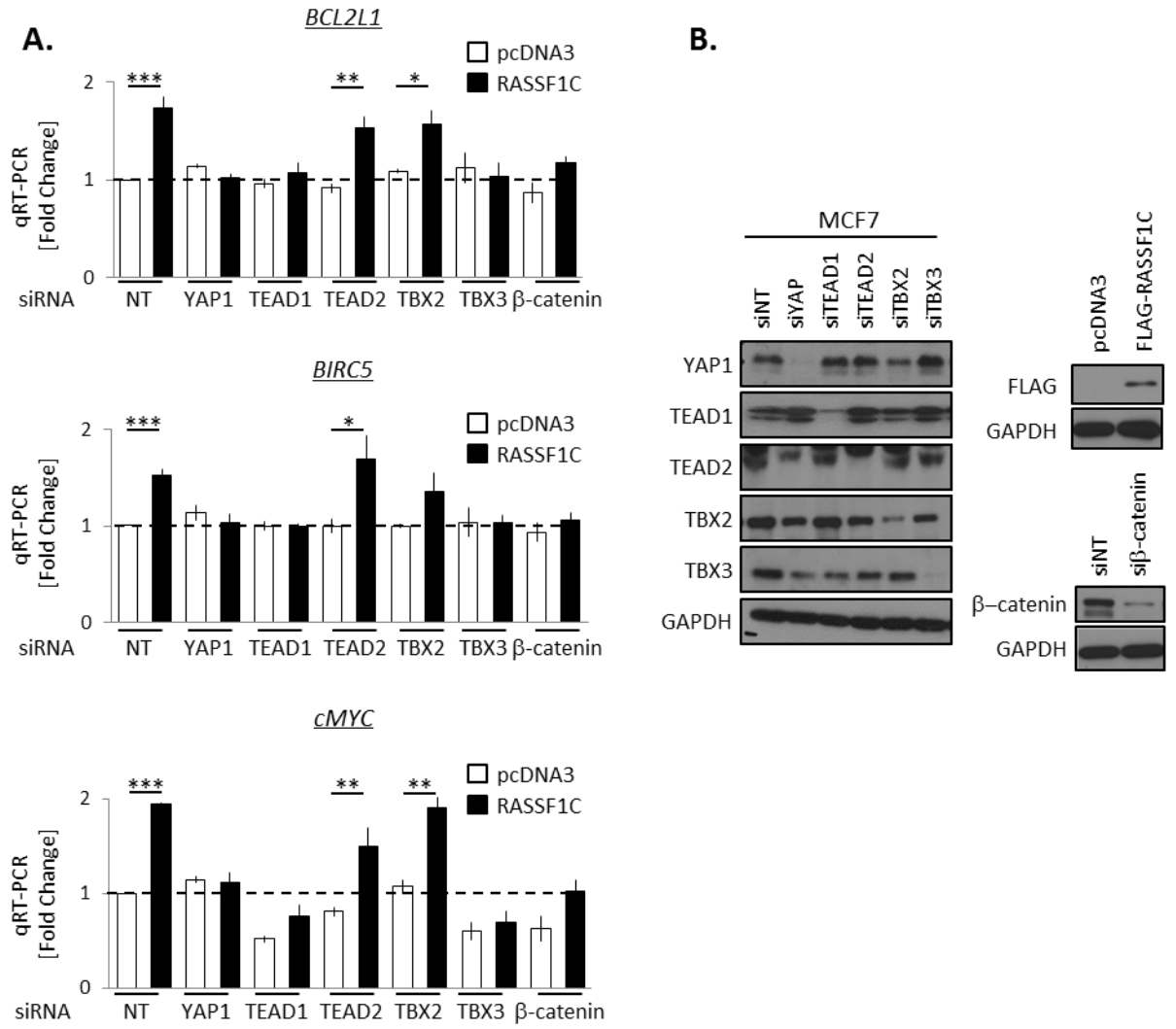


Figure 4.11. RASSF1C Promotes YAP1-TEAD1-β-catenin-TBX3 Dependent Transcription. A. Quantification of qRT-PCR for the β-catenin-YAP-target genes *BCL2L1*, *BIRC5* and *cMYC* in MCF7 cells (2 x 10^5 cells/well) transfected with empty vector or FLAG-RASSF1C and indicated siRNAs. After 48 hrs the cells were collected and 50,000 cells were lysed and cDNA prepared. qPCR was performed on an Applied Biosystems 7500 Fast Real Time PCR system. Expression of 18S was used as an internal control. Expression of RASSF1C promotes the upregulation of *BCL2L1*, *BIRC5* and *cMYC* that is dependent on YAP1, TEAD1, TBX3 and β-catenin. Data is representative of three independent experiments. * $p \leq 0.05$, ** $p \leq 0.01$, *** $p \leq 0.001$. Error bars represent 1 x SEM. **B**. Lysates from MCF7 cells with the indicated siRNAs, showing the knockdown of the gene targets by the siRNAs used in (**A.**). Cells were cultured for a total of 48 hrs and lysed with laemmli lysis buffer and analysed by SDS-PAGE and western blot with the indicated antibodies.

`

4.8 Discussion

In this chapter I have shown that loss of RASSF1A, but not of RASSF1C, leads to nuclear localisation of YAP1 and decreased levels of pS127-YAP1. The expression of RASSF1C promotes the phosphorylation of YAP1 at Y357 and the nuclear accumulation of YAP1 and β-catenin, which results in increased transcription of the anti-apoptotic and invasion promoting genes *BCL2L1*, *BIRC5* and *c-MYC.* I have also shown that the expression of these target genes is YAP1/TEAD1 and β-catenin/TBX3-dependent, providing an explanation for the invasive and aggressive phenotype observed in Chapter 3.

In Chapter 3 I showed that RASSF1A and RASSF1C had opposing effects on the activity of SRC (Figure 3.1), and that RASSF1C is only able to activate SRC in cell lines that have lost RASSF1A expression. During our early studies of co-expressing RASSF1A and RASSF1C constructs we observed that RASSF1C expression was lower when RASSF1A was co-expressed compared to when RASSF1C was expressed alone. Preliminary data has shown that this could be due to RASSF1A binding to and regulating RASSF1C (Figure 8.6) and that this interaction occurred through the RA domain (Scrace and University of Oxford). We have observed that dual expression of RASSF1A and RASSF1C leads to loss of RASSF1C, suggesting that RASSF1A could be involved in the degradation of RASSF1A (Data not shown). This suggests that when both isoforms are expressed, RASSF1A is dominant. It would be interesting to further investigate the dynamics of this observation using biochemical methods, such as a protein kinase assay to identify how RASSF1C is targeted for degradation by RASSF1A and by which ubiquitin ligase.

It has been shown that the adherens junctions can sense epidermal cell density (Lien et al., 2006) and that E-cadherin is required for Hippo pathway-dependent control of the cellular density via the regulation of YAP1 subcellular localisation (Kim et al., 2011; Zhao et al., 2007). Therefore loss of adherens junctions can lead to loss of Hippo pathway activation and YAP1 translocation to the nucleus (Kim et al., 2011). The adherens junction is a complex of proteins including E-cadherin, β-catenin and α-catenin, all of which have been associated with activation of the Hippo pathway (Kim

`

et al., 2011). In our system, RASSF1C expression activates SRC, which phosphorylates and destabilises E-cadherin (Figure 3.6) and phosphorylates β-catenin (Figure 8.4). YAP1 staining of MCF7 cells showed that RASSF1C induced nuclear localisation of YAP1, only in the presence of the WT E-cadherin, which is susceptible to SRC phosphorylation (Figure 4.2). RASSF1C failed to induce nuclear localisation in cells expressing the E-cadherin Y3F mutant, which is not susceptible to SRC phosphorylation. This is in agreement with the literature that showed that loss of E-cadherin leads to YAP1 accumulation in the nucleus (Kim et al., 2011). Further validation of this data could be achieved by doing a nuclear/cytoplasmic fractionation in cells expressing RASSF1C and either WT E-cadherin or the E-cadherin Y3F mutant, which would show the increase in nuclear YAP1 when RASSF1C expression leads to SRC activity and phosphorylation of WT E-cadherin. Furthermore, given that depletion of α-catenin led to a reduction in the inhibitory phosphorylation of YAP1 at S127, a process that is MST/LATS independent (Schlegelmilch et al., 2011) and that phosphorylated α-catenin leads to increase in the stability of β-catenin, which can be reversed by the use of the SRC inhibitor Dasatinib, we would want to investigate if RASSF1C expression also downregulates the functions of α-catenin, thus positively affecting both β-catenin and YAP.

RASSF1A is an upstream component of the mammalian Hippo pathway, regulating the activation of MST1/2 and LATS1/2, leading to phosphorylation of YAP1 at S127. However, the RASSF1A-dependent phosphorylation of YAP1 retains pS127-YAP1 in the nucleus, where it leads to a YAP1 transcriptional switch away from regulation of proliferation through TEAD or differentiation through RUNX2, but towards tumour suppression via YAP1/p73 transcription (Hamilton et al., 2009; Matallanas et al., 2007; van der Weyden and Adams, 2007; van der Weyden et al., 2012). However, in U2OS cells, in which RASSF1A expression has been knocked down, but RASSF1C retained, we observed an accumulation of YAP1 in the nucleus (Figure 4.3). The specific ablation of RASSF1A indicated that the reduced pS127-YAP1 appears to be required, but is insufficient for the nuclear localisation of YAP1 (Figure 4.4), suggesting that the mechanisms that drives the nuclear retention of YAP1 in cells expressing RASSF1A is different from the one in cells expressing RASSF1C. We hypothesised that in

`

cells with depleted RASSF1A and RASSF1C, the observed loss in nuclear YAP1 was predominantly due to the loss of RASSF1C. We confirmed this by using resistant forms of RASSF1A and RASSF1C to siRNA targeting the *RASSF1* gene (Figure 4.5 and 4.6). Use of the siRNA resistant sequences of RASSF1A and RASSF1C enabled us to identify the individual contributions of RASSF1A and RASSF1C to the phenotype observed with siRASSF1 and confirm the results we observed with specific knockdown of RASSF1A. However, we could further confirm these results by knocking down both RASSF1A and RASSF1C individually. Although we had difficulties with generating effective siRNAs that were specific to RASSF1C, we might have more success with other technologies such as shRNA, or CRISPR. We have had some moderate success using cells stably expressing shRNAs targeting *RASSF1*, *RASSF1A* and *RASSF1C*, but further investigation is required in order to confirm the data. We would hypothesise that the knockdown of *RASSF1A*, but not of *RASSF1C*, would induce an increase in the nuclear localisation of YAP.

Cells expressing RASSF1C can activate the three major members of the SRC family kinase – SRC (Figure 3.1), FYN (Data not shown) and YES (Figure 4.11B). Since YAP1 has the YXXP motif (Levy et al., 2008) and was shown to be phosphorylated by YES1 (Rosenbluh et al., 2012), we sought to investigate whether RASSF1C induces tyrosine phosphorylation of YAP1. We saw that the cells expressing RASSF1C show higher levels of phospho-tyrosine YAP1 compared to the control cells (Figure 4.7A). We also observed that in cells that have lost RASSF1A and RASSF1C, but not RASSF1A alone, there was an increase in the accumulated nuclear pY357-YAP1 (Figure 4.7B and C), further confirming that the increase in phospho-tyrosine YAP1 in cells that retain RASSF1C was indeed the pY357. Interestingly, we observed that basal level of YAP1 phosphorylation in the control cells was higher than the expected levels if YAP1 is not phosphorylated. This could be explained by a phosphorylation of the Y357-YAP1 site by the SRC family member c-Abl, which has been reported to activate MST1/2 (Liu et al., 2012; Xiao et al., 2011) and lead to pY357-YAP1 binding to p73 and association with pro-apoptotic promoters (Levy et al., 2008). Given the levels of RASSF1A in the U2OS

`

cells and the reported RASSF1A-dependent upregulation of the YAP1/p73 complex (Hamilton et al., 2009), c-Abl could be acting concurrently with RASSF1A, to an increase the basal pY357 levels.

We further observed that the phosphorylation on YAP1 at Y357 was SRC- and YES-dependent, in agreement with the published data (Rosenbluh et al., 2012). The overexpression of RASSF1C led to a SRC- and YES1-dependent increase in the phosphorylation of Y357-YAP1 (Figure 4.8). Given that treatment with the tyrosine kinase inhibitor Dasatinib (Lombardo et al., 2004) can inhibit the tyrosine phosphorylation of YAP1 (Rosenbluh et al., 2012), future research could investigate how pY357-YAP1 localisation is affected in RASSF1C-expressing cells in the presence of SRC inhibitor. We would predict that the use of SRC inhibitor will reduce the levels of RASSF1C-dependent YAP1 phosphorylation and consequently a decrease in the localisation of YAP1 in the nucleus. This could be shown by immunofluorescence, or by nuclear/cytoplasmic fractionation.

The phosphorylation of β-catenin following the activation of Rho-family small GTP-ase Rac1 has been shown to affect the activity and localisation of β-catenin (Wu et al., 2008b). E-cadherin association protects β-catenin from degradation (Huber and Weis, 2001), but both proteins dissociate from the membrane following phosphorylation by SRC (Coluccia et al., 2006; Roura et al., 1999). We observed that RASSF1C expression promotes SRC-mediated β-catenin phosphorylation (Figure 8.4) and consequently its accumulation in the nucleus (Figure 4.9). Given that RASSF1C expression leads to SRC- or YES1- dependent phosphorylation and nuclear localisation of YAP1, we hypothesised that the induced nuclear β-catenin would be able to associate with the nuclear YAP1, in accordance with previously published data, showing a complex between active β-catenin, YAP1 and YES1 in the nucleus (Rosenbluh et al., 2012).

Our results suggest that, β-catenin acts, in part, in a TCF-4 and Wnt-signalling independent manner, since we did not observe any transcriptional activation of TCF-4 (Data not shown). Given that we have observed that RASSF1C promotes β-catenin and YAP1 localisation in the nucleus, it would be interesting to see how it alters other members of the Wnt pathway, such as the adenomatous

`

polyposis coli (APC), glycogen synthase kinase-3 (GSK3) and the casein kinase 1 (CK1). RASSF1C has previously been linked to Wnt signalling. It was shown that RASSF1C was able to inhibit the βTrCP-mediated degradation of β-catenin (Estrabaud et al., 2007). Also, nuclear YAP1/TAZ have been associated with the Wnt destruction complex, protecting β-catenin from degradation and inducing its nuclear localisation (Azzolin et al., 2014). Since APC has been shown to regulate the suppression of β-catenin and YAP1/TAZ under physiological conditions, and, consequently, inhibit the development of tubular adenomas (Cai et al., 2015), it would be interesting to see if the functions of APC are impaired by RASSF1C, or promoted by RASSF1A expression. Given the role of RASSF1A expression in the inactivation of the Hippo pathway or the loss of MST1/2 and SAV1; and its role in the nuclear YAP1/TAZ localisation and the consequent stabilisation of β-catenin (Azzolin et al., 2014; Heallen et al., 2011), the observed RASSF1C-dependent YAP-β-catenin nuclear accumulation could be reversed by the expression of RASSF1A.

Since loss of RASSF1A, or exogenous expression of RASSF1C led to YAP1 and β-catenin nuclear localisation, it was important to find out whether their activity in the nucleus was associated with an increase in gene transcription, leading to upregulation of the anti-apoptotic signals *BCL2L1* and *BIRC5*, as previously reported in the literature (Rosenbluh et al., 2012). We therefore examined the expression of *BCL2L1*, *BIRC5* and the canonical β-catenin transcriptional target, *c-MYC* in cells where we had transiently knocked down RASSF1A expression and observed upregulation of all three genes (Figure 4.10A). We further confirmed the role of RASSF1C by exogenously expressing it and seeing the upregulation of *BCL2L1, BIRC5* and *c-MYC* (Figure 4.11A).

The YAP1-β-catenin targets we have identified have been linked to a number of oncogenic processes. The B Cell Lymphoma 2-Like 1 (BCL2L1), a member of the BCL2 family, is involved in the regulation of apoptosis (Hossini and Eberle, 2008). The BCL2L1 pre-mRNA can give rise to several splice variants, including BCL-XL, which inhibits apoptosis (Boise et al., 1993). Overexpression of BCL-XL contributes to resistance to apoptosis, tumour cell survival, metastasis and poor response to chemotherapy

`

(Fernandez et al., 2002; Zhang et al., 2008). It has also been reported that *BCL2L1* affects the 20q gain-driven colorectal adenoma-to-carcinoma progression (Sillars-Hardebol et al., 2012). The Baculoviral IAP Repeat Containing 5 (BIRC5, Survivin) is a member of the Inhibitor of Apoptosis gene family that has been previously linked to resistance in cell death induction in high-stage neuroblastoma (Hagenbuchner et al., 2015); increase in EMT, invasion and development of gastric cancer (Li et al., 2015) and prostate cancer metastasis (Wang et al., 2015). MYC was selected due to its β-catenin-dependent transcription (He et al., 1998) and functional regulation of pro- and anti-apoptotic proteins in the BCL-2/BH3 family (Youle and Strasser, 2008) and invasion (Wolfer and Ramaswamy, 2011). Also, double-hit (BCL2 – MYC) and triple-hit lymphomas with BCL2, BCL6 and MYC translocations have extremely poor prognosis (Hashimoto et al., 2015; Yoshida et al., 2015a; Yoshida et al., 2015b). Taken together, the upregulation of these genes could explain some of the phenotypes seen in RASSF1C-expressing cells. We could further investigate this by using shRNA to stably knock down each of these targets in the mammosphere growth assay. If the RASSF1C-induced phenotype is dependent on these targets, we would see a decrease in mammosphere growth.

In order to examine the role of SFK activation in the regulation of the gene transcription, we used two different SRC inhibitors – Dasatinib and AZD0530. We observed that treatment of the cells expressing RASSF1C led to a downregulation of the three target genes (Figure 4.10B). This fits with our hypothesis that RASSF1C activation of SRC drives YAP-β-catenin to the nucleus through disruption of the junctions and through direct phosphorylation of YAP1 and β-catenin, as well as previously published data which showed that Dasatinib treatment inhibited the binding of β-catenin and YAP1 to the *BCL2L1* and *BIRC5* promoters (Rosenbluh et al., 2012).

Both YAP1 and β-catenin are transcriptional coregulators, which interact with transcription factors in order to promote or repress the transcription of target genes (Kaidi et al., 2007; Zhao et al., 2008). YAP1 induces transcription by associating with TEAD1 or TEAD2 transcription factors (Vassilev et al., 2001; Wu et al., 2008a; Zhao, 2008), whereas β-catenin binds to the TCF/LEF transcription factors

`

(Valenta et al., 2012). Since Rosenbluh *et al.* have shown that *BIRC5* and *BCL2L1* are the transcriptional targets of the β-catenin-YAP1 when bound to the transcription factor TBX5 (Rosenbluh et al., 2012), we investigated whether in RASSF1C-expressing cells the transcription factor TBX5 led to upregulation of *BIRC5* and *BCL2L1*. siRNA depletion of TBX5 showed no downregulation of the *BIRC5* and *BCL2L1* gene expression (Data not shown). Therefore, we decided to investigate the roles of the TBX5 homologues TBX2 and TBX3. TBX2 and TBX3 were chosen due to their link to cancer and high homology to TBX5. TBX2 and TBX3 are associated with TGF β, fibroblast growth factor (FGF) and Wnt pathways (Abrahams et al., 2010) and are upregulated in breast cancer (Fan et al., 2004; Sinclair et al., 2002) and invasive cellular behaviour (Mowla et al., 2011; Peres and Prince, 2013; Stephens et al., 2012). siRNA depletion of YAP1, β-catenin and TEAD1 and TBX3 led to the downregulation of *BCL2L1, BIRC5* and *c-MYC* gene expression in RASSF1C-expressing cells. This showed that in RASSF1C-expressing cells, the upregulation of *BCL2L1, BIRC5* and *c-MYC* was dependent on a YAP1-TEAD1-β-catenin-TBX3 complex (Figure 4.11A). These results further support the invasive phenotype we observed in Chapter 3, where the RASSF1C-dependent activation of SRC led to E-cadherin internalisation and increased tumourigenesis. The YAP-dependent mammosphere formation and growth in soft agar have been attributed to BIRC5 expression (Dong et al., 2007; Rosenbluh et al., 2012), which together with c-MYC-mediated invasion (Wolfer and Ramaswamy, 2011) is in line with the RASSF1C-expressing cells forming larger, more aggressive mammospheres *in vitro* and larger tumours *in vivo* (Figure 3.18 and 3.19). In agreement with our data, TBX3 was recently linked with YAP1 in the generation of invasive cancers (Mowla et al., 2011; Nallet-Staub et al., 2014; Peres and Prince, 2013; Vlug et al., 2013) and the increase in motility during development (Fukui et al., 2014; Shen et al., 2014). It would be interesting to validate the formation of the YAP1-TEAD1-β-catenin-TBX3 complex in RASSF1C-expressing cells by immunoprecipitation or by multiplex PLA that would allow the simultaneous visualisation of all four protein complexes (Leuchowius et al., 2013). It would also be interesting to confirm by siRNA or shRNA that these genes are regulating the increase in mammosphere formation and growth, in cells expressing RASSF1C.

`

TBX3 has also been shown to be regulated in a number of other ways all linked to oncogenesis, such as the phorbol ester PMA which can activate the Protein Kinase C family of enzymes (Basu et al., 1990) and the Activator Protein-1 (AP-1) family of transcription factors (Lamph et al., 1988), c-Jun, JunB and c-Fos, which can mediate expression and activation of TBX3 (Mowla et al., 2011). The PMA-induced migration of MCF7 cells is positively regulated by TBX3 expression (Mowla et al., 2011). This is thought to be due to the fact that TBX3 has been reported to repress the expression of E-cadherin and to enhance invasiveness in melanoma (Peres et al., 2010; Rodriguez et al., 2008). It would be interesting to investigate whether RASSF1C expression, as well as disrupting E-cadherin at cell-cell junctions via SRC, also downregulates E-cadherin levels via the YAP-TEAD-β-catenin-TBX3 complex (Figure 4.11B). Although we have not seen any changes to E-cadherin expression in the presence of RASSF1C, it may be the case that continued expression over a long time period may lead to these changes. This will be a matter of future investigation, which would involve following the levels of E-cadherin over several passages.

Recently it has been shown that the YAP1/TAZ transcriptional response is mediated by AP-1 transcription factors, recruited to the same genomic regions as the TEAD factors (Zanconato et al., 2015). The YAP1/TAZ-dependent oncogenic growth was shown to be strongly enhanced by the gain of AP-1 (Zanconato et al., 2015). The AP-1 factors c-fos and c-Jun play critical roles in processes like proliferation, differentiation, oncogene-induced transformation and invasion (Jochum et al., 2001; Karin, 1995). AP-1 also regulates JunB expression in human mature granulocytes where JunB loss leads to higher expression of members of the Bcl2 family of anti-apoptotic genes (Passegue et al., 2001). RASSF1A has been implicated in the regulation of c-fos and c-jun. RASSF1A has been shown to interact with and negatively regulate the transcription factor EWS, thus preventing it from positively regulating c-fos (Kim et al., 2006). Also, RASSF1A has also been reported to downregulate JNK signalling and consequently inhibit the phosphorylation of target proteins such as the transcription factor c-jun (Derijard et al., 1994; Gupta et al., 1995). It would be really interesting to see if RASSF1A

`

or RASSF1C expression regulated AP-1-dependent transcription and whether this shifted AP-1 activity from tumour-suppressing to oncogenic, respectively.

Taken together these data led us to create a working model (Figure 4.12) in which RASSF1C leads to SRC activation, promoting E-cadherin and β-catenin phosphorylation and internalisation. Loss of cell junctions and SRC phosphorylation of YAP1 lead to the translocation of YAP1 in the nucleus, where it associates with internalised β-catenin to create a transcriptional complex. This complex, together with the transcriptional factors TEAD1 and TBX3 induce the expression of the *BCL2L1, BIRC5* and *c-MYC*, which promote the tumourigenesis of the RASSF1C-expressing cells.

`

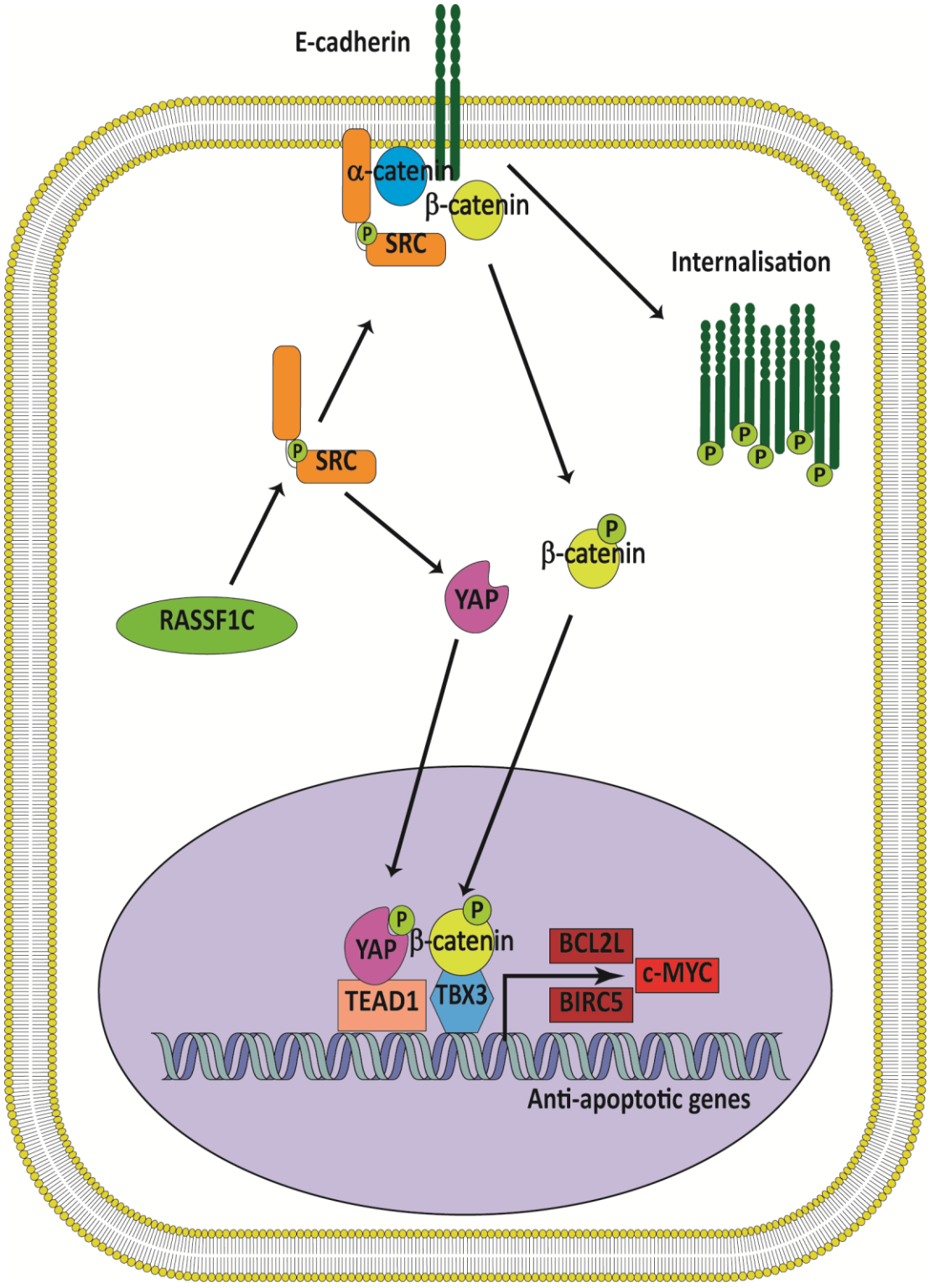


Figure 4.12. Cartoon Depicting the Hypothesis Generated from the Results in Chapter 4. SRC family kinases are activated in the perinuclear region by the binding of RASSF1C, promoting their translocation to the plasma membrane and subsequent activation, which then disrupts E-cadherin, leading to E-cadherin internalisation and loss of cell-cell junctions. SRC also leads to β-catenin and YAP1 tyrosine phosphorylation, driving them into the nucleus, where they associate with the TEAD1 and TBX3 transcription factors to promote the expression of the anti-apoptotic genes *BCL2L1, BIRC5* and *c-MYC,* driving survival and potentially metastasis.

`

Chapter 5 RASSF1C Expression Increases the Rates of Secretion and Alters the Proteins Packaged in Exosomes

5.1 Introduction

In Chapter 4, we showed that the loss of RASSF1A led to the phosphorylation of YAP1 and its nuclear localisation. We also identified that this was due to activation of SRC by stabilised RASSF1C. Further analysis showed that RASSF1C expression induced nuclear localisation of β-catenin. This led to the formation of a transcriptional complex between YAP1-TEAD1-β-catenin-TBX3, resulting in the upregulation of genes that have been associated with inhibition of apoptosis and general tumourigenicity. Interestingly, the activation of these genes in tumour cells has previously been associated with secretion of exosomes.

5.1.1 Exosomes

An essential hallmark of multicellular organisms is the intercellular communication, achieved either by direct cell-cell contact or by the transfer of secreted molecules. A recently discovered third mechanism involves the intercellular transfer of extracellular vesicles. The origin, nature, features and names of these vesicles are diverse and are a subject of extensive research. The term exosome was initially used for vesicles released by a variety of cultured cells and ranging from 40 to 1000 nm, however the term was later adopted for small vesicles of endosomal origin, ranging from 30-150 nm (Johnstone et al., 1987; Taylor et al., 1983; Trams et al., 1981). A variety of cell types have been reported to release exosomes, including neurons, oligodendrocytes, platelets, cytotoxic T cells and

`

intestinal epithelial cells (Colombo et al., 2014; Raposo and Stoorvogel, 2013). Vesicles with hallmarks of exosomes have been isolated from seveal body fluids, including bile, cerebrospinal fluid, ascites fluid, amniotic fluid, saliva, breast milk, blood, urine and semen (Colombo et al., 2014; Raposo and Stoorvogel, 2013).

Exosomes originate from internal budding of the plasma membrane that occurs during endocytic internalisation. Through an interaction with the Golgi complex, the early endosome matures to form a late endosome. The bilayer of the late endosomes gives rise to intraluminal vesicles – exosomes. The exosomes are then contained within the multivesicular bodies (MVBs). The formation of MVBs is driven by the endosomal sorting complex required for transport (ESCRT), which is composed of approximately thirty proteins that assemble into four complexes (ESCRT-0, -I, -II and –III) with associated proteins (VPS4, VTA1 and ALIX) conserved from yeast to mammals (Hanson and Cashikar, 2012). The ESCRT-0, -I, and –II complexes are involved in the recognition and sequestration of ubiquitinated membrane proteins at the endosomal delimiting membrane, whereas ESCRT-III complex is involved in membrane budding and actual scission of intraluminal vesicles (Hurley, 2010; Raiborg and Stenmark, 2009). The MVBs can fuse with the plasma membrane to release exosomes through exocytosis or can be sent for degradation to the lysosomes (Pant et al., 2012). The MVB fusion with the plasma membrane depends on several Rab GTPase proteins (Pfeffer, 2010), studied by their selective inactivation in order to understand their role in the exosome release process. Inhibition of RAB11 decreased secretion of HSP70-containing exosomes (Savina et al., 2002); RAB35 was shown to be necessary for PLP-bearing exosome secretion (Hsu et al., 2010); shRNA silencing of RAB2B, RAB5A, RAB9A and RAB27A and RAB27B decreased secretion of exosomes containing CD63, CD81, and MHC class II (Ostrowski et al., 2010). RAB27A/B and RAB35 were shown to allow docking of MVBs to the plasma membrane (Hsu et al., 2010; Ostrowski et al., 2010). Little is known about the machinery that drives MVB fusion with the plasma membrane, however the SNARE proteins (soluble *N*-ethylmaleimide-sensitive fusion attachment protein (SNAP) receptors) SNAP-23, VAMP8 or VAMP7 have been reported to promote exocytosis of MVBs (Fader et al., 2009; Zylbersztejn and Galli, 2011).

`

Exosomes are composed of proteins, lipids and nucleic acids. Exosomes have been shown to contain a variety of proteins, including endosome –associated proteins (e.g., flotillin, Annexins, SNAREs and Rab GTPase); proteins involved in MVB biogenesis (e.g., ALIX and TSG101); membrane proteins, including tetraspanins (e.g., CD63, CD81, CD82, CD53) and integrins (e.g., $\alpha5\beta1$ and $\alpha2\beta1$); cytoskeletal proteins (e.g., actin, cofilin, tubulin); and signal transduction proteins (e.g., heterotrimeric G proteins, 14-3-3 and syntenin) (Colombo et al., 2014; Kim et al., 2012a; Kourembanas, 2015; Raposo and Stoorvogel, 2013). The lipid composition of exosomes varies depending on the cells of origin, secreting the exosomes, however the most commonly found lipids include phosphoglycerides, cholesterol, ceramide, and long fatty-acyl chains, all of which may provide structural stability (Choi et al., 2013). Exosomes have been reported to carry mRNA, miRNA, single-stranded DNA, genomic DNA, cDNA, and transposable elements (Valadi et al., 2007). The overall composition of the exosomes is representative of mixed populations and has been reported to change due to a variety of extracellular signals. For example, the protein and RNA composition of the released exosomes from dendritic, endothelial or mesenchymal stem cells can be altered due to inflammatory signals (e.g., TNFα, IFNγ) (de Jong et al., 2012; Kilpinen et al., 2013; Segura et al., 2005). In addition, expression of oncogenic forms of either *K-RAS* or *H-RAS* changes the composition of the secreted vesicles (Demory Beckler et al., 2013; Tauro et al., 2013).

5.1.2 Exosomes in Cancer

The shedding of membrane-enclosed vesicles by normal and neoplastic cells was originally reported in the early 1980s, but the secretion of tumour-derived exosomes was only reported in 2001 (Wolfers et al., 2001). Since then, exosomes have been shown to play a bimodal role, aiding cancer growth and dissemination and also re-programming the immune system by inhibiting an anti-tumour response (Colombo et al., 2014).

`

Exosomes are involved in the transfer of oncogenic proteins between cancer cells. The exchange of proteins between cancer cells in exosomes has been shown to promote oncogenesis and also chemoresistance (Corcoran et al., 2012). For example, in glioma cells, a mutant EGFR can be delivered via exosomes to the cells lacking the mutant form, which triggers upregulation of anti-apoptotic genes and anchorage independent growth (Al-Nedawi et al., 2008). Also, colon cancer cells with mutant K-RAS can release exosomes with the mutant form and send them to cells expressing the wild-type K-RAS, inducing growth and tumourigenicity (Demory Beckler et al., 2013).

Exosomes can also modulate the tumour microenvironment, promoting many aspects of oncogenesis, including formation of tumour-promoting stroma, angiogenesis and metastasis. A biologically active TGF-β1 protein can be transferred to recipient cells via exosomes from prostate cancer and mesothelioma cells, leading to differentiation of fibroblasts to myofibroblasts, thus forming tumour-promoting stroma, indicative of poor survival prognosis (Moorman et al., 2012; Webber et al., 2010). Breast cancer exosomes have been reported to possess the ability to convert mesenchymal stem cells into myofibroblasts via the SMAD pathway, contributing to cancer progression and malignancy (Cho et al., 2012). Melanoma derived exosomes can deliver microRNA-9, leading to endothelial cell migration *in vitro* and angiogenesis *in vivo* (Zhuang et al., 2012). Another study has shown that melanoma exosomes can increase lung endothelial permeability and recruit bone-marrow derived cells to initiate a pre-metastatic niche and increase lung metastasis *in vivo* (Peinado et al., 2012). Increased motility has been linked to a complex interplay between exosome release and activation of the surrounding fibroblasts and stroma (Luga et al., 2012). This is thought to be through the regulation of invadopodia biogenesis and matrix degradation by the exosomes (Hoshino et al., 2013).

The recruitment of pro-tumorigenic immune cells by the tumour cells is mediated by exosome secretion. In murine breast cancer, the inhibition of Rab27a-mediated release of exosomes is associated with decrease mobilisation of neutrophils, leading to an increase in the tumour growth

`

(Bobrie et al., 2012). Cancer derived exosomes are thought to regulate the immune system by inducing interleukin-6 production in myeloid-derived suppressor cells, which leads to STAT3-dependent immunosuppression (Chalmin et al., 2010; Nagaraj and Gabrilovich, 2012; Taylor et al., 2003). Intriguingly, exosomes can transport antigens from tumour cells to antigen presenting dendritic cells, leading to efficient induction of antitumour immune responses (Andre et al., 2002; Dai et al., 2006; Wolfers et al., 2001), however the immune consequences of exosome secretion by tumours *in vivo* remains not fully understood.

Exosomes have been recognised as critical mediators of health and disease and could be used as biomarkers for specific conditions. Due to their secretion by the tumour cells and the distinct compositions from the ones derived from non-malignant cells, exosomes have been detected in human plasma, urine and saliva (Gallo et al., 2012; Keller et al., 2011; Skog et al., 2008). They have been used for tumour diagnosis in brain, ovarian, colorectal and skin cancers (Peinado et al., 2012; Silva et al., 2012; Skog et al., 2008; Taylor and Gercel-Taylor, 2008). Exosome-associated signatures from various malignancies could potentially be used to predict the presence of early disease, before the use of classic methods, such as PET scan, CT or MRI (Anderson and Butler, 2014).

Exosomes have also been linked to SRC and β-catenin. Exosomes can also promote angiogenesis in a SRC-dependent manner and Dasatinib can negatively regulate the exosome-induced FAK and Akt (Mineo et al., 2012). The loss of the tetraspanins CD82 and CD9 has been shown to induce β-catenin export via exosomes, leading to down-regulation of the Wnt signalling pathway and potential increase in tumour metastasis (Chairoungdua et al., 2010).

5.1.3 Aims

The work in Chapters 3 and 4 have highlighted a novel role for RASSF1C in the regulation of SRC, YAP1 and β-catenin, in cell tumourigenicity. We observed RASSF1C-dependent nuclear localisation of

`

YAP1 and β-catenin led to the upregulation of target genes, such as *BCL2L1*, *BIRC5 (also known as Survivin)* and *c-MYC* in a TEAD1- and TBX3-dependent manner. We hypothesised that this gene regulation was responsible for the increased tumourigenicity observed in Chapter 3. It has been shown that HCT116 cells, depleted for Werner syndrome protein, can condition media by releasing BCL2, BCL-X and BCL-XL, potentially via exosomes (Fausti et al., 2013; Yang and Robbins, 2011). Survivin has also been found to be released from HeLa cells via exosome secretion (Khan et al., 2011). In addition, *c-MYC* transformation of mesenchymal stem cells has been associated with the infinite supply of cells for the production of exosomes as therapeutic agents of delivery vesicles (Chen et al., 2011). Finally, in Chapter 3, we showed that cells expressing RASSF1C can release membranous vesicles (Figure 3.18). Therefore we wanted to investigate the role of RASSF1C in the production and secretion of exosomes.

5.2 Exosomal Marker Activity is Associated with RASSF1C-Expressing Cells

Exosomes originate in the MVBs and are released from the cells by the fusion of the MVBs with the plasma membrane (Colombo et al., 2014). The formation of MVBs is associated with the functions of the ESCRT complexes, acting as cargo sequestering and sorting machinery in the generation of MVBs and subsequently exosomes. ESCRT-III, which binds ESCRT-I via ALIX (also known as PDCD6IP), promote the budding of the membrane (Akers et al., 2013) and loss of ALIX has been shown to impair exosome release (Baietti et al., 2012). However, some evidence suggests that MVBs can form in absence of ESCRT function since the concomitant inactivation of the four different ESCRT complexes does not abolish MVB formation (Stuffers et al., 2009). The expression of the tetraspanins CD63 and CD81 have been linked to ESCRT independent secretion of exosomes (Perez-Hernandez et al., 2013; van Niel et al., 2011). The tetraspanins are a 4-transmembrane protein family that are highly

`

enriched in exosomes. They are able to form complexes by interacting among themselves and with a large variety of transmembrane and cytosolic proteins (Charrin et al., 2009).

Exosomes have been shown to promote angiogenesis in a SRC-dependent manner (Mineo et al., 2012). SRC is able to phosphorylate ALIX, negatively regulating its activity. This inhibition prevents ALIX from interacting with, and inactivating focal adhesion kinase (FAK), which has been associated with increased motility and metastasis (Schmidt et al., 2005). Interestingly, expression of CD63 has been shown to stimulate the activation of SRC by the phosphorylation at pY416 and to decrease the inhibitory phosphorylation at pY527-SRC (Lin et al., 2008). CD81 has been shown to bind to Rac2 and Rac1, localizing Rac to the leading edge of the cell adhesions and thus regulating cell migration (Tejera et al., 2013). Also, exosomes containing CD81 stimulate the protrusive activity, motility and metastasis of breast cancer cells (Luga et al., 2012), phenotypes we observed in Chapter 3. Therefore, in order to better understand the activity of the ESCRT complex and the potential secretion of exosomes in cells expressing RASSF1C and active SRC, we sought to investigate the localisation of ALIX, CD63 and CD81. We used MCF7, which we have shown before (Chapter 3) to have active SRC and to secrete vesicles in the presence of RASSF1C (Figure 3.17). Cells were transiently transfected with ZsGreen-empty vector or ZsGreen-RASSF1C and were incubated for 36 hrs in complete media and then 12 hrs in DMEM media supplemented with 0.1 % FBS. Cells were then collected and stained with ALIX, CD63 or CD81 antibodies. We observed an increase in the ALIX levels in cells expressing RASSF1C, compared to control cells (Figure 5.1A). We also saw that the cells expressing RASSF1C have higher cytoplasmic levels of CD63 (Figure 5.1B). Staining for CD81 expression, revealed that in RASSF1C-expressing cells the levels of CD81 were higher than in control cells (Figure 5.1C). This data suggests that expression of RASSF1C can promote the increase in the levels of ALIX, CD63 and CD81. Given that these proteins are associated with the exosome secretory machinery and are consistently found in the secreted exosomes (Colombo et al., 2014), we wanted to investigate whether the expression of RASSF1C led to an increase in the levels of secreted exosomes.

`

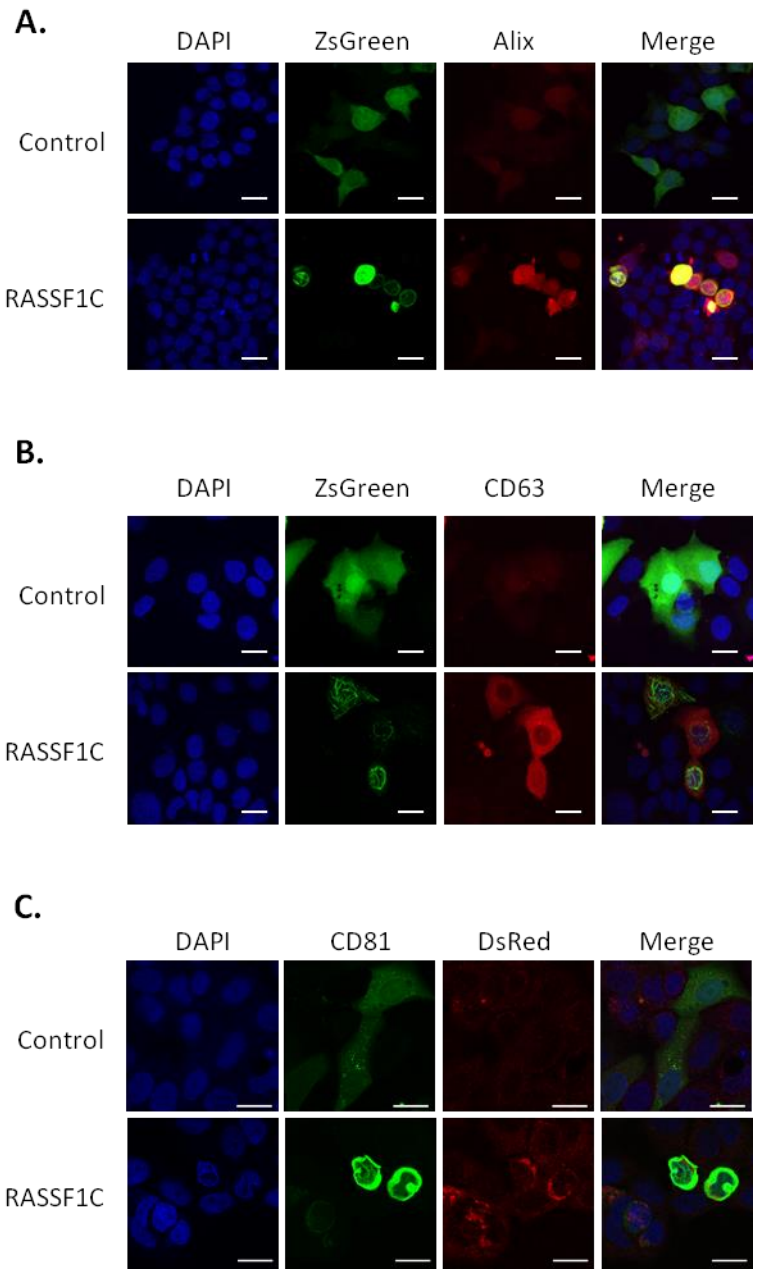


Figure 5.1. The Levels of ALIX, CD63 and CD81 Are Higher In RASSF1C-Expressing Cells. MCF7 cells (3 x 10^5 cells/well) were plated on glass coverslips and transfected with ZsGreen-empty vector or ZsGreen-RASSF1C. Cells were grown in complete media for 36 hrs and 12 hrs in DMEM media supplemented with 0.1 % FBS. Cells were fixed for 15 mins with 4 % PFA, permeabilised for 5 mins with 0.2 % Triton X solution and blocked for 30 mins with 0.2 % FSG. Cells were probed with the indicated antibodies. Cover slips were mounted onto slides using mounting media containing DAPI. Images were taken using a Zeiss LSM 780 microscope at 63 x magnification. Scale bars represent 20 μm. Data is representative of two independent experiments. The expression of RASSF1C leads to the increase in the cytoplasmic levels of ALIX (**A.**), CD63 (**B.**) and CD81 (**C.**), compared to control cells, indicating an upregulation of the exosome secreting machinery.

`

5.3 Cells Expressing RASSF1C Produce More Exosomes

Due to the observed expression of proteins involved in the production, packaging and secretion of exosomes, we hypothesised that RASSF1C-expressing cells could release a greater number of exosomes. RASSF1C expression drove the increase in aggressiveness and size of MDA-MB-231 mammospheres grown in matrigel (Figure 3.18). It has been shown that CD81-contatinig exosomes increase the protrusive activity, motility and metastasis of MDA-MB-231 cells (Hoshino et al., 2013; Luga et al., 2012).We observed an increase in the levels of CD81 (Figure 5.1C), therefore we decided to measure the amount of exosomes, secreted by the RASSF1C-expressing cells. We transiently transfected MDA-MB-231 cells with either pcDNA3 or FLAG-RASSF1C. The cells were grown in DMEM supplemented with 0.1 % (v/v) FBS (which had the bovine extracellular vesicle contaminants removed via ultracentrifugation) for 3 days in order to condition the media. The media was then sequentially ultracentrifuged in order to purify the exosomes that might have been secreted into the media. The produced pellet was then resuspended in 1 X PBS and adjusted depending on the final cell number count to yield equivalent secreted exosome concentrations (Hoshino et al., 2013). A device allowing Nanoparticle Tracking Analysis (NTA) has been previously designed to measure the size distribution and concentration of nanoparticles (Dragovic et al., 2011), by tracking the movement of laser-illuminated individual particles under Brownian motion. The device then calculates their diameter using statistical methods, generating a simple way to analyse large numbers of particles simultaneously. Most articles using this technique to analyse exosomes show a major population of particles between 100 and 150 nm in diameter, consistent with the sizes observed by transmission electron microscopy (Baietti et al., 2012; Colombo et al., 2013). The isolated exosomes were processed using NTA and the size and concentration of the exosomes were measured, following previously established protocol (Garnier et al., 2013). The exosomes derived from the control cells were around 100 nm and at a concentration of 15.28 x 10^8/ml. In contrast, the cells expressing RASSF1C were producing more extracellular vesicles, at a concentration of 23.79 x 10^8/ml, with a size peak between 100 and 150 nm, which fits the description of exosomes (Figure 5.2A). In order to

`

better understand the process of increased production and secretion of the exosomes, we collected the conditioned media from plates containing MDA-MB-231 cells, transiently transfected with either pcDNA3 or FLAG-RASSF1C, grown in DMEM with 0.1 % FBS for one, two or three consecutive days. We observed that the increase in the exosome population from the RASSF1C cells occurred between the second and the third day of production (Figure 5.2B), which is in accordance with the published literature where the enrichment of the media with exosomes was achieved after 3 days of incubation (Luga et al., 2012). There were not significant changes to the size of the secreted vesicles between the three days and between the pcDNA3 and RASSF1C-expressing cells (Figure 5.2C). Taken together this data confirms that the extracellular vesicles secreted by the MDA-MB-231 cells are exosomes and that RASSF1C cells release higher number of exosomes.

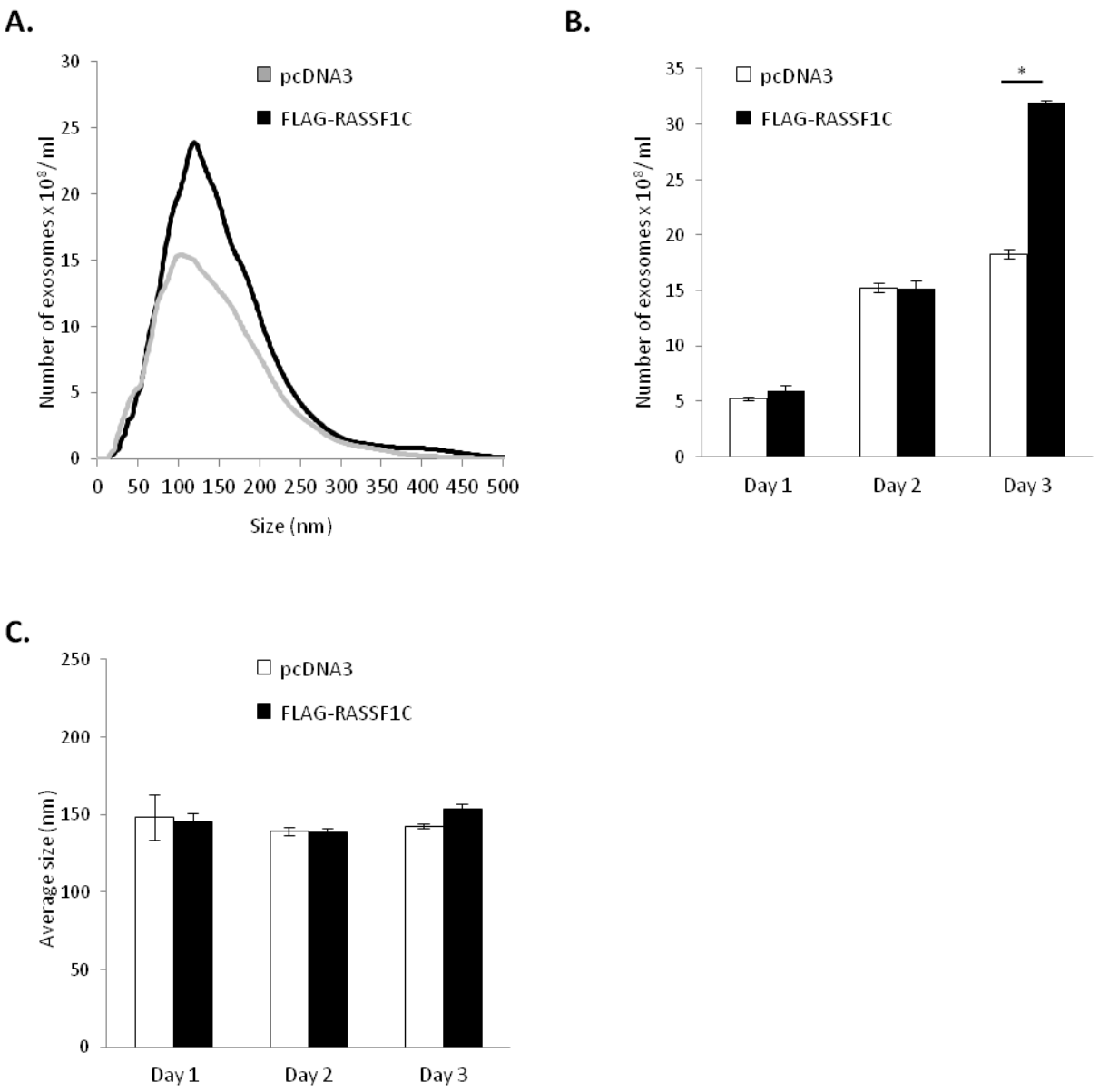


Figure 5.2. RASSF1C Cells Produce More Exosomes. A. MDA-MB-231 cells (5 x 10^6 cells/plate) were transfected with pcDNA3 or FLAG-RASSF1C. Cells were grown in DMEM media supplemented with 0.1 % FBS for 3 days. Exosomes were extracted from the conditioned media using sequential ultracentrifugation. Cells were counted at the end of the experiment and levels of exosomes were adjusted for the amount of cells per plate. Exosomes were then diluted 1:500 in PBS and counted using NanoSight NS300. Representative graph of the NTA exosome analysis. Data is representative of three independent experiments. RASSF1C-expressing MDA-MB-231 cells produce more exosomes. **B.** Quantification of exosome numbers from MDA-MB-231 cells transfected with either pcDNA3 or FLAG-RASSF1C. Cells were grown in DMEM media supplemented with 0.1 % FBS for 1, 2 or 3 days and the exosomes extracted and analysed as in **A.** The RASSF1C cells produce more exosomes compared to the control after day 2. Data is representative of three independent experiments. * $p \leq 0.05$. **C.** Quantification of the average size of the isolated exosomes from **B.** Data is representative of three independent experiments. Error bars represent 1 x SEM. The most significant increase in the production of exosomes by RASSF1C-expressing cells can be observed at day 3 after transfection.

`

5.4 Exosomes Secreted by RASSF1C Cells Vary in Their Protein Contents

Having shown that RASSF1C expression increases the number of exosomes produced in MDA-MB-231 cells, we wished to investigate whether expression of RASSF1C also altered the contents of the secreted vesicles. MDA-MB-231 cells were transiently transfected with either pcDNA3 or FLAG-RASSF1C and exosomes allowed to be released into the media for 3 days. The exosomes were then purified, lysed using 1 X RIPA buffer and analysed by SDS-PAGE and western blot. The blot was probed for a variety of known exosome proteins and for proteins that have been shown to be affected by RASSF1C expression. We observed that the exosomes, derived from the MDA-MB-231 cells expressing RASSF1C, contained significantly more exosomes-associated proteins, such as ALIX, CD81, and PDCD6, compared to controls (Figure 5.3). Interestingly we found that Caveolin levels were lower in the exosomes from RASSF1C-expressing cells compared to controls. Both SRC and the active pY416-SRC were increased in the exosomes derived from RASSF1C-expressing cells. We also saw an increase in the LFA-1 and β-catenin level in the RASSF1C-derived exosomes. No FLAG-RASSF1C was detected in the exosomes, suggesting that RASSF1C could be promoting the secretion of exosomes, but is not actively associated with the secretion or packaging mechanisms of the exosomes.

`

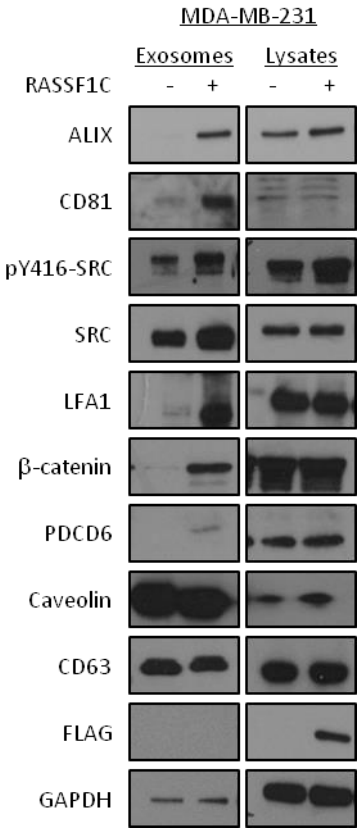


Figure 5.3. RASSF1C Expression Leads to an Increase in Exosome Cargo. MDA-MB-231 cells (5 x 10^6 cells/plate) were transfected with pcDNA3 or FLAG-RASSF1C. Cells were grown in DMEM media supplemented with 0.1 % FBS for 3 days. Exosomes were extracted from the conditioned media using sequential ultracentrifugation. Cells and exosomes were lysed using 1 X RIPA buffer. The number of cells/plate at the end of the experiment was used for protein levels normalisation of lysates and exosome samples. Samples were analysed by SDS-PAGE and western blot for the indicated antibodies. Cells transfected with RASSF1C produce more exosomes and affect the level of proteins carried by the exosomes.

`

In order to confirm that the RASSF1C-dependent changes in the exosome cargo were not unique to MDA-MB-231 cells, we tested exosomes derived from CaCo2, H1299 and MCF7 cells either expressing pcDNA or FLAG-RASSF1C. The purified exosomes and corresponding cell lysates were analysed by SDS-PAGE and western blotted for the exosome targets ALIX, CD81, PDCD6, CD63, TSG101, and for β-catenin and FLAG. In CaCo2 cells the observed differences between the control and the RASSF1C derived exosomes were not as pronounced as we observed for the MDA-MB-231 cells. However, we were still able to observe a significant increase in CD81, PDCD6 and TSG101 levels, but no levels of CD63 were detected in the exosomes (Figure 5.4A). The H1299 control and the RASSF1C cells and exosomes showed no difference in their protein contents (Figure 5.4B). In MCF7 cells, we observed increase in the levels of ALIX, CD63 and TSG101 (Figure 5.4C). Surprisingly, we were not able to detect the high upregulation of ALIX in the MCF7, as the one previously observed (Figure 5.1A). However, the exosomes did show an increase in both ALIX and CD63, suggesting that the phenotype seen previously (Figure 5.1) could be due to an increase in the packaged exosomes, ready to be released. All three cell lines showed upregulation of packaged β-catenin in exosomes derived from RASSF1C-expressing cells. Combined, these results show that the expression of RASSF1C leads to not only increase in exosome production, but that their cargo varies between cell lines and that the secretion is increased in the mesenchymal and invasive MDA-MB-231, compared to the more epithelial CaCo2 and H1299 cells.

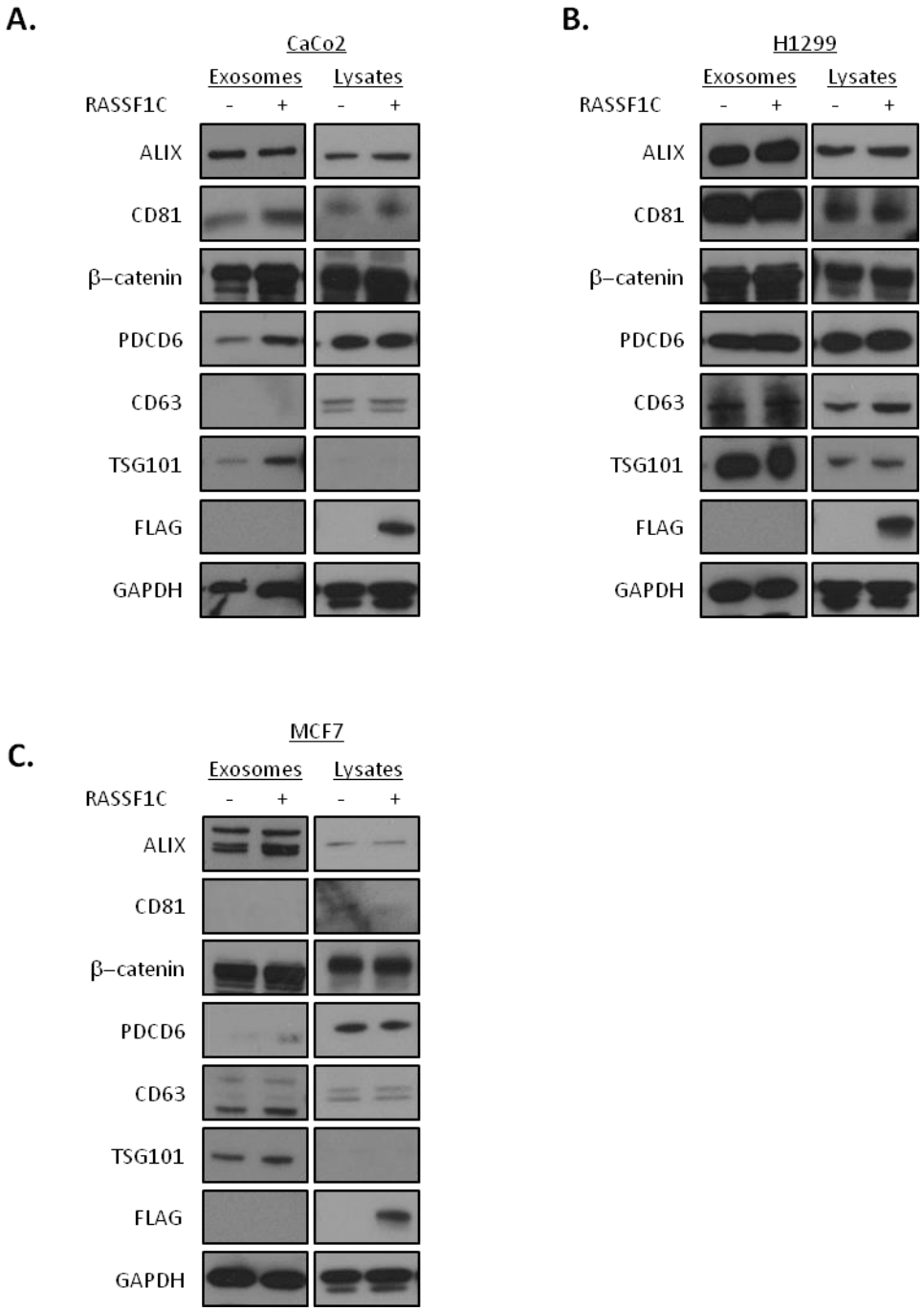


Figure 5.4. The Packaging of Proteins in Exosomes from RASSF1C-Expressing Cells is Cell Line Dependent. CaCo2 (**A.**), H1299 (**B.**) and MCF7 (**C.**) cells (5 x 10^6 cells/plate) were transfected with pcDNA3 or FLAG-RASSF1C. Cells were grown in DMEM media supplemented with 0.1 % FBS for 3 days. Exosomes were purified using sequential ultracentrifugation. Cells and exosomes were lysed using 1 X RIPA buffer. The number of cells/plate at the end of the experiment was used protein levels normalisation of lysates and exosome samples. Samples were analysed by SDS-PAGE and western blot for the indicated antibodies. All data is representative of three independent experiments. **A.** Expression of RASSF1C in CaCo2 cells led to an increase in the levels of CD81, β-catenin, PDCD6 and TSG101 in the secreted exosomes. **B**. Expression of RASSF1C in H1299 cells did not affect the protein contents of the exosomes, compared to ones derived from control cells. **C.** RASSF1C-derived exosomes from MCF7 cells led to an increase in ALIX and TSG101. Taken together, this data shows that RASSF1C promotes the upregulation of proteins packaged in exosomes in a cell-line dependent manner.

`

5.5 The Changes in Exosome Cargo Do not Alter the Rates of Internalisation

One of the properties of the exosomes as extracellular vesicles is that they can act as messengers between cells. Exosomes secreted by one cell can interact with and be internalised by other cells inducing changes in their physiology. We sought to better understand whether the exosomes secreted by the RASSF1C cells, despite their obvious differences in cargo and number, remain biologically active and are still able to be internalised by naïve cells. We isolated exosomes from MDA-MB-231 cells, either transfected with pcDNA3 or FLAG-RASSF1C, by ultracentrifugation. In this case the protein content was measured using a Bicinchonic acid (BCA) Micro Protein Assay kit, due to its high sensitivity in protein detection, in order to load the same amount of exosomes from the control and RASSF1C cells onto naïve MDA-MB-231 cells. The exosomes were then stained using the PKH67 dye, which stains the exosome membrane, as previously reported (Sheldon et al., 2010). Naïve MDA-MB-231 cells were then treated with the PKH67 stained exosomes derived from pcDNA3- or FLAG-RASSF1C-transfected cells, or were left untreated for 18 hrs. Cells were then fixed and co-stained with anti-CD63 antibody and imaged. We observed that the naïve cells internalised the exosomes from both pcDNA3 and FLAG-RASSF1C-expressing cells shown by the presence of the PKH67 and CD63 stained vesicles within the cells. Furthermore, the PKH67 vesicles co-localize with CD63, clearly demonstrating that the exosomes present in the cells (CD63 positive) had been internalised from the media and not generated by the naïve cells (Figure 5.5). However, the intensity of the cells treated with exosomes, derived from RASSF1C-expressing cells appears to be increased, compared to the control, with an increase in the level of co-localisation between exosomes and CD63 staining.

`

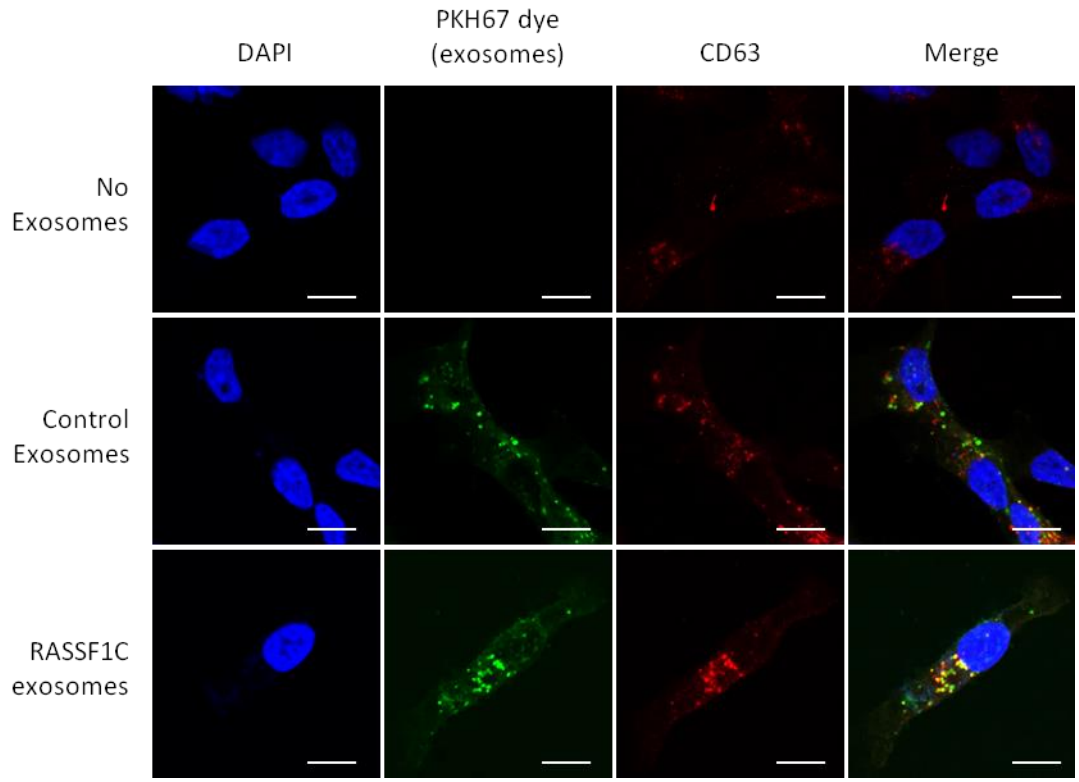


Figure 5.5. The Exosomes Secreted by the Control or RASSF1C Cells are Able to Be Internalised. MDA-MB-231 cells (5 x 10^6 cells/plate) were transfected with pcDNA3 or FLAG-RASSF1C. Cells were grown in DMEM media supplemented with 0.1 % FBS for 3 days. Exosomes were extracted from the conditioned media using sequential ultracentrifugation. Cells and a fraction of the exosomes were lysed using 1 X RIPA buffer and the protein content measured using BCA Micro kit to ensure equal loading of 50 μg/ml of exosomes per well. Exosomes were stained using the PKH67 kit following manufacturer's instructions prior to their addition to naïve MDA-MB-231 cells, plated at 2 x 10^5 cells/plate in 6 well plates. The cells were treated with the exosomes for 18 hrs.. Scale bars represent 20 μm. Data is representative of three independent experiments. Both the exosomes derived from pcDNA3 and RASSF1C were internalised by the naïve cells, but the levels of internalised exosomes appear higher in the cells treated with RASSF1C exosomes.

In order to further validate whether more cells are internalising the exosomes, we used Flow cytometry to analyse and quantitate the uptake of PKH67-stained exosomes isolated from MDA-MB-231 or MCF7 cells, transfected with either pcDNA3 or FLAG-RASSF1C. Exosomes isolated from MDA-MB-231 cells were used on naïve MDA-MB-231 cells and MCF7 exosomes were used on MCF7 naïve cells. We used a FACScalibur FACS analyser in order to count the PKH67 positive (green) cells that had internalised exosomes and compared the relative intensities per cell. Contrary to our observation that the levels of exosome uptake was increased when cells were treated with RASSF1C-

`

derived exosomes (Figure 5.5), we did not observe any difference in the internalisation rates of exosomes secreted by either pcDNA- or RASSF1C-expressing cells for both MDA-MB-231 cells (Figure 5.6A) or the MCF7 cells (Figure 5.6B). These results suggested that if any, a response of the exosome-treated naïve cells will not be based on the amount of internalised exosomes, but potentially of their contents and the mechanisms they trigger when internalised. We therefore decided to investigate what effect do the RASSF1C exosomes have on tumourigenesis of naïve cells.

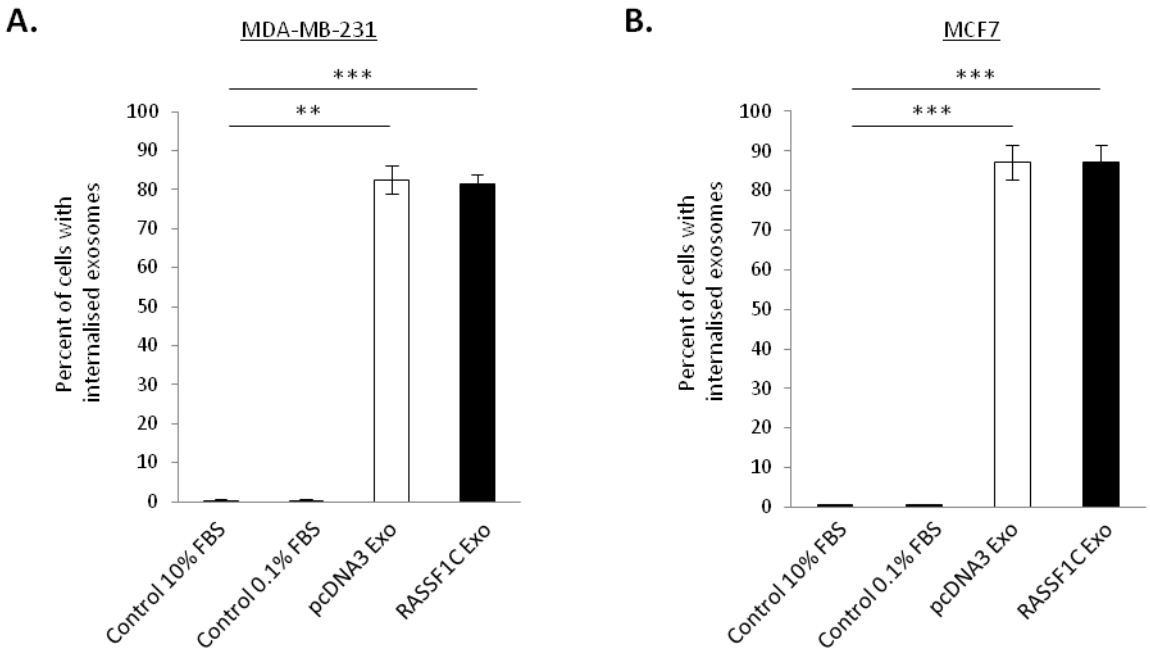


Figure 5.6. The Exosomes Secreted by the Control or RASSF1C Cells are Internalised by Equal Numbers of Naïve Cells. MDA-MB-231 (**A.**) and MCF7 (**B.**) cells (5 x 10^6 cells/plate) were transfected with pcDNA3 or FLAG-RASSF1C. Cells were grown in DMEM media supplemented with 0.1 % FBS for 3 days. Exosomes were extracted from the conditioned media using sequential ultracentrifugation. Cells and exosomes were lysed using 1 X RIPA buffer and the protein content measured using BCA Micro kit to ensure equal loading of 50 μg of exosomes per well. Exosomes were stained using the PKH67 kit following manufacturer's instructions and added to naïve cells, previously plated at 2 x 10^5 in 6 well plates. Naïve MDA-MB-231 cells were treated with exosomes from MDA-MB-231 cells, and MFC7 cells were treated with exosomes from MCF7 cells. The cells were treated with the exosomes for 18 hrs. Cells were then trypsinised, blocked with 3 % BSA in 1 X PBS and processed using FACScalibur FACS analyser. Data is representative of three independent experiments. Error bars represent 1 x SEM. ** $p \leq 0.01$, *** $p \leq 0.001$. **A.** Both the exosomes derived from pcDNA3 and RASSF1C were equally internalised by the naïve MDA-MB-231 cells. **B.** The exosomes derived from pcDNA3 and RASSF1C were internalised by equal numbers of naïve MCF7 cells.

`

5.6 Exosomes from RASSF1C Cells Increase the Growth of Mammospheres

So far, we observed that RASSF1C expression promotes the increased generation and release of exosomes and alters the exosome cargo. Also, we showed that the released exosomes are active and can be internalised by other cells. Once secreted from the cell, exosomes can deliver their cargo to adjacent or distant cells, leading to modifications in the target cell's gene expression, signalling, and overall function, which, in tumours, can lead to an increase in angiogenesis, EMT, invasiveness and metastasis (Barres et al., 2010; Fausti et al., 2013; Garnier et al., 2012; Hoshino et al., 2013; Luga et al., 2012; Morelli et al., 2004; Segura et al., 2005). Therefore, we wanted to investigate the potential physiological changes that the recipient cells undergo. One of the oncogenic phenotypes we observed for cells expressing RASSF1C was increased mammosphere growth and aggressiveness (Figure 3.18). We decided to investigate the role that exosomes derived from RASSF1C-expressing cells might play in this. We transiently transfected MDA-MB-231 cells with either pcDNA3 or FLAG-RASSF1C. Media was conditioned for 3 days, after which the exosomes were purified by ultracentrifugation and the protein content measured in order to ensure equal loading, since we wanted any effects that the exosomes would have to be attributed to the contents of the exosomes and not their numbers. Naïve MDA-MB-231 cells were plated on matrigel for 24 hrs prior to the treatment with exosomes from pcDNA3 cells, exosomes from RASSF1C-expressing cells or left untreated. Mammospheres were treated every three days with 50 μg/ml of exosomes per well, in accordance with previously published reports (Sheldon et al., 2010) and were grown for a total of 10 days. We observed that both the mammospheres treated with exosomes from pcDNA3- or RASSF1C-expressing cells were bigger (Figure 5.7A) and were more aggressive (Figure 5.7B) than the mammospheres not treated with exosomes. This could be attributed to the fact that the exosomes derived from the control cells were positive for active SRC, which, as seen in Figure 3.18 could have induced the increase in the mammosphere growth. However, the mammospheres treated with

`

exosomes derived from RASSF1C cells grew larger (Figure 5.7A) and had more aggressive phenotype (Figure 5.7B), compared to the control and untreated mammospheres (Figure 5.7C). Taken together, this data suggests that RASSF1C-expressing cells not only generate and release more exosomes than control cells, but that the changes to the protein content of the exosomes have biological activity that stimulates cell growth and invasion. In order to completely understand the mechanism through which RASSF1C-derived exosomes promote oncogenesis, we further analysed their contents, by isolating mRNA from these exosomes. This work will be covered in Chapter 6.

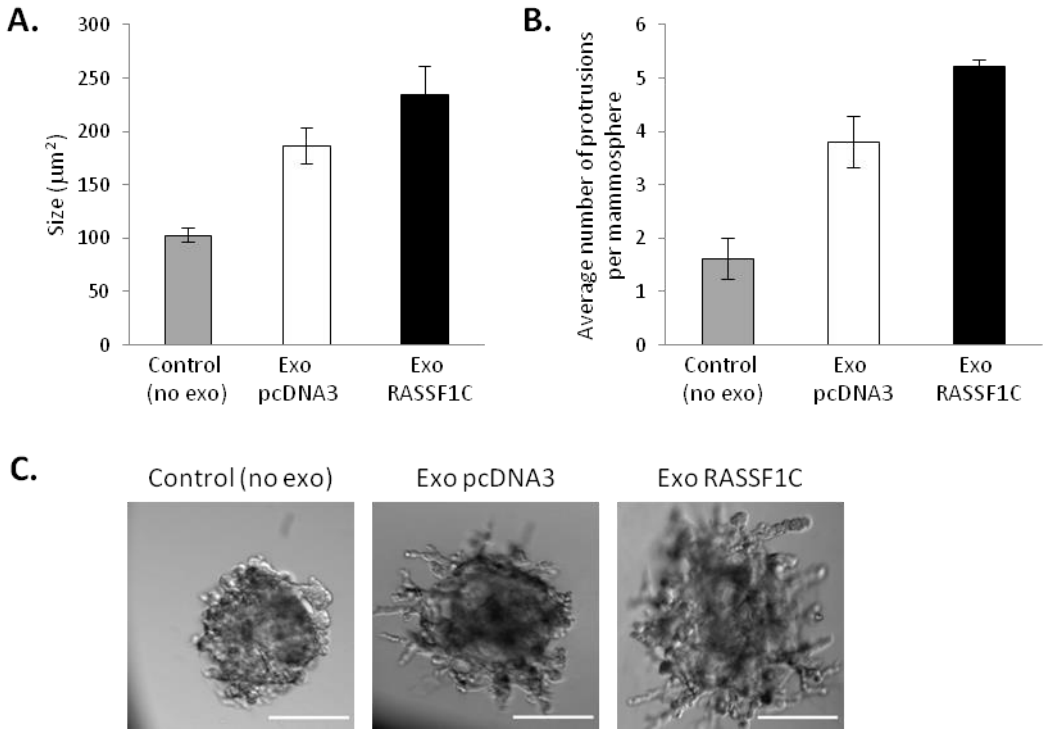


Figure 5.7. MDA-MB-231 Cells treated with Exosomes Derived from RASSF1C Cells Are More Invasive. MDA-MB-231 cells (5 x 10^5 cells/plate) were transfected with pcDNA3 or FLAG-RASSF1C. Cells were grown in DMEM media supplemented with 0.1 % FBS for 3 days. Exosomes were extracted from the conditioned media using sequential ultracentrifugation. The protein content measured of the exosomes was measured to ensure equal loading of 50 μg/ml of exosomes per well. MDA-MB-231 cells were seeded onto growth factor reduced matrigel (2500 cells/well) and grown for a day before the extracted exosomes were added. Media and fresh exosomes were added every 3 days. Images were taken at 10 X magnification using a Nikon TE2000 Eclipse microscope. Mammosphere area (**A.**) and number of protrusions (**B.**) were measured using Nikon NIS Elements. Data is representative of two independent experiments and includes quantification of 40 mammospheres per condition per experiment. Error bars represent 1 x SD. **C.** Representative images of mammospheres of control cells, cells treated with exosomes from pcDNA3 transfected cell and cells transfected with FLAG-RASSF1C. Scale bars represent 200 μm.

`

5.7 Discussion

In this chapter I have shown that the expression of RASSF1C leads to upregulation of known exosome proteins. RASSF1C-expressing cells were also found to release significantly more exosomes *in vitro* and that this release was time dependent. In addition, the packaging of proteins in the secreted active exosomes is altered by RASSF1C expression, leading to increased levels in the exosomes of the exosomal biogenesis proteins ALIX and TSG101, the tetraspanins CD63 and CD81 and the tumour-associated marker Caveolin. However, the proteins packaged in the exosomes varied between cell lines. We have also shown that RASSF1A-expressing cells release less exosomes, compared to the control and RASSF1C ones. Finally, we showed that RASSF1C derived exosomes induce an increase in cellular growth and aggressiveness, in keeping with the idea that RASSF1C is an oncogene, which is also supported by the higher levels in the exosomes of the oncogenes β-catenin and SRC.

Given that we identified vesicles in RASSF1C-expressing cells in Chapter 3, and that exosomes are known to play a role in cancer development, we decided to investigate whether expression of RASSF1C leads to upregulation in the exosome production by investigating the levels of ALIX, CD63 and CD81. Exosomes are vesicles of 50-150 nm in size, made from a protective lipid bilayer. They can contain proteins, mRNA and miRNA (Colombo et al., 2014). The list of proteins found in exosomes is highly variable and is constantly changing, however some proteins appear to remain constant, such as ALIX, CD63 and CD81, making them good markers for identifying exosomes (Thery et al., 2006). In the cell, ALIX (also known as PDCD6IP) is a protein that interacts with several ESCRT proteins (including TSG101 and CHMP4) and is thought to participate in endosomal sorting processes, vesicle budding and abscission (Bowers et al., 2004; Katoh et al., 2003; Matsuo et al., 2004; Odorizzi, 2006). CD63 is a member of the tetraspanin family of transmembrane and cytosolic proteins, often referred to as lysosomal membrane protein that can translocate between lysosomes and endosomes (Pols and Klumperman, 2009). The other member of the tetraspanins, CD81 has been shown to associate with CD63 (Radford et al., 1996) and both CD63 and CD81, have been linked to ESCRT-independent

`

secretion of exosomes (Perez-Hernandez et al., 2013; van Niel et al., 2011). Staining of MCF7 cells, expressing RASSF1C showed that all three proteins, ALIX, CD63 and CD81 were upregulated (Figure 5.1). This led us to believe that RASSF1C expression could lead to an activation of both ESCRT-dependent and -independent exosome production mechanisms. However it did not show us if RASSF1C plays a role in exosome secretion, or whether this was ESCRT-dependent or –independent. In Chapter 3, we showed that expression of RASSF1C leads to activation of SRC. Interestingly, SRC has been shown to phosphorylate and inactivate ALIX and to lead to its sequestration away from the focal adhesions, which it normally inhibits (Schmidt et al., 2005). The inhibition of ALIX by SRC has been linked to the assembly and stabilisation of focal adhesion, but its role in regulating ALIXs functions in exosome secretion or the ESCRT-dependent biogenesis of exosomes has not been studied. It would be interesting to investigate if SRC, activated by RASSF1C expression, is able to phosphorylate and inactivate ALIX. This may give us more insight into whether the exosomes production we observe is ESCRT-dependent or independent. We would hypothesise that if the SRC-dependent inhibition of ALIX prevents its association with the ESCRT-dependent packaging of exosomes, then the generation of exosomes could be ESCRT-independent via CD63 and CD81 activity, which are upregulated in RASSF1C-expressing cells (Figure 5.1B and C). However, SRC localisation to the focal adhesions is thought to be dependent on functioning ESCRT pathway (Tu et al., 2010), suggesting that RASSF1C could be involved in processes that are ESCRT-dependent (stabilisation of focal adhesions) and –independent (secreting exosomes). Therefore, it would be interesting to see if RASSF1C plays a role in exosome formation or translocation by investigating if RASSF1C interacts directly with the ESCRT machinery or with proteins involved in MVB formation. In addition, the levels of active Focal Adhesion Kinase (FAK) should be assessed in RASSF1C-expresing cells, in order to further understand if RASSF1C can lead to stabilisation of the focal adhesions by recruiting SRC and inactivating ALIX.

The increase in the levels of CD63, CD81 and ALIX in RASSF1C-expressing cells led us to investigate the levels of exosomes produced by the RASSF1C cells. We hypothesised that RASSF1C expression

`

would lead to increased production of exosomes, which is exactly what we observed in MDA-MB-231 cells (Figure 5.2A). Intriguingly, a time course experiment for the secretion of exosomes showed that the major increase in the quantity of RASSF1C-derived exosomes was achieved between the second and the third day (Figure 5.2B). This could be due to a steady increase in the RASSF1C expression levels that reaches its peak at day 2/3. Or potentially could be associated with autocrine signalling, where at certain concentration, the exosomes produced by the RASSF1C-expressing cells upregulate the exosome production in the rest of the cells or in the same cells in a positive feedback-loop (Luga et al., 2012; Riches et al., 2014). Also, the conditioning of the media for 3 days has been used in the literature (Luga et al., 2012). The observed increase in the secretion at day 3 could also be explained with the expression of RASSF1C that requires a build-up of transcriptional upregulation of genes associated with the exosomes, followed by the sudden release of exosomes. We could investigate this further by tracking the changes in levels of RASSF1C and the amount of exosomes released. We could also follow the secretion of exosomes beyond day 3, however, initially, we decided not to continue the time course beyond 3 days due to the fact that cells were left in media containing 0.1 % FBS for prolonged periods of time and serum cell starvation can have detrimental effects on cell division, exosome secretion and morphology and cell viability, leading to off target effects. As seen in Figure 5.2C, there were no significant changes in the size of the exosomes during the short time course of 3 days. Therefore, we wanted to see if there were any changes in the contents of the exosomes.

In order to further assess the exosomes from RASSF1C-expressing cells, we investigated the protein content of the purified exosomes. We observed that in MDA-MB-231 cells, the expression of RASSF1C leads not only to increase in the levels of exosomes, but also to the differential packaging of the RASSF1C-derived exosomes compared to the control ones (Figure 5.3). We investigated the presence of the common proteins secreted in exosomes and found that RASSF1C expression led to an increased packaging of these core exosome proteins. We also investigated whether targets associated with RASSF1C signalling were packaged into exosomes. We examined β-catenin and SRC,

`

which are known to package into exosomes (Chairoungdua et al., 2010; Mineo et al., 2012). Secreted exosomal SRC has been previously shown to promote Focal Adhesion Kinase (FAK) activation and angiogenesis (Mineo et al., 2012). Given the previously discussed role of SRC in ALIX inhibition (Schmidt et al., 2005), we observed an increase in the levels of both pY416-SRC and ALIX in the exosomes and the cell lysates from RASSF1C cells (Figure 5.3). Given the phosphorylation of SRC in these cells and its role in junctional stability (Figure 3.5), it would be interesting to examine the role of the secretion of active SRC via exosomes. If RASSF1C-expressing cells have inhibited ALIX, due to increase in SRC activity, we would hypothesise that secreted exosomes containing pY416-SRC can induce a similar phenotype in the surrounding cells lacking RASSF1C: loss of junctions, increase in focal adhesion and a YAP1/β-catenin gene transcriptional activation, thus leading to increased invasiveness and aggressiveness.

The levels of CD81 in the exosomes derived from RASSF1C-expressing cells were also increased (Figure 5.3). MDA-MB-231 cells secreting CD81 have been shown to promote stromal mobilisation and enhance metastasis (Luga et al., 2012). We could hypothesise that the exosomes secreted by RASSF1C-expressing cells and containing CD81 could also facilitate the invasion of the surrounding cells, even if they do not express RASSF1C.

We also found an upregulation of the integrin LFA-1 in the exosomes. LFA-1 expression has been associated with the expression of CD63, which we observed was upregulated in RASSF1C-expressing cells (Radford et al., 1995). The increase in LFA-1 was only observed in the MDA-MB-231 cells, which could be explained with their mesenchymal and metastatic potential due to RASSF1C expression. We are currently investigating the role of LFA-1 upregulation in metastasis, to see if packaging of LFA-1 into exosomes could help modify of the site of distant metastasis.

It is important to note that contrary to the increase in ALIX, CD63 and CD81 levels, shown by immunofluorescence in Figure 5.1, we did not see a similar level of upregulation in the lysates from the MCF7 cells (Figure 5.4). Since the transfection efficiency for RASSF1C is generally quite poor, we

`

could assess the upregulation of the exosome factors in the MDA-MB-231, H1299 and Caco2 cells by immunofluorescence, as we did for the MCF7 cells, however, a more stringent method would be to use Flow cytometry to analyse RASSF1C-expressing cells and compare the levels of these factors in RASSF1C positive and negative cells. We are currently carrying out these experiments.

Interestingly, we observed variability in the proteins that were upregulated and their levels in the exosomes derived from RASSF1C-expressing cells (Figure 5.4). This is in agreement with previous work that showed that the protein contents of the exosomes is cell line dependent (Melo et al., 2015), but further investigation is required to understand how RASSF1C affects the decision for changes in the packaged proteins in the exosomes. We would address this by analysing exosomes from different cell lines using mass spectrometry. Also, in order to better understand the reasoning behind the difference in the packaged proteins in the exosomes, we are investigating novel mechanisms that can control the packaging of exosomes, independently of RASSF1C expression. We have seen that inhibition of PI3K or Akt can affect the packaging of CD63 and Caveolin in the exosomes (Figures 8.8 and 8.9), and that the differentially packaged exosomes can affect the growth of mammospheres (Figure 8.10). This is part of ongoing work.

Extracellular vesicles like exosomes can act as messengers at the cell surface and in intercellular communication. The internalisation of exosomes can occur through various processes, including actin polymerisation-, dynamin- and PI3-kinase-dependent phagocytosis (Barres et al., 2010; Feng et al., 2010); receptor-mediated endocytosis (Morelli et al., 2004); clathrin-dependent (Fruhbeis et al., 2013); or caveolae-dependent endocytosis (Nanbo et al., 2013). Even though we observed that RASSF1C-derived exosomes were internalised (Figures 5.5 and 5.6), it remains unclear which pathway of internalisation the cells are using. This should be an important point for investigation for future studies since it could be used as a target in order to prevent the spreading of the tumourigenic signals carried by the exosomes.

`

It would be interesting to follow the internalisation of exosomes by different organs *in vivo*. This has been achieved recently by the use of Cre-LoxP system, where in MDA-MB-231 cells Cre recombinase is packaged onto the secreted extracellular vesicles. When the vesicles are released and they are internalised by the recipient cells, the Cre recombinase will induce change in colour from DsRed to GFP, thus facilitating the detection of cells which have internalised the vesicles (Zomer et al., 2015). We could use this system to knock-down expression of crucial internalisation pathway members, such as clathrin, but also this system can be used to follow to follow the secretion of the exosomes and what tissues are more responsive to the signals carried within the vesicles. We would hypothesise that the exosomes could either promote the dissemination of cells from the initial tumour, or facilitate the establishment of the travelling cancer cells at a site of distant metastasis. This would be tested both *in vitro* and *in vivo*.

In order to further understand the signals carried by the RASSF1C-derived exosomes and their potential role in tumourigenesis and invasiveness, we grew mammospheres from naïve MDA-MB-231 cells, which we treated with exosomes. We observed that RASSF1C-derived exosomes increase the size and invasiveness of the mammospheres, compared to mammospheres treated with control exosomes (Figure 5.7). Given that we identified increased levels of SRC and β-catenin in the RASSF1C derived exosomes we could be driving a phenotype similar to the one observed in Chapter 3, where the expression of RASSF1C leads to SRC activation and increased mammosphere growth and aggressiveness. However, SRC and β-catenin could also be increasing tumourigenicity via the upregulation of *BCL2L1*, *BIRC5* and *c-MYC*, as shown in Figure 4.11. SRC could be involved in the ALIX/Caveolin/β-catenin induced growth. Taken together, this data suggests that RASSF1C-expressing cells change the protein content of the exosomes and induce biological activity that stimulates cell growth and invasion. In order to completely understand the mechanism through which RASSF1C-derived exosomes promote oncogenesis and increase mammosphere growth, we further analysed their contents, isolating packaged mRNA. This matter will be further investigated in Chapter 6.

`

Together the work presented in this chapter (summarised in Figure 5.8) shows that RASSF1C expression drives a mechanism that leads to the upregulation of CD63 and CD81 and the consequent increase in exosome release. RASSF1C can activate SRC and SRC could then phosphorylate and inactivate ALIX, stabilising the focal adhesions. In addition, exosomes released from RASSF1C-expressing cells can contain active SRC and β-catenin, which can induce mammosphere growth and aggressiveness in matrigel.

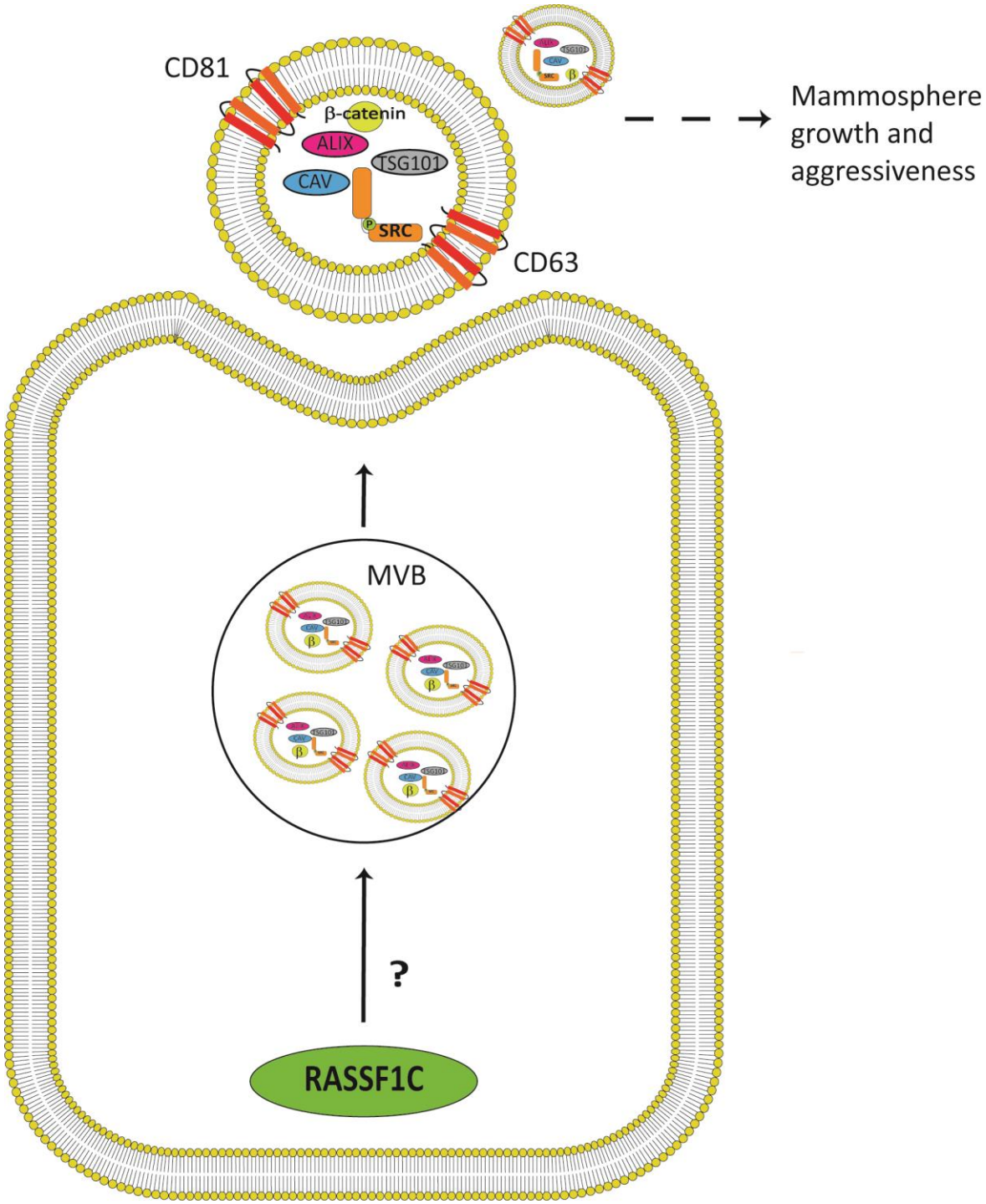


Figure 5.8. Cartoon Depicting the Hypothesis Generated from the Work in Chapter 5. RASSF1C expression leads to upregulation of proteins associated with the packaging of exosomes and consequentially leads to increased exosome secretion. The proteins packaged in the exosomes released from RASSF1C-expressing cells include ALIX, TSG101, CD63, CD81, active SRC and β-catenin. The secreted RASSF1C-derived exosomes can be internalised by naïve cells and promote growth and aggressiveness of mammospheres in matrigel.

`

Chapter 6 RASSF1C Promotes a Cancer Stem Cell Phenotype

6.1 Introduction

In Chapter 5, we identified the role of RASSF1C in the production and secretion of extracellular vesicles, particularly of exosomes. We observed that RASSF1C plays a role in the differential packaging of the exosomes in MCF7 and MDA-MB-231 breast cancer cell lines, but not in lung cell line H1299. Finally, it was shown that these exosomes are internalised by naïve cells and that their internalisation triggers an increase in the growth and aggressiveness of mammospheres.

6.1.1 Cancer Stem Cells

The Cancer Stem Cell (CSC) model suggests a cellular mechanism that leads to phenotypic and functional heterogeneity in a variety of cancer types. CSCs, like embryonic stem cells, show properties of self-renewal and differentiation, but unlike somatic stem cells, CSC are not omnipotent, but are known to only differentiate into one cell type – the cells involved in the formation of the tumour. Interestingly, CSCs are not thought to originate from somatic stem cells, but are thought to develop through de-differentiation of differentiated cells. Recent reports have shown that CSCs could have the potential for multilineage differentiation in colon cancer and leukaemia (Vermeulen et al., 2008; Wiseman et al., 2014). The concept for CSCs was first introduced in AML, where the CSCs, termed leukaemia-initiating cells, were grown as xenografts in severe combined immunodeficient mice, by injecting different numbers of cells per mouse and establishing a linear correlation with engraftment and establishing that AML is organized as a hierarchy with differential expression of the

`

cell membrane markers CD34 and CD38 (Bonnet and Dick, 1997; Lapidot et al., 1994). After this initial study, CSCs have been identified in the populations of breast (Ginestier et al., 2007), brain (Singh et al., 2003), prostate (Collins et al., 2005), ovarian (Bapat et al., 2005), colon (Dalerba et al., 2007), liver (Hermann et al., 2007), lung (Eramo et al., 2008), and pancreatic tumours (Hermann et al., 2007). Generally, these stem cells have been shown to have a higher tumourigenic capacity when seeded for xenografts. However, within tumour, distinct populations of stem cells can be identified. Single-cell sequencing of human breast cancer samples has shown that there are distinct subpopulations of cells within the tumour and that a particular population can be identified as the dominant, metastasis-seeding one (Navin et al., 2011). Interestingly, since tumour initiation is one of the defining features of CSCs, xenografting is central to the CSC model. However, a limitation of xenograft studies is that even orthotopic transplantation may not faithfully reproduce the growth factor milieu found within a patient's tumour. For example, some murine growth factors, such as Tumour Necrosis Factor, are not cross-species reactive and these environmental differences can apply selective forces on tumour cells, resulting in CSCs from humans not displaying growth as xenografts (Kreso and Dick, 2014; Rongvaux et al., 2013).

The identification of CSCs has been predominantly done using combinations of cell-surface antigens, including CD133, CD44, EpCAM and ALDH activity. However none of these markers are exclusively expressed by the CSCs, as they often exhibit much broader expression than what could be expected from the low CSC numbers, identified in tumours by xenotransplatation assays (Ricci-Vitiani et al., 2007). The CD133 antigen has been used as a CSC marker in various cancers, including brain (Singh et al., 2003), lung (Eramo et al., 2008), pancreas (Hermann et al., 2007) and prostate (Collins et al., 2005). It has also been used as a marker for stem/progenitor cells in normal somatic tissues, including brain (Lee et al., 2005) and liver (am Esch et al., 2005). Aldehyde dehydrogenase 1 (ALDH1) is a protein used to mark CSCs in leukaemias and breast (Ginestier et al., 2007), colon (Carpentino et al., 2009) and lung (Ma et al., 2008) carcinomas. CSCs from breast cancer have also been characterised by the $CD44^{high}/CD24^{low}$ surface marker levels (Al-Hajj et al., 2003), however these

`

markers fail to selectively enrich for CSCs in ER-negative and triple-negative breast tumours (Meyer et al., 2010). In addition, in patients with non-small lung cancer, CD166 emerged as a better marker for CSCs in 50% of the cases, compared to CD133, CD44 and EpCAM (Zhang et al., 2012). Therefore, although a number of markers have been identified, they appear to vary not just between cancers from different tissue types, but also within tumours of one tissue type. This may be due to different mutations causing the cancer and resulting in different stem cell markers being expressed.

A process that has been shown to result in the generation of cells with stem-like properties is EMT (Mani et al., 2008). TGFβ as well as canonical and non-canonical WNT/β-catenin signalling have been linked to EMT and production of CSCs (Thiery et al., 2009). Such signalling cascades induce the expression of EMT transcription factors, like SNAIL, TWIST and ZEB. ZEB has been shown to respond to TGFβ and to induce a switch between non-CSC and CSC state (Chaffer et al., 2013). This switch can also explain the reports that in breast, ovarian and squamous cell carcinomas there is a phenotypic and functional heterogeneity in the CSC population (Meyer et al., 2010; Schober and Fuchs, 2011; Stewart et al., 2011). In addition, β-catenin-dependent transcription has been associated with the generation of colorectal CSCs, due to stimulation by hepatocyte growth factor, a known inducer of EMT (Vermeulen et al., 2010).

Interestingly, the microenvironment plays an important role in the generation and maintenance of CSCs (Kucia et al., 2005). In some glioblastomas, there is a bidirectional relationship between the CSC and the local environment (Safa et al., 2015). The communication between the microenvironment and the CSCs is observed even in nonsolid tumours, where cytokines and growth factors can instruct and determine the lineage fate of leukemic stem cells (Wei et al., 2008).

Most CSCs seem to be resistant and evade cytotoxic therapies and radiotherapy. There is evidence for a subpopulation of chemotherapy-resistant CSCs in a variety of solid tumours (Li et al., 2008; Yu et al., 2007). One interesting property of CSCs, given that they are thought to give rise to the tumour, is quiescence. In leukaemia, CSCs have been targeted by using cytokines to induce entry into the cell

`

cycle (Saito et al., 2010); inhibition of DNA repair mechanisms (Viale et al., 2009); or by using monoclonal antibodies against targets like CD44 (Jin et al., 2006) or CD47 (Chao et al., 2011). Currently, studies are focusing on targeting the radioresistance of CSCs (Hambardzumyan et al., 2008) through inhibiting receptor signalling inhibition using small molecule (Beck et al., 2011; Vermeulen et al., 2010); or micro-RNAs (Liu et al., 2011a).

6.1.2 Cancer Stem Cells and Hippo Signalling

As discussed in Chapter 5, the Hippo pathway plays a key role in the regulation of organ size and tumourigenesis. Cellular signalling activates MST1/2 and LATS1/2 to inhibit YAP/TAZ localisation to the nucleus. Failure to inactivate YAP/TAZ leads to their nuclear localisation, where they form a complex with the transcription factors TEAD1-4, which promotes cell and tumour growth. In breast cancer, TAZ has been shown to be a key regulator of CSCs. In a cohort of 993 primary tumours, poor histological differentiation of the tumours was associated an increase of TAZ levels in CSCs, which has been shown to have a negative prognostic value (Cordenonsi et al., 2011). Also, YAP1 and TEAD have been shown to be highly expressed in the CSCs of medulloblastoma (Fernandez et al., 2009), whereas TAZ has been highly expressed in glioblastomas, where it leads to increased invasion, self-renewal and generation of mesenchymal-like stem cells (Bhat et al., 2011). High YAP/TAZ activity has also been linked to the CSC content in well-differentiated, less aggressive tumours (Pece et al., 2010). Also, TAZ has been linked to EMT (Chan et al., 2008b) which has been shown to disrupt the inhibitory association of MST/LATS with TAZ, leading to the generation of breast CSCs, demonstrated by the change in the expression of cell surface markers CD44 and CD24 (Cordenonsi et al., 2011).

`

6.1.3 Aims

The work in Chapter 5 indicated a role of RASSF1C in extracellular communication via the secretion of exosomes. Exosome secretion has also been linked to the CSCs (Kumar et al., 2015). Given the oncogenic roles of RASSF1C upregulating YAP1 and β-catenin, promoting a partial EMT phenotype and upregulating the secretion of exosomes, we sought to investigate whether cells expressing RASSF1C undergo phenotypical changes suggestive of CSC generation.

6.2 Expression of RASSF1C Leads to Changes in Cell Morphology

In Chapter 3 we demonstrated that the expression of RASSF1C promotes the loss of cell-cell junctions (Figure 3.4) and increased motility (Figure 3.17). The loss of cell-cell junctions has been associated with EMT, which leads to the generation of CSCs (Scheel and Weinberg, 2012). During our experiments designed to investigate the loss of cell-cell junctions, we have observed that epithelial cells (MCF7, CaCo2 and H1299), expressing RASSF1C, can undergo loss of cell-cell contact, which results in cells rounding-up and escaping the monolayer. In order to quantify this, we transfected MCF7 cells with ZsGreen-empty vector or ZsGreen-RASSF1C. The cells were directly imaged from the plate 48 hrs after transfection in order to minimise disturbance to the plate that might result in loss of cells from the monolayer. All rounded cells, both in and out of the monolayer were counted. We observed, as in our previous experiments, that expression of RASSF1C leads to an increase in cells with a rounded morphology (Figure 6.1 A and B). This is in agreement with the SRC-mediated loss of junctions via RASSF1C expression (Figure 3.1 and Figure 8.4).

`

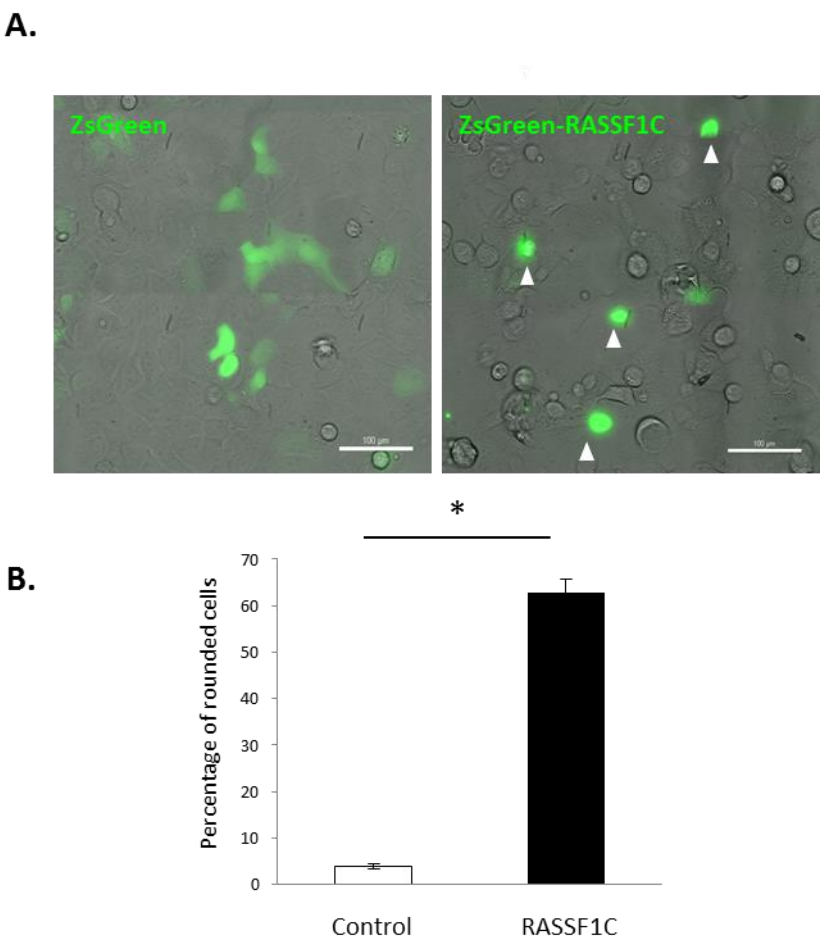


Figure 6.1. RASSF1C-Expressing Cells Become Rounded. A. Representative images of MCF7 cells (3 x 10^5 cells/condition), which were plated onto 12 well plates and transfected with ZsGreen-empty vector or ZsGreen-RASSF1C. Cells were imaged 48 hrs after transfection on a Nikon TE2000 Eclipse microscope, at 20 X magnification. Scale bars represent 100 μm. **B.** Quantification of the rounded morphology of the cells in **A.** Rounded cells were defined as circular cells that had left the monolayer. Data is representative of three independent experiments. On average 5000 cells were processed per experiment. The percentage of RASSF1C-expressing cells with a rounded phenotype is higher than the control cells.

`

6.3 The Rounded RASSF1C-Expressing Cells are Functional and Not Dividing

Cells round-up in the observed manner for a number of reasons, including: during apoptosis, cell division and senescence. In order to investigate whether the rounded RASSF1C-expressing cells are undergoing cell division, we transiently transfected MCF7 cells with ZsGreen-empty vector or Zs-Green-RASSF1C. After three days we stained the cells for phospho-Histone H3 (pH3). Histone H3 is specifically phosphorylated during mitosis and therefore can be used as a marker (Hans and Dimitrov, 2001). We observed that there was no increased staining of pH3 in the Zs-Green-RASSF1C cells, compared to the control (Figure 6.2). In order to quantify the number of cells undergoing mitosis, we stained the cells with propidium iodide, a counterstain which binds to DNA. We observed that there was a decrease in the amount of cells in G2/M in cells expressing RASSF1C compared to controls (Figure 8.7). These data suggest that the rounded cells expressing RASSF1C are not rounding-up for cell division.

Next we assessed whether the RASSF1C-expressing cells were rounding-up due to them undergoing cell death. We stained MCF7 cells with the proliferation marker Ki-67. Ki-67 is a molecule expressed throughout all points of the cell cycle except in the G0 resting phase. We transiently transfected MCF7 cells with ZsGreen-empty vector or Zs-Green-RASSF1C. After three days we stained the cells for Ki-67. We found that both the control cells and the RASSF1C-expressing cells showed clear nuclear staining of Ki-67, indicating that the RASSF1C-expressing cells were proliferative, not arrested in G0 and were potentially spending very little time in mitosis (Figure 6.3).

To further confirm this, we tested whether the RASSF1C-expressing cells were apoptotic. In order to do this, we stained the cells with the apoptosis marker FITC-VAD that shows the caspase activity in situ. We did not observe any staining with FITC-VAD in the RASSF1C-expressing population,

`

suggesting that the cells were not undergoing apoptosis (Figure 6.4). Together these findings suggest that there must be another reason for the rounding-up of the RASSF1C-expressing cells.

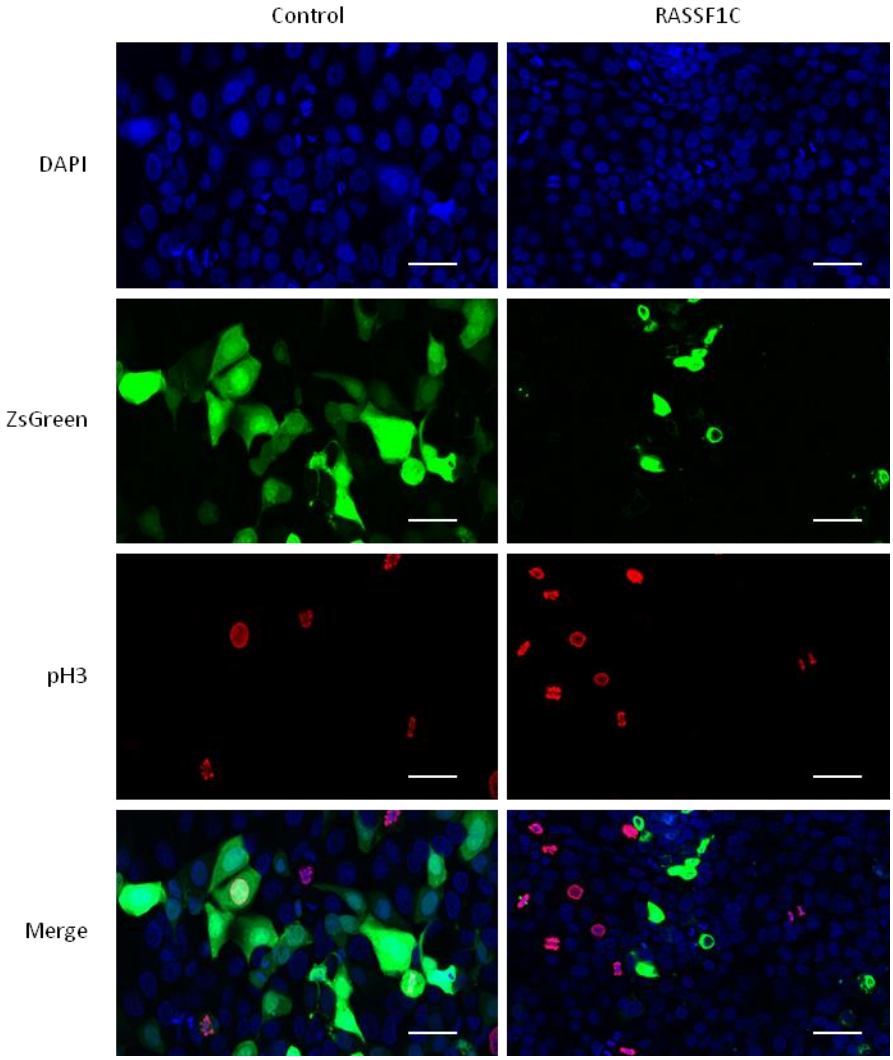


Figure 6.2. The Rounded RASSF1C-Expressing Cells Are Not in Mitosis. Representative images showing the expression of phospho-Histone H3 in MCF7 cells (3 x 10^5 cells/condition), which were plated onto glass cover slips and transfected with ZsGreen-empty vector or ZsGreen-RASSF1C. Cells were fixed for 15 mins with 4 % PFA, permeabilised for 5 mins with 0.2 % Triton X solution and blocked for 30 mins with 0.2 % FSG. Cells were probed with anti-phospho-Histone H3 antibody. Secondary antibody was Alexa-fluor 594 nm. Cover slips were mounted onto slides using mounting media containing DAPI. Images were taken using a Zeiss LSM 780 microscope at 63 x magnification. Scale bars represent 20 μm. The pH3 staining does not co-localise with RASSF1C-expressing cells, suggesting that the rounded cells are not in mitosis.

`

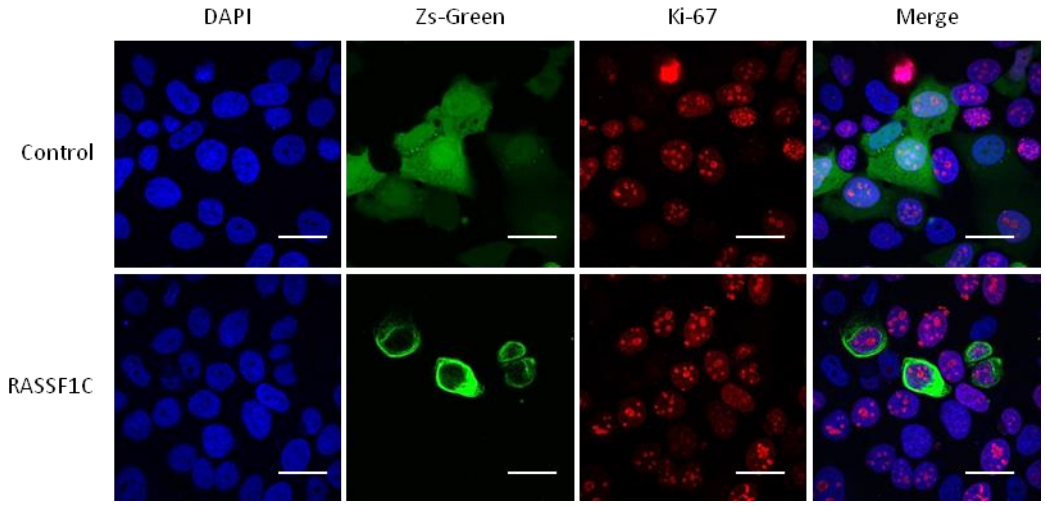


Figure 6.3. RASSF1C-Expressing Cells are Proliferative. Representative images showing the localisation of Ki-67 in MCF7 cells (3 x 10^5 cells/condition), which were plated onto glass cover slips and transfected with ZsGreen-empty vector or ZsGreen-RASSF1C. Cells were fixed for 15 mins with 4 % PFA, permeabilised for 5 mins with 0.2 % Triton X solution and blocked for 30 mins with 0.2 % FSG. Cells were probed with anti-Ki-67 antibody. Secondary antibody was Alexa-fluor 594 nm. Cover slips were mounted onto slides using mounting media containing DAPI. Images were taken using a Zeiss LSM 780 microscope at 63 x magnification. Scale bars represent 20 μm. RASSF1C-expressing cells are Ki-67 positive, suggesting that the cells are proliferating, and not dying.

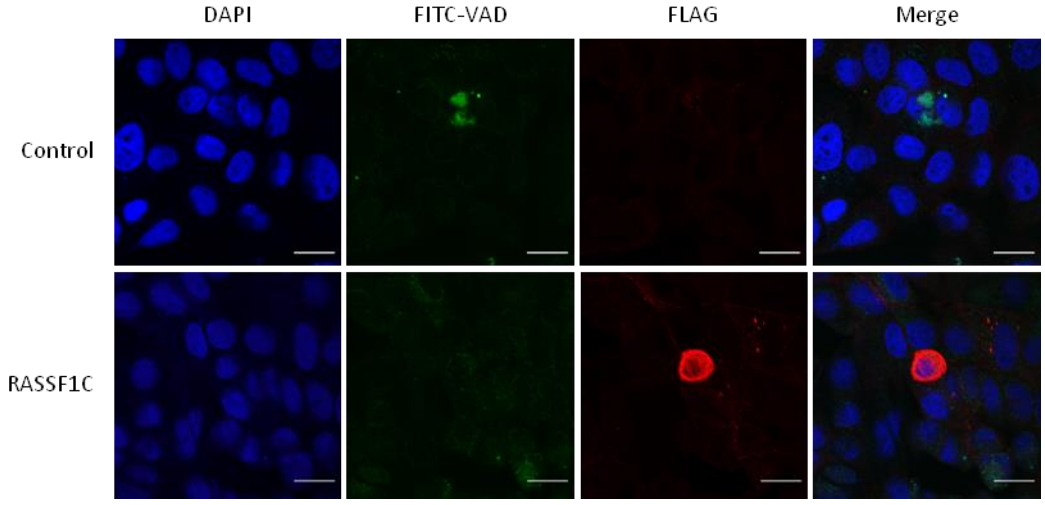


Figure 6.4. RASSF1C-Expressing Cells are Not Apoptotic. Representative images showing the localisation of FITC-VAD positive apoptotic cells. MCF7 cells (3 x 10^5 cells/condition), which were plated onto glass cover slips and transfected with ZsGreen-empty vector or ZsGreen-RASSF1C. Cells were fixed for 15 mins with 4 % PFA, permeabilised for 5 mins with 0.2 % Triton X solution and blocked for 30 mins with 0.2 % FSG. Cells were probed with FITC-VAD-FMK In Situ Marker. Cover slips were mounted onto slides using mounting media containing DAPI. Images were taken using a Zeiss LSM 780 microscope at 63 x magnification. Scale bars represent 20 μm. RASSF1C-expressing cells are not positive for FITC-VAD, suggesting that the RASSF1C-expressing cells are not rounded due to apoptosis.

`

6.4 RASSF1C-Expressing Cells Remain in the Centre of the Mammospheres

Since RASSF1C expression led to the rounding-up of cells and this was not due to apoptosis, senescence or division, we hypothesised that the partial EMT phenotype observed in RASSF1C-expressing cells (Figure 3.15) and the change in the morphology of the cells towards a more rounded phenotype, was able to induce a stem-like properties. Given the evasion from the monolayer observed in Figure 6.1, we wanted to investigate the behaviour of these cells in matrigel. Previously, we observed that RASSF1C expression led to increased motility (Figure 3.17), and invasion (Figure 3.18). In order to investigate this further, we stably transfected MDA-MB-231 cells with either ZsGreen-empty vector or ZsGreen-RASSF1C. Cells were then plated onto matrigel and in 10 days the formed groups of cells, or mammospheres, were imaged. As previously shown in Figure 3.18, the expression of RASSF1C led to significantly larger, more aggressive mammospheres. Given that RASSF1C expression drives motility and invasion, we predicted that the green, RASSF1C-expressing cells would be at the invasive edge of the mammosphere. Surprisingly, we observed that RASSF1C-expressing cells remained in the centre of each mammosphere, in comparison to ZsGreen-empty vector which was found to be evenly expressed across the mammosphere (Figure 6.5A and B). Interestingly, quantification of the RASSF1C-expressing mammospheres showed that on average, they contained 1.6 green cells in the centre of the mammospheres. Further quantification of the images showed a significant increase in the size (Figure 6.5C) and number of protrusions (Figure 6.5C) in the mammospheres expressing ZsGreen-RASSF1C, compared to the control. This data would suggest that potentially the RASSF1C-expressing cell is a stem cell since it is similar to the intestinal organoid culture and crypts (Sato et al., 2011). It would also suggest that the invasion seen in the mammospheres in Figure 3.18 could have been driven by signalling from a small population of RASSF1C-expressing cells, driving the invasion by communication achieved via exosome secretion.

`

Therefore we decided to investigate if the secreted exosomes from RASSF1C-expressing cells were changing the phenotype of the recipient cells.

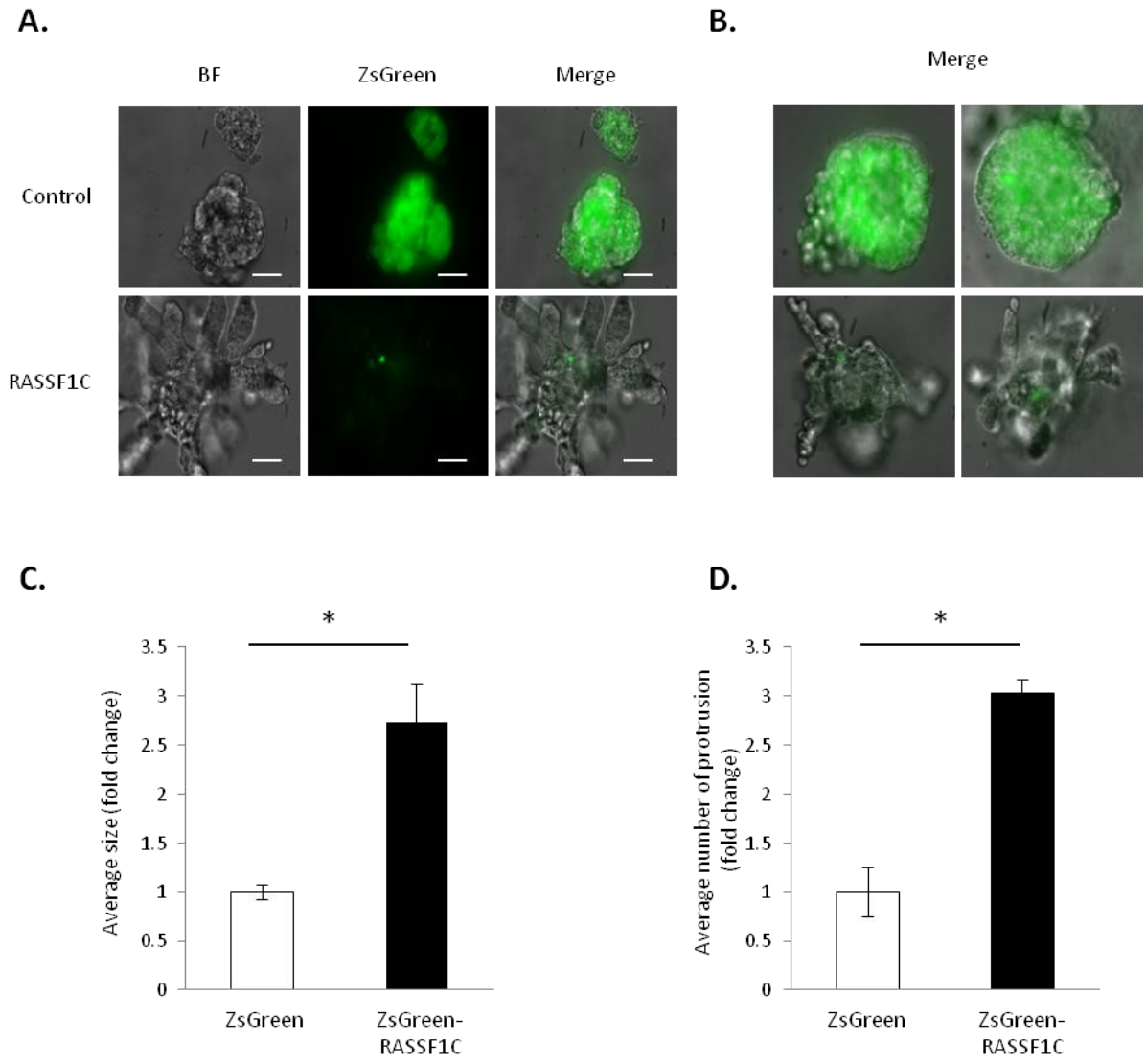


Figure 6.5. RASSF1C-Expressing Cells Are Located in the Centre of the Mammospheres. **A.** Representative images of MDA-MB-231 mammospheres expressing ZsGreen-empty vector, or ZsGreen-RASSF1C. MDA-MB-231 cells, stably expressing either ZsGreen-empty vector or ZsGreen-RASSF1C, were seeded onto matrigel at 2500 cells/well and cultured for 10 days, changing media every 3 days to allow mammospheres formation. Images were taken at 10 X magnification using a Nikon TE2000 Eclipse microscope. Scale bars represent 200 μm. **B.** Representative merged images showing the localisation of the ZsGreen-RASSF1C in the mammospheres. ZsGreen in control cells is evenly distributed throughout the mammosphere. RASSF1C is only expressed in cells located in the centre of the mammosphere. The fold change of the average mammosphere area (**C.**) and number of protrusions (**D.**) were measured using Nikon NIS Elements 4.20 software. Data is representative of three independent experiments. * $p \leq 0.05$. The expression of ZsGreen-RASSF1C leads to the formation of significantly larger and more aggressive mammospheres in matrigel.

`

6.5 RASSF1C Exosomes Induce the Upregulation of Vimentin

Given that RASSF1C-expressing cells are only located in the centre of the mammospheres, and not at the invasive tips as we had predicted, we hypothesised that the RASSF1C positive cells could be sending signals to the remaining cells in order to promote their invasiveness. In Chapter 5, we saw that RASSF1C-expressing cells increase the secretion of exosomes. The mesenchymal marker Vimentin was upregulated in RASSF1C-expressing cells (Figure 3.15). Overexpression of Vimentin has been associated with elevated cell motility and directional migration, EMT phenotypes (Haudenschild et al., 2011) and has been shown to be packaged and secreted with exosomes (Jeppesen et al., 2014). Therefore, we investigated whether the secreted exosomes could carry a signal to the surrounding cells and whether this signal was Vimentin. We isolated exosomes from the MCF7 cells transfected with either pcDNA3 or FLAG-RASSF1C. We then treated naïve MCF7 cells with the extracted exosomes for 18 hrs. Exosomes have been reported to carry proteins and lipids, but also mRNA (Valadi et al., 2007). We isolated mRNA from the treated cells and quantified the levels of Vimentin gene expression using RT-qPCR. The cells treated with exosomes, derived from RASSF1C-expressing cells, had higher Vimentin mRNA, compared to the controls (Figure 6.6A). In order to exclude the possibility that the exosomes are packaged with Vimentin mRNA, we isolated mRNA from the exosomes used for the treatment of the naïve cells. RT-qPCR showed that even though the cells treated with exosomes from RASSF1C-expressing cells had upregulation of Vimentin, the actual exosomes did not contain higher levels of Vimentin mRNA (Figure 6.6B). We therefore concluded that cells expressing RASSF1C can secrete exosomes that can induce the upregulation of Vimentin, and that potentially, the RASSF1C-expressing cells in the centre of the mammospheres could be sending signals to the surrounding cells, triggering Vimentin expression and inducing invasion.

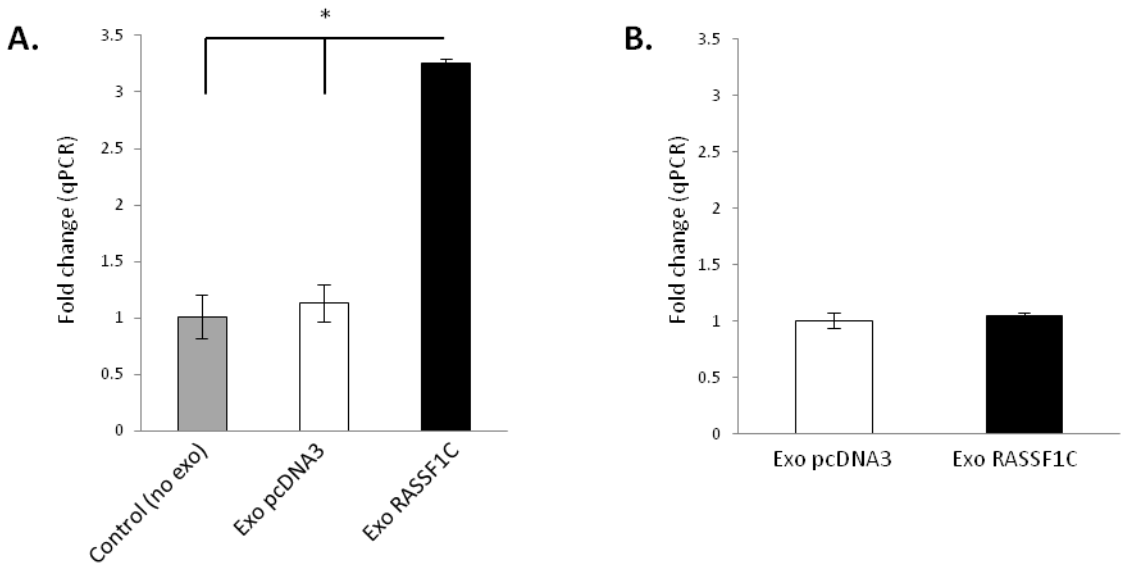


Figure 6.6. Exosomes Derived From RASSF1C-Expressing Cells Induce Upregulation of Vimentin. A. MCF7 cells (5 x 10^6 cells/plate) were transfected with pcDNA3 or FLAG-RASSF1C. Cells were grown in DMEM media supplemented with 0.1 % FBS for 3 days. Exosomes were extracted from the conditioned media using sequential ultracentrifugation. Cells and a fraction of the exosomes were lysed and the protein content was measured to ensure equal loading of 50 μg of exosomes per well. Extracted exosomes were added to naïve MCF7 cells, previously plated at 2 x 10^5 in 6 well plates. The cells were treated with the exosomes for 18 hrs. Cells were then collected and 50,000 cells were lysed and cDNA prepared for qPCR. Expression of 18S was used as an internal control. Data is representative of three independent experiments. * $p \leq 0.05$. Exosomes from RASSF1C promote upregulation of Vimentin in naïve MCF7 cells. **B.** MCF7 cells (5 x 10^6 cells/plate) were transfected with pcDNA3 or FLAG-RASSF1C. Cells were grown in DMEM media supplemented with 0.1 % FBS for 3 days. Exosomes were extracted from the conditioned media using sequential ultracentrifugation. Exosomes were lysed, RNA extracted and 1 μg of RNA was used for qPCR. Expression of 18S was used as an internal control. Data is representative of two independent experiments. The increase in Vimentin expression was not due to physical transport of Vimentin mRNA carried by the exosomes.

`

6.6 RASSF1C Exosomes Induce the Upregulation of Stem Cell Genes

We identified very few highly expressing RASSF1C cells in the middle of the mammospheres and that exosomes from these cells appear to contain Vimentin. Vimentin has been shown to promote elevated cell motility and EMT phenotypes (Haudenschild et al., 2011). Also, Vimentin has been found on the cell surface of liver CSCs and associated with increased growth in matrigel and expression of stem cell genes like *OCT4* and *SOX2* (Mitra et al., 2015). The POU domain-containing OCT4 (OCT3/4), along with the high mobility group domain-containing SOX2 (SRY-related HMG-box gene 2) and the homeodomain-containing transcription factor NANOG, are part of the key set of transcription factors, involved in the maintenance of pluripotency and self-renewal in undifferentiated embryonic stem cells (Avilion et al., 2003; Mitsui et al., 2003; Pesce and Scholer, 2001; Wang et al., 2006). The expression of all three has been linked to the generation and maintenance of CSCs (Ben-Porath et al., 2008; Chiou et al., 2008; Gu et al., 2007; Hochedlinger et al., 2005; Shi et al., 2008; Tay et al., 2008). We therefore hypothesised that the RASSF1C-expressing cells in the middle of the mammosphere are acting like a CSC, modulating the functions of the surrounding cells via the secreted exosomes. We wanted to investigate whether the exosomes can induce self-renewal, pro-survival signals to the surrounding cells. In order to test this, we measured the upregulation of the stem-cell transcription factors *NANOG*, *OCT4* and *SOX2* in the recipient cells. We therefore isolated exosomes from MDA-MB-231 cells, transfected with either pcDNA3 or FLAG-RASSF1C. The exosomes were then added for 18 hrs onto naïve MDA-MB-231 and MCF7 cells. The cells were then collected and analysed by RT-qPCR. We observed that the exosomes from RASSF1C-expressing cells induced upregulation of *NANOG*, *OCT4* and *SOX2* in MDA-MB-231 cells (Figure 6.7A) and MCF7 cells (Figure 6.7B). Taken together, this data suggests a role for RASSF1C in the communication and upregulation of CSC-associated stem cell genes. Therefore, the cells expressing RASSF1C in the middle of the mammospheres could promote the secretion of exosomes, which would carry signals which would trigger Vimentin expression, which could promote invasiveness and stem cell phenotype into the surrounding cells.

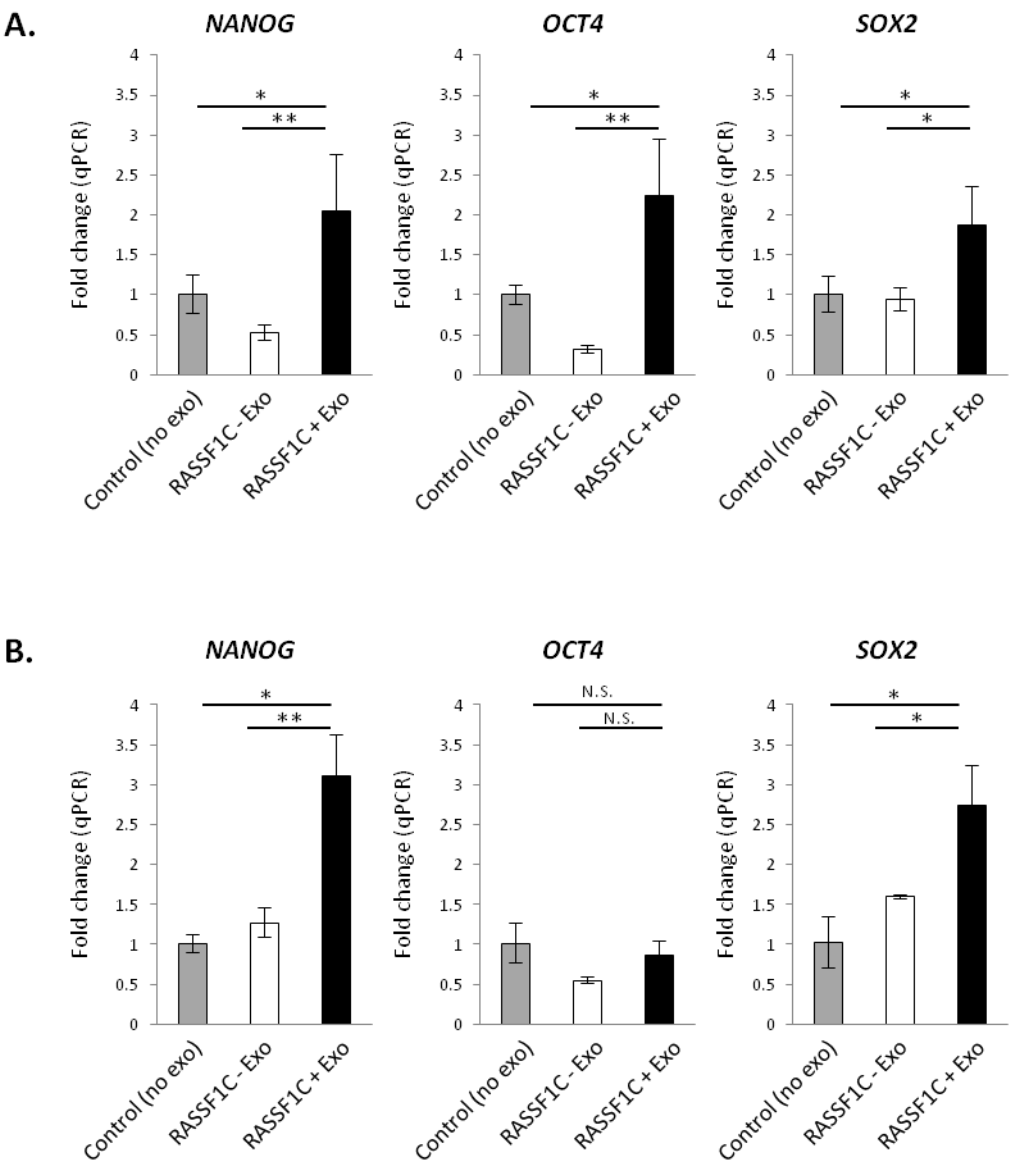


Figure 6.7. Exosomes From RASSF1C-Expressing Cells Induce Upregulation of Stem Cell Genes. MDA-MB-231 cells (5 x 10^6 cells/plate) were transfected with pcDNA3, or FLAG-RASSF1C. Cells were grown in DMEM media supplemented with 0.1 % (v/v) FBS for 3 days. Exosomes were extracted from the conditioned media using sequential ultracentrifugation. Cells, and a fraction of the exosomes, were lysed using 1 X RIPA buffer and the protein content measured to ensure equal loading of 50 μg of exosomes per well. Extracted Exosomes were added to naïve MCF7 cells (**A.**), or MDA-MB-231 cells (**B.**), previously plated at 2 x 10^5 in 6 well plates. The cells were treated with the exosomes for 18 hrs. Cells were then collected and 50,000 cells were lysed and cDNA prepared. qPCR was performed on Applied Biosystems 7500 Fast Real Time PCR system. Expression of 18S was used as an internal control. Data is representative of three independent experiments. N.S $p > 0.05$, * $p \leq 0.05$, ** $p \leq 0.01$. Error bars represent 1 x SEM. Exosomes derived from RASSF1C-expressing cells promotes the upregulation of stem cell markers *NANOG*, *OCT4* and *SOX2* in naïve MCF7 and MDA-MB-231 cells.

`

6.7 Stem Cell Genes are Upregulated in RASSF1C-Expressing cells

As RASSF1C-expressing cells are releasing exosomes which are able to induce the upregulation of stem cell transcription factors in naïve cells, we wanted to investigate whether cells transfected with RASSF1C would express the same pluripotency transcription factors. Therefore, we transfected MCF7 cells with either ZsGreen-empty vector or Zs-Green-RASSF1C plasmids. Cells were incubated for 2 days after which were sorted by flow cytometry in order to better understand the expression profile of the cells highly expressing Zs-Green-RASSF1C, such as those found in the middle of the mammospheres (Figure 6.5). The sorted cells were then analysed using RT-qPCR. We saw that in MCF7 cells, the expression of ZsGreen-RASSF1C promoted the upregulation of both *NANOG* (Figure 6.8A) and *OCT4* (Figure 6.8B). Interestingly, we were unable to detect *SOX2* in the cells (Data not shown). These findings confirm our hypothesis that cells expressing RASSF1C have upregulated CSC transcription factors, suggesting a potential role of RASSF1C as inducer of the CSC phenotype.

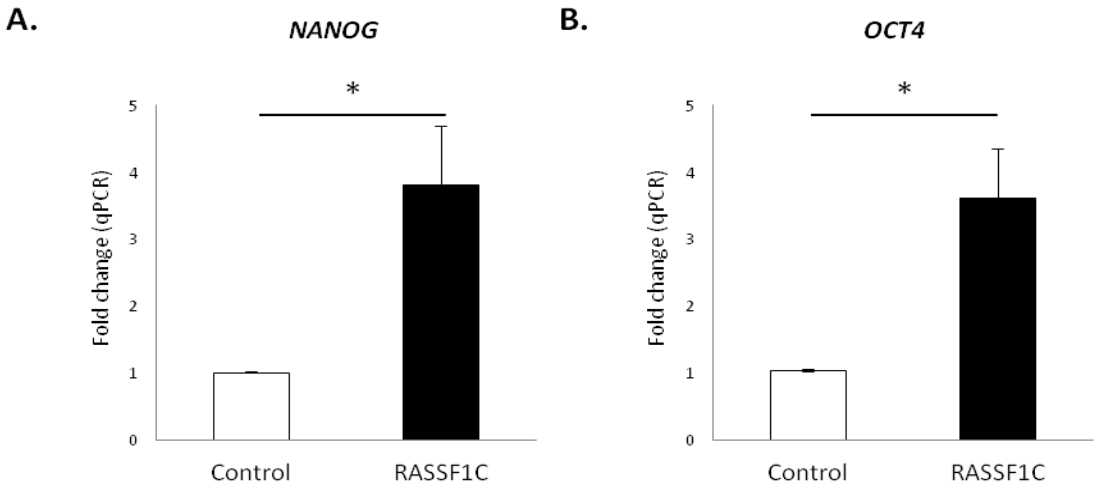


Figure 6.8. RASSF1C Expression Promotes the Upregulation of Stem Cell Genes. MCF7 cells (2 x 10^5 cells/well) were plated and transfected with ZsGreen-empty vector or ZsGreen-RASSF1C. After 48 hrs the cells were trypsinised, resuspended in 1 X PBS and 50,000 cells FACS sorted the positive green cells. The cells were then lysed, cDNA prepared and qPCR was performed on an Applied Biosystems 7500 Fast Real Time PCR system. Expression of 18S was used as an internal control. RASSF1C expression in MCF7 cells leads to the upregulation of *NANOG* (**A.**) and *OCT4* (**B.**). Data is representative of three independent experiments. * $p \leq 0.05$. Error bars represent 1 x SEM.

`

6.8 RASSF1C Expression Induces a $CD44^{high}/CD24^{low}$ Phenotype

It has been previously shown that the increase in the activity of the YAP1 homolog TAZ, leads to a shift in the profile of secondary breast cancer spheroids from $CD44^{low}/CD24^{low}$ to $CD44^{high}/CD24^{low}$ (Cordenonsi et al., 2011). This shift has been associated with breast CSCs (Al-Hajj et al., 2003). Also, high levels of Vimentin expression have been linked to increased levels in $CD44^{high}/CD24^{low}$ breast CSCs (Cufi et al., 2011). The $CD44^{high}/CD24^{low}$ phenotype has been associated with high expression levels of *NANOG* and *OCT4* in non-small lung cancer (Leung et al., 2010), which have been shown to down-regulate E-cadherin in breast cancer (Wang et al., 2014a). We hypothesised that given RASSF1C expression leads to upregulation of *NANOG* and *OCT4*, changes in E-cadherin stability and increases in Vimentin mRNA levels, the expression of RASSF1C also promotes a $CD44^{high}/CD24^{low}$ CSC profile, further suggesting that RASSF1C expression occurs in CSCs. In order to test this we generated MCF7 cells stably expressing pcDNA3 or MYC-RASSF1C. The cells were grown up until confluent, after which were trypsinised and plated as single cell suspensions on ultra-low attachment plates. The spheroids formed were passaged 3 times, each after 5 days of growth. The cells were then detached using a mild trypsin solution, resuspended, blocked and incubated with anti-human CD44 (APC-conjugated) and anti-human CD24 (FITC-conjugated) antibodies. Cells were then analysed by flow cytometry. We observed that RASSF1C-expressing cells had an increase in the $CD44^{high}/CD24^{low}$ levels, compared to both the control and RASSF1A-expressing cells (Figure 6.9).

Combined, the data from this chapter suggests a role of RASSF1C in the generation of CSCs, which leads to export of Vimentin and stem cell signals to surrounding cells via exosomes.

`

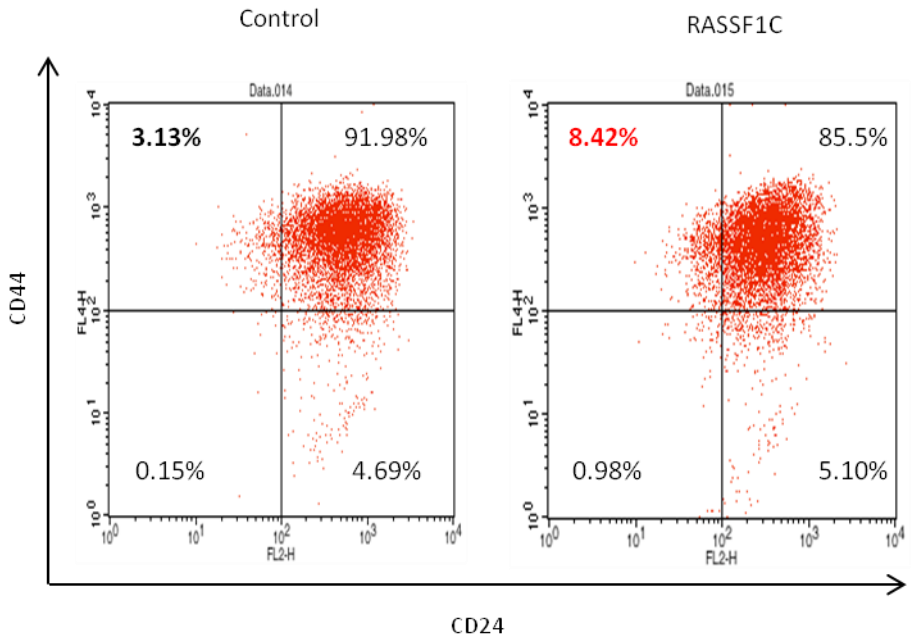


Figure 6.9. RASSF1C Expression Shifts Cell Population Towards CD44^{high}/CD24^{low} CSC Phenotype. MCF7 cells, stably transfected with pcDNA3 or MYC-RASSF1C were grown to confluency on a 6 well plate. Cells were then trypsinised, counted and plated as single-cell suspensions (1000 cells/well) on 24 well ultra-low attachment plates. The cells were left to form spheroids for 5 days, after which time they were dissociated and reseeded for a second round of spheroid formation. After another 5 days the procedure was repeated. The tertiary spheroids were then detached from plates with TrypLE (Life Technologies), resuspended at concentration of 5 x 10^5 cells/ml in running buffer (1 X PBS, 0.5 % (w/v) BSA and 5 mM EDTA). Cells were then stained with FITC-CD24 and APC-CD44 antibodies overnight at 4 ^{o}C. Cells were then analysed using flow cytometry, counting 10000 cells. The cells expressing RASSF1C have an increased proportion of cells with the breast cancer stem cells markers CD24^{low}/CD44^{high}, compared to control cells. Data is representative of 2 independent experiments.

`

6.9 Discussion

In this chapter I have demonstrated that the expression of RASSF1C leads to changes in the morphology of the cells *in vitro*, as they round-up and leave the monolayer. I confirmed that this change in morphology was not a result of entry into mitosis, or senescence and that the cells were not apoptotic. On the contrary, the cells were shown to be proliferative and can grow in a 3D culture. Using 3D culture, we identified that cells actively expressing RASSF1C are only located at the centre of mammospheres, and suggested that this subset of cells was able to drive the aggressive phenotype observed in RASSF1C-expressing cells by sending signals, via exosomes, to the surrounding cells. Further, we identified that these signals upregulate the mesenchymal gene *VIMENTIN* and the stem cell genes *NANOG*, *OCT4* and *SOX2*. Finally, we have shown that cells expressing RASSF1C have gene expression and cell surface receptors consistent with the cancer stem cells.

Throughout the experiments done in this thesis, we had noticed that the epithelial cells expressing RASSF1C behaved differently *in vitro* approximately 3 days after transfection (Figure 6.1). The cells that highly expressed RASSF1C were more prone to round-up and then leave the monolayer. In Chapter 3 we observed that the expression of RASSF1C leads to activation of SRC and the loss of adherens junctions. Given this, we hypothesised that the rounded phenotype observed, could be due to the loss of cell-cell junctions. This could be tested by quantifying the rounded cells in the presence of SRC inhibitors, either Dasatinib or AZD0530, or by dual expression of RASSF1A and RASSF1C, since RASSF1A expression led to the inhibitory phosphorylation of SRC (Figure 3.2B).

The detachment from the cell monolayer suggests that the RASSF1C-expressing cells could be growing in an anchorage-independent manner. Anchorage-independent growth has been shown to be a characteristic of stem cells of various types of self-renewing tissue (Reynolds and Weiss, 1992; Toma et al., 2001) and of CSCs (Cordenonsi et al., 2011; Kunjithapatham et al., 2014). These growth conditions have also been attributed to the selection of more metastatic and aggressive cells,

`

partially due to the fact that not all cells can survive the anchorage-independent conditions (Kunjithapatham et al., 2014). Given that we had also observed that RASSF1C-expressing cells can grow under anchorage-independent conditions such as matrigel (Figure 3.18), it would be interesting to further investigate this phenotype by using other types of anchorage-independent assays, including growing RASSF1C-expressing cells in methyl-cellulose media (Mori et al., 2009) or noble agar (Rosenbluh et al., 2012). In accordance with our hypothesis, RASSF1C-expressing cells were able to grow onto low-attachment plates for several sequential passages, which also led to the upregulation of surface CSC markers (Figure 6.9).

Our previous data led us to hypothesise that the rounding up of the RASSF1C-expressing cells was due to cells losing junctions and undergoing a partial EMT. However, we wanted to confirm that the rounded phenotype of the RASSF1C-expressing cells observed in Figure 6.1 was not due to any other changes, related to the cells leaving the monolayer. Similar phenotypes have been linked to cell division, where cells lose their junctions and round-up during mitosis (Lancaster et al., 2013); and cell death, via necrosis or apoptosis, during which the cells round-up as they proceed through pathways associated with cell death (Elmore, 2007). We did not find any staining for the mitotic marker phospho-Histone H3 in cells expressing RASSF1C, ruling out that cell division was responsible for the observed rounded phenotype (Figure 6.2). However, we did observe that the RASSF1C-expessing cells were positive for Ki-67 staining suggesting that cell division was occurring and that the cells were not senescent (Figure 6.3). This is because Ki-67 is present during all active phases of the cell cycle and mitosis, but is absent in cells arrested in G0 (Scholzen and Gerdes, 2000). Interestingly, reports have shown that Ki-67 positive cells are the differentiated cells from a tumour, not the CSCs (Felthaus et al., 2011). Given our hypothesis that rounded RASSF1C-expressing cells are becoming CSCs, the identification that some of the RASSF1C-expressing cells are Ki-67 positive may suggest that not all RASSF1C-expressing cells obtain the CSC traits, as previously reported (Sathi et al., 2012). It would be interesting to measure the frequency of proliferative CSCs in the presence of RASSF1C by staining the RASSF1C-expressing cells for Ki-67 and a cancer stem cell marker, depending on the cell

`

type, for example CD44 and CD24 cell markers in breast CSCs (Figure 6.9). This will be a matter of future research.

In Chapter 3 we demonstrated that mammospheres from MDA-MB-231 cells, expressing MYC-RASSF1C, grow significantly bigger and aggressive (Figure 3.18). The aggressiveness was measured by the number of protrusions coming out of the mammospheres. Given that RASSF1C-expressing cells were more prone to migrate (Figure 3.17) we wanted to know if the level of expression of RASSF1C was changing, based on the position of the cells in the mammosphere. We hypothesised that the cells with high RASSF1C expression would be concentrated at the sites of protrusions, driving the invasion. Surprisingly, the cells expressing high levels of RASSF1C were localised at the centre of the mammosphere (Figure 6.5). Given the results from Figures 6.7 and 6.8, which showed an upregulation in the stem cell genes *NANOG* and *OCT4* (Figure 6.7) and in the cell surface marker CD44 (Figure 6.8) we could speculate that this population in the centre of the mammosphere represents the CSCs. This would fit the model for one subset of CSCs that are present in the tumour, generating heterogeneity through differentiation. Since there has been a correlation between the aggressive behaviour of tumours from patients and the amount of CSC in them (Boiko et al., 2010; Pece et al., 2010; Zhang et al., 2012), it would be interesting to correlate the invasive phenotype of the mammosphere with the amount of active RASSF1C-expressing cells in the centre. This could be achieved by the quantification of the ZsGreen-RASSF1C-expressing cells to look for correlation between the number of protrusions and the size of the mammosphere. Also, the mammospheres could be collected by the digestion of the matrigel and the green cells could be sorted using flow cytometry, analysed by qPCR for the upregulation of stem cell genes or stained for CD44 and CD24 expression.

Heterogeneous CSC compartments can exist in solid tumours (Welte et al., 2010). In breast, ovarian and squamous cell carcinomas there is a phenotypic and functional heterogeneity in the CSC population (Meyer et al., 2010; Schober and Fuchs, 2011; Stewart et al., 2011). In addition, in primary

`

colorectal cancers, three different subtypes of CSCs exist: a subset that maintained tumour growth on serial transplantation; a tumour-initiating cell with limited self-renewal capabilities; and a more latent CSCs that was activated in secondary, or tertiary transplantation assays (Dieter et al., 2011). Therefore it would be important to isolate and investigate the active RASSF1C-expressing cells, to better understand if there is any heterogeneity within the CSC population which would explain the timeframe for the generation of RASSF1C-expressing CSCs. Given the upregulation of *NANOG* and *OCT4* after transfection (Figure 6.8) and the tertiary spheroid cultures grown (Figure 6.9) we would hypothesise that the RASSF1C-expressing CSCs maintain tumour growth on serial transplantation. The use of mouse transplantation assay can be used to further confirm this hypothesis.

The secretion of exosomes has been linked to CSCs. Exosome secretion by stromal cells surrounding the tumour has been shown to promote the generation and maintenance of CSCs in a tumour (Gernapudi et al., 2015; Ramteke et al., 2015). Conversely, CSCs can use exosomes to communicate with the surrounding stroma, reprogramming it to support local cancer growth (Marzesco, 2013). Exosomes contain many factors that can promote growth of tumours and modulate the microenvironment (Kahlert and Kalluri, 2013). Breast CSCs have been shown to directly secrete exosomes containing CD63, CD81, ALIX and TSG101 proteins (Kumar et al., 2015). We also identified these proteins in the exosomes secreted by the RASSF1C-expressing breast cancer cell lines (Figure 5.6 and 5.7). Our investigation identified that exosomes derived from RASSF1C-expressing cells were able to induce a cellular response, upregulating of both mesenchymal (Figure 6.5) and stem cell genes (Figure 6.6). It has been previously reported that exosomes from embryonic stem cells can contain mRNA for NANOG and OCT4 (Ratajczak et al., 2006), but we did not identify these mRNAs in our exosomes. Instead, our finding suggests that the exosomes derived from RASSF1C-expressing CSCs contain factors that upregulate these stem cell genes in the surrounding cells, increasing their proliferative and invasive capacity. Nevertheless a crucial experiment for future work will be the better understanding of the mRNA profile of the exosomes derived from the RASSF1C-expressing cells, which we could address using an mRNA expression array.

`

In Chapter 3 we identified that RASSF1C-expressing cells had undergone a partial EMT, failing to downregulate E-cadherin expression, but upregulating the mesenchymal gene Vimentin (Figure 3.15). In this chapter we identified that these same cells also release exosomes that can induce the upregulation of Vimentin in the surrounding cells (Figure 6.6). Vimentin protein has previously been identified in exosomes (Jeppesen et al., 2014). In addition, these Vimentin containing exosomes have been shown to play a role in the induction of EMT, thus enhancing the invasiveness and stemness of prostate cancer cells (Ramteke et al., 2015). In addition, cell surface Vimentin positive cells have been shown to exhibit stem-like properties, including the formation of spheres in matrigel and the upregulation of the stem cell genes *OCT4* and *SOX2*. Therefore, we believe that in our system, the exosomes released by the RASSF1C-expressing cells activate the mesenchymal, invasive phenotype of the surrounding cells, as characterised by the upregulation of Vimentin. The level of invasiveness of cells treated with RASSF1C-derived exosomes will be investigated in the future and would include the knock down of Vimentin in order to further confirm its role in the cell invasiveness in the matrigel system, but also to investigate its role in the promotion of CSCs by serial mouse transplantation.

In our model, we saw not only that exosomes derived from RASSF1C cells can induce *NANOG*, *OCT4* and *SOX2* expression, but the cells transfected with RASSF1C can also upregulate *NANOG* and *OCT4* expression (Figure 6.7). *NANOG* and *OCT4* expression has been linked to down-regulation of E-cadherin expression and up-regulation of Vimentin (Wang et al., 2014a). Interestingly, cells expressing cell surface Vimentin have been identified as CSCs and shown to express OCT4 and SOX2. It would be interesting to see if the stem cell marker expression is creating a loop with Vimentin, leading to constant expression. Knocking down Vimentin could show us if it is responsible for *OCT4* and *SOX2* gene upregulation. Surprisingly, in our system, we do not see RASSF1C-dependent E-cadherin degradation. Potentially an experiment over a longer time course would show that E-cadherin is being degraded. Although we have yet to identify the actual signalling factors in the exosomes that induce the changes we see in the naïve cells, a plausible hypothesis might involve the packaging of RASSF1C into the exosomes. We have not detected any RASSF1C in the exosomes

`

(Figures 5.3 and 5.4); however we are currently investigating whether the exosomes can transport RASSF1C mRNA. Nevertheless, it is important to point out that the RASSF1C-expressing exosome-secreting cells are able to transfer most of the stem cell and invasion traits using the extracellular vesicles. Using Mass spectrometry we would like to identify key proteins that are packaged in the exosomes and that could link the exosome secretion with the generation of CSCs. Also, we would like to use an *in vivo* experiment in order to show whether the exosomes can modulate the tumour stroma or the sites of distant metastasis, as previously reported for other extracellular vesicles (Zomer et al., 2015).

It has been previously shown that the increase in TAZ activity leads to a shift in the profile of secondary breast cancer spheroids from $CD44^{low}/CD24^{low}$ to $CD44^{high}/CD24^{low}$ (Cordenonsi et al., 2011), a shift that has been associated with breast CSCs (Al-Hajj et al., 2003). In our system we see a shift in the $CD44^{high}/CD24^{low}$ in MCF7 cells expressing RASSF1C (Figure 6.9). So far this experiment has been done *in vitro* using low attachment plate to culture tertiary spheroids. An important validation of the experiment will be the use of *in vivo* xenograft model to further demonstrate the CSC potential of the RASSF1C-expressing cells, where sorting by flow cytometry of the RASSF1C-expressing positive and negative cells can be used in order to enrich the population with RASSF1C CSCs.

CD44/CD24 cannot be used as universal markers of CSCs, due to the fact that in ER-negative and triple-negative breast tumours, CSCs were found in both $CD44^{high}/CD24^{low}$ and $CD44^{high}/CD24^{high}$ populations (Meyer et al., 2010). Therefore, another marker might be useful to further characterise the CSC properties of RASSF1C-expressing cells. However, the CSC markers are not universal for all cancer types, meaning that in other cancer cells, such as glioblastoma, the CSCs are CD133 positive (Lathia et al., 2011). Interestingly, in hepatocellular carcinoma the CD133 negative and cell surface Vimentin positive cells were identified as the CSC population and expressing OCT4 and SOX2. Therefore the marker that could be used for further validation is CD133 and Vimentin. The YAP1 homolog TAZ has been identified in the literature to be involved in the generation of CSCs

`

(Cordenonsi et al., 2011). Given that we identify that RASSF1C expression can activate YAP1, a homolog of TAZ, it would be interesting to find out if in our system, YAP1 plays a role in the observed phenotype, or whether RASSF1C is also able to activate TAZ.

Given that we have shown that RASSF1A is able to bind to RASSF1C and potentially inhibit RASSF1C function by inactivating SRC, and that RASSF1C expression led to upregulation of *NANOG* and *OCT4*, it would be really interesting to investigate whether RASSF1A and RASSF1C can co-exist or co-localise in a spheroid. Our model would suggest that RASSF1A would inhibit RASSF1C from promoting anchorage-independent growth. We would investigate this by following the mammosphere formation of cells expressing either RASSF1A or RASSF1C. We would hypothesise that RASSF1A cells would fail to grow in the matrigel.

The data presented in this chapter (Summarised in Figure 6.10) shows that expression of RASSF1C leads to changes in the cell shape and its evasion from the cell monolayer, potentially due to the loss of cell junctions (Chapter 3), but also due to cancer stem cell traits, including stem cell gene expression of *NANOG* and *OCT4.* The RASSF1C-expressing cells can be located in the centre of the mammosphere, from where, potentially via exosome secretion, can induce the invasion and transfer of the cancer stem cell phenotype to the surrounding cells, not expressing RASSF1C.

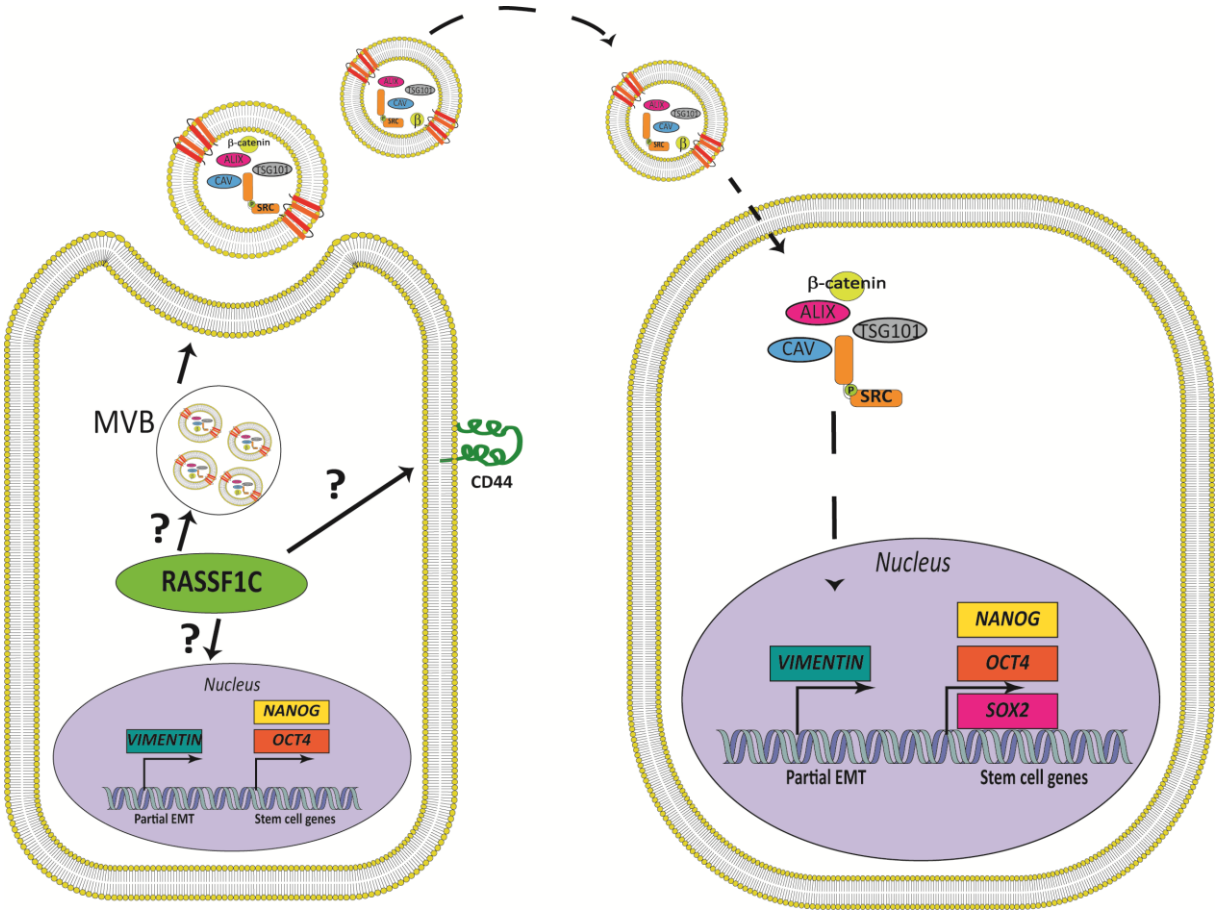


Figure 6.10. Cartoon Depicting the Hypothesis Generated from the Work in Chapter 6. RASSF1C expression leads to upregulation of the mesenchymal marker Vimentin and the stem cell genes *NANOG* and *OCT4,* suggesting a phenotype associated with cancer stem cells. This was confirmed by the expression of the cell surface markers CD44 and CD24, further confirming the cancer stem cell status. In addition, the RASSF1C-expressing cells can secrete exosomes that can induce the upregulation of Vimentin and the stem cell genes *NANOG*, *OCT4* and *SOX2* in cells not expressing RASSF1C.

`

Chapter 7 Discussion

The development and progression of tumours to more invasive and malignant cancer have been associated with a variety of cellular events or hallmarks, including upregulation of oncogenes, such as *SRC;* the loss of tumour suppressor genes, like *RASSF1A;* and control of pathways that involve increase in cell growth, loss of cell attachments, evasion of apoptotic signals, modulation of the surrounding environment and generation of self-proliferative cells that can survive potential treatment. The loss of *RASSF1A* is one of the most frequent epigenetically inactivated tumour-suppressor genes in sporadic human malignancies (Donninger et al., 2007; Grawenda and O'Neill, 2015; Hesson et al., 2007; van der Weyden and Adams, 2007). Therefore we wanted to address the fate of its oncogenic isoform, RASSF1C, in the development of cancer.

The data presented in this thesis described a novel regulation of SRC family kinases, gene transcription, exosome production and cancer stem cell generation, all regulated by RASSF1 isoforms. We have shown that when RASSF1A is lost in tumours, RASSF1C behaves as an oncogene and that its expression is essential for SRC activation. Moreover, RASSF1C leads to accumulation of SRC at the sites of cell-cell junctions, where it can engage with and phosphorylate target proteins, such as the known substrate E-cadherin. Further investigation has shown that RASSF1C, via SRC, can drive the destabilisation and loss of E-cadherin from the sites of cell-cell junctions and its further internalisation and accumulation into the cytoplasm. In agreement with the activation of SRC, we showed that RASSF1C expression promotes cell migration and aggressive phenotype, forming large, invasive mammospheres in matrigel and larger tumours *in vivo*. Furthermore, we find that RASSF1A loss, and consequently RASSF1C expression, have been associated with an increase in the phosphorylation of YAP1 and its further localisation into the nucleus. RASSF1C has previously been implicated in promoting the internalisation of β-catenin by the inhibition of the negative regulator β-TRCP (Estrabaud et al., 2007); however, we provide evidence for a novel, RASSF1C-dependent mechanism through which SRC phosphorylated β-catenin, is released from the cell-cell junctions

`

and its translocated to the nucleus. There, internalised nuclear β-catenin, together with YAP1, leads to an increase in the transcription of the anti-apoptotic and pro-survival genes *BCL2L*, *BIRC5* and *c-MYC* (Rosenbluh et al., 2012).

Moreover, we have shown that RASSF1C alters the cargo and increases the secretion of exosomes, transferring tumourigenic signals to the surrounding cells. Finally, we have shown that cancer cells, expressing RASSF1C, can obtain a stem cell phenotype which can also be transferred to the surrounding cells, via exosomes, to induce increased growth and invasion. Taken together this data gives an explanation to the processes that occur when RASSF1A, but not RASSF1C, expression is lost in tumours. This could explain why RASSF1A is downregulated by promoter methylation, but not mutation. A mutation would potentially inactivate both RASSF1A and RASSF1C, since there is a high sequence similarity between the two isoforms.

The methylation of the promoter for RASSF1A leads to a transcriptional silencing. This has been studied extensively in a vast number of human cancers: bladder (Gao et al., 2012; Jarmalaite et al., 2008; Kim et al., 2012b; Maruyama et al., 2001), cervix (Neyaz et al., 2008), endometrium (Jo et al., 2006; Liao et al., 2008; Pallares et al., 2008), prostate (Jeronimo et al., 2004; Kawamoto et al., 2007; Liu et al., 2011b; Liu et al., 2002; Maruyama et al., 2002), lung (Buckingham et al., 2010; Endoh et al., 2003; Kubo et al., 2009; Lee et al., 2012; Tomizawa et al., 2002; Wang et al., 2007), breast (Muller et al., 2003), head and neck (Fendri et al., 2009; Li et al., 2005; Yang et al., 2014; Zhang et al., 2014a), kidney (Kawai et al., 2010), melanoma (Tanemura et al., 2009), and brain tumours, such as glioma (Hesson et al., 2004), neuroblastoma (Stutterheim et al., 2012) and pituitary adenomas (Qian et al., 2005). Meta-analysis of eight breast cancer studies involving 1795 patients and 19 non-small cell lung carcinoma studies involving 2802 patients further demonstrated the importance of RASSF1A promoter methylation as a prognostic marker due to the significant correlation between RASSF1A methylation and both overall survival and relapse-free survival (Jiang et al., 2012; Wang et al., 2011a). It is therefore clear that the loss of RASSF1A expression is associated with more aggressive

`

and metastatic cancers. The data presented in this thesis would predict that this is due to the functions of RASSF1C. We suggest that one of the tumour suppressor roles of RASSF1A is to modulate the activity of SRC family kinases. RASSF1A prevents the activation of SRC and the consequent loss of cell junctions. Inhibition of SRC would also impair the anti-apoptotic YAP1- and β-catenin-dependent gene transcription. We have also seen evidence suggesting that RASSF1A can bind to and inactivate RASSF1C. This would suggest that in cancers that have lost RASSF1A, RASSF1C is also able to promote the generation of cancer stem cells and modulate their environment via the secretion of exosomes, containing active SRC and also stem cell and EMT genes.

In some cancers the methylation of the *RASSF1* gene promoter (Figure 1.1) would extend beyond the CpG island containing the 1α promoter (RASSF1A) and would reach the second downstream CpG island, containing the 2γ promoter from which RASSF1C is transcribed. In such cases both the isoforms of the *RASSF1* gene are silenced (Dreijerink et al., 2001; Vos et al., 2000). Given the evidence supporting the utility of the RASSF1A promoter methylation as a biomarker for cancer risk and poor outcome (Grawenda and O'Neill, 2015), it would be interesting to observe if the prognostic power of RASSF1A methylation could be improved by measuring the promoter methylation across both 1α and 2γ promoters. Having seen the metastatic and aggressive potential of cancer cells expressing RASSF1C, we would predict that in patients with DNA methylation only at the 1α promoter, the retention of RASSF1C expression would result in a worse prognosis than those methylated at both the 1α and 2γ promoters, which will not have both RASSF1A and RASSF1C.

The data presented in this thesis, in accordance with previously published reports, show that RASSF1C is an oncogene (Amaar et al., 2006a; Reeves et al., 2010; Reeves et al., 2013; Reeves et al., 2014). We also show that the RASSF1 isoforms have opposing roles in the activation of SRC. In keeping with this work, compared to wild type mice, both homozygous and heterozygous *Rassf1A* knockout mice show increased incidence of spontaneous tumourigenesis and decreased survival rate (Tommasi et al., 2005; van der Weyden et al., 2005) and *Rassf1A* null mice show a more severe

`

tumour susceptibility phenotype after exposure to irradiation or chemical mutagens (benzo[a]pyrene and urethane) (Tommasi et al., 2005; van der Weyden et al., 2005). However, homozygous mice with a minimal deletion region encompassing the 12 genes located at Chromosome 3p21.3 (the *Rassf1* locus were embryonic lethal, but not the heterozygous mice, which showed no increase in spontaneous tumourigenesis (Smith et al., 2002). This would suggest that, in the absence of *Rassf1A*, one of the other proteins produced from the 12 genes promotes tumourigenesis. Our work suggests that this may be caused by the expression of *Rassf1C*.

SRC is a non-receptor tyrosine kinase that is often overexpressed or activated in tumours, where it regulates a variety of cancer-associated processes, including cell adhesion complex assembly and turnover, motility, proliferation and survival. SRC expression has been linked to the development of tumours, particularly breast, lung and colorectal cancers (Cartwright et al., 1989; Mazurenko et al., 1992; Verbeek et al., 1996). SRC has been correlated with advanced stage and metastatic potential (Cartwright et al., 1990; Irby et al., 1999), similar to the epigenetic loss of RASSF1A (Fendri et al., 2009; Tommasi et al., 2011b). SRC is activated by phosphorylation at Y416 (Xu et al., 1997) and inhibited by CSK-mediated phosphorylation at Y527 (Cartwright et al., 1987; Okada and Nakagawa, 1989). We have identified a role for RASSF1C in promoting SRC activatory phosphorylation and translocation to the membrane. However, it remains unclear how RASSF1C does this. It is also unclear whether RASSF1C is also translocated to the membrane, since all our observations have been done at a stage where RASSF1C expression is at its peak, and it could be localised to the membrane at an earlier point of expression. We have shown that contrary to the RASSF1C activation of SRC, RASSF1A has opposing roles, since it binds to CSK and leads to phosphorylation of SRC at Y527, thus leading to its inhibition. Interestingly, RASSF1C fails to activate SRC in the presence of RASSF1A, suggesting that the RASSF1A binding to CSK and SRC is stronger and would explain a novel role of RASSF1A in the regulation of both SRC and RASSF1C. SRC has been mutated in a subset of advanced metastatic colon cancers where a truncation mutation at codon 531 in the C-terminal regulatory domain prevents SRC regulation by CSK, which results in a constitutively active SRC protein (Irby et

`

al., 1999). In tumours, evidence exists for growth factor or cytokine-induced increase in the activity of SRC, but a clear somatic event is lacking (Irby and Yeatman, 2000; Liu et al., 2013). Given the novel link between RASSF1C and SRC activation and the regulation of CSK by RASSF1A, we would predict that in patient samples, RASSF1A methylation will be correlated with either increase in the active SRC, or a decrease in the inactive one. This would also suggest that SRC inhibitors like Dasatinib, Bosutinib, Saracatinib and AZD0530 would be an effective treatment in cells in which RASSF1A has been silenced. Also, since RASSF1A promotes senescence and apoptosis in response to oncogenic K-Ras signalling, but RASSF1A methylation correlates poorly with *K-RAS* or *BRAF* mutations (Matallanas et al., 2011; Thaler et al., 2009). However, *SRC* mutations, similar to the *K-RAS* ones, would not correlate with RASSF1A methylation. A possible explanation for this would be that a mutation of *SRC* would disrupt the requirement for SRC activation by RASSF1C, thus decreasing the selection pressure on cells to downregulate RASSF1A.

SRC family kinases can phosphorylate both E-cadherin and the catenin proteins on tyrosine residues, leading to the destabilisation of the cadherin-catenin complex. Active SRC has been shown to promote E-cadherin internalisation through Arf6 GTPase (Palacios et al., 2001) and the SRC-dependent phosphorylation of E-cadherin leads to its ubiquitination by the E3 ubiquitin ligase HAKAI, which promotes the internalisation and degradation of E-cadherin in the lysosomes (Behrens et al., 1993; Fujita et al., 2002; Palacios et al., 2005). We have also shown that the RASSF1C-dependent phosphorylation of SRC leads to the phosphorylation of junctional components, such as E-cadherin and β-catenin, leading to the disruption of the cell-cell junctions. Previous studies have shown that RASSF1C expression led to an increase in the HAKAI binding to E-cadherin and SRC, however the RASSF1C-induced internalisation did not lead to a degradation and decrease of the total levels of E-cadherin. E-cadherin trafficking from the plasma membrane to the cytoplasm is important in the maintenance of the adherens junctions. Dynamin controls the endocytosis of E-cadherin and in the formation of mature junctions the chemical inhibition of Dynamin leads to loss of endocytosis and failure of E-cadherin to return to the site of photobleach (FRAP analysis) (de Beco et al., 2009). In our

`

system, we have observed that in RASSF1C-expressing cells, the return of the E-cadherin molecules to the site of photobleach is impaired. Further investigation showed that the junctions were significantly weaker when RASSF1C was expressed, both physically, as well as in terms of return after Ca^{2+} depletion assay. Potentially, RASSF1C could inhibit Dynamin via activation of SRC and ARF6, preventing the formation of strong, mature junctions. We also found that E-cadherin was highly accumulated in the cytoplasm, however it remains unclear whether it's kept in the cytoplasm or internalised in a cell organelle like the endosomes or the lysosomes. Preliminary results have shown that RASSF1C does not associate with ARF6 and that the integrated E-cadherin is not localised into the lysosomes, however further investigations would be required to fully understand this potentially novel method through which E-cadherin is internalised and accumulated in the cytoplasm, thus leading to loss of cell adherence, which would facilitate motility. Interestingly, in ovarian cancer high levels of E-cadherin are maintained during metastasis (Kobel et al., 2011) and E-cadherin has been shown to be important for the collective cell migration (Friedl et al., 2004). This would suggest that the accumulated E-cadherin in the RASSF1C-expressing cells could be stored in the cytoplasm in order to be used in the attachment of the metastatic, invasive cell to the stroma of the site of distant metastasis. We have also seen by immunofluorescence that motile RASSF1C-expressing cells can secrete vesicles containing E-cadherin. However, it remains unclear to whether these particular vesicles are exosomes and whether they would help the invasion.

E-cadherin stability at adherens junctions is controlled by the Rho family of GTPases (Menke and Giehl, 2012). Rac also stabilises the junctions (Hordijk et al., 1997; Sander et al., 1999). SRC recruitment of GEFs and GAPs can regulate the activity of both Rho and Rac (Huveneers and Danen, 2009), but both are spatially regulated and not active in the same part of the cell. Rac and Rho can antagonise each other (Nimnual et al., 2003; Ohta et al., 2006), which is important since loss of Rho makes cells more elongated, whereas cells that have lost Rac become rounded (Sequeira et al., 2008). This shows that cell rounding is promoted by Rho and is due to ROCK-driven actomyosin contractility (Amano et al., 1997; Kimura et al., 1996). We have shown that cells that express

`

RASSF1C become small and rounded and leave the monolayer. We find that these cells have lost their adherens junctions and become more motile. However, it remains unclear whether this motility is Rho- or Rac- driven. RASSF1C may promote Rho activation through SRC recruitment of a Rho-GEF. Rho also promotes the formation of Actin stress fibre (Ridley and Hall, 1992) and loss of RASSF1A expression has been linked to an increase in the Actin stress fibre formation (Dallol et al., 2005). Therefore, in the presence of RASSF1C and active SRC, the inhibition of the mediator of Rho contractility, ROCK, via the inhibitor Y27632, could lead to decreased myosin light chain (MLC) phosphorylation and avoid rounding-up of the cells. ROCK has been shown to promote myosin contractility through upregulation and direct phosphorylation of MLC and by phosphorylation and inactivation of myosin phosphatase (Kimura et al., 1996; Kureishi et al., 1997). This regulation of the MLC can be of great importance since MLC phosphorylation has been linked to increase in proliferation and migration of breast cancer cells and upregulation of β-catenin, BIRC5 and c-MYC (Zhou et al., 2008), a phenotype shown in this thesis to be connected to RASSF1C expression.

The Hippo pathway controls organ size by regulating cell contact inhibition, triggered by the activation of a cascade of phosphorylation events, including MST1/2, LATS1/2 and finally YAP1 on S127, leading to YAP1 inactivation and degradation (Johnson and Halder, 2014). We have shown that RASSF1A activation of the Hippo pathway maintains phosphorylation of YAP1 at S127 (Zaidi et al., 2004), preventing association with TEAD (van der Weyden et al., 2012). However, the loss of RASSF1A, but not of RASSF1C, leads to downregulation of the pathway. After the loss of the pS127, YAP1 is permissive for activation, but requires additional modifications to promote its nuclear localisation and transcriptional functionality (Ahn et al., 2013; Rosenbluh et al., 2012; Taniguchi et al., 2015; Zaidi et al., 2004). We find that these modifications are dependent on the expression of RASSF1C. We believe that together these data argue that upon RASSF1A loss, YAP1 is regulated in a Hippo-independent manner, which shifts its phosphorylation to RASSF1C-activated SFK.

`

The Hippo pathway effectors YAP1 and its homolog TAZ have been shown to be activated by Rho-mediated actomyosin contractility (Dupont et al., 2011). Therefore, RASSF1C activation of Rho may contribute to the activation of YAP1 and could explain the aggressive phenotypes seen in the mammospheres growth assay. Also, contact inhibition induced by E-cadherin signalling is mediated by the inhibition of YAP1 by the Hippo pathway (Kim et al., 2011) and YAP/TAZ are known to be sequestered to the sights of cell-cell junctions by α-catenin and Angiomotin (Chan, 2011; Schlegelmilch et al., 2011; Zhao, 2011). We have shown that in cells expressing RASSF1C, loss of E-cadherin can induce YAP1 localisation to the nucleus, but the role of Angiomotin in the system remains unclear. Since E-cadherin plays an important role in the localisation of YAP1 and contact growth inhibition (Kim et al., 2011), we investigated the expression of RASSF1C, and the consequent loss of E-cadherin and observed YAP1 nuclear localisation and increased cellular growth.

Indeed, in cells expressing RASSF1C, YAP1 is localised into the nucleus, after being phosphorylated at pY357 site by SFK. Interestingly, we observed that basal level of YAP1 phosphorylation in the control cells was higher than the expected levels when RASSF1C is not expressed. This could be explained by a phosphorylation of the Y357-YAP1 site by the SRC family member c-Abl, which has been reported to activate MST1/2 (Liu et al., 2012; Xiao et al., 2011) and lead to pY357-YAP1 binding to p73 and association with pro-apoptotic promoters (Levy et al., 2008). Given the levels of RASSF1A in the U2OS cells and the reported RASSF1A-dependent upregulation of the YAP1/p73 complex (Hamilton et al., 2009), c-Abl could be acting concurrently with RASSF1A, to increase the basal pY357 levels.

The phosphorylation of Y357 in the presence of RASSF1C confirms previously published data, showing the role for SFK-mediated phosphorylation of YAP1 for nuclear targeting (Rosenbluh et al., 2012), as has also been previously implicated for RUNX2 complexes (Zaidi et al., 2004) and in cancer-associated fibroblasts (CAFs) in response to mechanical stress (Calvo et al., 2013). We have shown that RASSF1C expression leads to SRC activation and loss of cell junctions due to phosphorylation of E-cadherin. We found that active SRC was also able to phosphorylate the transcriptional activator

`

and member of the junctional complex β-catenin, sequestering it away from the junctions and leading to its nuclear localisation. In the nucleus, β-catenin and YAP1 form a complex, leading to upregulation of transcriptional targets, in accordance with previously published data (Rosenbluh et al., 2012). We have shown that in breast cancer cells YAP1/β-catenin forms a complex with TBX3, which copies the TBX5 expression phenotype for *BCL2L1* and *BIRC5* and additionally promotes *c-MYC* expression, by combining known TEAD and TBX3 binding elements (Han et al., 2010; Heallen et al., 2011; Zhao et al., 2007). Mammosphere formation and growth in soft agar have been previously attributed to *BIRC5* expression (Dong et al., 2007; Rosenbluh et al., 2012), and c-MYC has been associated with increased invasion (Wolfer and Ramaswamy, 2011). This would further explain the formation of larger, more aggressive mammospheres in cells expressing RASSF1C. However, the upregulation of the anti-apoptotic genes *BCL2L1* and *BIRC5*, would suggest that in tumours that have lost *RASSF1A* due to methylation, selective inhibitors that would trigger apoptosis might not have an effect on the tumour (Hagenbuchner et al., 2013; Park et al., 2015). This could mean that treatment of tumours with drugs that restore the expression of RASSF1A, like DMNT inhibitors could result in the increased sensitivity towards treatments that target the apoptotic pathways.

The phosphorylation of β-catenin following the activation of Rho-family small GTP-ase Rac1 has been shown to affect the activity and localisation of β-catenin (Wu et al., 2008b). E-cadherin association protects β-catenin from degradation (Huber and Weis, 2001), but both proteins dissociate from the membrane following phosphorylation by SRC (Coluccia et al., 2006; Roura et al., 1999). We observed that RASSF1C expression promotes SRC-mediated β-catenin phosphorylation and consequently its accumulation in the nucleus. Interestingly, β-catenin has been shown to upregulate TBX3 expression (Renard et al., 2007). Furthermore, TBX3 has been reported to repress the expression of E-cadherin and to enhance invasiveness in melanoma (Peres et al., 2010; Rodriguez et al., 2008). Therefore in the cells expressing RASSF1C, the loss of cell junctions and the internalisation of E-cadherin could occur prior to the nuclear localisation of β-catenin which would cause the activation of TBX3 and the

`

inhibition of E-cadherin expression. This potentially could occur in order for the cells to undergo EMT, or to act as a second mechanism through which RASSF1C could impair E-cadherin. Further investigation would be required to confirm this hypothesis. Interestingly, the expression of *NANOG* and *OCT4* have been linked to the down-regulation of E-cadherin (Wang et al., 2014a), suggesting that RASSF1C expression could potentially lead to two separate ways to inhibit the further expression of E-cadherin.

The data presented in this thesis provides an explanation for the prognostic value of *RASSF1A* methylation and also suggests a possible approach in the treatment of such tumours by using SRC inhibitors. Methylation of *RASSF1A* in colorectal cancer has been associated with tumour dissemination (Wang et al., 2014b) and was found to be dramatically elevated in liver metastasis compared to primary tumours (Tommasi et al., 2011a). Since the loss of RASSF1A cooperates with loss of APC to promote intestinal tumours (van der Weyden et al., 2008), the observed RASSF1C-dependent SRC activation may contribute to colorectal tumourigenesis by inducing the tyrosine phosphorylations of both β-catenin and YAP1, leading to their nuclear localisation and transcriptional activation (Rosenbluh et al., 2012; Zaidi et al., 2004).

In Chapter 5 it was shown that RASSF1C expression promoted the secretion of exosomes and affected their cargo. Also, RASSF1C-derived exosomes were able to increase the growth rate of naïve cells in matrigel, suggesting that these microvesicles are able to induce the phenotype seen in MDA-MB-231 cells, expressing RASSF1C. Recent report shows that *in vivo*, extracellular vesicles released by malignant MDA-MB-231 cells were taken up by less malignant cells, located either within the same or distant tumours and led to enhanced migratory and metastatic capacity (Zomer et al., 2015). This is in accordance with our findings that the cells recipient for the exosomes were subjected to a similar transcriptional activity of upregulation of the stem cell genes *NANOG*, *OCT4* and *SOX2* and mesenchymal gene Vimentin, and an increase in the invasive behaviour, as the ones seen in the RASSF1C-expressing cells releasing the exosomes. Communication between cancer cells and their

`

surroundings plays a key role in driving tumour progression. It has been previously reported that CD81-positive exosomes were able to promote motility and metastasis of MDA-MB-231 cells (Luga et al., 2012). Furthermore, secreted vesicles like exosomes have been linked to the establishment of a pre-metastatic niche formation in the liver, that allows the colonisation and growth of disseminated tumour cells of pancreatic ductal adenocarcinoma (Costa-Silva et al., 2015). We showed that the RASSF1C expression increases the release of exosomes, which are able to modulate the cells surrounding the tumour and induce an exosome–mediated phenocopying of the aggressive and potentially metastatic behaviour. It remains unclear whether these exosomes will be able to travel to a pre-metastatic site and establish a niche for the disseminated RASSF1C cells. It would be interesting to find out if RASSF1C-derived exosomes can change the surrounding stroma and induce increase in the adhesiveness of endothelial cells or CAFs. Another unanswered question is how RASSF1C is inducing the increased secretion of exosomes. The secretion of exosomes is highly dependent on the ESCRT complex and the MVB. However, the ESCRT pathway is important for SRC functionality and localisation of active SRC at the sites of focal adhesions (Tu et al., 2010). Therefore RASSF1C could also be involved in the upregulation of SRC-mediated stabilisation of focal adhesions, promoting invasiveness.

The RASSF1C-derived exosomes were able to induce transcription of stem cell genes, in a pattern similar to the one observed in the RASSF1C-expressing cells. YAP1 has been shown to promote self-renewal in mouse embryonic stem cells in response to LIF signalling (Tamm et al., 2011) and its homolog, TAZ has been shown to induce stem cell markers in breast cancer cells (Cordenonsi et al., 2011). This suggests that RASSF1C activation of YAP, could lead to cancer cells gaining stem-like properties. Interestingly, RASSF1C expression in H1299 cells has been shown to upregulate the expression of LIF and the stem cell marker PIWIL (Reeves et al., 2012). LIF is a member of the IL-6 family of cytokines and is essential for stem cell pluripotency and inhibition of leukemic cell differentiation (Gough et al., 1988; Smith et al., 1992). LIF binds to receptors that contain the gp130 subunit, leading to the upregulation of *NANOG* through *SOX2* and *OCT4* (Gearing, 1993). NANOG is a

`

transcription factor that directly regulates the expression of other factors including KLF4, which RASSF1C can also potentially upregulate (Reeves et al., 2012). KLF4, like LIF-1, is a member of the Yamanaka cocktail of genes, used for re-programming of somatic cells into induced pluripotent stem cells (Takahashi and Yamanaka, 2006). KLF4 also regulates NANOG by direct interaction with OCT4, creating a positive feedback loop and maintaining pluripotency (Bourillot et al., 2009; Hall et al., 2009; Niwa et al., 2009; Zhang et al., 2010). We have shown that RASSF1C expression leads to the upregulation of both *NANOG* and *OCT4*, however it remains unclear whether this upregulation is achieved through LIF-1 and KLF4. The Yamanaka cocktail induces the expression of OCT4, SOX2, c-MYC and KLF4. RASSF1C expression has upregulated transcription of *OCT4*, *SOX2* and *c-MYC*. Therefore it would be interesting to further investigate whether *KLF4* is also upregulated in our system and whether RASSF1C can induce re-programming of somatic cells. Nevertheless, we show that the expression of RASSF1C promotes the enrichment of a tumour with cancer stem cells, tumour cells that contain self-renewal capacity and multilineage differentiation capacity (Medema, 2013). These findings are in accordance with previous reports showing an unknown mechanism leading to the upregulation of stem cell markers in RASSF1C-expressing breast and lung cancer cell lines (Amaar et al., 2006a; Reeves et al., 2012; Reeves et al., 2010). Further investigation will be required and would involve the examination of the stem cell population on xenografts with or without RASSF1A expression. We would predict that a tumour, formed from RASSF1A-expressing cells, would have a smaller stem cell population and a $CD44^{low}/CD24^{low}$ profile.

These findings are is in accordance with the association between loss of RASSF1A and a decrease in cell differentiation. It has been published that tumour formation in *RASSF1A* null mice is statistically associated with loss of the differentiation factor RUNX2, leading to a significantly faster tumour development, specifically of poorly differentiated lymphomas or CD3-positive T-cell lymphomas (van der Weyden et al., 2012). Also, the loss of RASSF1A and RUNX2 led to a loss of the association of YAP1 and p73 and promoted enhanced YAP-TEAD binding (van der Weyden et al., 2012) which would lead to EMT and inhibition of differentiation (Zhang et al., 2009).

`

Cancer stem cells are proposed to be more chemo and radio-resistant (Bao et al., 2006; Diehn et al., 2009; Krause et al., 2011). Therefore tumours that have lost RASSF1A, but expressing RASSF1C, would be more resistant to therapy. This is indeed the case. The decreased responsiveness to DNA damaging therapies has been correlated to RASSF1A methylation (Catto et al., 2005; Dote et al., 2005; Honda et al., 2008). A potential way of addressing the loss of RASSF1A due to methylation can be the use of a DNMT inhibitor, which would re-sensitise the tumours to the therapeutic regimes through the re-expression of RASSF1A. This treatment, used in combination with an inhibitor of SRC, should reverse the effects of RASSF1C expression and the downstream events following the activation of SRC in RASSF1C-expressing cells. It has been shown that the re-expression of RASSF1A using DNMT inhibitors in cell lines and mouse models have resulted in an increase in sensitivity to DNA damaging agents like radiation and cisplatin, and have also shown increased sensitivity to other chemotherapeutics such as, fluorouracil and mitomycin (Balch et al., 2005; Dote et al., 2005; Zhao and Dou, 2007). In patients, decitabine (5-aza-2'-deoxycytidine) has been successfully used to enhance the cisplatin sensitivity of testicular germ cell tumours (Beyrouthy et al., 2009). The treatment correlated with DNMT3B expression and therefore DNA methylation. This is important since one of the most significant targets for DNMT3B has been shown to be RASSF1A (Palakurthy et al., 2009) suggesting that treatment effectiveness depends on the re-expression of RASSF1A. Finally, in a phase 2 clinical, the usage of low dose decitabine in heavily pre-treated ovarian cancer patients, was able to restore sensitivity to carboplatin, resulting in high response rates and prolonged progression free survival (Matei et al., 2012). The restored expression of RASSF1A would not only have effect on the increase in radiosensitivity due to the induction of RASSF1A stress response pathways, but also should decrease the expression levels of RASSF1C, affecting SRC activity, loss of junctions, YAP1 transcription and invasion. Therefore, the role of RASSF1C in cells treated with DNMT inhibitors should be further examined by investigating predominantly SRC activity, but also the presence of stem cell markers. We would predict that treatment of tumours, methylated for

`

RASSF1A, with DNMT inhibitors would lead to inactive SRC, downregulation of BCL2L, BIRC5 and c-MYC and tumours with a decreased stem cell population that is more sensitive to radiotherapy.

Effective treatment of tumours methylated for RASSF1A could include the use of SRC inhibitors. From the various SRC inhibitors in development, the three best studied are Dasatinib, bosutinib and AZD0530 (saracatinib). All three of these drugs have been associated with a robust anti-tumour and anti-proliferative effects, blocking cell growth, invasion and angiogenesis in preclinical trials (Aleshin and Finn, 2010). Our data suggests that inhibition of SRC activity reduces the destabilisation of E-cadherin, inhibits the growth in matrigel and downregulates *BCL2L1*, *BIRC5* and *c-MYC*. It yet remains to understand the role of SRC inhibition in exosome packaging; however we have seen active SRC packaged in the exosomes derived from RASSF1C-expressing cells. Preliminary data has indicated that cells treated with RASSF1C-derived exosomes can lead to an increase in the pY416-SRC protein levels. Therefore the inhibition of SRC can potentially cease the packaging of the active SRC in the exosomes. In colon carcinoma cells, Dasatinib was shown to increase the sensitivity to oxaliplatin (Kopetz et al., 2009) in lung cancer, the one to cisplatin (Ceppi et al., 2009). Having in mind the variety of phase 1 and 2 clinical trials progressing with these drugs, used either as single agents or in combination with drugs, and the data shown in this thesis, any future treatment of patients with methylated RASSF1A gene should include a combination of both SRC inhibitors and DNMT inhibitors. A suggested combined treatment could lead to a decrease in the rate of metastasis.

Taking the data presented in this thesis, in context with the literature, allows us to propose a final testable model (Figure 7.1). In normal cells, RASSF1A regulates the activity of SRC family kinases through the interaction with CSK, allowing CSK to phosphorylate and inactivate SRC. RASSF1A also inhibits the interaction between RASSF1C and SRC. In cancers, when RASSF1A is lost, RASSF1C levels become elevated and lead to activation of SRC and its translocation to the membrane. Once at the membrane active SRC leads to phosphorylation and loss of E-cadherin from the sites of cell-cell junctions. E-cadherin is then accumulated in the cytoplasm. The loss of junctions induces a partial

`

EMT and translocation of β-catenin from the junctional complex to the nucleus. This leads to an increase in cell motility. RASSF1C-activated SFK are also able to phosphorylate YAP1 and translocate it to the nucleus, where with β−catenin and TBX3 and TEAD are able to induce the upregulation of pro-survival and migratory genes.

RASSF1C expression also leads to increase in the CD63/CD81 levels and the upregulation of exosome secretion and affecting the surrounding cancer cells in a pattern, which phenocopies the one of the RASSF1C cell. This increases the aggressiveness and pro-survival mechanisms of the cell surroundings, potentially leading to establishing a pre-metastatic niche at the site of distant metastasis. RASSF1C-expressing cells also undergo upregulation of stem cell genes and present surface markers associating them with cancer stem cells. We propose a model where expression of RASSF1C could affect the surroundings via exosomes, establish a niche and invade there due to the loss of cell adhesion. When it reaches the site of metastasis, it would use the pro-survival and stem cell gene upregulation to increase the potential for establishing a new tumour at that site. The proposed model predicts that due to these properties, the resulting population of cells will be less sensitive to radio- and chemotherapies. Re-sensitisation of this cell population may occur through treatment with DMNT inhibitors which would induce the re-expression of RASSF1A or by direct inhibition of SRC family kinases.

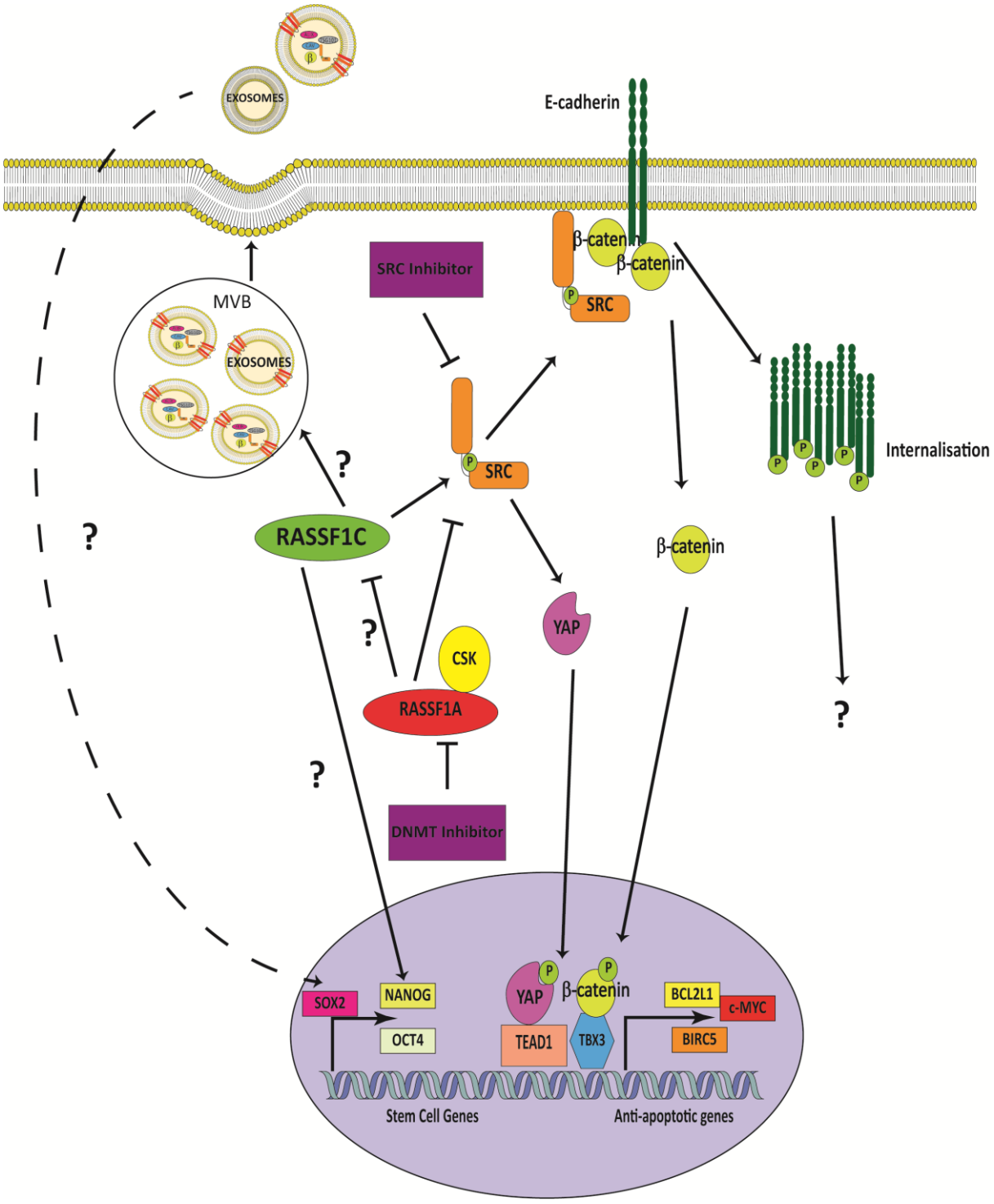


Figure 7.1. Cartoon Depicting the Model Generated from the Results in this Thesis. When RASSF1A is lost, RASSF1C can activate SRC, promoting translocation of SRC to the plasma membrane. At the plasma membrane SRC phosphorylates target proteins such as E-cadherin and β-catenin. This leads to the internalisation of E-cadherin and its accumulation in the cytoplasm. Phosphorylated β-catenin is translocated into the nucleus. RASSF1C, via SRC, can phosphorylate YAP leading to its accumulation in the nucleus. There, YAP and β-catenin associate with the transcription factors TEAD1 and TBX3 to induce the expression of the anti-apoptotic genes *BCL2L1*, *BIRC5* and *c-MYC*. RASSF1C expression can also alter the secretion and packaging of exosomes. These exosomes can be internalised by neighbouring cells to induce the expression of the stem cell genes *NANOG*, *OCT4* and *SOX2*. RASSF1C-expressing cells can only upregulate the expression of *NANOG* and *OCT4*. Re-expression of RASSF1A, using DNMT inhibitor, may inhibit SRC activation by binding to CSK. SRC may also be targeted directly using a SRC inhibitor.

`

Chapter 8 Appendix

8.1 CSK Binds to RASSF1A

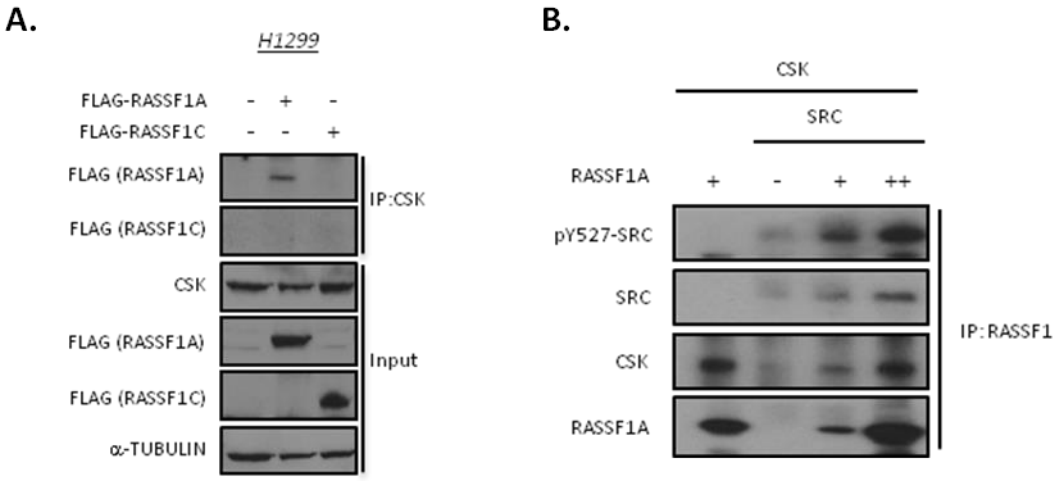


Figure 8.1. RASSF1A Binds to CSK and SRC. A. H1299 cells (1 x 10^6 cells/plate) were transfected with FLAG-RASSF1A and FLAG-RASSF1C and cultured for 48 hrs prior to lysis with a 0.5 % NP40, 150 mM NaCl lysis buffer and immunoprecipitated with an anti-CSK antibodies bound to protein G sepharose beads. Inputs and precipitates were analysed by SDS-PAGE and western blot for the presence of RASSF1A and RASSF1C using antibodies against FLAG-tag. RASSF1A immunoprecipitated with CSK. Data is representative of three independent experiments. This experiment was done by Simon Scrace. **B.** Recombinant His-tagged RASSF1A (1 μg (+) or 2 μg (++)) (Fitzgerald Industries, USA) was mixed with either recombinant, kinase active His-tagged CSK (1 μg) (Active Motif) or His-tagged SRC (1 μg) (Active Motif) in a reaction tube with mild lysis buffer (0.1% NP40, 20 mM HEPES pH 7.5, 150 mM NaCl, 0.5 mM EDTA, 50 mM NaF, 10 mM β-glycerophosphate and 0.5 mM Sodium orthovanidate) supplemented with protease inhibitors (Roche) in 20 μl volume. The tubes were then incubated for 30 minutes at 37^{o} C after which 5 μl of each reaction was used for immunoprecipitation. The pull-downs were achieved with either SRC (Cell Signalling) or RASSF1 (Santa Cruz) antibodies bound to agarose beads for 1.5 hours at 4^{o} C under constant rotation. The beads were washed four times with the lysis buffer by centrifugation (2150 x g, 4^{o} C, 5 min) prior to resuspension in loading buffer (10 % Glycerol, 62.5 mM Tris-HCl pH 6.8, 2 % SDS, 2 % 2-Mercaptoethanol plus bromophenol blue). Data represents one independent experiment. Purified RASSF1A binds to SRC via CSK, and they can bind to pY527-SRC.

`

8.2 Opposing Roles for SRC Regulation by RASSF1A and RASSF1C

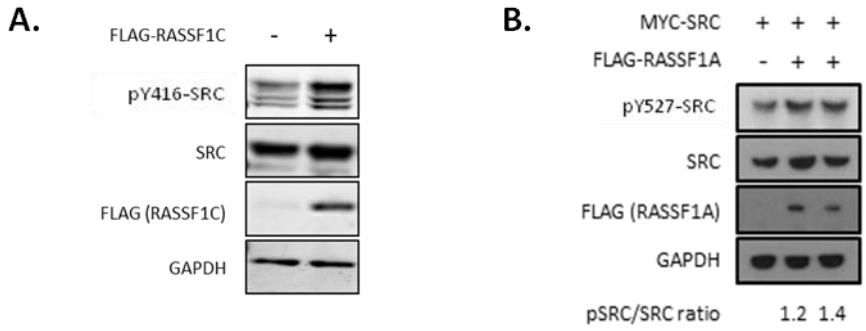


Figure 8.2. RASSF1A and RASSF1C Show Opposing Roles in SRC Activation. A. H1299 cells (2 x 10^5 cells/plate) were transfected with pcDNA3 or FLAG-RASSF1C. Cells were cultured in DMEM containing 0.1 % FBS 16 hrs before lysis with Laemmli lysis buffer. Lysates were analysed by SDS-PAGE and western blot for activated SRC using antibodies against phospho-SRC Y416 and total SRC. Anti-FLAG antibodies were used to confirm RASSF1C expression. GAPDH is a loading control. Phosphorylated, active, SRC clearly increases with RASSF1C expression. Data is representative of three independent experiments. **B.** H1299 cells (2 x 10^5 cells/plate) were transfected with MYC-SRC and pcDNA3 or FLAG-RASSF1A. Cells were cultured in DMEM containing 0.1 % FBS 16 hrs before being lysed and analysed by SDS-PAGE and western blot. Blots were stained using the indicated antibodies. RASSF1A leads to phosphorylation of SRC at Y527 site. Data is representative of three independent experiments. These experiments were done by Simon Scrace.

8.3 RASSF1C Can Only Activate SRC in RASSF1A-Negative Cell Lines

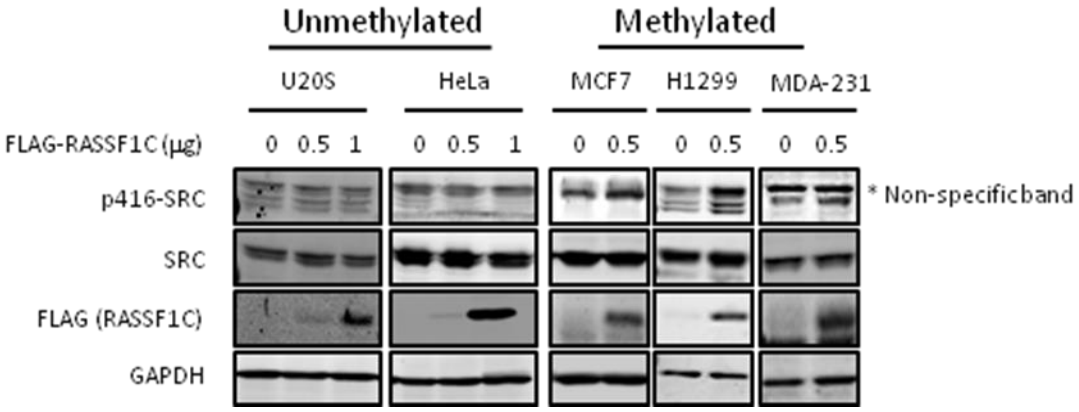


Figure 8.3. The Expression of RASSF1C Can Only Activate SRC in RASSF1A-Negative Cell Lines. RASSF1A-expressing cell lines (U20S, SW480 and HeLa) and RASSF1A negative (RASSF1A methylated) cell lines (MCF7 and MDA-MB-231) (2 x 10^5 cells/plate) were transfected with 0, 0.5 or 1 μg FLAG-RASSF1C. Cells were cultured in DMEM containing 0.1 % FBS for 16 hrs prior to lysis with Laemmli lysis buffer. Lysates were analysed by SDS-PAGE and western blot for activated SRC with antibodies against phospho-SRC Y416 and total SRC. Anti-FLAG antibodies confirmed RASSF1C expression and GAPDH is a loading control. Phosphorylated SRC increases with RASSF1C expression in MCF7 and MDA-MB-231 cells, but not in U2OS, SW480 or HeLa cells as indicated by the Phospho-SRC to SRC ratio. Data represents one independent experiment. This experiment was done by Simon Scrace.

`

8.4 RASSF1C Leads to SRC-Dependent Phosphorylation of E-cadherin

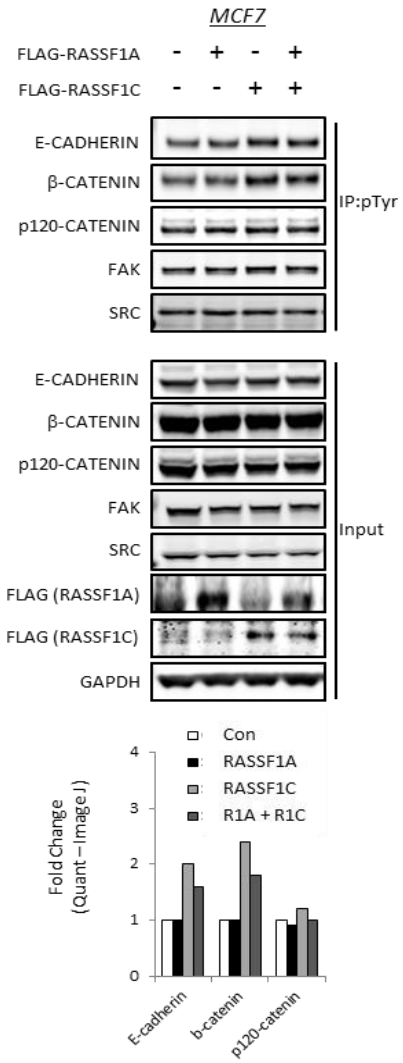


Figure 8.4. RASSF1C Activation of SRC Leads to Tyrosine Phosphorylation of SRC Targets. MCF7 cells (1 x 10^6 cells/plate) were transfected with FLAG-RASSF1A and FLAG-RASSF1C, either alone or together, at a ratio such that equal expression of each construct was achieved. Cells were lysed by scraping into 0.5 % NP40, 150 mM NaCl lysis buffer supplemented with protease and phosphatase inhibitors. Cells were immunoprecipitated for 6 hrs with anti-pY 4G10 antibody. Protein was recovered from the beads by boiling into 1 x loading buffer for 5 mins. Samples were analysed by SDS-PAGE and western blot for SRC targets: E-cadherin, β-catenin, p120-catenin, FAK and SRC. Inputs were also probed with an anti-FLAG antibody to confirm RASSF1A and RASSF1C expression. Tyrosine phosphorylation of E-cadherin and β-catenin was elevated in cells expressing RASSF1C Blot is representative of three independent experiments which have been quantified using ImageJ software. This experiment was done by Simon Scrace.

`

8.5 E-cadherin is Not Accumulated in the Cell Organelles

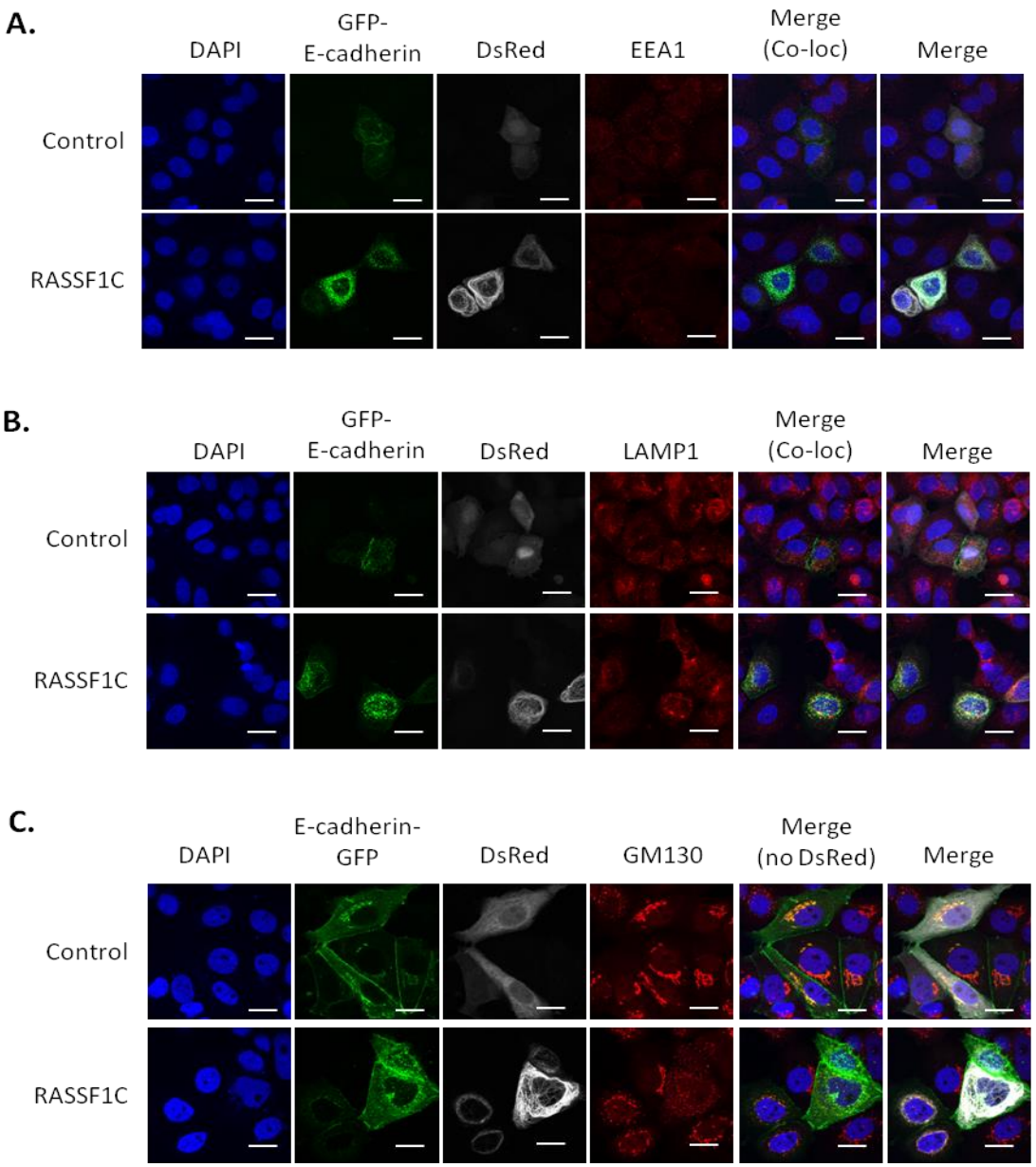


Figure 8.5. RASSF1C Does Not Send E-cadherin to the Endosomes, Lysosomes or Golgi. MCF7 cells (3 x 10^5 cells/condition), were plated onto glass cover slips and transfected with E-cadherin-GFP and DsRed or DsRed-RASSF1C. Cells were fixed for 15 mins with 4 % PFA, permeabilised for 5 mins with 0.2 % Triton X solution and blocked for 30 mins with 0.2 % FSG. Cells were probed with the anti-YAP1 or anti p127-YAP1 antibodies. Secondary antibody was Alexa-fluor 633 nm. Cover slips were mounted onto slides using mounting media containing DAPI. Images were taken using a Zeiss LSM 780 microscope at 63 x magnification. Scale bars represent 10 mm. The DsRed channel was left grey, so that the co-localisation can be observed, if any, with the 633 channel. **A.** E-cadherin expressing cells stained with the endosome marker EEA1. **B.** E-cadherin expressing cells stained with the lysosome marker LAMP1. **C.** E-cadherin expressing cells stained with the Golgi marker GM130. RASSF1C does not lead to accumulation of E-cadherin into the endosomes, lysosomes or the Golgi complex.

`

8.6 RASSF1A Binds to RASSF1C

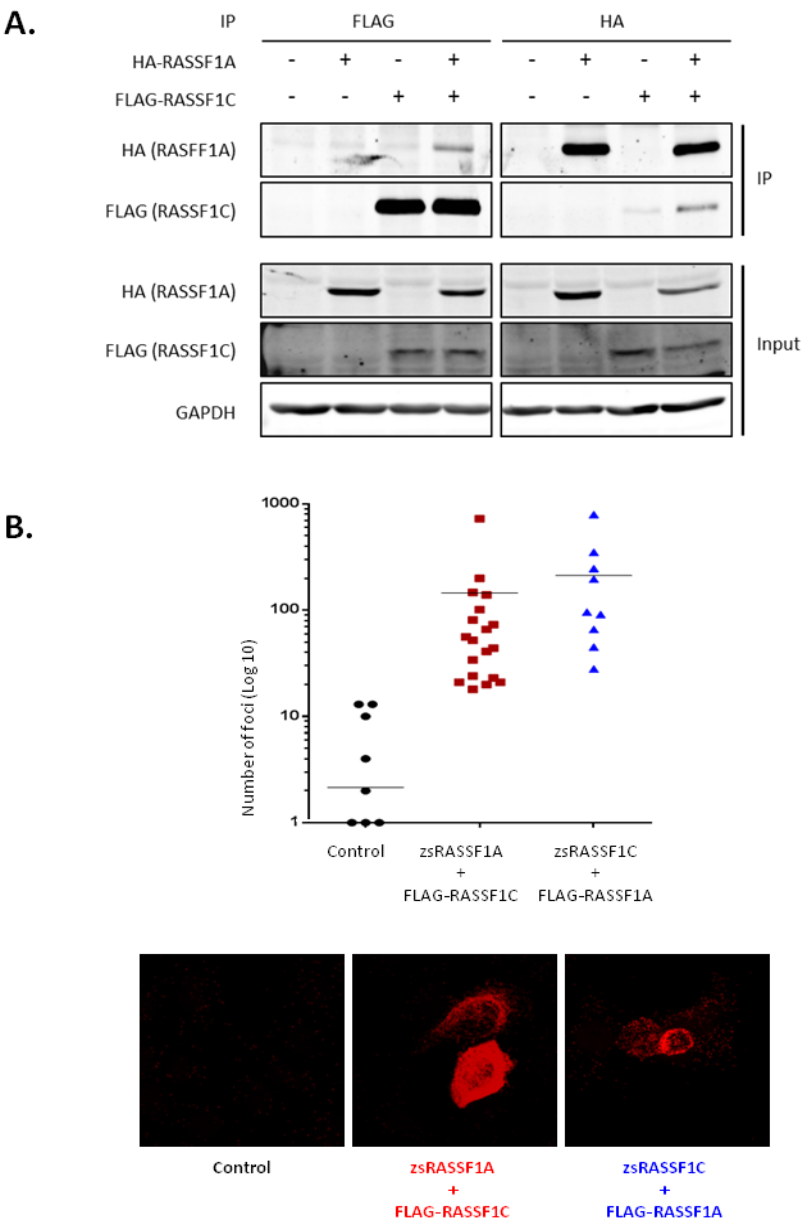


Figure 8.6. RASSF1A Binds to RASSF1C. A. H1299 cells (1 x 10^6 cells/plate) were transfected with either pcDNA3, HA-RASSF1A, FLAG-RASSF1C or both. Empty vector was used to balance the amount of DNA transfected. Cells were cultured for 48 hrs before cells were lysed using a 0.5 % NP40, 150 mM NaCl lysis buffer and immunoprecipitated with either anti-HA antibodies bound to protein G sepharose beads or with anti-FLAG M2-conjugated agarose beads. Cells were cultured for a total of 48 hrs and lysed with laemmli lysis buffer and analysed by SDS-PAGE and western blot with the indicated antibodies. RASSF1A binds to RASSF1C. This experiment was done by Simon Scrace. **B.** H1299 cells (1 x 10^4 cells/well) were plated on 16-well chamber slide (Thermo Scientific)) and transfected with either ZsGreen, ZsGreen-RASSF1A or ZsGreen-RASSF1C or either FLAG-RASSF1A or FLAG-RASSF1C. Wells were and treated with the Duolink PLA assay kit as per instructions, before overnight incubation with primary anti-ZsGreen (bait) and anti-FLAG (prey) antibodies and secondary antibodies for 1 h. Hybridisation was performed for 30 minutes in a humidified chamber, ligation reactions for 30 minutes, amplification for 100 minutes and DAPI was used for cell nucleus detection. Scale bars represent 10 μm. The PLA reaction occurs only if two proteins are in close proximity (40nm). Data represents two independent experiments.

`

8.7 RASSF1C-Expressing Cells Accumulate in G1/S Phase

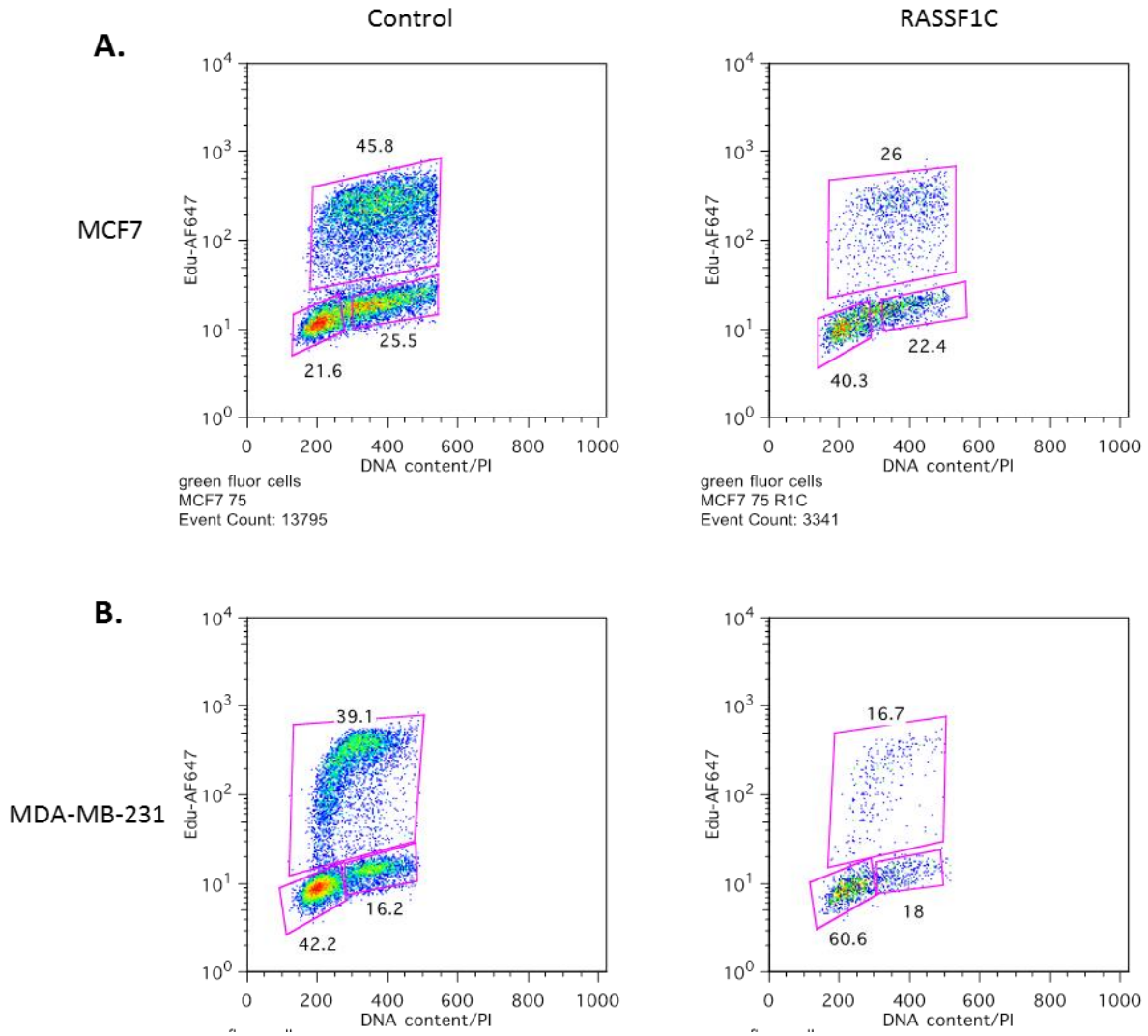


Figure 8.7. RASSF1C-Expressing Cells are Predominantly in G1. Flow cytometry analysis of MCF7 cells (**A.)** and MDA-MB-231 (**B.**) cells (1 x 10^6 cells/plate) transfected with either ZsGreen-control or ZsGreen-RASSF1C. After 3 days cells were collected and stained with propidium iodide, followed by flow cytometry analysis. The cells expressing RASSF1C are concentrated in the G1/M phase, compared to the control cells.

`

8.8 Analysis of Exosomes Treated with mTOR and PI3K Inhibitors

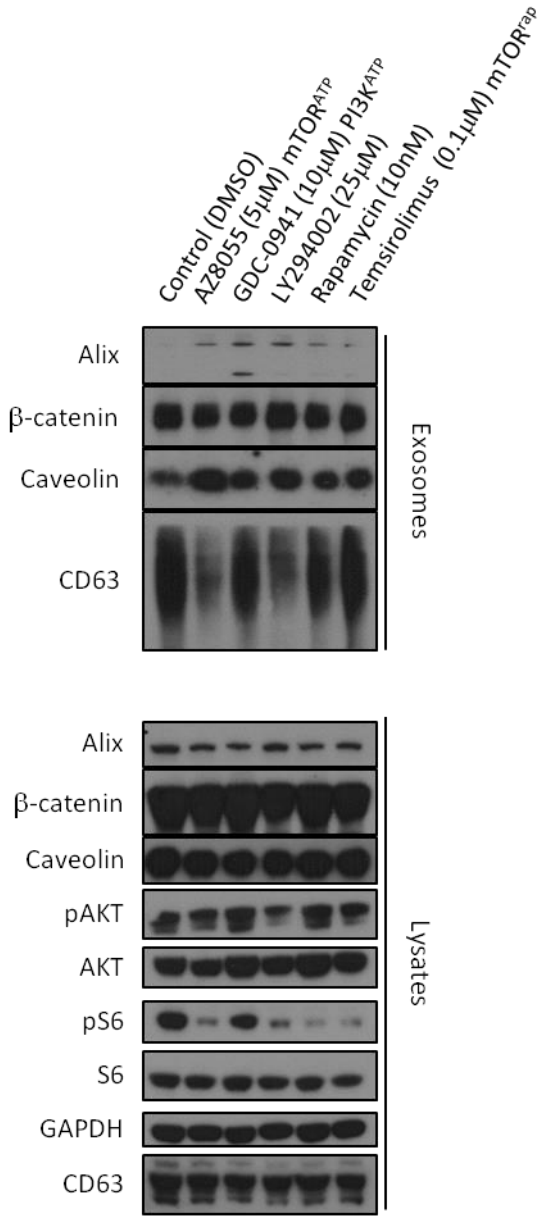


Figure 8.8. The Packaging of Proteins in Exosomes Depends on mTOR Activity in HCT116 Cells. HCT116 cells (5 x 10^6 cells/plate) were treated with the indicated drugs. Cells were grown in DMEM media supplemented with 0.1 % FBS for 1 day. Exosomes were extracted from the conditioned media using sequential ultracentrifugation. Cells and exosomes were lysed using 1 X RIPA buffer. The number of cells/plate at the end of the experiment was used for protein levels normalisation. Samples were analysed by SDS-PAGE and western blot for the indicated antibodies. Cells in treated with mTOR inhibitors switch between exosomes containing high caveolin and low CD63; and low caveolin and high CD63. All data is representative of three independent experiments.

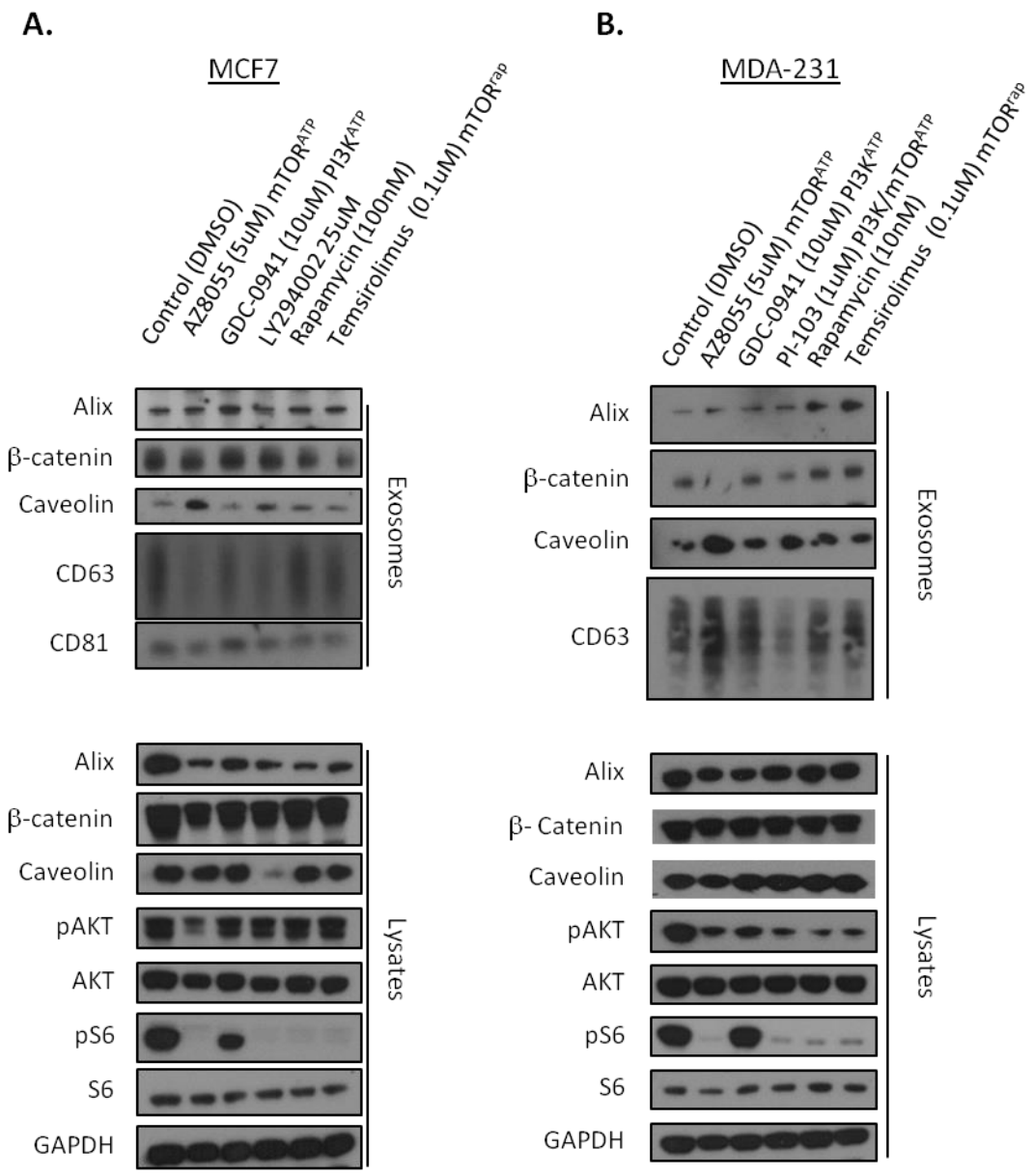


Figure 8.9. The Packaging of Proteins in Exosomes Depends on mTOR Activity in Breast Cancer Cell Lines. MCF7 (**A.**) and MDA-MB-231 (**B.**) cells (5 x 10^6 cells/plate) were treated with the indicated drugs. Cells were grown in DMEM media supplemented with 0.1 % FBS for 1 day. Exosomes were extracted from the conditioned media using sequential ultracentrifugation. Cells and exosomes were lysed using 1 X RIPA buffer. The number of cells/plate at the end of the experiment was used for protein levels normalisation. Samples were analysed by SDS-PAGE and western blot for the indicated antibodies. Cells in treated with mTOR inhibitors switch between exosomes containing high caveolin and low CD63; and low caveolin and high CD63. All data is representative of three independent experiments.

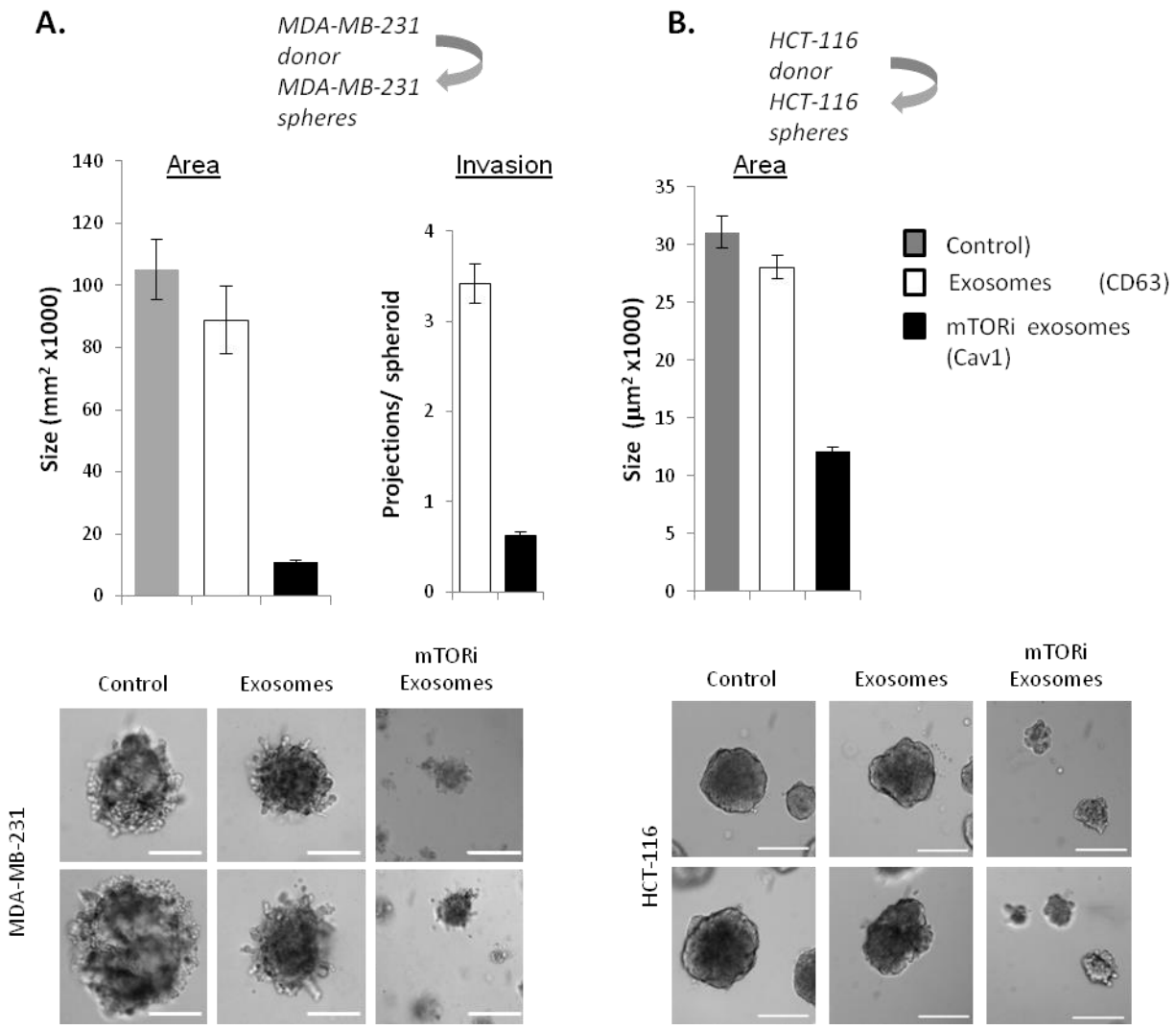


Figure 8.10. Exosomes Derived from Cells Treated with mTOR Inhibitor Reduce the Growth of Mammospheres. MDA-MB-231 cells (**A.**) or HCT-116 cells (**B.**) (5 x 10^6 cells/plate) were transfected with pcDNA3 or FLAG-RASSF1C. Cells were grown in DMEM media supplemented with 0.1 % FBS for 1 days. Exosomes were extracted from the conditioned media using sequential ultracentrifugation. MDA-MB-231 cells (**A.**) or HCT-116 cells (**B.**) were plated onto matrigel and treated with the respective purified exosomes every three days for up to 10 days in total. Images were taken using a Nikon TE2000 microscope at 10 X magnification. In both cases exosomes derived from cells treated with the mTOR inhibitor AZD8055 reduced the size of the mammosphere, compared to the control or mammospheres treated with DMSO.

`

Chapter 9 References

Abrahams, A., M.I. Parker, and S. Prince. 2010. The T-box transcription factor Tbx2: its role in development and possible implication in cancer. *IUBMB Life*. 62:92-102.

Adams, C.L., Y.T. Chen, S.J. Smith, and W.J. Nelson. 1998. Mechanisms of epithelial cell-cell adhesion and cell compaction revealed by high-resolution tracking of E-cadherin-green fluorescent protein. *J Cell Biol*. 142:1105-1119.

Ahn, E.Y., J.S. Kim, G.J. Kim, and Y.N. Park. 2013. RASSF1A-mediated regulation of AREG via the Hippo pathway in hepatocellular carcinoma. *Mol Cancer Res*. 11:748-758.

Akers, J.C., D. Gonda, R. Kim, B.S. Carter, and C.C. Chen. 2013. Biogenesis of extracellular vesicles (EV): exosomes, microvesicles, retrovirus-like vesicles, and apoptotic bodies. *J Neurooncol*. 113:1-11.

Al-Hajj, M., M.S. Wicha, A. Benito-Hernandez, S.J. Morrison, and M.F. Clarke. 2003. Prospective identification of tumorigenic breast cancer cells. *Proc Natl Acad Sci U S A*. 100:3983-3988.

Al-Nedawi, K., B. Meehan, J. Micallef, V. Lhotak, L. May, A. Guha, and J. Rak. 2008. Intercellular transfer of the oncogenic receptor EGFRvIII by microvesicles derived from tumour cells. *Nat Cell Biol*. 10:619-624.

Aleshin, A., and R.S. Finn. 2010. SRC: a century of science brought to the clinic. *Neoplasia*. 12:599-607.

Allalou, A., and C. Wahlby. 2009. BlobFinder, a tool for fluorescence microscopy image cytometry. *Computer methods and programs in biomedicine*. 94:58-65.

am Esch, J.S., 2nd, W.T. Knoefel, M. Klein, A. Ghodsizad, G. Fuerst, L.W. Poll, C. Piechaczek, E.R. Burchardt, N. Feifel, V. Stoldt, M. Stockschlader, N. Stoecklein, R.Y. Tustas, C.F. Eisenberger, M. Peiper, D. Haussinger, and S.B. Hosch. 2005. Portal application of autologous CD133+ bone marrow cells to the liver: a novel concept to support hepatic regeneration. *Stem Cells*. 23:463-470.

Amaar, Y.G., D.J. Baylink, and S. Mohan. 2005. Ras-association domain family 1 protein, RASSF1C, is an IGFBP-5 binding partner and a potential regulator of osteoblast cell proliferation. *J Bone Miner Res*. 20:1430-1439.

Amaar, Y.G., M.G. Minera, L.K. Hatran, D.D. Strong, S. Mohan, and M.E. Reeves. 2006a. Ras association domain family 1C protein stimulates human lung cancer cell proliferation. *Am J Physiol Lung Cell Mol Physiol*. 291:L1185-1190.

Amaar, Y.G., B. Tapia, S.T. Chen, D.J. Baylink, and S. Mohan. 2006b. Identification and characterization of novel IGFBP5 interacting protein: evidence IGFBP5-IP is a potential regulator of osteoblast cell proliferation. *Am J Physiol Cell Physiol*. 290:C900-906.

Amano, M., K. Chihara, K. Kimura, Y. Fukata, N. Nakamura, Y. Matsuura, and K. Kaibuchi. 1997. Formation of actin stress fibers and focal adhesions enhanced by Rho-kinase. *Science*. 275:1308-1311.

Anderson, N.G., and A.P. Butler. 2014. Clinical applications of spectral molecular imaging: potential and challenges. *Contrast Media Mol Imaging*. 9:3-12.

Andre, F., N.E. Schartz, M. Movassagh, C. Flament, P. Pautier, P. Morice, C. Pomel, C. Lhomme, B. Escudier, T. Le Chevalier, T. Tursz, S. Amigorena, G. Raposo, E. Angevin, and L. Zitvogel. 2002. Malignant effusions and immunogenic tumour-derived exosomes. *Lancet*. 360:295-305.

Aragona, M., T. Panciera, A. Manfrin, S. Giulitti, F. Michielin, N. Elvassore, S. Dupont, and S. Piccolo. 2013. A mechanical checkpoint controls multicellular growth through YAP/TAZ regulation by actin-processing factors. *Cell*. 154:1047-1059.

`

Arnette, C., N. Efimova, X. Zhu, G.J. Clark, and I. Kaverina. 2014. Microtubule segment stabilization by RASSF1A is required for proper microtubule dynamics and Golgi integrity. *Mol Biol Cell*. 25:800-810.

Arthur, W.T., and K. Burridge. 2001. RhoA inactivation by p190RhoGAP regulates cell spreading and migration by promoting membrane protrusion and polarity. *Mol Biol Cell*. 12:2711-2720.

Arvand, A., and C.T. Denny. 2001. Biology of EWS/ETS fusions in Ewing's family tumors. *Oncogene*. 20:5747-5754.

Avilion, A.A., S.K. Nicolis, L.H. Pevny, L. Perez, N. Vivian, and R. Lovell-Badge. 2003. Multipotent cell lineages in early mouse development depend on SOX2 function. *Genes Dev*. 17:126-140.

Avizienyte, E., V.J. Fincham, V.G. Brunton, and M.C. Frame. 2004. Src SH3/2 domain-mediated peripheral accumulation of Src and phospho-myosin is linked to deregulation of E-cadherin and the epithelial-mesenchymal transition. *Mol Biol Cell*. 15:2794-2803.

Avizienyte, E., A.W. Wyke, R.J. Jones, G.W. McLean, M.A. Westhoff, V.G. Brunton, and M.C. Frame. 2002. Src-induced de-regulation of E-cadherin in colon cancer cells requires integrin signalling. *Nat Cell Biol*. 4:632-638.

Aylon, Y., Y. Ofir-Rosenfeld, N. Yabuta, E. Lapi, H. Nojima, X. Lu, and M. Oren. 2010. The Lats2 tumor suppressor augments p53-mediated apoptosis by promoting the nuclear proapoptotic function of ASPP1. *Genes Dev*. 24:2420-2429.

Aylon, Y., N. Yabuta, H. Besserglick, Y. Buganim, V. Rotter, H. Nojima, and M. Oren. 2009. Silencing of the Lats2 tumor suppressor overrides a p53-dependent oncogenic stress checkpoint and enables mutant H-Ras-driven cell transformation. *Oncogene*. 28:4469-4479.

Azzolin, L., T. Panciera, S. Soligo, E. Enzo, S. Bicciato, S. Dupont, S. Bresolin, C. Frasson, G. Basso, V. Guzzardo, A. Fassina, M. Cordenonsi, and S. Piccolo. 2014. YAP/TAZ incorporation in the beta-catenin destruction complex orchestrates the Wnt response. *Cell*. 158:157-170.

Baietti, M.F., Z. Zhang, E. Mortier, A. Melchior, G. Degeest, A. Geeraerts, Y. Ivarsson, F. Depoortere, C. Coomans, E. Vermeiren, P. Zimmermann, and G. David. 2012. Syndecan-syntenin-ALIX regulates the biogenesis of exosomes. *Nat Cell Biol*. 14:677-685.

Baksh, S., S. Tommasi, S. Fenton, V.C. Yu, L.M. Martins, G.P. Pfeifer, F. Latif, J. Downward, and B.G. Neel. 2005. The tumor suppressor RASSF1A and MAP-1 link death receptor signaling to Bax conformational change and cell death. *Molecular cell*. 18:637-650.

Balch, C., P. Yan, T. Craft, S. Young, D.G. Skalnik, T.H. Huang, and K.P. Nephew. 2005. Antimitogenic and chemosensitizing effects of the methylation inhibitor zebularine in ovarian cancer. *Mol Cancer Ther*. 4:1505-1514.

Bao, S., Q. Wu, R.E. McLendon, Y. Hao, Q. Shi, A.B. Hjelmeland, M.W. Dewhirst, D.D. Bigner, and J.N. Rich. 2006. Glioma stem cells promote radioresistance by preferential activation of the DNA damage response. *Nature*. 444:756-760.

Bapat, S.A., A.M. Mali, C.B. Koppikar, and N.K. Kurrey. 2005. Stem and progenitor-like cells contribute to the aggressive behavior of human epithelial ovarian cancer. *Cancer Res*. 65:3025-3029.

Barbacid, M. 1987. ras genes. *Annual review of biochemistry*. 56:779-827.

Barres, C., L. Blanc, P. Bette-Bobillo, S. Andre, R. Mamoun, H.J. Gabius, and M. Vidal. 2010. Galectin-5 is bound onto the surface of rat reticulocyte exosomes and modulates vesicle uptake by macrophages. *Blood*. 115:696-705.

Basu, A., B.A. Teicher, and J.S. Lazo. 1990. Involvement of protein kinase C in phorbol ester-induced sensitization of HeLa cells to cis-diamminedichloroplatinum(II). *J Biol Chem*. 265:8451-8457.

Basu, S., N.F. Totty, M.S. Irwin, M. Sudol, and J. Downward. 2003. Akt phosphorylates the Yes-associated protein, YAP, to induce interaction with 14-3-3 and attenuation of p73-mediated apoptosis. *Molecular cell*. 11:11-23.

Baum, B., and N. Perrimon. 2001. Spatial control of the actin cytoskeleton in Drosophila epithelial cells. *Nat Cell Biol*. 3:883-890.

Baum, B., J. Settleman, and M.P. Quinlan. 2008. Transitions between epithelial and mesenchymal states in development and disease. *Semin Cell Dev Biol*. 19:294-308.

`

Beck, B., G. Driessens, S. Goossens, K.K. Youssef, A. Kuchnio, A. Caauwe, P.A. Sotiropoulou, S. Loges, G. Lapouge, A. Candi, G. Mascre, B. Drogat, S. Dekoninck, J.J. Haigh, P. Carmeliet, and C. Blanpain. 2011. A vascular niche and a VEGF-Nrp1 loop regulate the initiation and stemness of skin tumours. *Nature*. 478:399-403.

Behrens, J., L. Vakaet, R. Friis, E. Winterhager, F. Van Roy, M.M. Mareel, and W. Birchmeier. 1993. Loss of epithelial differentiation and gain of invasiveness correlates with tyrosine phosphorylation of the E-cadherin/beta-catenin complex in cells transformed with a temperature-sensitive v-SRC gene. *J Cell Biol*. 120:757-766.

Ben-Porath, I., M.W. Thomson, V.J. Carey, R. Ge, G.W. Bell, A. Regev, and R.A. Weinberg. 2008. An embryonic stem cell-like gene expression signature in poorly differentiated aggressive human tumors. *Nature genetics*. 40:499-507.

Bernardi, R., P.P. Scaglioni, S. Bergmann, H.F. Horn, K.H. Vousden, and P.P. Pandolfi. 2004. PML regulates p53 stability by sequestering Mdm2 to the nucleolus. *Nat Cell Biol*. 6:665-672.

Berx, G., and F. van Roy. 2009. Involvement of members of the cadherin superfamily in cancer. *Cold Spring Harb Perspect Biol*. 1:a003129.

Beyrouthy, M.J., K.M. Garner, M.P. Hever, S.J. Freemantle, A. Eastman, E. Dmitrovsky, and M.J. Spinella. 2009. High DNA methyltransferase 3B expression mediates 5-aza-deoxycytidine hypersensitivity in testicular germ cell tumors. *Cancer Res*. 69:9360-9366.

Bhat, K.P., K.L. Salazar, V. Balasubramaniyan, K. Wani, L. Heathcock, F. Hollingsworth, J.D. James, J. Gumin, K.L. Diefes, S.H. Kim, A. Turski, Y. Azodi, Y. Yang, T. Doucette, H. Colman, E.P. Sulman, F.F. Lang, G. Rao, S. Copray, B.D. Vaillant, and K.D. Aldape. 2011. The transcriptional coactivator TAZ regulates mesenchymal differentiation in malignant glioma. *Genes Dev*. 25:2594-2609.

Bird, A. 2002. DNA methylation patterns and epigenetic memory. *Genes Dev*. 16:6-21.

Bivona, T.G., S.E. Quatela, B.O. Bodemann, I.M. Ahearn, M.J. Soskis, A. Mor, J. Miura, H.H. Wiener, L. Wright, S.G. Saba, D. Yim, A. Fein, I. Perez de Castro, C. Li, C.B. Thompson, A.D. Cox, and M.R. Philips. 2006. PKC regulates a farnesyl-electrostatic switch on K-Ras that promotes its association with Bcl-XL on mitochondria and induces apoptosis. *Molecular cell*. 21:481-493.

Bobrie, A., S. Krumeich, F. Reyal, C. Recchi, L.F. Moita, M.C. Seabra, M. Ostrowski, and C. Thery. 2012. Rab27a supports exosome-dependent and -independent mechanisms that modify the tumor microenvironment and can promote tumor progression. *Cancer Res*. 72:4920-4930.

Boggiano, J.C., P.J. Vanderzalm, and R.G. Fehon. 2011. Tao-1 phosphorylates Hippo/MST kinases to regulate the Hippo-Salvador-Warts tumor suppressor pathway. *Dev. Cell*. 21:888-895.

Boiko, A.D., O.V. Razorenova, M. van de Rijn, S.M. Swetter, D.L. Johnson, D.P. Ly, P.D. Butler, G.P. Yang, B. Joshua, M.J. Kaplan, M.T. Longaker, and I.L. Weissman. 2010. Human melanoma-initiating cells express neural crest nerve growth factor receptor CD271. *Nature*. 466:133-137.

Boise, L.H., M. Gonzalez-Garcia, C.E. Postema, L. Ding, T. Lindsten, L.A. Turka, X. Mao, G. Nunez, and C.B. Thompson. 1993. bcl-x, a bcl-2-related gene that functions as a dominant regulator of apoptotic cell death. *Cell*. 74:597-608.

Bonnet, D., and J.E. Dick. 1997. Human acute myeloid leukemia is organized as a hierarchy that originates from a primitive hematopoietic cell. *Nature medicine*. 3:730-737.

Bonnomet, A., L. Syne, A. Brysse, E. Feyereisen, E.W. Thompson, A. Noel, J.M. Foidart, P. Birembaut, M. Polette, and C. Gilles. 2012. A dynamic in vivo model of epithelial-to-mesenchymal transitions in circulating tumor cells and metastases of breast cancer. *Oncogene*. 31:3741-3753.

Bourillot, P.Y., I. Aksoy, V. Schreiber, F. Wianny, H. Schulz, O. Hummel, N. Hubner, and P. Savatier. 2009. Novel STAT3 target genes exert distinct roles in the inhibition of mesoderm and endoderm differentiation in cooperation with Nanog. *Stem Cells*. 27:1760-1771.

Bowers, K., J. Lottridge, S.B. Helliwell, L.M. Goldthwaite, J.P. Luzio, and T.H. Stevens. 2004. Protein-protein interactions of ESCRT complexes in the yeast Saccharomyces cerevisiae. *Traffic*. 5:194-210.

Boyer, B., and J.P. Thiery. 1993. Epithelium-mesenchyme interconversion as example of epithelial plasticity. *Apmis*. 101:257-268.

Boyer, B., G.C. Tucker, A.M. Valles, J. Gavrilovic, and J.P. Thiery. 1989. Reversible transition towards a fibroblastic phenotype in a rat carcinoma cell line. *Int J Cancer Suppl*. 4:69-75.

Braga, V.M., L.M. Machesky, A. Hall, and N.A. Hotchin. 1997. The small GTPases Rho and Rac are required for the establishment of cadherin-dependent cell-cell contacts. *J Cell Biol*. 137:1421-1431.

Brahmbhatt, A.A., and R.L. Klemke. 2003. ERK and RhoA differentially regulate pseudopodia growth and retraction during chemotaxis. *J Biol Chem*. 278:13016-13025.

Brugnera, E., L. Haney, C. Grimsley, M. Lu, S.F. Walk, A.C. Tosello-Trampont, I.G. Macara, H. Madhani, G.R. Fink, and K.S. Ravichandran. 2002. Unconventional Rac-GEF activity is mediated through the Dock180-ELMO complex. *Nature cell biology*. 4:574-582.

Brunton, V.G., I.R. MacPherson, and M.C. Frame. 2004. Cell adhesion receptors, tyrosine kinases and actin modulators: a complex three-way circuitry. *Biochim Biophys Acta*. 1692:121-144.

Bryant, D.M., M.C. Kerr, L.A. Hammond, S.R. Joseph, K.E. Mostov, R.D. Teasdale, and J.L. Stow. 2007. EGF induces macropinocytosis and SNX1-modulated recycling of E-cadherin. *J Cell Sci*. 120:1818-1828.

Bucci, C., R.G. Parton, I.H. Mather, H. Stunnenberg, K. Simons, B. Hoflack, and M. Zerial. 1992. The small GTPase rab5 functions as a regulatory factor in the early endocytic pathway. *Cell*. 70:715-728.

Buckingham, L., L. Penfield Faber, A. Kim, M. Liptay, C. Barger, S. Basu, M. Fidler, K. Walters, P. Bonomi, and J. Coon. 2010. PTEN, RASSF1 and DAPK site-specific hypermethylation and outcome in surgically treated stage I and II nonsmall cell lung cancer patients. *Int J Cancer*. 126:1630-1639.

Burbee, D.G., E. Forgacs, S. Zochbauer-Muller, L. Shivakumar, K. Fong, B. Gao, D. Randle, M. Kondo, A. Virmani, S. Bader, Y. Sekido, F. Latif, S. Milchgrub, S. Toyooka, A.F. Gazdar, M.I. Lerman, E. Zabarovsky, M. White, and J.D. Minna. 2001. Epigenetic inactivation of RASSF1A in lung and breast cancers and malignant phenotype suppression. *J Natl Cancer Inst*. 93:691-699.

Cai, H., K. Reinisch, and S. Ferro-Novick. 2007. Coats, tethers, Rabs, and SNAREs work together to mediate the intracellular destination of a transport vesicle. *Dev Cell*. 12:671-682.

Cai, J., A. Maitra, R.A. Anders, M.M. Taketo, and D. Pan. 2015. beta-Catenin destruction complex-independent regulation of Hippo-YAP signaling by APC in intestinal tumorigenesis. *Genes Dev*. 29:1493-1506.

Callus, B.A., A.M. Verhagen, and D.L. Vaux. 2006. Association of mammalian sterile twenty kinases, Mst1 and Mst2, with hSalvador via C-terminal coiled-coil domains, leads to its stabilization and phosphorylation. *FEBS J.* 273:4264-4276.

Calvo, F., N. Ege, A. Grande-Garcia, S. Hooper, R.P. Jenkins, S.I. Chaudhry, K. Harrington, P. Williamson, E. Moeendarbary, G. Charras, and E. Sahai. 2013. Mechanotransduction and YAP-dependent matrix remodelling is required for the generation and maintenance of cancer-associated fibroblasts. *Nat Cell Biol*. 15:637-646.

Canel, M., A. Serrels, D. Miller, P. Timpson, B. Serrels, M.C. Frame, and V.G. Brunton. 2010. Quantitative in vivo imaging of the effects of inhibiting integrin signaling via Src and FAK on cancer cell movement: effects on E-cadherin dynamics. *Cancer Res*. 70:9413-9422.

Cano, A., M.A. Perez-Moreno, I. Rodrigo, A. Locascio, M.J. Blanco, M.G. del Barrio, F. Portillo, and M.A. Nieto. 2000. The transcription factor snail controls epithelial-mesenchymal transitions by repressing E-cadherin expression. *Nat Cell Biol*. 2:76-83.

Cantley, L.C. 2002. The phosphoinositide 3-kinase pathway. *Science*. 296:1655-1657.

Carlton, J., M. Bujny, A. Rutherford, and P. Cullen. 2005. Sorting nexins--unifying trends and new perspectives. *Traffic*. 6:75-82.

Carpentino, J.E., M.J. Hynes, H.D. Appelman, T. Zheng, D.A. Steindler, E.W. Scott, and E.H. Huang. 2009. Aldehyde dehydrogenase-expressing colon stem cells contribute to tumorigenesis in the transition from colitis to cancer. *Cancer Res*. 69:8208-8215.

`

Carragher, N.O., S.M. Walker, L.A. Scott Carragher, F. Harris, T.K. Sawyer, V.G. Brunton, B.W. Ozanne, and M.C. Frame. 2006. Calpain 2 and Src dependence distinguishes mesenchymal and amoeboid modes of tumour cell invasion: a link to integrin function. *Oncogene*. 25:5726-5740.

Cartwright, C.A., W. Eckhart, S. Simon, and P.L. Kaplan. 1987. Cell transformation by pp60c-src mutated in the carboxy-terminal regulatory domain. *Cell*. 49:83-91.

Cartwright, C.A., M.P. Kamps, A.I. Meisler, J.M. Pipas, and W. Eckhart. 1989. pp60c-src activation in human colon carcinoma. *J Clin Invest*. 83:2025-2033.

Cartwright, C.A., A.I. Meisler, and W. Eckhart. 1990. Activation of the pp60c-src protein kinase is an early event in colonic carcinogenesis. *Proc Natl Acad Sci U S A*. 87:558-562.

Catto, J.W., A.R. Azzouzi, I. Rehman, K.M. Feeley, S.S. Cross, N. Amira, G. Fromont, M. Sibony, O. Cussenot, M. Meuth, and F.C. Hamdy. 2005. Promoter hypermethylation is associated with tumor location, stage, and subsequent progression in transitional cell carcinoma. *J Clin Oncol*. 23:2903-2910.

Cavey, M., M. Rauzi, P.F. Lenne, and T. Lecuit. 2008. A two-tiered mechanism for stabilization and immobilization of E-cadherin. *Nature*. 453:751-756.

Ceppi, P., M. Papotti, V. Monica, M. Lo Iacono, S. Saviozzi, M. Pautasso, S. Novello, S. Mussino, E. Bracco, M. Volante, and G.V. Scagliotti. 2009. Effects of Src kinase inhibition induced by dasatinib in non-small cell lung cancer cell lines treated with cisplatin. *Mol Cancer Ther*. 8:3066-3074.

Ceresa, B.P. 2006. Regulation of EGFR endocytic trafficking by rab proteins. *Histol Histopathol*. 21:987-993.

Chaffer, C.L., N.D. Marjanovic, T. Lee, G. Bell, C.G. Kleer, F. Reinhardt, A.C. D'Alessio, R.A. Young, and R.A. Weinberg. 2013. Poised chromatin at the ZEB1 promoter enables breast cancer cell plasticity and enhances tumorigenicity. *Cell*. 154:61-74.

Chairoungdua, A., D.L. Smith, P. Pochard, M. Hull, and M.J. Caplan. 2010. Exosome release of beta-catenin: a novel mechanism that antagonizes Wnt signaling. *J Cell Biol*. 190:1079-1091.

Chalmin, F., S. Ladoire, G. Mignot, J. Vincent, M. Bruchard, J.P. Remy-Martin, W. Boireau, A. Rouleau, B. Simon, D. Lanneau, A. De Thonel, G. Multhoff, A. Hamman, F. Martin, B. Chauffert, E. Solary, L. Zitvogel, C. Garrido, B. Ryffel, C. Borg, L. Apetoh, C. Rebe, and F. Ghiringhelli. 2010. Membrane-associated Hsp72 from tumor-derived exosomes mediates STAT3-dependent immunosuppressive function of mouse and human myeloid-derived suppressor cells. *J Clin Invest*. 120:457-471.

Chan, D., J.W. Tyner, W.J. Chng, C. Bi, R. Okamoto, J. Said, B.D. Ngan, G.D. Braunstein, and H.P. Koeffler. 2012. Effect of dasatinib against thyroid cancer cell lines in vitro and a xenograft model in vivo. *Oncol Lett*. 3:807-815.

Chan, E.H. 2005. The Ste20-like kinase Mst2 activates the human large tumor suppressor kinase Lats1. *Oncogene*. 24:2076-2086.

Chan, K., P. Lai, T. Mok, H.L. Chan, C. Ding, S.W. Yeung, and Y.M. Lo. 2008a. Quantitative analysis of circulating methylated DNA as a biomarker for hepatocellular carcinoma. *Clin Chem*. 54:1528-1536.

Chan, S.W. 2011. Hippo pathway-independent restriction of TAZ and YAP by angiomotin. *J. Biol. Chem.* 286:7018-7026.

Chan, S.W., C.J. Lim, K. Guo, C.P. Ng, I. Lee, W. Hunziker, Q. Zeng, and W. Hong. 2008b. A role for TAZ in migration, invasion, and tumorigenesis of breast cancer cells. *Cancer Res*. 68:2592-2598.

Chao, C., S. Saito, C.W. Anderson, E. Appella, and Y. Xu. 2000. Phosphorylation of murine p53 at ser-18 regulates the p53 responses to DNA damage. *Proc Natl Acad Sci U S A*. 97:11936-11941.

Chao, M.P., A.A. Alizadeh, C. Tang, M. Jan, R. Weissman-Tsukamoto, F. Zhao, C.Y. Park, I.L. Weissman, and R. Majeti. 2011. Therapeutic antibody targeting of CD47 eliminates human acute lymphoblastic leukemia. *Cancer Res*. 71:1374-1384.

Charrin, S., F. le Naour, O. Silvie, P.E. Milhiet, C. Boucheix, and E. Rubinstein. 2009. Lateral organization of membrane proteins: tetraspanins spin their web. *Biochem J*. 420:133-154.

`

Chen, C.L. 2010. The apical-basal cell polarity determinant Crumbs regulates Hippo signaling in Drosophila. *Proc. Natl Acad. Sci. USA*. 107:15810-15815.

Chen, C.L., M.C. Schroeder, M. Kango-Singh, C. Tao, and G. Halder. 2012a. Tumor suppression by cell competition through regulation of the Hippo pathway. *Proc. Natl Acad. Sci. USA*. 109:484-489.

Chen, D., Y. Sun, Y. Wei, P. Zhang, A.H. Rezaeian, J. Teruya-Feldstein, S. Gupta, H. Liang, H.K. Lin, M.C. Hung, and L. Ma. 2012b. LIFR is a breast cancer metastasis suppressor upstream of the Hippo-YAP pathway and a prognostic marker. *Nature medicine*. 18:1511-1517.

Chen, T.S., F. Arslan, Y. Yin, S.S. Tan, R.C. Lai, A.B. Choo, J. Padmanabhan, C.N. Lee, D.P. de Kleijn, and S.K. Lim. 2011. Enabling a robust scalable manufacturing process for therapeutic exosomes through oncogenic immortalization of human ESC-derived MSCs. *J Transl Med*. 9:47.

Chin, L., A. Tam, J. Pomerantz, M. Wong, J. Holash, N. Bardeesy, Q. Shen, R. O'Hagan, J. Pantginis, H. Zhou, J.W. Horner, 2nd, C. Cordon-Cardo, G.D. Yancopoulos, and R.A. DePinho. 1999. Essential role for oncogenic Ras in tumour maintenance. *Nature*. 400:468-472.

Chiou, S.H., C.C. Yu, C.Y. Huang, S.C. Lin, C.J. Liu, T.H. Tsai, S.H. Chou, C.S. Chien, H.H. Ku, and J.F. Lo. 2008. Positive correlations of Oct-4 and Nanog in oral cancer stem-like cells and high-grade oral squamous cell carcinoma. *Clin Cancer Res*. 14:4085-4095.

Cho, J.A., H. Park, E.H. Lim, and K.W. Lee. 2012. Exosomes from breast cancer cells can convert adipose tissue-derived mesenchymal stem cells into myofibroblast-like cells. *Int J Oncol*. 40:130-138.

Choi, D.S., D.K. Kim, Y.K. Kim, and Y.S. Gho. 2013. Proteomics, transcriptomics and lipidomics of exosomes and ectosomes. *Proteomics*. 13:1554-1571.

Chow, C., N. Wong, M. Pagano, S.W. Lun, K.I. Nakayama, K. Nakayama, and K.W. Lo. 2012. Regulation of APC/CCdc20 activity by RASSF1A-APC/CCdc20 circuitry. *Oncogene*. 31:1975-1987.

Chuang, J.C., and P.A. Jones. 2007. Epigenetics and microRNAs. *Pediatric research*. 61:24R-29R.

Cinar, B., P.K. Fang, M. Lutchman, D. Di Vizio, R.M. Adam, N. Pavlova, M.A. Rubin, P.C. Yelick, and M.R. Freeman. 2007. The pro-apoptotic kinase Mst1 and its caspase cleavage products are direct inhibitors of Akt1. *Embo J*. 26:4523-4534.

Cleton-Jansen, A.M., D.F. Callen, R. Seshadri, S. Goldup, B. McCallum, J. Crawford, J.A. Powell, C. Settasatian, H. van Beerendonk, E.W. Moerland, V.T. Smit, W.H. Harris, R. Millis, N.V. Morgan, D. Barnes, C.G. Mathew, and C.J. Cornelisse. 2001. Loss of heterozygosity mapping at chromosome arm 16q in 712 breast tumors reveals factors that influence delineation of candidate regions. *Cancer Res*. 61:1171-1177.

Collins, A.T., P.A. Berry, C. Hyde, M.J. Stower, and N.J. Maitland. 2005. Prospective identification of tumorigenic prostate cancer stem cells. *Cancer Res*. 65:10946-10951.

Colombani, J., C. Polesello, F. Josue, and N. Tapon. 2006. Dmp53 activates the Hippo pathway to promote cell death in response to DNA damage. *Curr Biol*. 16:1453-1458.

Colombo, M., C. Moita, G. van Niel, J. Kowal, J. Vigneron, P. Benaroch, N. Manel, L.F. Moita, C. Thery, and G. Raposo. 2013. Analysis of ESCRT functions in exosome biogenesis, composition and secretion highlights the heterogeneity of extracellular vesicles. *J Cell Sci*. 126:5553-5565.

Colombo, M., G. Raposo, and C. Thery. 2014. Biogenesis, secretion, and intercellular interactions of exosomes and other extracellular vesicles. *Annu Rev Cell Dev Biol*. 30:255-289.

Coluccia, A.M., D. Benati, H. Dekhil, A. De Filippo, C. Lan, and C. Gambacorti-Passerini. 2006. SKI-606 decreases growth and motility of colorectal cancer cells by preventing pp60(c-Src)-dependent tyrosine phosphorylation of beta-catenin and its nuclear signaling. *Cancer Res*. 66:2279-2286.

Corcoran, C., S. Rani, K. O'Brien, A. O'Neill, M. Prencipe, R. Sheikh, G. Webb, R. McDermott, W. Watson, J. Crown, and L. O'Driscoll. 2012. Docetaxel-resistance in prostate cancer: evaluating associated phenotypic changes and potential for resistance transfer via exosomes. *PLoS One*. 7:e50999.

Cordenonsi, M., F. Zanconato, L. Azzolin, M. Forcato, A. Rosato, C. Frasson, M. Inui, M. Montagner, A.R. Parenti, A. Poletti, M.G. Daidone, S. Dupont, G. Basso, S. Bicciato, and S. Piccolo. 2011. The Hippo transducer TAZ confers cancer stem cell-related traits on breast cancer cells. *Cell*. 147:759-772.

`

Costa-Silva, B., N.M. Aiello, A.J. Ocean, S. Singh, H. Zhang, B.K. Thakur, A. Becker, A. Hoshino, M.T. Mark, H. Molina, J. Xiang, T. Zhang, T.M. Theilen, G. Garcia-Santos, C. Williams, Y. Ararso, Y. Huang, G. Rodrigues, T.L. Shen, K.J. Labori, I.M. Lothe, E.H. Kure, J. Hernandez, A. Doussot, S.H. Ebbesen, P.M. Grandgenett, M.A. Hollingsworth, M. Jain, K. Mallya, S.K. Batra, W.R. Jarnagin, R.E. Schwartz, I. Matei, H. Peinado, B.Z. Stanger, J. Bromberg, and D. Lyden. 2015. Pancreatic cancer exosomes initiate pre-metastatic niche formation in the liver. *Nat Cell Biol*. 17:816-826.

Coulombe, P.A., and P. Wong. 2004. Cytoplasmic intermediate filaments revealed as dynamic and multipurpose scaffolds. *Nat Cell Biol*. 6:699-706.

Courtneidge, S.A., A.D. Levinson, and J.M. Bishop. 1980. The protein encoded by the transforming gene of avian sarcoma virus (pp60src) and a homologous protein in normal cells (pp60proto-src) are associated with the plasma membrane. *Proc Natl Acad Sci U S A*. 77:3783-3787.

Cox, A.D., and C.J. Der. 2003. The dark side of Ras: regulation of apoptosis. *Oncogene*. 22:8999-9006.

Cufi, S., A. Vazquez-Martin, C. Oliveras-Ferraros, B. Martin-Castillo, L. Vellon, and J.A. Menendez. 2011. Autophagy positively regulates the CD44(+) CD24(-/low) breast cancer stem-like phenotype. *Cell Cycle*. 10:3871-3885.

da Costa Prando, E., L.R. Cavalli, and C.A. Rainho. 2011. Evidence of epigenetic regulation of the tumor suppressor gene cluster flanking RASSF1 in breast cancer cell lines. *Epigenetics*. 6:1413-1424.

Dai, S., X. Zhou, B. Wang, Q. Wang, Y. Fu, T. Chen, T. Wan, Y. Yu, and X. Cao. 2006. Enhanced induction of dendritic cell maturation and HLA-A*0201-restricted CEA-specific CD8(+) CTL response by exosomes derived from IL-18 gene-modified CEA-positive tumor cells. *J Mol Med (Berl)*. 84:1067-1076.

Dalerba, P., S.J. Dylla, I.K. Park, R. Liu, X. Wang, R.W. Cho, T. Hoey, A. Gurney, E.H. Huang, D.M. Simeone, A.A. Shelton, G. Parmiani, C. Castelli, and M.F. Clarke. 2007. Phenotypic characterization of human colorectal cancer stem cells. *Proc Natl Acad Sci U S A*. 104:10158-10163.

Dallol, A., A. Agathanggelou, S.L. Fenton, J. Ahmed-Choudhury, L. Hesson, M.D. Vos, G.J. Clark, J. Downward, E.R. Maher, and F. Latif. 2004. RASSF1A interacts with microtubule-associated proteins and modulates microtubule dynamics. *Cancer Res*. 64:4112-4116.

Dallol, A., A. Agathanggelou, S. Tommasi, G.P. Pfeifer, E.R. Maher, and F. Latif. 2005. Involvement of the RASSF1A tumor suppressor gene in controlling cell migration. *Cancer Res*. 65:7653-7659.

Dallol, A., L.B. Hesson, D. Matallanas, W.N. Cooper, E. O'Neill, E.R. Maher, W. Kolch, and F. Latif. 2009. RAN GTPase is a RASSF1A effector involved in controlling microtubule organization. *Curr Biol*. 19:1227-1232.

Dammann, R., C. Li, J.H. Yoon, P.L. Chin, S. Bates, and G.P. Pfeifer. 2000. Epigenetic inactivation of a RAS association domain family protein from the lung tumour suppressor locus 3p21.3. *Nature genetics*. 25:315-319.

Dammann, R., U. Schagdarsurengin, C. Seidel, M. Strunnikova, M. Rastetter, K. Baier, and G.P. Pfeifer. 2005. The tumor suppressor RASSF1A in human carcinogenesis: an update. *Histol Histopathol*. 20:645-663.

Daniel, J.M., and A.B. Reynolds. 1997. Tyrosine phosphorylation and cadherin/catenin function. *Bioessays*. 19:883-891.

Danielsen, S.A., G.E. Lind, M. Kolberg, M. Holand, B. Bjerkehagen, K. Sundby Hall, E. van den Berg, F. Mertens, S. Smeland, P. Picci, and R.A. Lothe. 2014. Methylated RASSF1A in malignant peripheral nerve sheath tumors identifies neurofibromatosis type 1 patients with inferior prognosis. *Neuro Oncol*. 17:63-69.

Das Thakur, M. 2010. Ajuba LIM proteins are negative regulators of the Hippo signaling pathway. *Curr. Biol.* 20:657-662.

Datta, A., F. Huber, and D. Boettiger. 2002. Phosphorylation of beta3 integrin controls ligand binding strength. *J Biol Chem*. 277:3943-3949.

Davis, R.J. 2000. Signal transduction by the JNK group of MAP kinases. *Cell*. 103:239-252.

de Beco, S., C. Gueudry, F. Amblard, and S. Coscoy. 2009. Endocytosis is required for E-cadherin redistribution at mature adherens junctions. *Proc Natl Acad Sci U S A*. 106:7010-7015.

de Jong, O.G., M.C. Verhaar, Y. Chen, P. Vader, H. Gremmels, G. Posthuma, R.M. Schiffelers, M. Gucek, and B.W. van Balkom. 2012. Cellular stress conditions are reflected in the protein and RNA content of endothelial cell-derived exosomes. *J Extracell Vesicles*. 1.

De Roock, W., V. De Vriendt, N. Normanno, F. Ciardiello, and S. Tejpar. 2011. KRAS, BRAF, PIK3CA, and PTEN mutations: implications for targeted therapies in metastatic colorectal cancer. *Lancet Oncol*. 12:594-603.

DeFeo, D., M.A. Gonda, H.A. Young, E.H. Chang, D.R. Lowy, E.M. Scolnick, and R.W. Ellis. 1981. Analysis of two divergent rat genomic clones homologous to the transforming gene of Harvey murine sarcoma virus. *Proc Natl Acad Sci U S A*. 78:3328-3332.

Demory Beckler, M., J.N. Higginbotham, J.L. Franklin, A.J. Ham, P.J. Halvey, I.E. Imasuen, C. Whitwell, M. Li, D.C. Liebler, and R.J. Coffey. 2013. Proteomic analysis of exosomes from mutant KRAS colon cancer cells identifies intercellular transfer of mutant KRAS. *Mol Cell Proteomics*. 12:343-355.

den Elzen, N., and J. Pines. 2001. Cyclin A is destroyed in prometaphase and can delay chromosome alignment and anaphase. *J Cell Biol*. 153:121-136.

Derijard, B., M. Hibi, I.H. Wu, T. Barrett, B. Su, T. Deng, M. Karin, and R.J. Davis. 1994. JNK1: a protein kinase stimulated by UV light and Ha-Ras that binds and phosphorylates the c-Jun activation domain. *Cell*. 76:1025-1037.

Diehn, M., R.W. Cho, N.A. Lobo, T. Kalisky, M.J. Dorie, A.N. Kulp, D. Qian, J.S. Lam, L.E. Ailles, M. Wong, B. Joshua, M.J. Kaplan, I. Wapnir, F.M. Dirbas, G. Somlo, C. Garberoglio, B. Paz, J. Shen, S.K. Lau, S.R. Quake, J.M. Brown, I.L. Weissman, and M.F. Clarke. 2009. Association of reactive oxygen species levels and radioresistance in cancer stem cells. *Nature*. 458:780-783.

Dieter, S.M., C.R. Ball, C.M. Hoffmann, A. Nowrouzi, F. Herbst, O. Zavidij, U. Abel, A. Arens, W. Weichert, K. Brand, M. Koch, J. Weitz, M. Schmidt, C. von Kalle, and H. Glimm. 2011. Distinct types of tumor-initiating cells form human colon cancer tumors and metastases. *Cell Stem Cell*. 9:357-365.

Dobbelstein, M., S. Strano, J. Roth, and G. Blandino. 2005. p73-induced apoptosis: a question of compartments and cooperation. *Biochem Biophys Res Commun*. 331:688-693.

Dong, J., G. Feldmann, J. Huang, S. Wu, N. Zhang, S.A. Comerford, M.F. Gayyed, R.A. Anders, A. Maitra, and D. Pan. 2007. Elucidation of a universal size-control mechanism in Drosophila and mammals. *Cell*. 130:1120-1133.

Donninger, H., N. Allen, A. Henson, J. Pogue, A. Williams, L. Gordon, S. Kassler, T. Dunwell, F. Latif, and G.J. Clark. 2011. Salvador protein is a tumor suppressor effector of RASSF1A with hippo pathway-independent functions. *J Biol Chem*. 286:18483-18491.

Donninger, H., M.D. Vos, and G.J. Clark. 2007. The RASSF1A tumor suppressor. *J Cell Sci*. 120:3163-3172.

Dote, H., D. Cerna, W.E. Burgan, D.J. Carter, M.A. Cerra, M.G. Hollingshead, K. Camphausen, and P.J. Tofilon. 2005. Enhancement of in vitro and in vivo tumor cell radiosensitivity by the DNA methylation inhibitor zebularine. *Clin Cancer Res*. 11:4571-4579.

Downward, J. 2003. Targeting RAS signalling pathways in cancer therapy. *Nat Rev Cancer*. 3:11-22.

Dragovic, R.A., C. Gardiner, A.S. Brooks, D.S. Tannetta, D.J. Ferguson, P. Hole, B. Carr, C.W. Redman, A.L. Harris, P.J. Dobson, P. Harrison, and I.L. Sargent. 2011. Sizing and phenotyping of cellular vesicles using Nanoparticle Tracking Analysis. *Nanomedicine*. 7:780-788.

Dreijerink, K., E. Braga, I. Kuzmin, L. Geil, F.M. Duh, D. Angeloni, B. Zbar, M.I. Lerman, E.J. Stanbridge, J.D. Minna, A. Protopopov, J. Li, V. Kashuba, G. Klein, and E.R. Zabarovsky. 2001. The candidate tumor suppressor gene, RASSF1A, from human chromosome 3p21.3 is involved in kidney tumorigenesis. *Proc Natl Acad Sci U S A*. 98:7504-7509.

Dupont, S., L. Morsut, M. Aragona, E. Enzo, S. Giulitti, M. Cordenonsi, F. Zanconato, J. Le Digabel, M. Forcato, S. Bicciato, N. Elvassore, and S. Piccolo. 2011. Role of YAP/TAZ in mechanotransduction. *Nature*. 474:179-183.

Durocher, D., and S.P. Jackson. 2001. DNA-PK, ATM and ATR as sensors of DNA damage: variations on a theme? *Curr Opin Cell Biol*. 13:225-231.

Edelman, G.M., W.J. Gallin, A. Delouvee, B.A. Cunningham, and J.P. Thiery. 1983. Early epochal maps of two different cell adhesion molecules. *Proc Natl Acad Sci U S A*. 80:4384-4388.

Eden, A., F. Gaudet, A. Waghmare, and R. Jaenisch. 2003. Chromosomal instability and tumors promoted by DNA hypomethylation. *Science*. 300:455.

Eger, A., A. Stockinger, B. Schaffhauser, H. Beug, and R. Foisner. 2000. Epithelial mesenchymal transition by c-Fos estrogen receptor activation involves nuclear translocation of beta-catenin and upregulation of beta-catenin/lymphoid enhancer binding factor-1 transcriptional activity. *J Cell Biol*. 148:173-188.

Ellis, S., and H. Mellor. 2000. Regulation of endocytic traffic by rho family GTPases. *Trends Cell Biol*. 10:85-88.

Elmore, S. 2007. Apoptosis: a review of programmed cell death. *Toxicol Pathol*. 35:495-516.

Endoh, H., Y. Yatabe, S. Shimizu, K. Tajima, H. Kuwano, T. Takahashi, and T. Mitsudomi. 2003. RASSF1A gene inactivation in non-small cell lung cancer and its clinical implication. *Int J Cancer*. 106:45-51.

Eramo, A., F. Lotti, G. Sette, E. Pilozzi, M. Biffoni, A. Di Virgilio, C. Conticello, L. Ruco, C. Peschle, and R. De Maria. 2008. Identification and expansion of the tumorigenic lung cancer stem cell population. *Cell Death Differ*. 15:504-514.

Escobar-Cabrera, E., D.K. Lau, S. Giovinazzi, A.M. Ishov, and L.P. McIntosh. 2010. Structural characterization of the DAXX N-terminal helical bundle domain and its complex with Rassf1C. *Structure*. 18:1642-1653.

Esteller, M. 2007. Cancer epigenomics: DNA methylomes and histone-modification maps. *Nat Rev Genet*. 8:286-298.

Estrabaud, E., I. Lassot, G. Blot, E. Le Rouzic, V. Tanchou, E. Quemeneur, L. Daviet, F. Margottin-Goguet, and R. Benarous. 2007. RASSF1C, an isoform of the tumor suppressor RASSF1A, promotes the accumulation of beta-catenin by interacting with betaTrCP. *Cancer Res*. 67:1054-1061.

Fader, C.M., D.G. Sanchez, M.B. Mestre, and M.I. Colombo. 2009. TI-VAMP/VAMP7 and VAMP3/cellubrevin: two v-SNARE proteins involved in specific steps of the autophagy/multivesicular body pathways. *Biochim Biophys Acta*. 1793:1901-1916.

Fan, W., X. Huang, C. Chen, J. Gray, and T. Huang. 2004. TBX3 and its isoform TBX3+2a are functionally distinctive in inhibition of senescence and are overexpressed in a subset of breast cancer cell lines. *Cancer Res*. 64:5132-5139.

Fang, G., H. Yu, and M.W. Kirschner. 1998. The checkpoint protein MAD2 and the mitotic regulator CDC20 form a ternary complex with the anaphase-promoting complex to control anaphase initiation. *Genes Dev*. 12:1871-1883.

Fausti, F., S. Di Agostino, M. Cioce, P. Bielli, C. Sette, P.P. Pandolfi, M. Oren, M. Sudol, S. Strano, and G. Blandino. 2013. ATM kinase enables the functional axis of YAP, PML and p53 to ameliorate loss of Werner protein-mediated oncogenic senescence. *Cell Death Differ*. 20:1498-1509.

Felthaus, O., T. Ettl, M. Gosau, O. Driemel, G. Brockhoff, A. Reck, K. Zeitler, M. Hautmann, T.E. Reichert, G. Schmalz, and C. Morsczeck. 2011. Cancer stem cell-like cells from a single cell of oral squamous carcinoma cell lines. *Biochem Biophys Res Commun*. 407:28-33.

Fendri, A., A. Masmoudi, A. Khabir, T. Sellami-Boudawara, J. Daoud, M. Frikha, A. Ghorbel, A. Gargouri, and R. Mokdad-Gargouri. 2009. Inactivation of RASSF1A, RAR[beta]2 and DAP-kinase by promoter methylation cosrrelates with lymph node metastasis in nasopharyngeal carcinoma. *Cancer Biol*. 8:444-451.

Feng, D., W.L. Zhao, Y.Y. Ye, X.C. Bai, R.Q. Liu, L.F. Chang, Q. Zhou, and S.F. Sui. 2010. Cellular internalization of exosomes occurs through phagocytosis. *Traffic*. 11:675-687.

Fernandes, M.S., F. Carneiro, C. Oliveira, and R. Seruca. 2012. Colorectal cancer and RASSF family-A special emphasis on RASSF1A. *Int J Cancer*.

`

Fernandez, B.G. 2011. Actin-capping protein and the Hippo pathway regulate F-actin and tissue growth in Drosophila. *Development*. 138:2337-2346.

Fernandez, L.A., P.A. Northcott, J. Dalton, C. Fraga, D. Ellison, S. Angers, M.D. Taylor, and A.M. Kenney. 2009. YAP1 is amplified and up-regulated in hedgehog-associated medulloblastomas and mediates Sonic hedgehog-driven neural precursor proliferation. *Genes Dev*. 23:2729-2741.

Fernandez, Y., B. Gu, A. Martinez, A. Torregrosa, and A. Sierra. 2002. Inhibition of apoptosis in human breast cancer cells: role in tumor progression to the metastatic state. *Int J Cancer*. 101:317-326.

Fidler, I.J. 2003. The pathogenesis of cancer metastasis: the 'seed and soil' hypothesis revisited. *Nat Rev Cancer*. 3:453-458.

Foley, C.J., H. Freedman, S.L. Choo, C. Onyskiw, N.Y. Fu, V.C. Yu, J. Tuszynski, J.C. Pratt, and S. Baksh. 2008. Dynamics of RASSF1A/MOAP-1 association with death receptors. *Mol Cell Biol*. 28:4520-4535.

Franco, M., P.J. Peters, J. Boretto, E. van Donselaar, A. Neri, C. D'Souza-Schorey, and P. Chavrier. 1999. EFA6, a sec7 domain-containing exchange factor for ARF6, coordinates membrane recycling and actin cytoskeleton organization. *Embo J*. 18:1480-1491.

Freed-Pastor, W.A., and C. Prives. 2012. Mutant p53: one name, many proteins. *Genes Dev*. 26:1268-1286.

Friedl, P., Y. Hegerfeldt, and M. Tusch. 2004. Collective cell migration in morphogenesis and cancer. *Int J Dev Biol*. 48:441-449.

Frisch, S.M. 2008. Caspase-8: fly or die. *Cancer Res*. 68:4491-4493.

Fristrom, D. 1988. The cellular basis of epithelial morphogenesis. A review. *Tissue Cell*. 20:645-690.

Frixen, U.H., J. Behrens, M. Sachs, G. Eberle, B. Voss, A. Warda, D. Lochner, and W. Birchmeier. 1991. E-cadherin-mediated cell-cell adhesion prevents invasiveness of human carcinoma cells. *J Cell Biol*. 113:173-185.

Fruhbeis, C., D. Frohlich, W.P. Kuo, J. Amphornrat, S. Thilemann, A.S. Saab, F. Kirchhoff, W. Mobius, S. Goebbels, K.A. Nave, A. Schneider, M. Simons, M. Klugmann, J. Trotter, and E.M. Kramer-Albers. 2013. Neurotransmitter-triggered transfer of exosomes mediates oligodendrocyte-neuron communication. *PLoS Biol*. 11:e1001604.

Fujita, Y., G. Krause, M. Scheffner, D. Zechner, H.E. Leddy, J. Behrens, T. Sommer, and W. Birchmeier. 2002. Hakai, a c-Cbl-like protein, ubiquitinates and induces endocytosis of the E-cadherin complex. *Nat Cell Biol*. 4:222-231.

Fukui, H., K. Terai, H. Nakajima, A. Chiba, S. Fukuhara, and N. Mochizuki. 2014. S1P-Yap1 Signaling Regulates Endoderm Formation Required for Cardiac Precursor Cell Migration in Zebrafish. *Dev Cell*. 31:128-136.

Gallo, A., M. Tandon, I. Alevizos, and G.G. Illei. 2012. The majority of microRNAs detectable in serum and saliva is concentrated in exosomes. *PLoS One*. 7:e30679.

Gao, B., X. Xie, C. Huang, D. Shames, T. Chen, C. Lewis, A. Bian, B. Zhang, O. Olopade, J. Garber, D. Euhus, G. Tomlinson, and J. Minna. 2008. RASSF1A polymorphism A133S is associated with early onset breast cancer in BRCA1/2 mutation carriers. *Cancer Res*. 68:22-25.

Gao, T., S. Wang, B. He, Y. Pan, G. Song, L. Gu, L. Chen, Z. Nie, Y. Xu, and R. Li. 2012. The association of RAS association domain family Protein1A (RASSF1A) methylation states and bladder cancer risk: a systematic review and meta-analysis. *PLoS One*. 7:e48300.

Garcia-Manero, G., H.M. Kantarjian, B. Sanchez-Gonzalez, H. Yang, G. Rosner, S. Verstovsek, M. Rytting, W.G. Wierda, F. Ravandi, C. Koller, L. Xiao, S. Faderl, Z. Estrov, J. Cortes, S. O'Brien, E. Estey, C. Bueso-Ramos, J. Fiorentino, E. Jabbour, and J.P. Issa. 2006. Phase 1/2 study of the combination of 5-aza-2'-deoxycytidine with valproic acid in patients with leukemia. *Blood*. 108:3271-3279.

Garnier, D., N. Jabado, and J. Rak. 2013. Extracellular vesicles as prospective carriers of oncogenic protein signatures in adult and paediatric brain tumours. *Proteomics*. 13:1595-1607.

`

Garnier, D., N. Magnus, T.H. Lee, V. Bentley, B. Meehan, C. Milsom, L. Montermini, T. Kislinger, and J. Rak. 2012. Cancer cells induced to express mesenchymal phenotype release exosome-like extracellular vesicles carrying tissue factor. *J Biol Chem*. 287:43565-43572.

Gasman, S., S. Chasserot-Golaz, M.F. Bader, and N. Vitale. 2003a. Regulation of exocytosis in adrenal chromaffin cells: focus on ARF and Rho GTPases. *Cell Signal*. 15:893-899.

Gasman, S., Y. Kalaidzidis, and M. Zerial. 2003b. RhoD regulates endosome dynamics through Diaphanous-related Formin and Src tyrosine kinase. *Nat Cell Biol*. 5:195-204.

Ge, Y.Z., L.W. Xu, R.P. Jia, Z. Xu, Y.M. Feng, R. Wu, P. Yu, Y. Zhao, Z.L. Gui, S.J. Tan, and Q. Song. 2014. The association between RASSF1A promoter methylation and prostate cancer: evidence from 19 published studies. *Tumour Biol*. 35:3881-3890.

Gearing, D.P. 1993. The leukemia inhibitory factor and its receptor. *Adv Immunol*. 53:31-58.

Geley, S., E. Kramer, C. Gieffers, J. Gannon, J.M. Peters, and T. Hunt. 2001. Anaphase-promoting complex/cyclosome-dependent proteolysis of human cyclin A starts at the beginning of mitosis and is not subject to the spindle assembly checkpoint. *The Journal of cell biology*. 153:137-148.

Genevet, A., and N. Tapon. 2011. The Hippo pathway and apico-basal cell polarity. *Biochem J*. 436:213-224.

Genevet, A., M.C. Wehr, R. Brain, B.J. Thompson, and N. Tapon. 2010. Kibra is a regulator of the Salvador/Warts/Hippo signaling network. *Dev. Cell*. 18:300-308.

Georgiou, M., E. Marinari, J. Burden, and B. Baum. 2008. Cdc42, Par6, and aPKC regulate Arp2/3-mediated endocytosis to control local adherens junction stability. *Curr Biol*. 18:1631-1638.

Gernapudi, R., Y. Yao, Y. Zhang, B. Wolfson, S. Roy, N. Duru, G. Eades, P. Yang, and Q. Zhou. 2015. Targeting exosomes from preadipocytes inhibits preadipocyte to cancer stem cell signaling in early-stage breast cancer. *Breast Cancer Res Treat*. 150:685-695.

Giannone, G., B.J. Dubin-Thaler, H.G. Dobereiner, N. Kieffer, A.R. Bresnick, and M.P. Sheetz. 2004. Periodic lamellipodial contractions correlate with rearward actin waves. *Cell*. 116:431-443.

Gilles, C., M. Polette, M. Mestdagt, B. Nawrocki-Raby, P. Ruggeri, P. Birembaut, and J.M. Foidart. 2003. Transactivation of Vimentin by beta-catenin in human breast cancer cells. *Cancer Res*. 63:2658-2664.

Gimond, C., A. van Der Flier, S. van Delft, C. Brakebusch, I. Kuikman, J.G. Collard, R. Fassler, and A. Sonnenberg. 1999. Induction of cell scattering by expression of beta1 integrins in beta1-deficient epithelial cells requires activation of members of the rho family of GTPases and downregulation of cadherin and catenin function. *The Journal of cell biology*. 147:1325-1340.

Ginestier, C., M.H. Hur, E. Charafe-Jauffret, F. Monville, J. Dutcher, M. Brown, J. Jacquemier, P. Viens, C.G. Kleer, S. Liu, A. Schott, D. Hayes, D. Birnbaum, M.S. Wicha, and G. Dontu. 2007. ALDH1 is a marker of normal and malignant human mammary stem cells and a predictor of poor clinical outcome. *Cell Stem Cell*. 1:555-567.

Glantschnig, H., G.A. Rodan, and A.A. Reszka. 2002. Mapping of MST1 kinase sites of phosphorylation. Activation and autophosphorylation. *J Biol Chem*. 277:42987-42996.

Gobel, G., D. Auer, I. Gaugg, A. Schneitter, R. Lesche, E. Muller-Holzner, C. Marth, and G. Daxenbichler. 2011. Prognostic significance of methylated RASSF1A and PITX2 genes in blood- and bone marrow plasma of breast cancer patients. *Breast Cancer Res Treat*. 130:109-117.

Gomez-Casares, M.T., E. Garcia-Alegria, C.E. Lopez-Jorge, N. Ferrandiz, R. Blanco, S. Alvarez, J.P. Vaque, G. Bretones, J.M. Caraballo, P. Sanchez-Bailon, M.D. Delgado, J. Martin-Perez, J.C. Cigudosa, and J. Leon. 2013. MYC antagonizes the differentiation induced by imatinib in chronic myeloid leukemia cells through downregulation of p27(KIP1.). *Oncogene*. 32:2239-2246.

Gonzalez-Garcia, A., C.A. Pritchard, H.F. Paterson, G. Mavria, G. Stamp, and C.J. Marshall. 2005. RalGDS is required for tumor formation in a model of skin carcinogenesis. *Cancer Cell*. 7:219-226.

Gorvel, J.P., P. Chavrier, M. Zerial, and J. Gruenberg. 1991. rab5 controls early endosome fusion in vitro. *Cell*. 64:915-925.

`

Gottardi, C.J., E. Wong, and B.M. Gumbiner. 2001. E-cadherin suppresses cellular transformation by inhibiting beta-catenin signaling in an adhesion-independent manner. *J Cell Biol*. 153:1049-1060.

Gough, N.M., D.P. Gearing, J.A. King, T.A. Willson, D.J. Hilton, N.A. Nicola, and D. Metcalf. 1988. Molecular cloning and expression of the human homologue of the murine gene encoding myeloid leukemia-inhibitory factor. *Proc Natl Acad Sci U S A*. 85:2623-2627.

Goulev, Y. 2008. SCALLOPED interacts with YORKIE, the nuclear effector of the hippo tumor-suppressor pathway in Drosophila. *Curr. Biol.* 18:435-441.

Graff, J.R., J.G. Herman, R.G. Lapidus, H. Chopra, R. Xu, D.F. Jarrard, W.B. Isaacs, P.M. Pitha, N.E. Davidson, and S.B. Baylin. 1995. E-cadherin expression is silenced by DNA hypermethylation in human breast and prostate carcinomas. *Cancer Res*. 55:5195-5199.

Grande, M.T., B. Sanchez-Laorden, C. Lopez-Blau, C.A. De Frutos, A. Boutet, M. Arevalo, R.G. Rowe, S.J. Weiss, J.M. Lopez-Novoa, and M.A. Nieto. 2015. Snail1-induced partial epithelial-to-mesenchymal transition drives renal fibrosis in mice and can be targeted to reverse established disease. *Nature medicine*. 21:989-997.

Grawenda, A.M., and E. O'Neill. 2015. Clinical utility of RASSF1A methylation in human malignancies. *Br J Cancer*. 113:372-381.

Grigoryan, G., and A.E. Keating. 2008. Structural specificity in coiled-coil interactions. *Curr Opin Struct Biol*. 18:477-483.

Gu, G., J. Yuan, M. Wills, and S. Kasper. 2007. Prostate cancer cells with stem cell characteristics reconstitute the original human tumor in vivo. *Cancer Res*. 67:4807-4815.

Guarino, M. 2010. Src signaling in cancer invasion. *Journal of cellular physiology*. 223:14-26.

Gumbiner, B., B. Stevenson, and A. Grimaldi. 1988. The role of the cell adhesion molecule uvomorulin in the formation and maintenance of the epithelial junctional complex. *J Cell Biol*. 107:1575-1587.

Gumbiner, B.M. 2005. Regulation of cadherin-mediated adhesion in morphogenesis. *Nat Rev Mol Cell Biol*. 6:622-634.

Guo, C., S. Tommasi, L. Liu, J.K. Yee, R. Dammann, and G.P. Pfeifer. 2007. RASSF1A is part of a complex similar to the Drosophila Hippo/Salvador/Lats tumor-suppressor network. *Curr Biol*. 17:700-705.

Guo, C., X. Zhang, and G.P. Pfeifer. 2011. The Tumor Suppressor RASSF1A Prevents Dephosphorylation of the Mammalian STE20-like Kinases MST1 and MST2. *J Biol Chem*. 286:6253-6261.

Gupta, S., D. Campbell, B. Derijard, and R.J. Davis. 1995. Transcription factor ATF2 regulation by the JNK signal transduction pathway. *Science*. 267:389-393.

Hagenbuchner, J., U. Kiechl-Kohlendorfer, P. Obexer, and M.J. Ausserlechner. 2015. BIRC5/Survivin as a target for glycolysis inhibition in high-stage neuroblastoma. *Oncogene*.

Hagenbuchner, J., A.V. Kuznetsov, P. Obexer, and M.J. Ausserlechner. 2013. BIRC5/Survivin enhances aerobic glycolysis and drug resistance by altered regulation of the mitochondrial fusion/fission machinery. *Oncogene*. 32:4748-4757.

Hagting, A., N. Den Elzen, H.C. Vodermaier, I.C. Waizenegger, J.M. Peters, and J. Pines. 2002. Human securin proteolysis is controlled by the spindle checkpoint and reveals when the APC/C switches from activation by Cdc20 to Cdh1. *J Cell Biol*. 157:1125-1137.

Hall, J., G. Guo, J. Wray, I. Eyres, J. Nichols, L. Grotewold, S. Morfopoulou, P. Humphreys, W. Mansfield, R. Walker, S. Tomlinson, and A. Smith. 2009. Oct4 and LIF/Stat3 additively induce Kruppel factors to sustain embryonic stem cell self-renewal. *Cell stem cell*. 5:597-609.

Hamaratoglu, F. 2006. The tumour-suppressor genes NF2/Merlin and Expanded act through Hippo signalling to regulate cell proliferation and apoptosis. *Nature Cell Biol.* 8:27-36.

Hambardzumyan, D., O.J. Becher, M.K. Rosenblum, P.P. Pandolfi, K. Manova-Todorova, and E.C. Holland. 2008. PI3K pathway regulates survival of cancer stem cells residing in the perivascular niche following radiation in medulloblastoma in vivo. *Genes Dev*. 22:436-448.

`

Hamilton, G., K.S. Yee, S. Scrace, and E. O'Neill. 2009. ATM regulates a RASSF1A-dependent DNA damage response. *Curr Biol*. 19:2020-2025.

Han, J., P. Yuan, H. Yang, J. Zhang, B.S. Soh, P. Li, S.L. Lim, S. Cao, J. Tay, Y.L. Orlov, T. Lufkin, H.H. Ng, W.L. Tam, and B. Lim. 2010. Tbx3 improves the germ-line competency of induced pluripotent stem cells. *Nature*. 463:1096-1100.

Hanahan, D., and R.A. Weinberg. 2000. The hallmarks of cancer. *Cell*. 100:57-70.

Hanahan, D., and R.A. Weinberg. 2011. Hallmarks of cancer: the next generation. *Cell*. 144:646-674.

Hans, F., and S. Dimitrov. 2001. Histone H3 phosphorylation and cell division. *Oncogene*. 20:3021-3027.

Hanson, P.I., and A. Cashikar. 2012. Multivesicular body morphogenesis. *Annu Rev Cell Dev Biol*. 28:337-362.

Hao, Y., A. Chun, K. Cheung, B. Rashidi, and X. Yang. 2008. Tumor suppressor LATS1 is a negative regulator of oncogene YAP. *J. Biol. Chem.* 283:5496-5509.

Harada, K., S. Toyooka, A. Maitra, R. Maruyama, K.O. Toyooka, C.F. Timmons, G.E. Tomlinson, D. Mastrangelo, R.J. Hay, J.D. Minna, and A.F. Gazdar. 2002. Aberrant promoter methylation and silencing of the RASSF1A gene in pediatric tumors and cell lines. *Oncogene*. 21:4345-4349.

Harjes, E., S. Harjes, S. Wohlgemuth, K.H. Muller, E. Krieger, C. Herrmann, and P. Bayer. 2006. GTP-Ras disrupts the intramolecular complex of C1 and RA domains of Nore1. *Structure*. 14:881-888.

Hartsock, A., and W.J. Nelson. 2008. Adherens and tight junctions: structure, function and connections to the actin cytoskeleton. *Biochim Biophys Acta*. 1778:660-669.

Harvey, K.F., X. Zhang, and D.M. Thomas. 2013. The Hippo pathway and human cancer. *Nature Rev. Cancer*. 13:246-257.

Hashimoto, A., A. Fujimi, Y. Kanisawa, C. Nakajima, N. Hayasaka, S. Yamada, T. Okuda, S. Minami, T. Matsumoto, T. Shibata, K. Hamaguchi, Y. Kamihara, S. Iwasaki, and J. Kato. 2015. Successful treatment with dose-adjusted EPOCH-R for triple-hit lymphoma having BCL2, BCL6 and MYC translocations. *Rinsho Ketsueki*. 56:905-910.

Haudenschild, D.R., J. Chen, N. Pang, N. Steklov, S.P. Grogan, M.K. Lotz, and D.D. D'Lima. 2011. Vimentin contributes to changes in chondrocyte stiffness in osteoarthritis. *J Orthop Res*. 29:20-25.

Hay, E.D., and A. Zuk. 1995. Transformations between epithelium and mesenchyme: normal, pathological, and experimentally induced. *Am J Kidney Dis*. 26:678-690.

He, T.C., A.B. Sparks, C. Rago, H. Hermeking, L. Zawel, L.T. da Costa, P.J. Morin, B. Vogelstein, and K.W. Kinzler. 1998. Identification of c-MYC as a target of the APC pathway. *Science*. 281:1509-1512.

Heallen, T., M. Zhang, J. Wang, M. Bonilla-Claudio, E. Klysik, R.L. Johnson, and J.F. Martin. 2011. Hippo pathway inhibits Wnt signaling to restrain cardiomyocyte proliferation and heart size. *Science*. 332:458-461.

Hermann, P.C., S.L. Huber, T. Herrler, A. Aicher, J.W. Ellwart, M. Guba, C.J. Bruns, and C. Heeschen. 2007. Distinct populations of cancer stem cells determine tumor growth and metastatic activity in human pancreatic cancer. *Cell Stem Cell*. 1:313-323.

Hesson, L., I. Bieche, D. Krex, E. Criniere, K. Hoang-Xuan, E.R. Maher, and F. Latif. 2004. Frequent epigenetic inactivation of RASSF1A and BLU genes located within the critical 3p21.3 region in gliomas. *Oncogene*. 23:2408-2419.

Hesson, L.B., W.N. Cooper, and F. Latif. 2007. The role of RASSF1A methylation in cancer. *Dis Markers*. 23:73-87.

Hidalgo-Carcedo, C., S. Hooper, S.I. Chaudhry, P. Williamson, K. Harrington, B. Leitinger, and E. Sahai. 2011. Collective cell migration requires suppression of actomyosin at cell-cell contacts mediated by DDR1 and the cell polarity regulators Par3 and Par6. *Nature cell biology*. 13:49-58.

Hochedlinger, K., Y. Yamada, C. Beard, and R. Jaenisch. 2005. Ectopic expression of Oct-4 blocks progenitor-cell differentiation and causes dysplasia in epithelial tissues. *Cell*. 121:465-477.

Hoeller, D., C.M. Hecker, and I. Dikic. 2006. Ubiquitin and ubiquitin-like proteins in cancer pathogenesis. *Nat Rev Cancer*. 6:776-788.

Honda, S., M. Haruta, W. Sugawara, F. Sasaki, M. Ohira, T. Matsunaga, H. Yamaoka, H. Horie, N. Ohnuma, A. Nakagawara, E. Hiyama, S. Todo, and Y. Kaneko. 2008. The methylation status of RASSF1A promoter predicts responsiveness to chemotherapy and eventual cure in hepatoblastoma patients. *Int J Cancer*. 123:1117-1125.

Hong, X., H.T. Nguyen, Q. Chen, R. Zhang, Z. Hagman, P.M. Voorhoeve, and S.M. Cohen. 2014. Opposing activities of the Ras and Hippo pathways converge on regulation of YAP protein turnover. *Embo J*.

Hordijk, P.L., J.P. ten Klooster, R.A. van der Kammen, F. Michiels, L.C. Oomen, and J.G. Collard. 1997. Inhibition of invasion of epithelial cells by Tiam1-Rac signaling. *Science*. 278:1464-1466.

Hoshino, D., K.C. Kirkbride, K. Costello, E.S. Clark, S. Sinha, N. Grega-Larson, M.J. Tyska, and A.M. Weaver. 2013. Exosome secretion is enhanced by invadopodia and drives invasive behavior. *Cell Rep*. 5:1159-1168.

Hossini, A.M., and J. Eberle. 2008. Apoptosis induction by Bcl-2 proteins independent of the BH3 domain. *Biochem Pharmacol*. 76:1612-1619.

Hsia, D.A., S.K. Mitra, C.R. Hauck, D.N. Streblow, J.A. Nelson, D. Ilic, S. Huang, E. Li, G.R. Nemerow, J. Leng, K.S. Spencer, D.A. Cheresh, and D.D. Schlaepfer. 2003. Differential regulation of cell motility and invasion by FAK. *The Journal of cell biology*. 160:753-767.

Hsu, C., Y. Morohashi, S. Yoshimura, N. Manrique-Hoyos, S. Jung, M.A. Lauterbach, M. Bakhti, M. Gronborg, W. Mobius, J. Rhee, F.A. Barr, and M. Simons. 2010. Regulation of exosome secretion by Rab35 and its GTPase-activating proteins TBC1D10A-C. *J Cell Biol*. 189:223-232.

Huang, H.L. 2013. Par-1 regulates tissue growth by influencing Hippo phosphorylation status and Hippo-salvador association. *PLoS Biol.* 11:e1001620.

Huang, J., S. Wu, J. Barrera, K. Matthews, and D. Pan. 2005. The Hippo signaling pathway coordinately regulates cell proliferation and apoptosis by inactivating Yorkie, the Drosophila Homolog of YAP. *Cell*. 122:421-434.

Huber, A.H., and W.I. Weis. 2001. The structure of the beta-catenin/E-cadherin complex and the molecular basis of diverse ligand recognition by beta-catenin. *Cell*. 105:391-402.

Huber, M.A., N. Kraut, and H. Beug. 2005. Molecular requirements for epithelial-mesenchymal transition during tumor progression. *Curr Opin Cell Biol*. 17:548-558.

Hung, J., Y. Kishimoto, K. Sugio, A. Virmani, D.D. McIntire, J.D. Minna, and A.F. Gazdar. 1995. Allele-specific chromosome 3p deletions occur at an early stage in the pathogenesis of lung carcinoma. *JAMA*. 273:1908.

Hurley, J.H. 2010. The ESCRT complexes. *Crit Rev Biochem Mol Biol*. 45:463-487.

Huveneers, S., and E.H. Danen. 2009. Adhesion signaling - crosstalk between integrins, Src and Rho. *J Cell Sci*. 122:1059-1069.

Hwang, E., K.S. Ryu, K. Paakkonen, P. Guntert, H.K. Cheong, D.S. Lim, J.O. Lee, Y.H. Jeon, and C. Cheong. 2007. Structural insight into dimeric interaction of the SARAH domains from Mst1 and RASSF family proteins in the apoptosis pathway. *Proc Natl Acad Sci U S A*. 104:9236-9241.

Irby, R.B., W. Mao, D. Coppola, J. Kang, J.M. Loubeau, W. Trudeau, R. Karl, D.J. Fujita, R. Jove, and T.J. Yeatman. 1999. Activating SRC mutation in a subset of advanced human colon cancers. *Nat Genet*. 21:187-190.

Irby, R.B., and T.J. Yeatman. 2000. Role of Src expression and activation in human cancer. *Oncogene*. 19:5636-5642.

Jacobs, J.J., P. Keblusek, E. Robanus-Maandag, P. Kristel, M. Lingbeek, P.M. Nederlof, T. van Welsem, M.J. van de Vijver, E.Y. Koh, G.Q. Daley, and M. van Lohuizen. 2000. Senescence bypass screen identifies TBX2, which represses Cdkn2a (p19(ARF)) and is amplified in a subset of human breast cancers. *Nature genetics*. 26:291-299.

Jaffe, A.B., P. Aspenstrom, and A. Hall. 2004. Human CNK1 acts as a scaffold protein, linking Rho and Ras signal transduction pathways. *Mol Cell Biol*. 24:1736-1746.

`

Jarmalaite, S., F. Jankevicius, K. Kurgonaite, K. Suziedelis, P. Mutanen, and K. Husgafvel-Pursiainen. 2008. Promoter hypermethylation in tumour suppressor genes shows association with stage, grade and invasiveness of bladder cancer. *Oncology*. 75:145-151.

Jaspersen, S.L., J.F. Charles, and D.O. Morgan. 1999. Inhibitory phosphorylation of the APC regulator Hct1 is controlled by the kinase Cdc28 and the phosphatase Cdc14. *Curr Biol*. 9:227-236.

Jeanes, A., C.J. Gottardi, and A.S. Yap. 2008. Cadherins and cancer: how does cadherin dysfunction promote tumor progression? *Oncogene*. 27:6920-6929.

Jeppesen, D.K., A. Nawrocki, S.G. Jensen, K. Thorsen, B. Whitehead, K.A. Howard, L. Dyrskjot, T.F. Orntoft, M.R. Larsen, and M.S. Ostenfeld. 2014. Quantitative proteomics of fractionated membrane and lumen exosome proteins from isogenic metastatic and nonmetastatic bladder cancer cells reveal differential expression of EMT factors. *Proteomics*. 14:699-712.

Jeronimo, C., R. Henrique, M. Hoque, E. Mambo, F.R. Ribeiro, G. Varzim, J. Oliveira, M.R. Teixeira, C. Lopes, and D. Sidransky. 2004. A quantitative promoter methylation profile of prostate cancer. *Clin Cancer*. 10:8472-8478.

Jiang, Y., L. Cui, W.D. Chen, S.H. Shen, and L.D. Ding. 2012. The prognostic role of RASSF1A promoter methylation in breast cancer: a meta-analysis of published data. *PLoS One*. 7:e36780.

Jin, L., K.J. Hope, Q. Zhai, F. Smadja-Joffe, and J.E. Dick. 2006. Targeting of CD44 eradicates human acute myeloid leukemic stem cells. *Nature medicine*. 12:1167-1174.

Jo, H., J. Kim, G. Kang, N. Park, Y. Song, S. Kang, and H. Lee. 2006. Association of promoter hypermethylation of the RASSF1A gene with prognostic parameters in endometrial cancer. *Clin Cancer Res*. 16:205-209.

Jochum, W., E. Passegue, and E.F. Wagner. 2001. AP-1 in mouse development and tumorigenesis. *Oncogene*. 20:2401-2412.

Johnson, R., and G. Halder. 2014. The two faces of Hippo: targeting the Hippo pathway for regenerative medicine and cancer treatment. *Nat Rev Drug Discov*. 13:63-79.

Johnstone, R.M., M. Adam, J.R. Hammond, L. Orr, and C. Turbide. 1987. Vesicle formation during reticulocyte maturation. Association of plasma membrane activities with released vesicles (exosomes). *J Biol Chem*. 262:9412-9420.

Jones, P.A., and S.B. Baylin. 2002. The fundamental role of epigenetic events in cancer. *Nat Rev Genet*. 3:415-428.

Jones, P.A., and S.B. Baylin. 2007. The epigenomics of cancer. *Cell*. 128:683-692.

Jones, P.L., G.J. Veenstra, P.A. Wade, D. Vermaak, S.U. Kass, N. Landsberger, J. Strouboulis, and A.P. Wolffe. 1998. Methylated DNA and MeCP2 recruit histone deacetylase to repress transcription. *Nature genetics*. 19:187-191.

Kahlert, C., and R. Kalluri. 2013. Exosomes in tumor microenvironment influence cancer progression and metastasis. *J Mol Med (Berl)*. 91:431-437.

Kaidi, A., A.C. Williams, and C. Paraskeva. 2007. Interaction between beta-catenin and HIF-1 promotes cellular adaptation to hypoxia. *Nat Cell Biol*. 9:210-217.

Kalluri, R., and E.G. Neilson. 2003. Epithelial-mesenchymal transition and its implications for fibrosis. *J Clin Invest*. 112:1776-1784.

Kalluri, R., and R.A. Weinberg. 2009. The basics of epithelial-mesenchymal transition. *J Clin Invest*. 119:1420-1428.

Kamei, T., T. Matozaki, T. Sakisaka, A. Kodama, S. Yokoyama, Y.F. Peng, K. Nakano, K. Takaishi, and Y. Takai. 1999. Coendocytosis of cadherin and c-Met coupled to disruption of cell-cell adhesion in MDCK cells--regulation by Rho, Rac and Rab small G proteins. *Oncogene*. 18:6776-6784.

Kaplan, K.B., K.B. Bibbins, J.R. Swedlow, M. Arnaud, D.O. Morgan, and H.E. Varmus. 1994. Association of the amino-terminal half of c-Src with focal adhesions alters their properties and is regulated by phosphorylation of tyrosine 527. *EMBO J*. 13:4745-4756.

Kaplan, K.B., J.R. Swedlow, H.E. Varmus, and D.O. Morgan. 1992. Association of p60c-src with endosomal membranes in mammalian fibroblasts. *J Cell Biol*. 118:321-333.

Kapoor, A., W. Yao, H. Ying, S. Hua, A. Liewen, Q. Wang, Y. Zhong, C.J. Wu, A. Sadanandam, B. Hu, Q. Chang, G.C. Chu, R. Al-Khalil, S. Jiang, H. Xia, E. Fletcher-Sananikone, C. Lim, G.I. Horwitz, A.

Viale, P. Pettazzoni, N. Sanchez, H. Wang, A. Protopopov, J. Zhang, T. Heffernan, R.L. Johnson, L. Chin, Y.A. Wang, G. Draetta, and R.A. DePinho. 2014. Yap1 activation enables bypass of oncogenic Kras addiction in pancreatic cancer. *Cell*. 158:185-197.

Karin, M. 1995. The regulation of AP-1 activity by mitogen-activated protein kinases. *J Biol Chem*. 270:16483-16486.

Karnoub, A.E., and R.A. Weinberg. 2008. Ras oncogenes: split personalities. *Nat Rev Mol Cell Biol*. 9:517-531.

Katoh, K., H. Shibata, H. Suzuki, A. Nara, K. Ishidoh, E. Kominami, T. Yoshimori, and M. Maki. 2003. The ALG-2-interacting protein Alix associates with CHMP4b, a human homologue of yeast Snf7 that is involved in multivesicular body sorting. *J Biol Chem*. 278:39104-39113.

Kawai, Y., S. Sakano, Y. Suehiro, T. Okada, Y. Korenaga, T. Hara, K. Naito, H. Matsuyama, and Y. Hinoda. 2010. Methylation level of the RASSF1A promoter is an independent prognostic factor for clear-cell renal cell carcinoma. *Ann Oncol*. 21:1612-1617.

Kawamoto, K., S.T. Okino, R.F. Place, S. Urakami, H. Hirata, N. Kikuno, T. Kawakami, Y. Tanaka, D. Pookot, Z. Chen, S. Majid, H. Enokida, M. Nakagawa, and R. Dahiya. 2007. Epigenetic modifications of RASSF1A gene through chromatin remodeling in prostate cancer. *Clin Cancer Res*. 13:2541-2548.

Keller, S., J. Ridinger, A.K. Rupp, J.W. Janssen, and P. Altevogt. 2011. Body fluid derived exosomes as a novel template for clinical diagnostics. *J Transl Med*. 9:86.

Khan, S., J.M. Jutzy, J.R. Aspe, D.W. McGregor, J.W. Neidigh, and N.R. Wall. 2011. Survivin is released from cancer cells via exosomes. *Apoptosis*. 16:1-12.

Khokhlatchev, A., S. Rabizadeh, R. Xavier, M. Nedwidek, T. Chen, X.F. Zhang, B. Seed, and J. Avruch. 2002. Identification of a novel Ras-regulated proapoptotic pathway. *Curr Biol*. 12:253-265.

Kilpinen, L., U. Impola, L. Sankkila, I. Ritamo, M. Aatonen, S. Kilpinen, J. Tuimala, L. Valmu, J. Levijoki, P. Finckenberg, P. Siljander, E. Kankuri, E. Mervaala, and S. Laitinen. 2013. Extracellular membrane vesicles from umbilical cord blood-derived MSC protect against ischemic acute kidney injury, a feature that is lost after inflammatory conditioning. *J Extracell Vesicles*. 2.

Kim, H.S., D.Y. Choi, S.J. Yun, S.M. Choi, J.W. Kang, J.W. Jung, D. Hwang, K.P. Kim, and D.W. Kim. 2012a. Proteomic analysis of microvesicles derived from human mesenchymal stem cells. *J Proteome Res*. 11:839-849.

Kim, J.S., Y. Chae, Y.S. Ha, I.Y. Kim, S.S. Byun, S.J. Yun, and W.J. Kim. 2012b. Ras association domain family 1A: a promising prognostic marker in recurrent nonmuscle invasive bladder cancer. *Clin Genitourin Cancer*. 10:114-120.

Kim, K., Z. Lu, and E.D. Hay. 2002. Direct evidence for a role of beta-catenin/LEF-1 signaling pathway in induction of EMT. *Cell Biol Int*. 26:463-476.

Kim, L.C., L. Song, and E.B. Haura. 2009. Src kinases as therapeutic targets for cancer. *Nat Rev Clin Oncol*. 6:587-595.

Kim, N.G., E. Koh, X. Chen, and B.M. Gumbiner. 2011. E-cadherin mediates contact inhibition of proliferation through Hippo signaling-pathway components. *Proc Natl Acad Sci U S A*. 108:11930-11935.

Kim, S., C.T. Denny, and R. Wisdom. 2006. Cooperative DNA binding with AP-1 proteins is required for transformation by EWS-Ets fusion proteins. *Mol Cell Biol*. 26:2467-2478.

Kim, S.T., D.S. Lim, C.E. Canman, and M.B. Kastan. 1999. Substrate specificities and identification of putative substrates of ATM kinase family members. *J Biol Chem*. 274:37538-37543.

Kimura, K., M. Ito, M. Amano, K. Chihara, Y. Fukata, M. Nakafuku, B. Yamamori, J. Feng, T. Nakano, K. Okawa, A. Iwamatsu, and K. Kaibuchi. 1996. Regulation of myosin phosphatase by Rho and Rho-associated kinase (Rho-kinase). *Science*. 273:245-248.

Kitagawa, D., H. Kajiho, T. Negishi, S. Ura, T. Watanabe, T. Wada, H. Ichijo, T. Katada, and H. Nishina. 2006. Release of RASSF1C from the nucleus by Daxx degradation links DNA damage and SAPK/JNK activation. *Embo J*. 25:3286-3297.

Kiyokawa, E., Y. Hashimoto, S. Kobayashi, H. Sugimura, T. Kurata, and M. Matsuda. 1998. Activation of Rac1 by a Crk SH3-binding protein, DOCK180. *Genes Dev*. 12:3331-3336.

Klingelhofer, J., O.Y. Laur, R.B. Troyanovsky, and S.M. Troyanovsky. 2002. Dynamic interplay between adhesive and lateral E-cadherin dimers. *Mol Cell Biol*. 22:7449-7458.

Kobel, M., D. Turbin, S.E. Kalloger, D. Gao, D.G. Huntsman, and C.B. Gilks. 2011. Biomarker expression in pelvic high-grade serous carcinoma: comparison of ovarian and omental sites. *Int J Gynecol Pathol*. 30:366-371.

Kok, K., S.L. Naylor, and C.H. Buys. 1997. Deletions of the short arm of chromosome 3 in solid tumors and the search for suppressor genes. *Adv Cancer Res*. 71:27-92.

Kopetz, S., D.P. Lesslie, N.A. Dallas, S.I. Park, M. Johnson, N.U. Parikh, M.P. Kim, J.L. Abbruzzese, L.M. Ellis, J. Chandra, and G.E. Gallick. 2009. Synergistic activity of the SRC family kinase inhibitor dasatinib and oxaliplatin in colon carcinoma cells is mediated by oxidative stress. *Cancer Res*. 69:3842-3849.

Korinek, V., N. Barker, P.J. Morin, D. van Wichen, R. de Weger, K.W. Kinzler, B. Vogelstein, and H. Clevers. 1997. Constitutive transcriptional activation by a beta-catenin-Tcf complex in APC-/- colon carcinoma. *Science*. 275:1784-1787.

Kornberg, L., H.S. Earp, J.T. Parsons, M. Schaller, and R.L. Juliano. 1992. Cell adhesion or integrin clustering increases phosphorylation of a focal adhesion-associated tyrosine kinase. *J Biol Chem*. 267:23439-23442.

Kourembanas, S. 2015. Exosomes: vehicles of intercellular signaling, biomarkers, and vectors of cell therapy. *Annu Rev Physiol*. 77:13-27.

Kramer, E.R., N. Scheuringer, A.V. Podtelejnikov, M. Mann, and J.M. Peters. 2000. Mitotic regulation of the APC activator proteins CDC20 and CDH1. *Mol Biol Cell*. 11:1555-1569.

Krause, M., A. Yaromina, W. Eicheler, U. Koch, and M. Baumann. 2011. Cancer stem cells: targets and potential biomarkers for radiotherapy. *Clin Cancer Res*. 17:7224-7229.

Kreso, A., and J.E. Dick. 2014. Evolution of the cancer stem cell model. *Cell Stem Cell*. 14:275-291.

Kubo, T., H. Yamamoto, K. Ichimura, M. Jida, T. Hayashi, H. Otani, K. Tsukuda, Y. Sano, K. Kiura, and S. Toyooka. 2009. DNA methylation in small lung adenocarcinoma with bronchioloalveolar carcinoma components. *Lung Cancer*. 65:328-332.

Kucia, M., R. Reca, K. Miekus, J. Wanzeck, W. Wojakowski, A. Janowska-Wieczorek, J. Ratajczak, and M.Z. Ratajczak. 2005. Trafficking of normal stem cells and metastasis of cancer stem cells involve similar mechanisms: pivotal role of the SDF-1-CXCR4 axis. *Stem Cells*. 23:879-894.

Kumar, D., D. Gupta, S. Shankar, and R.K. Srivastava. 2015. Biomolecular characterization of exosomes released from cancer stem cells: Possible implications for biomarker and treatment of cancer. *Oncotarget*. 6:3280-3291.

Kunjithapatham, R., S. Karthikeyan, J.F. Geschwind, E. Kieserman, M. Lin, D.X. Fu, and S. Ganapathy-Kanniappan. 2014. Reversal of anchorage-independent multicellular spheroid into a monolayer mimics a metastatic model. *Sci Rep*. 4:6816.

Kureishi, Y., S. Kobayashi, M. Amano, K. Kimura, H. Kanaide, T. Nakano, K. Kaibuchi, and M. Ito. 1997. Rho-associated kinase directly induces smooth muscle contraction through myosin light chain phosphorylation. *J Biol Chem*. 272:12257-12260.

Kurz, E.U., and S.P. Lees-Miller. 2004. DNA damage-induced activation of ATM and ATM-dependent signaling pathways. *DNA repair*. 3:889-900.

Kuzmin, I., J.W. Gillespie, A. Protopopov, L. Geil, K. Dreijerink, Y. Yang, C.D. Vocke, F.M. Duh, E. Zabarovsky, J.D. Minna, J.S. Rhim, M.R. Emmert-Buck, W.M. Linehan, and M.I. Lerman. 2002. The RASSF1A tumor suppressor gene is inactivated in prostate tumors and suppresses growth of prostate carcinoma cells. *Cancer Res*. 62:3498-3502.

Laemmli, U.K. 1970. Cleavage of structural proteins during the assembly of the head of bacteriophage T4. *Nature*. 227:680-685.

Lamar, J.M., P. Stern, H. Liu, J.W. Schindler, Z.G. Jiang, and R.O. Hynes. 2012. The Hippo pathway target, YAP, promotes metastasis through its TEAD-interaction domain. *Proc Natl Acad Sci U S A*. 109:E2441-2450.

Lamph, W.W., P. Wamsley, P. Sassone-Corsi, and I.M. Verma. 1988. Induction of proto-oncogene JUN/AP-1 by serum and TPA. *Nature*. 334:629-631.

`

Lancaster, O.M., M. Le Berre, A. Dimitracopoulos, D. Bonazzi, E. Zlotek-Zlotkiewicz, R. Picone, T. Duke, M. Piel, and B. Baum. 2013. Mitotic rounding alters cell geometry to ensure efficient bipolar spindle formation. *Dev Cell*. 25:270-283.

Lane, D.P. 1992. Cancer. p53, guardian of the genome. *Nature*. 358:15-16.

Langton, P.F., J. Colombani, E.H. Chan, A. Wepf, M. Gstaiger, and N. Tapon. 2009. The dASPP-dRASSF8 complex regulates cell-cell adhesion during Drosophila retinal morphogenesis. *Curr Biol*. 19:1969-1978.

Lapidot, T., C. Sirard, J. Vormoor, B. Murdoch, T. Hoang, J. Caceres-Cortes, M. Minden, B. Paterson, M.A. Caligiuri, and J.E. Dick. 1994. A cell initiating human acute myeloid leukaemia after transplantation into SCID mice. *Nature*. 367:645-648.

Lathia, J.D., J. Gallagher, J.T. Myers, M. Li, A. Vasanji, R.E. McLendon, A.B. Hjelmeland, A.Y. Huang, and J.N. Rich. 2011. Direct in vivo evidence for tumor propagation by glioblastoma cancer stem cells. *PLoS One*. 6:e24807.

Law, J., M. Salla, A. Zare, Y. Wong, L. Luong, N. Volodko, O. Svystun, K. Flood, J. Lim, M. Sung, J.R. Dyck, C.T. Tan, Y.C. Su, V.C. Yu, J. Mackey, and S. Baksh. 2015. Modulator of Apoptosis 1 (MOAP-1) is a tumor suppressor protein linked to RASSF1A. *J Biol Chem*.

Le, T.L., A.S. Yap, and J.L. Stow. 1999. Recycling of E-cadherin: a potential mechanism for regulating cadherin dynamics. *J Cell Biol*. 146:219-232.

Leckband, D., and S. Sivasankar. 2000. Mechanism of homophilic cadherin adhesion. *Curr Opin Cell Biol*. 12:587-592.

Lee, A., J.D. Kessler, T.A. Read, C. Kaiser, D. Corbeil, W.B. Huttner, J.E. Johnson, and R.J. Wechsler-Reya. 2005. Isolation of neural stem cells from the postnatal cerebellum. *Nat Neurosci*. 8:723-729.

Lee, S.M., W.K. Lee, D.S. Kim, and J.Y. Park. 2012. Quantitative promoter hypermethylation analysis of RASSF1A in lung cancer: comparison with methylation-specific PCR technique and clinical significance. *Mol Med Rep*. 5:239-244.

Lei, Q.Y. 2008. TAZ promotes cell proliferation and epithelial-mesenchymal transition and is inhibited by the hippo pathway. *Mol. Cell. Biol.* 28:2426-2436.

Leibfried, A., R. Fricke, M.J. Morgan, S. Bogdan, and Y. Bellaiche. 2008. Drosophila Cip4 and WASp define a branch of the Cdc42-Par6-aPKC pathway regulating E-cadherin endocytosis. *Curr Biol*. 18:1639-1648.

Lerman, M.I., and J.D. Minna. 2000. The 630-kb lung cancer homozygous deletion region on human chromosome 3p21.3: identification and evaluation of the resident candidate tumor suppressor genes. The International Lung Cancer Chromosome 3p21.3 Tumor Suppressor Gene Consortium. *Cancer Res*. 60:6116-6133.

Leuchowius, K.J., C.M. Clausson, K. Grannas, Y. Erbilgin, J. Botling, A. Zieba, U. Landegren, and O. Soderberg. 2013. Parallel visualization of multiple protein complexes in individual cells in tumor tissue. *Mol Cell Proteomics*. 12:1563-1571.

Leung, E.L., R.R. Fiscus, J.W. Tung, V.P. Tin, L.C. Cheng, A.D. Sihoe, L.M. Fink, Y. Ma, and M.P. Wong. 2010. Non-small cell lung cancer cells expressing CD44 are enriched for stem cell-like properties. *PLoS One*. 5:e14062.

Levesley, J., M.E. Lusher, J.C. Lindsey, S.C. Clifford, R. Grundy, and B. Coyle. 2011. RASSF1A and the BH3-only mimetic ABT-737 promote apoptosis in pediatric medulloblastoma cell lines. *Neuro Oncol*. 13:1265-1276.

Levine, A.J. 2009. The common mechanisms of transformation by the small DNA tumor viruses: The inactivation of tumor suppressor gene products: p53. *Virology*. 384:285-293.

Levine, A.J., M.C. Wu, A. Chang, A. Silver, E.F. Attiyeh, J. Lin, and C.B. Epstein. 1995. The spectrum of mutations at the p53 locus. Evidence for tissue-specific mutagenesis, selection of mutant alleles, and a "gain of function" phenotype. *Ann N Y Acad Sci*. 768:111-128.

Levy, D., Y. Adamovich, N. Reuven, and Y. Shaul. 2008. Yap1 phosphorylation by c-Abl is a critical step in selective activation of proapoptotic genes in response to DNA damage. *Molecular cell*. 29:350-361.

Li, C., J. Li, D. Wu, and G. Han. 2015. The involvement of survivin in insulin-like growth factor 1-induced epithelial-mesenchymal transition in gastric cancer. *Tumour Biol*.

Li, J., A. El-Naggar, and L. Mao. 2005. Promoter methylation of p16INK4a, RASSF1A, and DAPK is frequent in salivary adenoid cystic carcinoma. *Cancer*. 104:771-776.

Li, J., F. Wang, A. Protopopov, A. Malyukova, V. Kashuba, J.D. Minna, M.I. Lerman, G. Klein, and E. Zabarovsky. 2004. Inactivation of RASSF1C during in vivo tumor growth identifies it as a tumor suppressor gene. *Oncogene*. 23:5941-5949.

Li, X., M.T. Lewis, J. Huang, C. Gutierrez, C.K. Osborne, M.F. Wu, S.G. Hilsenbeck, A. Pavlick, X. Zhang, G.C. Chamness, H. Wong, J. Rosen, and J.C. Chang. 2008. Intrinsic resistance of tumorigenic breast cancer cells to chemotherapy. *J Natl Cancer Inst*. 100:672-679.

Liao, X., M.-Y. Siu, K.-K. Chan, E.-Y. Wong, H.-S. Ngan, Q.-Y. Chan, A.-M. Li, U.S. Khoo, and A.-Y. Cheung. 2008. Hypermethylation of RAS effector related genes and DNA methyltransferase 1 expression in endometrial carcinogenesis. *Int J Cancer*. 123:296-302.

Lien, W.H., O. Klezovitch, and V. Vasioukhin. 2006. Cadherin-catenin proteins in vertebrate development. *Curr Opin Cell Biol*. 18:499-506.

Lin, D., E.J. Kamsteeg, Y. Zhang, Y. Jin, H. Sterling, P. Yue, M. Roos, A. Duffield, J. Spencer, M. Caplan, and W.H. Wang. 2008. Expression of tetraspan protein CD63 activates protein-tyrosine kinase (PTK) and enhances the PTK-induced inhibition of ROMK channels. *J Biol Chem*. 283:7674-7681.

Liu, C., K. Kelnar, B. Liu, X. Chen, T. Calhoun-Davis, H. Li, L. Patrawala, H. Yan, C. Jeter, S. Honorio, J.F. Wiggins, A.G. Bader, R. Fagin, D. Brown, and D.G. Tang. 2011a. The microRNA miR-34a inhibits prostate cancer stem cells and metastasis by directly repressing CD44. *Nature medicine*. 17:211-215.

Liu, C.Y. 2010. The Hippo tumor pathway promotes TAZ degradation by phosphorylating a phosphodegron and recruiting the SCF[beta]-TrCP E3 ligase. *J. Biol. Chem.* 285:37159-37169.

Liu, L., K. Baier, R. Dammann, and G.P. Pfeifer. 2007. The tumor suppressor RASSF1A does not interact with Cdc20, an activator of the anaphase-promoting complex. *Cell Cycle*. 6:1663-1665.

Liu, L., C. Guo, R. Dammann, S. Tommasi, and G.P. Pfeifer. 2008. RASSF1A interacts with and activates the mitotic kinase Aurora-A. *Oncogene*. 27:6175-6186.

Liu, L., K.J. Kron, V.V. Pethe, N. Demetrashvili, M.E. Nesbitt, J. Trachtenberg, H. Ozcelik, N.E. Fleshner, L. Briollais, T.H. van der Kwast, and B. Bapat. 2011b. Association of tissue promoter methylation levels of APC, TGF[beta]2, HOXD3 and RASSF1A with prostate cancer progression. *Int J Cancer*. 129:2454-2462.

Liu, L., J.H. Yoon, R. Dammann, and G.P. Pfeifer. 2002. Frequent hypermethylation of the RASSF1A gene in prostate cancer. *Oncogene*. 21:6835-6840.

Liu, S.T., H. Pham, S.J. Pandol, and A. Ptasznik. 2013. Src as the link between inflammation and cancer. *Frontiers in physiology*. 4:416.

Liu, W., J. Wu, L. Xiao, Y. Bai, A. Qu, Z. Zheng, and Z. Yuan. 2012. Regulation of neuronal cell death by c-Abl-Hippo/MST2 signaling pathway. *PLoS One*. 7:e36562.

Liu, Z.G., H. Hsu, D.V. Goeddel, and M. Karin. 1996. Dissection of TNF receptor 1 effector functions: JNK activation is not linked to apoptosis while NF-kappaB activation prevents cell death. *Cell*. 87:565-576.

Livasy, C.A., G. Karaca, R. Nanda, M.S. Tretiakova, O.I. Olopade, D.T. Moore, and C.M. Perou. 2006. Phenotypic evaluation of the basal-like subtype of invasive breast carcinoma. *Modern pathology : an official journal of the United States and Canadian Academy of Pathology, Inc*. 19:264-271.

Llado, A., P. Timpson, S. Vila de Muga, J. Moreto, A. Pol, T. Grewal, R.J. Daly, C. Enrich, and F. Tebar. 2008. Protein kinase Cdelta and calmodulin regulate epidermal growth factor receptor recycling from early endosomes through Arp2/3 complex and cortactin. *Mol Biol Cell*. 19:17-29.

Lohia, M., Y. Qin, and I.G. Macara. 2012. The Scribble polarity protein stabilizes E-cadherin/p120-catenin binding and blocks retrieval of E-cadherin to the Golgi. *PLoS One*. 7:e51130.

Lombardo, L.J., F.Y. Lee, P. Chen, D. Norris, J.C. Barrish, K. Behnia, S. Castaneda, L.A. Cornelius, J. Das, A.M. Doweyko, C. Fairchild, J.T. Hunt, I. Inigo, K. Johnston, A. Kamath, D. Kan, H. Klei, P.

Marathe, S. Pang, R. Peterson, S. Pitt, G.L. Schieven, R.J. Schmidt, J. Tokarski, M.L. Wen, J. Wityak, and R.M. Borzilleri. 2004. Discovery of N-(2-chloro-6-methyl- phenyl)-2-(6-(4-(2-hydroxyethyl)- piperazin-1-yl)-2-methylpyrimidin-4- ylamino)thiazole-5-carboxamide (BMS-354825), a dual Src/Abl kinase inhibitor with potent antitumor activity in preclinical assays. *J Med Chem*. 47:6658-6661.

Londono, I., V. Marshansky, S. Bourgoin, P. Vinay, and M. Bendayan. 1999. Expression and distribution of adenosine diphosphate-ribosylation factors in the rat kidney. *Kidney Int*. 55:1407-1416.

Lopez, J., M. Percharde, H.M. Coley, A. Webb, and T. Crook. 2009. The context and potential of epigenetics in oncology. *Br J Cancer*. 100:571-577.

Lorenzato, A., C. Martino, N. Dani, Y. Oligschlager, A.M. Ferrero, N. Biglia, R. Calogero, M. Olivero, and M.F. Di Renzo. 2012. The cellular apoptosis susceptibility CAS/CSE1L gene protects ovarian cancer cells from death by suppressing RASSF1C. *Faseb J*. 26:2446-2456.

Luga, V., L. Zhang, A.M. Viloria-Petit, A.A. Ogunjimi, M.R. Inanlou, E. Chiu, M. Buchanan, A.N. Hosein, M. Basik, and J.L. Wrana. 2012. Exosomes mediate stromal mobilization of autocrine Wnt-PCP signaling in breast cancer cell migration. *Cell*. 151:1542-1556.

Ma, S., K.W. Chan, T.K. Lee, K.H. Tang, J.Y. Wo, B.J. Zheng, and X.Y. Guan. 2008. Aldehyde dehydrogenase discriminates the CD133 liver cancer stem cell populations. *Mol Cancer Res*. 6:1146-1153.

Machesky, L.M., and A. Hall. 1997. Role of actin polymerization and adhesion to extracellular matrix in Rac- and Rho-induced cytoskeletal reorganization. *The Journal of cell biology*. 138:913-926.

Malpeli, G., E. Amato, M. Dandrea, C. Fumagalli, V. Debattisti, L. Boninsegna, G. Pelosi, M. Falconi, and A. Scarpa. 2011. Methylation-associated down-regulation of RASSF1A and up-regulation of RASSF1C in pancreatic endocrine tumors. *BMC Cancer*. 11:351.

Malumbres, M., and A. Pellicer. 1998. RAS pathways to cell cycle control and cell transformation. *Frontiers in bioscience : a journal and virtual library*. 3:d887-912.

Manfredi, J.J. 2010. The Mdm2-p53 relationship evolves: Mdm2 swings both ways as an oncogene and a tumor suppressor. *Genes Dev*. 24:1580-1589.

Mani, S.A., W. Guo, M.J. Liao, E.N. Eaton, A. Ayyanan, A.Y. Zhou, M. Brooks, F. Reinhard, C.C. Zhang, M. Shipitsin, L.L. Campbell, K. Polyak, C. Brisken, J. Yang, and R.A. Weinberg. 2008. The epithelial-mesenchymal transition generates cells with properties of stem cells. *Cell*. 133:704-715.

Marcoux, N., and K. Vuori. 2003. EGF receptor mediates adhesion-dependent activation of the Rac GTPase: a role for phosphatidylinositol 3-kinase and Vav2. *Oncogene*. 22:6100-6106.

Marignani, P.A., and C.L. Carpenter. 2001. Vav2 is required for cell spreading. *J Cell Biol*. 154:177-186.

Marine, J.C., M.A. Dyer, and A.G. Jochemsen. 2007. MDMX: from bench to bedside. *J Cell Sci*. 120:371-378.

Marine, J.C., and G. Lozano. 2010. Mdm2-mediated ubiquitylation: p53 and beyond. *Cell Death Differ*. 17:93-102.

Mariner, D.J., P. Anastasiadis, H. Keilhack, F.D. Bohmer, J. Wang, and A.B. Reynolds. 2001. Identification of Src phosphorylation sites in the catenin p120ctn. *J Biol Chem*. 276:28006-28013.

Maruyama, R., S. Toyooka, K. Toyooka, A. Virmani, S. Zochbauer-Muller, A. Farinas, J. Minna, J. McConnell, E. Frenkel, and A. Gazdar. 2002. Aberrant promoter methylation profile of prostate cancers and its relationship to clinicopathological features. *Clin Cancer*. 8:514-519.

Maruyama, R., S. Toyooka, K.O. Toyooka, K. Harada, A.K. Virmani, S. Zochbauer-Muller, A.J. Farinas, F. Vakar-Lopez, J.D. Minna, A. Sagalowsky, B. Czerniak, and A.F. Gazdar. 2001. Aberrant promoter methylation profile of bladder cancer and its relationship to clinicopathological features. *Cancer Res*. 61:8659-8663.

Marzesco, A.M. 2013. Prominin-1-containing membrane vesicles: origins, formation, and utility. *Adv Exp Med Biol*. 777:41-54.

Marzese, D.M., R.A. Scolyer, M. Roque, L.M. Vargas-Roig, J.L. Huynh, J.S. Wilmott, R. Murali, M.E. Buckland, G. Barkhoudarian, J.F. Thompson, D.L. Morton, D.F. Kelly, and D.S. Hoon. 2014. DNA methylation and gene deletion analysis of brain metastases in melanoma patients identifies mutually exclusive molecular alterations. *Neuro Oncol*. 16:1499-1509.

Masaki, T., K. Igarashi, M. Tokuda, S. Yukimasa, F. Han, Y.J. Jin, J.Q. Li, H. Yoneyama, N. Uchida, J. Fujita, H. Yoshiji, S. Watanabe, K. Kurokohchi, and S. Kuriyama. 2003. pp60c-src activation in lung adenocarcinoma. *Eur J Cancer*. 39:1447-1455.

Matallanas, D., D. Romano, F. Al-Mulla, E. O'Neill, W. Al-Ali, P. Crespo, B. Doyle, C. Nixon, O. Sansom, M. Drosten, M. Barbacid, and W. Kolch. 2011. Mutant K-Ras Activation of the Proapoptotic MST2 Pathway Is Antagonized by Wild-Type K-Ras. *Molecular cell*. 44:893-906.

Matallanas, D., D. Romano, K. Yee, K. Meissl, L. Kucerova, D. Piazzolla, M. Baccarini, J.K. Vass, W. Kolch, and E. O'Neill. 2007. RASSF1A elicits apoptosis through an MST2 pathway directing proapoptotic transcription by the p73 tumor suppressor protein. *Molecular cell*. 27:962-975.

Matei, D., F. Fang, C. Shen, J. Schilder, A. Arnold, Y. Zeng, W.A. Berry, T. Huang, and K.P. Nephew. 2012. Epigenetic resensitization to platinum in ovarian cancer. *Cancer Res*. 72:2197-2205.

Matsuo, H., J. Chevallier, N. Mayran, I. Le Blanc, C. Ferguson, J. Faure, N.S. Blanc, S. Matile, J. Dubochet, R. Sadoul, R.G. Parton, F. Vilbois, and J. Gruenberg. 2004. Role of LBPA and Alix in multivesicular liposome formation and endosome organization. *Science*. 303:531-534.

Mazurenko, N.N., E.A. Kogan, I.B. Zborovskaya, and F.L. Kisseljov. 1992. Expression of pp60c-src in human small cell and non-small cell lung carcinomas. *Eur J Cancer*. 28:372-377.

McLauchlan, H., J. Newell, N. Morrice, A. Osborne, M. West, and E. Smythe. 1998. A novel role for Rab5-GDI in ligand sequestration into clathrin-coated pits. *Curr Biol*. 8:34-45.

Medema, J.P. 2013. Cancer stem cells: the challenges ahead. *Nat Cell Biol*. 15:338-344.

Melino, G., F. Bernassola, M. Ranalli, K. Yee, W.X. Zong, M. Corazzari, R.A. Knight, D.R. Green, C. Thompson, and K.H. Vousden. 2004. p73 Induces apoptosis via PUMA transactivation and Bax mitochondrial translocation. *J Biol Chem*. 279:8076-8083.

Melo, S.A., L.B. Luecke, C. Kahlert, A.F. Fernandez, S.T. Gammon, J. Kaye, V.S. LeBleu, E.A. Mittendorf, J. Weitz, N. Rahbari, C. Reissfelder, C. Pilarsky, M.F. Fraga, D. Piwnica-Worms, and R. Kalluri. 2015. Glypican-1 identifies cancer exosomes and detects early pancreatic cancer. *Nature*. 523:177-182.

Meng, W., A. Huebner, A. Shabsigh, A. Chakravarti, and T. Lautenschlaeger. 2012. Combined RASSF1A and RASSF2A promoter methylation analysis as diagnostic biomarker for bladder cancer. *Mol Biol Int*. 2012:701814.

Menke, A., and K. Giehl. 2012. Regulation of adherens junctions by Rho GTPases and p120-catenin. *Arch Biochem Biophys*. 524:48-55.

Meyer, M.J., J.M. Fleming, A.F. Lin, S.A. Hussnain, E. Ginsburg, and B.K. Vonderhaar. 2010. CD44posCD49fhiCD133/2hi defines xenograft-initiating cells in estrogen receptor-negative breast cancer. *Cancer Res*. 70:4624-4633.

Millband, D.N., and K.G. Hardwick. 2002. Fission yeast Mad3p is required for Mad2p to inhibit the anaphase-promoting complex and localizes to kinetochores in a Bub1p-, Bub3p-, and Mph1p-dependent manner. *Mol Cell Biol*. 22:2728-2742.

Miller, E. 2012. Identification of serum-derived sphingosine-1-phosphate as a small molecule regulator of YAP. *Chem. Biol.* 19:955-962.

Miller, J.R., and D.R. McClay. 1997. Characterization of the role of cadherin in regulating cell adhesion during sea urchin development. *Dev Biol*. 192:323-339.

Mineo, M., S.H. Garfield, S. Taverna, A. Flugy, G. De Leo, R. Alessandro, and E.C. Kohn. 2012. Exosomes released by K562 chronic myeloid leukemia cells promote angiogenesis in a Src-dependent fashion. *Angiogenesis*. 15:33-45.

Minn, A.J., G.P. Gupta, P.M. Siegel, P.D. Bos, W. Shu, D.D. Giri, A. Viale, A.B. Olshen, W.L. Gerald, and J. Massague. 2005. Genes that mediate breast cancer metastasis to lung. *Nature*. 436:518-524.

`

Miranda, K.C., T. Khromykh, P. Christy, T.L. Le, C.J. Gottardi, A.S. Yap, J.L. Stow, and R.D. Teasdale. 2001. A dileucine motif targets E-cadherin to the basolateral cell surface in Madin-Darby canine kidney and LLC-PK1 epithelial cells. *J Biol Chem*. 276:22565-22572.

Mitra, A., A. Satelli, X. Xia, J. Cutrera, L. Mishra, and S. Li. 2015. Cell-surface Vimentin: A mislocalized protein for isolating csVimentin(+) CD133(-) novel stem-like hepatocellular carcinoma cells expressing EMT markers. *Int J Cancer*. 137:491-496.

Mitra, S., D. Mazumder Indra, P.S. Basu, R.K. Mondal, A. Roy, S. Roychoudhury, and C.K. Panda. 2012. Alterations of RASSF1A in premalignant cervical lesions: clinical and prognostic significance. *Mol Carcinog*. 51:723-733.

Mitsui, K., Y. Tokuzawa, H. Itoh, K. Segawa, M. Murakami, K. Takahashi, M. Maruyama, M. Maeda, and S. Yamanaka. 2003. The homeoprotein Nanog is required for maintenance of pluripotency in mouse epiblast and ES cells. *Cell*. 113:631-642.

Miyashita, Y., and M. Ozawa. 2007. Increased internalization of p120-uncoupled E-cadherin and a requirement for a dileucine motif in the cytoplasmic domain for endocytosis of the protein. *J Biol Chem*. 282:11540-11548.

Mo, J.S., F.X. Yu, R. Gong, J.H. Brown, and K.L. Guan. 2012. Regulation of the Hippo-YAP pathway by protease-activated receptors (PARs). *Genes Dev.* 26:2138-2143.

Mohamed, T.M., M. Zi, S. Prehar, A. Maqsood, R. Abou-Leisa, L. Nguyen, G.P. Pfeifer, E.J. Cartwright, L. Neyses, and D. Oceandy. 2014. The tumour suppressor Ras-association domain family protein 1A (RASSF1A) regulates TNF-alpha signalling in cardiomyocytes. *Cardiovasc Res*. 103:47-59.

Moorman, A.M., R. Vink, H.J. Heijmans, J. van der Palen, and E.A. Kouwenhoven. 2012. The prognostic value of tumour-stroma ratio in triple-negative breast cancer. *Eur J Surg Oncol*. 38:307-313.

Morelli, A.E., A.T. Larregina, W.J. Shufesky, M.L. Sullivan, D.B. Stolz, G.D. Papworth, A.F. Zahorchak, A.J. Logar, Z. Wang, S.C. Watkins, L.D. Falo, Jr., and A.W. Thomson. 2004. Endocytosis, intracellular sorting, and processing of exosomes by dendritic cells. *Blood*. 104:3257-3266.

Mori, S., J.T. Chang, E.R. Andrechek, N. Matsumura, T. Baba, G. Yao, J.W. Kim, M. Gatza, S. Murphy, and J.R. Nevins. 2009. Anchorage-independent cell growth signature identifies tumors with metastatic potential. *Oncogene*. 28:2796-2805.

Morin, P.J., A.B. Sparks, V. Korinek, N. Barker, H. Clevers, B. Vogelstein, and K.W. Kinzler. 1997. Activation of beta-catenin-Tcf signaling in colon cancer by mutations in beta-catenin or APC. *Science*. 275:1787-1790.

Moroishi, T., C.G. Hansen, and K.L. Guan. 2015. The emerging roles of YAP and TAZ in cancer. *Nat Rev Cancer*. 15:73-79.

Mowla, S., R. Pinnock, V.D. Leaner, C.R. Goding, and S. Prince. 2011. PMA-induced up-regulation of TBX3 is mediated by AP-1 and contributes to breast cancer cell migration. *Biochem J*. 433:145-153.

Mukherjee, M., S.Y. Chow, P. Yusoff, J. Seetharaman, C. Ng, S. Sinniah, X.W. Koh, N.F. Asgar, D. Li, D. Yim, R.A. Jackson, J. Yew, J. Qian, A. Iyu, Y.P. Lim, X. Zhou, S.K. Sze, G.R. Guy, and J. Sivaraman. 2012. Structure of a novel phosphotyrosine-binding domain in Hakai that targets E-cadherin. *Embo J*. 31:1308-1319.

Mulholland, D.J., H. Cheng, K. Reid, P.S. Rennie, and C.C. Nelson. 2002. The androgen receptor can promote beta-catenin nuclear translocation independently of adenomatous polyposis coli. *J Biol Chem*. 277:17933-17943.

Muller, H.M., A. Widschwendter, H. Fiegl, L. Ivarsson, G. Goebel, E. Perkmann, C. Marth, and M. Widschwendter. 2003. DNA methylation in serum of breast cancer patients: an independent prognostic marker. *Cancer Res*. 63:7641-7645.

Murakami, M., M. Nakagawa, E.N. Olson, and O. Nakagawa. 2005. A WW domain protein TAZ is a critical coactivator for TBX5, a transcription factor implicated in Holt-Oram syndrome. *Proc Natl Acad Sci U S A*. 102:18034-18039.

Muthuswamy, S.K., and B. Xue. 2012. Cell polarity as a regulator of cancer cell behavior plasticity. *Annu. Rev. Cell Dev. Biol.* 28:599-625.

Myoui, A., R. Nishimura, P.J. Williams, T. Hiraga, D. Tamura, T. Michigami, G.R. Mundy, and T. Yoneda. 2003. C-SRC tyrosine kinase activity is associated with tumor colonization in bone and lung in an animal model of human breast cancer metastasis. *Cancer Res*. 63:5028-5033.

Nagaraj, S., and D.I. Gabrilovich. 2012. Regulation of suppressive function of myeloid-derived suppressor cells by CD4+ T cells. *Semin Cancer Biol*. 22:282-288.

Nallet-Staub, F., V. Marsaud, L. Li, C. Gilbert, S. Dodier, V. Bataille, M. Sudol, M. Herlyn, and A. Mauviel. 2014. Pro-invasive activity of the Hippo pathway effectors YAP and TAZ in cutaneous melanoma. *The Journal of investigative dermatology*. 134:123-132.

Nam, H.J., S.A. Im, D.Y. Oh, P. Elvin, H.P. Kim, Y.K. Yoon, A. Min, S.H. Song, S.W. Han, T.Y. Kim, and Y.J. Bang. 2013. Antitumor activity of saracatinib (AZD0530), a c-Src/Abl kinase inhibitor, alone or in combination with chemotherapeutic agents in gastric cancer. *Mol Cancer Ther*. 12:16-26.

Nan, X., H.H. Ng, C.A. Johnson, C.D. Laherty, B.M. Turner, R.N. Eisenman, and A. Bird. 1998. Transcriptional repression by the methyl-CpG-binding protein MeCP2 involves a histone deacetylase complex. *Nature*. 393:386-389.

Nanbo, A., E. Kawanishi, R. Yoshida, and H. Yoshiyama. 2013. Exosomes derived from Epstein-Barr virus-infected cells are internalized via caveola-dependent endocytosis and promote phenotypic modulation in target cells. *J Virol*. 87:10334-10347.

Navin, N., J. Kendall, J. Troge, P. Andrews, L. Rodgers, J. McIndoo, K. Cook, A. Stepansky, D. Levy, D. Esposito, L. Muthuswamy, A. Krasnitz, W.R. McCombie, J. Hicks, and M. Wigler. 2011. Tumour evolution inferred by single-cell sequencing. *Nature*. 472:90-94.

Newton, A.C. 1995. Protein kinase C. Seeing two domains. *Curr Biol*. 5:973-976.

Neyaz, M.K., R.S. Kumar, S. Hussain, S.H. Naqvi, I. Kohaar, N. Thakur, V. Kashyap, B.C. Das, S.A. Husain, and M. Bharadwaj. 2008. Effect of aberrant promoter methylation of FHIT and RASSF1A genes on susceptibility to cervical cancer in a North Indian population. *Biomarkers*. 13:597-606.

Nimnual, A.S., L.J. Taylor, and D. Bar-Sagi. 2003. Redox-dependent downregulation of Rho by Rac. *Nature cell biology*. 5:236-241.

Niwa, H., K. Ogawa, D. Shimosato, and K. Adachi. 2009. A parallel circuit of LIF signalling pathways maintains pluripotency of mouse ES cells. *Nature*. 460:118-122.

O'Neill, E.E., D. Matallanas, and W. Kolch. 2005. Mammalian sterile 20-like kinases in tumor suppression: an emerging pathway. *Cancer Res*. 65:5485-5487.

Ocana, O.H., R. Corcoles, A. Fabra, G. Moreno-Bueno, H. Acloque, S. Vega, A. Barrallo-Gimeno, A. Cano, and M.A. Nieto. 2012. Metastatic colonization requires the repression of the epithelial-mesenchymal transition inducer Prrx1. *Cancer Cell*. 22:709-724.

Odorizzi, G. 2006. The multiple personalities of Alix. *J Cell Sci*. 119:3025-3032.

Oh, H., and K.D. Irvine. 2008. In vivo regulation of Yorkie phosphorylation and localization. *Development*. 135:1081-1088.

Ohshima, J., M. Haruta, Y. Fujiwara, N. Watanabe, Y. Arai, T. Ariga, H. Okita, T. Koshinaga, T. Oue, S. Hinotsu, H. Nakadate, H. Horie, M. Fukuzawa, and Y. Kaneko. 2012. Methylation of the RASSF1A promoter is predictive of poor outcome among patients with Wilms tumor. *Pediatr Blood Cancer*. 59:499-505.

Ohta, Y., J.H. Hartwig, and T.P. Stossel. 2006. FilGAP, a Rho- and ROCK-regulated GAP for Rac binds filamin A to control actin remodelling. *Nature cell biology*. 8:803-814.

Oka, T., V. Mazack, and M. Sudol. 2008. Mst2 and Lats kinases regulate apoptotic function of Yes kinase-associated protein (YAP). *J Biol Chem*. 283:27534-27546.

Okada, M., and H. Nakagawa. 1989. A protein tyrosine kinase involved in regulation of pp60c-src function. *J Biol Chem*. 264:20886-20893.

Okada, T., L. You, and F.G. Giancotti. 2007. Shedding light on Merlin's wizardry. *Trends Cell Biol*. 17:222-229.

`

Oliveira, C., S. Velho, E. Domingo, A. Preto, R.M. Hofstra, R. Hamelin, H. Yamamoto, R. Seruca, and S. Schwartz, Jr. 2005. Concomitant RASSF1A hypermethylation and KRAS/BRAF mutations occur preferentially in MSI sporadic colorectal cancer. *Oncogene*. 24:7630-7634.

Ortiz-Vega, S., A. Khokhlatchev, M. Nedwidek, X.F. Zhang, R. Dammann, G.P. Pfeifer, and J. Avruch. 2002. The putative tumor suppressor RASSF1A homodimerizes and heterodimerizes with the Ras-GTP binding protein Nore1. *Oncogene*. 21:1381-1390.

Ostrowski, M., N.B. Carmo, S. Krumeich, I. Fanget, G. Raposo, A. Savina, C.F. Moita, K. Schauer, A.N. Hume, R.P. Freitas, B. Goud, P. Benaroch, N. Hacohen, M. Fukuda, C. Desnos, M.C. Seabra, F. Darchen, S. Amigorena, L.F. Moita, and C. Thery. 2010. Rab27a and Rab27b control different steps of the exosome secretion pathway. *Nat Cell Biol*. 12:19-30; sup pp 11-13.

Otsuki, Y., M. Tanaka, S. Yoshii, N. Kawazoe, K. Nakaya, and H. Sugimura. 2001. Tumor metastasis suppressor nm23H1 regulates Rac1 GTPase by interaction with Tiam1. *Proc Natl Acad Sci U S A*. 98:4385-4390.

Ozawa, M., H. Baribault, and R. Kemler. 1989. The cytoplasmic domain of the cell adhesion molecule uvomorulin associates with three independent proteins structurally related in different species. *Embo J*. 8:1711-1717.

Palacios, F., L. Price, J. Schweitzer, J.G. Collard, and C. D'Souza-Schorey. 2001. An essential role for ARF6-regulated membrane traffic in adherens junction turnover and epithelial cell migration. *Embo J*. 20:4973-4986.

Palacios, F., J.K. Schweitzer, R.L. Boshans, and C. D'Souza-Schorey. 2002. ARF6-GTP recruits Nm23-H1 to facilitate dynamin-mediated endocytosis during adherens junctions disassembly. *Nat Cell Biol*. 4:929-936.

Palacios, F., J.S. Tushir, Y. Fujita, and C. D'Souza-Schorey. 2005. Lysosomal targeting of E-cadherin: a unique mechanism for the down-regulation of cell-cell adhesion during epithelial to mesenchymal transitions. *Mol Cell Biol*. 25:389-402.

Palakurthy, R.K., N. Wajapeyee, M.K. Santra, C. Gazin, L. Lin, S. Gobeil, and M.R. Green. 2009. Epigenetic silencing of the RASSF1A tumor suppressor gene through HOXB3-mediated induction of DNMT3B expression. *Molecular cell*. 36:219-230.

Pallares, J., A. Velasco, N. Eritja, M. Santacana, X. Dolcet, M. Cuatrecasas, V. Palomar-Asenjo, L. Catasus, J. Prat, and X. Matias-Guiu. 2008. Promoter hypermethylation and reduced expression of RASSF1A are frequent molecular alterations of endometrial carcinoma. *Mod Pathol*. 21:691-699.

Pan, D. 2010. The hippo signaling pathway in development and cancer. *Dev. Cell*. 19:491-505.

Pant, S., H. Hilton, and M.E. Burczynski. 2012. The multifaceted exosome: biogenesis, role in normal and aberrant cellular function, and frontiers for pharmacological and biomarker opportunities. *Biochem Pharmacol*. 83:1484-1494.

Paramasivam, M., A. Sarkeshik, J.R. Yates, M.J. Fernandes, and D. McCollum. 2011. Angiomotin family proteins are novel activators of the LATS2 kinase tumor suppressor. *Mol. Biol. Cell*. 22:3725-3733.

Park, H., S.Y. Cho, H. Kim, D. Na, J.Y. Han, J. Chae, C. Park, O.K. Park, S. Min, J. Kang, B. Choi, J. Min, J.Y. Kwon, Y.S. Suh, S.H. Kong, H.J. Lee, E.T. Liu, J.I. Kim, S. Kim, H.K. Yang, and C. Lee. 2015. Genomic alterations in BCL2L1 and DLC1 contribute to drug sensitivity in gastric cancer. *Proc Natl Acad Sci U S A*.

Passegue, E., W. Jochum, M. Schorpp-Kistner, U. Mohle-Steinlein, and E.F. Wagner. 2001. Chronic myeloid leukemia with increased granulocyte progenitors in mice lacking junB expression in the myeloid lineage. *Cell*. 104:21-32.

Paterson, A.D., R.G. Parton, C. Ferguson, J.L. Stow, and A.S. Yap. 2003. Characterization of E-cadherin endocytosis in isolated MCF-7 and chinese hamster ovary cells: the initial fate of unbound E-cadherin. *J Biol Chem*. 278:21050-21057.

Pece, S., D. Tosoni, S. Confalonieri, G. Mazzarol, M. Vecchi, S. Ronzoni, L. Bernard, G. Viale, P.G. Pelicci, and P.P. Di Fiore. 2010. Biological and molecular heterogeneity of breast cancers correlates with their cancer stem cell content. *Cell*. 140:62-73.

Pefani, D.E., R. Latusek, I. Pires, A.M. Grawenda, K.S. Yee, G. Hamilton, L. van der Weyden, F. Esashi, E.M. Hammond, and E. O'Neill. 2014. RASSF1A-LATS1 signalling stabilizes replication forks by restricting CDK2-mediated phosphorylation of BRCA2. *Nat Cell Biol*. 16:962-971, 961-968.

Peinado, H., M. Aleckovic, S. Lavotshkin, I. Matei, B. Costa-Silva, G. Moreno-Bueno, M. Hergueta-Redondo, C. Williams, G. Garcia-Santos, C. Ghajar, A. Nitadori-Hoshino, C. Hoffman, K. Badal, B.A. Garcia, M.K. Callahan, J. Yuan, V.R. Martins, J. Skog, R.N. Kaplan, M.S. Brady, J.D. Wolchok, P.B. Chapman, Y. Kang, J. Bromberg, and D. Lyden. 2012. Melanoma exosomes educate bone marrow progenitor cells toward a pro-metastatic phenotype through MET. *Nature medicine*. 18:883-891.

Pelosi, G., C. Fumagalli, M. Trubia, A. Sonzogni, N. Rekhtman, P. Maisonneuve, D. Galetta, L. Spaggiari, G. Veronesi, A. Scarpa, G. Malpeli, and G. Viale. 2010. Dual role of RASSF1 as a tumor suppressor and an oncogene in neuroendocrine tumors of the lung. *Anticancer Res*. 30:4269-4281.

Peres, J., E. Davis, S. Mowla, D.C. Bennett, J.A. Li, S. Wansleben, and S. Prince. 2010. The Highly Homologous T-Box Transcription Factors, TBX2 and TBX3, Have Distinct Roles in the Oncogenic Process. *Genes Cancer*. 1:272-282.

Peres, J., and S. Prince. 2013. The T-box transcription factor, TBX3, is sufficient to promote melanoma formation and invasion. *Molecular cancer*. 12:117.

Perez-Hernandez, D., C. Gutierrez-Vazquez, I. Jorge, S. Lopez-Martin, A. Ursa, F. Sanchez-Madrid, J. Vazquez, and M. Yanez-Mo. 2013. The intracellular interactome of tetraspanin-enriched microdomains reveals their function as sorting machineries toward exosomes. *J Biol Chem*. 288:11649-11661.

Perez-Moreno, M., C. Jamora, and E. Fuchs. 2003. Sticky business: orchestrating cellular signals at adherens junctions. *Cell*. 112:535-548.

Pesce, M., and H.R. Scholer. 2001. Oct-4: gatekeeper in the beginnings of mammalian development. *Stem Cells*. 19:271-278.

Peters, U., S. Jiao, F.R. Schumacher, C.M. Hutter, A.K. Aragaki, J.A. Baron, S.I. Berndt, S. Bezieau, H. Brenner, K. Butterbach, B.J. Caan, P.T. Campbell, C.S. Carlson, G. Casey, A.T. Chan, J. Chang-Claude, S.J. Chanock, L.S. Chen, G.A. Coetzee, S.G. Coetzee, D.V. Conti, K.R. Curtis, D. Duggan, T. Edwards, C.S. Fuchs, S. Gallinger, E.L. Giovannucci, S.M. Gogarten, S.B. Gruber, R.W. Haile, T.A. Harrison, R.B. Hayes, B.E. Henderson, M. Hoffmeister, J.L. Hopper, T.J. Hudson, D.J. Hunter, R.D. Jackson, S.H. Jee, M.A. Jenkins, W.H. Jia, L.N. Kolonel, C. Kooperberg, S. Kury, A.Z. Lacroix, C.C. Laurie, C.A. Laurie, L. Le Marchand, M. Lemire, D. Levine, N.M. Lindor, Y. Liu, J. Ma, K.W. Makar, K. Matsuo, P.A. Newcomb, J.D. Potter, R.L. Prentice, C. Qu, T. Rohan, S.A. Rosse, R.E. Schoen, D. Seminara, M. Shrubsole, X.O. Shu, M.L. Slattery, D. Taverna, S.N. Thibodeau, C.M. Ulrich, E. White, Y. Xiang, B.W. Zanke, Y.X. Zeng, B. Zhang, W. Zheng, and L. Hsu. 2013. Identification of Genetic Susceptibility Loci for Colorectal Tumors in a Genome-Wide Meta-analysis. *Gastroenterology*. 144:799-807 e724.

Petitjean, A., E. Mathe, S. Kato, C. Ishioka, S.V. Tavtigian, P. Hainaut, and M. Olivier. 2007. Impact of mutant p53 functional properties on TP53 mutation patterns and tumor phenotype: lessons from recent developments in the IARC TP53 database. *Human mutation*. 28:622-629.

Pfeffer, S.R. 2010. Two Rabs for exosome release. *Nat Cell Biol*. 12:3-4.

Pilot, F., J.M. Philippe, C. Lemmers, and T. Lecuit. 2006. Spatial control of actin organization at adherens junctions by a synaptotagmin-like protein Btsz. *Nature*. 442:580-584.

Pines, J. 2006. Mitosis: a matter of getting rid of the right protein at the right time. *Trends Cell Biol*. 16:55-63.

Polesello, C., S. Huelsmann, N.H. Brown, and N. Tapon. 2006. The Drosophila RASSF homolog antagonizes the hippo pathway. *Curr Biol*. 16:2459-2465.

Pols, M.S., and J. Klumperman. 2009. Trafficking and function of the tetraspanin CD63. *Exp Cell Res*. 315:1584-1592.

Ponomaryova, A., E.Y. Rykova, N.V. Cherdyntseva, T.E. Skvortsova, A.Y. Dobrodeev, A. Zav/'yalov, L.O. Bryzgalov, S. Tuzikov, V.V. Vlassov, and P.P. Laktionov. 2013. Potentialities of aberrantly

methylated circulating DNA for diagnostics and post-treatment follow-up of lung cancer patients. *Lung Cancer*. 81:397-403.

Ponting, C.P., and D.R. Benjamin. 1996. A novel family of Ras-binding domains. *Trends Biochem Sci*. 21:422-425.

Poon, C.L., J.I. Lin, X. Zhang, and K.F. Harvey. 2011. The sterile 20-like kinase Tao-1 controls tissue growth by regulating the Salvador-Warts-Hippo pathway. *Dev. Cell*. 21:896-906.

Poyurovsky, M.V., and C. Prives. 2006. Unleashing the power of p53: lessons from mice and men. *Genes Dev*. 20:125-131.

Praskova, M., A. Khoklatchev, S. Ortiz-Vega, and J. Avruch. 2004. Regulation of the MST1 kinase by autophosphorylation, by the growth inhibitory proteins, RASSF1 and NORE1, and by Ras. *Biochem. J.* 381:453-462.

Praskova, M., F. Xia, and J. Avruch. 2008. MOBKL1A/MOBKL1B phosphorylation by MST1 and MST2 inhibits cell proliferation. *Curr Biol*. 18:311-321.

Price, L.S., A. Hajdo-Milasinovic, J. Zhao, F.J. Zwartkruis, J.G. Collard, and J.L. Bos. 2004. Rap1 regulates E-cadherin-mediated cell-cell adhesion. *J Biol Chem*. 279:35127-35132.

Qian, Z.R., T. Sano, K. Yoshimoto, S. Yamada, A. Ishizuka, N. Mizusawa, H. Horiguchi, M. Hirokawa, and S.L. Asa. 2005. Inactivation of RASSF1A tumor suppressor gene by aberrant promoter hypermethylation in human pituitary adenomas. *Lab Invest*. 85:464-473.

Qin, Y., C. Capaldo, B.M. Gumbiner, and I.G. Macara. 2005. The mammalian Scribble polarity protein regulates epithelial cell adhesion and migration through E-cadherin. *J Cell Biol*. 171:1061-1071.

Rabizadeh, S., R.J. Xavier, K. Ishiguro, J. Bernabeortiz, M. Lopez-Ilasaca, A. Khokhlatchev, P. Mollahan, G.P. Pfeifer, J. Avruch, and B. Seed. 2004. The scaffold protein CNK1 interacts with the tumor suppressor RASSF1A and augments RASSF1A-induced cell death. *J Biol Chem*. 279:29247-29254.

Radford, K.J., J. Mallesch, and P. Hersey. 1995. Suppression of human melanoma cell growth and metastasis by the melanoma-associated antigen CD63 (ME491). *Int J Cancer*. 62:631-635.

Radford, K.J., R.F. Thorne, and P. Hersey. 1996. CD63 associates with transmembrane 4 superfamily members, CD9 and CD81, and with beta 1 integrins in human melanoma. *Biochem Biophys Res Commun*. 222:13-18.

Raiborg, C., and H. Stenmark. 2009. The ESCRT machinery in endosomal sorting of ubiquitylated membrane proteins. *Nature*. 458:445-452.

Ramteke, A., H. Ting, C. Agarwal, S. Mateen, R. Somasagara, A. Hussain, M. Graner, B. Frederick, R. Agarwal, and G. Deep. 2015. Exosomes secreted under hypoxia enhance invasiveness and stemness of prostate cancer cells by targeting adherens junction molecules. *Mol Carcinog*. 54:554-565.

Raposo, G., and W. Stoorvogel. 2013. Extracellular vesicles: exosomes, microvesicles, and friends. *J Cell Biol*. 200:373-383.

Rapsomaniki, M.A., P. Kotsantis, I.E. Symeonidou, N.N. Giakoumakis, S. Taraviras, and Z. Lygerou. 2012. easyFRAP: an interactive, easy-to-use tool for qualitative and quantitative analysis of FRAP data. *Bioinformatics*. 28:1800-1801.

Ratajczak, J., K. Miekus, M. Kucia, J. Zhang, R. Reca, P. Dvorak, and M.Z. Ratajczak. 2006. Embryonic stem cell-derived microvesicles reprogram hematopoietic progenitors: evidence for horizontal transfer of mRNA and protein delivery. *Leukemia*. 20:847-856.

Raymond, W.A., and A.S. Leong. 1989. Vimentin--a new prognostic parameter in breast carcinoma? *J Pathol*. 158:107-114.

Reeves, M.E., M.L. Baldwin, R. Aragon, S. Baldwin, S.T. Chen, X. Li, S. Mohan, and Y.G. Amaar. 2012. RASSF1C modulates the expression of a stem cell renewal gene, PIWIL1. *BMC Res Notes*. 5:239.

Reeves, M.E., S.W. Baldwin, M.L. Baldwin, S.T. Chen, J.M. Moretz, R.J. Aragon, X. Li, D.D. Strong, S. Mohan, and Y.G. Amaar. 2010. Ras-association domain family 1C protein promotes breast cancer cell migration and attenuates apoptosis. *BMC Cancer*. 10:562.

Reeves, M.E., M. Firek, S.T. Chen, and Y. Amaar. 2013. The RASSF1 Gene and the Opposing Effects of the RASSF1A and RASSF1C Isoforms on Cell Proliferation and Apoptosis. *Mol Biol Int*. 2013:145096.

Reeves, M.E., M. Firek, S.T. Chen, and Y.G. Amaar. 2014. Evidence that RASSF1C stimulation of lung cancer cell proliferation depends on IGFBP-5 and PIWIL1 expression levels. *PLoS One*. 9:e101679.

Reichmann, E., H. Schwarz, E.M. Deiner, I. Leitner, M. Eilers, J. Berger, M. Busslinger, and H. Beug. 1992. Activation of an inducible c-FosER fusion protein causes loss of epithelial polarity and triggers epithelial-fibroblastoid cell conversion. *Cell*. 71:1103-1116.

Ren, F., L. Zhang, and J. Jiang. 2009. Hippo signaling regulates Yorkie nuclear localization and activity through 14-3-3 dependent and independent mechanisms. *Dev. Biol.* 337:303-312.

Ren, X.D., W.B. Kiosses, D.J. Sieg, C.A. Otey, D.D. Schlaepfer, and M.A. Schwartz. 2000. Focal adhesion kinase suppresses Rho activity to promote focal adhesion turnover. *J Cell Sci*. 113 (Pt 20):3673-3678.

Renard, C.A., C. Labalette, C. Armengol, D. Cougot, Y. Wei, S. Cairo, P. Pineau, C. Neuveut, A. de Reynies, A. Dejean, C. Perret, and M.A. Buendia. 2007. Tbx3 is a downstream target of the Wnt/beta-catenin pathway and a critical mediator of beta-catenin survival functions in liver cancer. *Cancer Res*. 67:901-910.

Reynolds, A.B., J. Daniel, P.D. McCrea, M.J. Wheelock, J. Wu, and Z. Zhang. 1994. Identification of a new catenin: the tyrosine kinase substrate p120cas associates with E-cadherin complexes. *Mol Cell Biol*. 14:8333-8342.

Reynolds, B.A., and S. Weiss. 1992. Generation of neurons and astrocytes from isolated cells of the adult mammalian central nervous system. *Science*. 255:1707-1710.

Ribeiro, P.S., F. Josue, A. Wepf, M.C. Wehr, O. Rinner, G. Kelly, N. Tapon, and M. Gstaiger. 2010. Combined functional genomic and proteomic approaches identify a PP2A complex as a negative regulator of Hippo signaling. *Molecular cell*. 39:521-534.

Ricci-Vitiani, L., D.G. Lombardi, E. Pilozzi, M. Biffoni, M. Todaro, C. Peschle, and R. De Maria. 2007. Identification and expansion of human colon-cancer-initiating cells. *Nature*. 445:111-115.

Riches, A., E. Campbell, E. Borger, and S. Powis. 2014. Regulation of exosome release from mammary epithelial and breast cancer cells - a new regulatory pathway. *Eur J Cancer*. 50:1025-1034.

Richter, A.M., G.P. Pfeifer, and R.H. Dammann. 2009. The RASSF proteins in cancer; from epigenetic silencing to functional characterization. *Biochim Biophys Acta*. 1796:114-128.

Richter, A.M., U. Schagdarsurengin, M. Rastetter, K. Steinmann, and R.H. Dammann. 2010. Protein kinase A-mediated phosphorylation of the RASSF1A tumour suppressor at Serine 203 and regulation of RASSF1A function. *Eur J Cancer*. 46:2986-2995.

Ridley, A.J., and A. Hall. 1992. The small GTP-binding protein rho regulates the assembly of focal adhesions and actin stress fibers in response to growth factors. *Cell*. 70:389-399.

Ridley, A.J., H.F. Paterson, C.L. Johnston, D. Diekmann, and A. Hall. 1992. The small GTP-binding protein rac regulates growth factor-induced membrane ruffling. *Cell*. 70:401-410.

Robinson, B.S., J. Huang, Y. Hong, and K.H. Moberg. 2010. Crumbs regulates Salvador/Warts/Hippo signaling in Drosophila via the FERM-domain protein expanded. *Curr. Biol.* 20:582-590.

Rodriguez, M., E. Aladowicz, L. Lanfrancone, and C.R. Goding. 2008. Tbx3 represses E-cadherin expression and enhances melanoma invasiveness. *Cancer Res*. 68:7872-7881.

Rohrschneider, L.R. 1979. Immunofluorescence on avian sarcoma virus-transformed cells: localization of the src gene product. *Cell*. 16:11-24.

Romano, D., D. Matallanas, G. Weitsman, C. Preisinger, T. Ng, and W. Kolch. 2010. Proapoptotic kinase MST2 coordinates signaling crosstalk between RASSF1A, Raf-1, and Akt. *Cancer Res*. 70:1195-1203.

Rong, R., L.Y. Jiang, M.S. Sheikh, and Y. Huang. 2007. Mitotic kinase Aurora-A phosphorylates RASSF1A and modulates RASSF1A-mediated microtubule interaction and M-phase cell cycle regulation. *Oncogene*. 26:7700-7708.

`

Rong, R., W. Jin, J. Zhang, M.S. Sheikh, and Y. Huang. 2004. Tumor suppressor RASSF1A is a microtubule-binding protein that stabilizes microtubules and induces G2/M arrest. *Oncogene*. 23:8216-8230.

Rongvaux, A., H. Takizawa, T. Strowig, T. Willinger, E.E. Eynon, R.A. Flavell, and M.G. Manz. 2013. Human hemato-lymphoid system mice: current use and future potential for medicine. *Annu Rev Immunol*. 31:635-674.

Rosenbluh, J., D. Nijhawan, A.G. Cox, X. Li, J.T. Neal, E.J. Schafer, T.I. Zack, X. Wang, A. Tsherniak, A.C. Schinzel, D.D. Shao, S.E. Schumacher, B.A. Weir, F. Vazquez, G.S. Cowley, D.E. Root, J.P. Mesirov, R. Beroukhim, C.J. Kuo, W. Goessling, and W.C. Hahn. 2012. beta-Catenin-driven cancers require a YAP1 transcriptional complex for survival and tumorigenesis. *Cell*. 151:1457-1473.

Roura, S., S. Miravet, J. Piedra, A. Garcia de Herreros, and M. Dunach. 1999. Regulation of E-cadherin/Catenin association by tyrosine phosphorylation. *J Biol Chem*. 274:36734-36740.

Ruter, B., P.W. Wijermans, and M. Lubbert. 2006. Superiority of prolonged low-dose azanucleoside administration? Results of 5-aza-2'-deoxycytidine retreatment in high-risk myelodysplasia patients. *Cancer*. 106:1744-1750.

Safa, A.R., M.R. Saadatzadeh, A.A. Cohen-Gadol, K.E. Pollok, and K. Bijangi-Vishehsaraei. 2015. Glioblastoma stem cells (GSCs) epigenetic plasticity and interconversion between differentiated non-GSCs and GSCs. *Genes Dis*. 2:152-163.

Saito, S., A.A. Goodarzi, Y. Higashimoto, Y. Noda, S.P. Lees-Miller, E. Appella, and C.W. Anderson. 2002. ATM mediates phosphorylation at multiple p53 sites, including Ser(46), in response to ionizing radiation. *J Biol Chem*. 277:12491-12494.

Saito, Y., N. Uchida, S. Tanaka, N. Suzuki, M. Tomizawa-Murasawa, A. Sone, Y. Najima, S. Takagi, Y. Aoki, A. Wake, S. Taniguchi, L.D. Shultz, and F. Ishikawa. 2010. Induction of cell cycle entry eliminates human leukemia stem cells in a mouse model of AML. *Nat Biotechnol*. 28:275-280.

Sakai, T., R. Jove, R. Fassler, and D.F. Mosher. 2001. Role of the cytoplasmic tyrosines of beta 1A integrins in transformation by v-src. *Proc Natl Acad Sci U S A*. 98:3808-3813.

Sakamoto, N., T. Terai, Y. Ajioka, S. Abe, O. Kobayasi, S. Hirai, O. Hino, H. Watanabe, N. Sato, T. Shimoda, and H. Fujii. 2004. Frequent hypermethylation of RASSF1A in early flat-type colorectal tumors. *Oncogene*. 23:8900-8907.

Sanchez-Bailon, M.P., A. Calcabrini, D. Gomez-Dominguez, B. Morte, E. Martin-Forero, G. Gomez-Lopez, A. Molinari, K.U. Wagner, and J. Martin-Perez. 2012. Src kinases catalytic activity regulates proliferation, migration and invasiveness of MDA-MB-231 breast cancer cells. *Cell Signal*. 24:1276-1286.

Sander, E.E., J.P. ten Klooster, S. van Delft, R.A. van der Kammen, and J.G. Collard. 1999. Rac downregulates Rho activity: reciprocal balance between both GTPases determines cellular morphology and migratory behavior. *J Cell Biol*. 147:1009-1022.

Sandilands, E., V.G. Brunton, and M.C. Frame. 2007. The membrane targeting and spatial activation of Src, Yes and Fyn is influenced by palmitoylation and distinct RhoB/RhoD endosome requirements. *J Cell Sci*. 120:2555-2564.

Sandilands, E., C. Cans, V.J. Fincham, V.G. Brunton, H. Mellor, G.C. Prendergast, J.C. Norman, G. Superti-Furga, and M.C. Frame. 2004. RhoB and actin polymerization coordinate Src activation with endosome-mediated delivery to the membrane. *Dev Cell*. 7:855-869.

Sandilands, E., and M.C. Frame. 2008. Endosomal trafficking of Src tyrosine kinase. *Trends Cell Biol*. 18:322-329.

Sansores-Garcia, L., W. Bossuyt, K. Wada, S. Yonemura, C. Tao, H. Sasaki, and G. Halder. 2011. Modulating F-actin organization induces organ growth by affecting the Hippo pathway. *Embo J*. 30:2325-2335.

Satelli, A., and S. Li. 2011. Vimentin in cancer and its potential as a molecular target for cancer therapy. *Cell Mol Life Sci*. 68:3033-3046.

Sathi, G.A., R. Tamamura, H. Tsujigiwa, N. Katase, M. Lefeuvre, C.H. Siar, H. Matsuda, and H. Nagatsuka. 2012. Analysis of immunoexpression of common cancer stem cell markers in ameloblastoma. *Exp Ther Med*. 3:397-402.

Sato, T., J.H. van Es, H.J. Snippert, D.E. Stange, R.G. Vries, M. van den Born, N. Barker, N.F. Shroyer, M. van de Wetering, and H. Clevers. 2011. Paneth cells constitute the niche for Lgr5 stem cells in intestinal crypts. *Nature*. 469:415-418.

Savina, A., M. Vidal, and M.I. Colombo. 2002. The exosome pathway in K562 cells is regulated by Rab11. *J Cell Sci*. 115:2505-2515.

Schaller, M.D., C.A. Borgman, B.S. Cobb, R.R. Vines, A.B. Reynolds, and J.T. Parsons. 1992. pp125FAK a structurally distinctive protein-tyrosine kinase associated with focal adhesions. *Proc Natl Acad Sci U S A*. 89:5192-5196.

Schaller, M.D., J.D. Hildebrand, J.D. Shannon, J.W. Fox, R.R. Vines, and J.T. Parsons. 1994. Autophosphorylation of the focal adhesion kinase, pp125FAK, directs SH2-dependent binding of pp60src. *Mol Cell Biol*. 14:1680-1688.

Scheel, C., and R.A. Weinberg. 2012. Cancer stem cells and epithelial-mesenchymal transition: concepts and molecular links. *Semin Cancer Biol*. 22:396-403.

Scheel, H., and K. Hofmann. 2003. A novel interaction motif, SARAH, connects three classes of tumor suppressor. *Curr Biol*. 13:R899-900.

Schlegelmilch, K., M. Mohseni, O. Kirak, J. Pruszak, J.R. Rodriguez, D. Zhou, B.T. Kreger, V. Vasioukhin, J. Avruch, T.R. Brummelkamp, and F.D. Camargo. 2011. Yap1 acts downstream of alpha-catenin to control epidermal proliferation. *Cell*. 144:782-795.

Schmidt, M.H., I. Dikic, and O. Bogler. 2005. Src phosphorylation of Alix/AIP1 modulates its interaction with binding partners and antagonizes its activities. *J Biol Chem*. 280:3414-3425.

Schober, M., and E. Fuchs. 2011. Tumor-initiating stem cells of squamous cell carcinomas and their control by TGF-beta and integrin/focal adhesion kinase (FAK) signaling. *Proc Natl Acad Sci U S A*. 108:10544-10549.

Scholzen, T., and J. Gerdes. 2000. The Ki-67 protein: from the known and the unknown. *Journal of cellular physiology*. 182:311-322.

Scrace, S., and University of Oxford. Novel regulation of SRC family kinase signalling by RASSF1 isoforms. xx, 230 leaves pp.

Segura, E., C. Nicco, B. Lombard, P. Veron, G. Raposo, F. Batteux, S. Amigorena, and C. Thery. 2005. ICAM-1 on exosomes from mature dendritic cells is critical for efficient naive T-cell priming. *Blood*. 106:216-223.

Seidel, C., F. Bartel, M. Rastetter, K. Bluemke, P. Wurl, H. Taubert, and R. Dammann. 2005. Alterations of cancer-related genes in soft tissue sarcomas: hypermethylation of RASSF1A is frequently detected in leiomyosarcoma and associated with poor prognosis in sarcoma. *Int J Cancer*. 114:442-447.

Seidel, C., U. Schagdarsurengin, K. Blumke, P. Wurl, G.P. Pfeifer, S. Hauptmann, H. Taubert, and R. Dammann. 2007. Frequent hypermethylation of MST1 and MST2 in soft tissue sarcoma. *Mol Carcinog*. 46:865-871.

Sekido, Y., M. Ahmadian, Wistuba, II, F. Latif, S. Bader, M.H. Wei, F.M. Duh, A.F. Gazdar, M.I. Lerman, and J.D. Minna. 1998a. Cloning of a breast cancer homozygous deletion junction narrows the region of search for a 3p21.3 tumor suppressor gene. *Oncogene*. 16:3151-3157.

Sekido, Y., K.M. Fong, and J.D. Minna. 1998b. Progress in understanding the molecular pathogenesis of human lung cancer. *Biochim Biophys Acta*. 1378:F21-59.

Sequeira, L., C.W. Dubyk, T.A. Riesenberger, C.R. Cooper, and K.L. van Golen. 2008. Rho GTPases in PC-3 prostate cancer cell morphology, invasion and tumor cell diapedesis. *Clinical & experimental metastasis*. 25:569-579.

Serrels, A., P. Timpson, M. Canel, J.P. Schwarz, N.O. Carragher, M.C. Frame, V.G. Brunton, and K.I. Anderson. 2009. Real-time study of E-cadherin and membrane dynamics in living animals: implications for disease modeling and drug development. *Cancer Res*. 69:2714-2719.

`

Shao, D.D., W. Xue, E.B. Krall, A. Bhutkar, F. Piccioni, X. Wang, A.C. Schinzel, S. Sood, J. Rosenbluh, J.W. Kim, Y. Zwang, T.M. Roberts, D.E. Root, T. Jacks, and W.C. Hahn. 2014. KRAS and YAP1 converge to regulate EMT and tumor survival. *Cell*. 158:171-184.

Sheldon, H., E. Heikamp, H. Turley, R. Dragovic, P. Thomas, C.E. Oon, R. Leek, M. Edelmann, B. Kessler, R.C. Sainson, I. Sargent, J.L. Li, and A.L. Harris. 2010. New mechanism for Notch signaling to endothelium at a distance by Delta-like 4 incorporation into exosomes. *Blood*. 116:2385-2394.

Shen, J., J. Lu, L. Sui, D. Wang, M. Yin, I. Hoffmann, A. Legler, and G.O. Pflugfelder. 2014. The orthologous Tbx transcription factors Omb and TBX2 induce epithelial cell migration and extrusion in vivo without involvement of matrix metalloproteinases. *Oncotarget*.

Shi, Y., C. Desponts, J.T. Do, H.S. Hahm, H.R. Scholer, and S. Ding. 2008. Induction of pluripotent stem cells from mouse embryonic fibroblasts by Oct4 and Klf4 with small-molecule compounds. *Cell Stem Cell*. 3:568-574.

Shimizu, Y., N. Yamamichi, K. Saitoh, A. Watanabe, T. Ito, M. Yamamichi-Nishina, M. Mizutani, N. Yahagi, T. Suzuki, C. Sasakawa, S. Yasugi, M. Ichinose, and H. Iba. 2003. Kinetics of v-src-induced epithelial-mesenchymal transition in developing glandular stomach. *Oncogene*. 22:884-893.

Shivakumar, L., J. Minna, T. Sakamaki, R. Pestell, and M.A. White. 2002. The RASSF1A tumor suppressor blocks cell cycle progression and inhibits cyclin D1 accumulation. *Mol Cell Biol*. 22:4309-4318.

Siliciano, J.D., C.E. Canman, Y. Taya, K. Sakaguchi, E. Appella, and M.B. Kastan. 1997. DNA damage induces phosphorylation of the amino terminus of p53. *Genes Dev*. 11:3471-3481.

Sillars-Hardebol, A.H., B. Carvalho, J.A. Belien, M. de Wit, P.M. Delis-van Diemen, M. Tijssen, M.A. van de Wiel, F. Ponten, R.J. Fijneman, and G.A. Meijer. 2012. BCL2L1 has a functional role in colorectal cancer and its protein expression is associated with chromosome 20q gain. *J Pathol*. 226:442-450.

Silva, J., V. Garcia, M. Rodriguez, M. Compte, E. Cisneros, P. Veguillas, J.M. Garcia, G. Dominguez, Y. Campos-Martin, J. Cuevas, C. Pena, M. Herrera, R. Diaz, N. Mohammed, and F. Bonilla. 2012. Analysis of exosome release and its prognostic value in human colorectal cancer. *Genes Chromosomes Cancer*. 51:409-418.

Silvis, M.R., B.T. Kreger, W.H. Lien, O. Klezovitch, G.M. Rudakova, F.D. Camargo, D.M. Lantz, J.T. Seykora, and V. Vasioukhin. 2011. alpha-catenin is a tumor suppressor that controls cell accumulation by regulating the localization and activity of the transcriptional coactivator Yap1. *Sci Signal*. 4:ra33.

Sinclair, C.S., C. Adem, A. Naderi, C.L. Soderberg, M. Johnson, K. Wu, L. Wadum, V.L. Couch, T.A. Sellers, D. Schaid, J. Slezak, Z. Fredericksen, J.N. Ingle, L. Hartmann, R.B. Jenkins, and F.J. Couch. 2002. TBX2 is preferentially amplified in BRCA1- and BRCA2-related breast tumors. *Cancer Res*. 62:3587-3591.

Singh, S.K., I.D. Clarke, M. Terasaki, V.E. Bonn, C. Hawkins, J. Squire, and P.B. Dirks. 2003. Identification of a cancer stem cell in human brain tumors. *Cancer Res*. 63:5821-5828.

Skog, J., T. Wurdinger, S. van Rijn, D.H. Meijer, L. Gainche, M. Sena-Esteves, W.T. Curry, Jr., B.S. Carter, A.M. Krichevsky, and X.O. Breakefield. 2008. Glioblastoma microvesicles transport RNA and proteins that promote tumour growth and provide diagnostic biomarkers. *Nat Cell Biol*. 10:1470-1476.

Smith, A.G., J. Nichols, M. Robertson, and P.D. Rathjen. 1992. Differentiation inhibiting activity (DIA/LIF) and mouse development. *Developmental biology*. 151:339-351.

Smith, A.J., J. Xian, M. Richardson, K.A. Johnstone, and P.H. Rabbitts. 2002. Cre-loxP chromosome engineering of a targeted deletion in the mouse corresponding to the 3p21.3 region of homozygous loss in human tumours. *Oncogene*. 21:4521-4529.

Soderberg, O., M. Gullberg, M. Jarvius, K. Ridderstrale, K.J. Leuchowius, J. Jarvius, K. Wester, P. Hydbring, F. Bahram, L.G. Larsson, and U. Landegren. 2006. Direct observation of individual endogenous protein complexes in situ by proximity ligation. *Nat Methods*. 3:995-1000.

`

Song, M.S., J.S. Chang, S.J. Song, T.H. Yang, H. Lee, and D.S. Lim. 2005. The centrosomal protein RAS association domain family protein 1A (RASSF1A)-binding protein 1 regulates mitotic progression by recruiting RASSF1A to spindle poles. *J Biol Chem*. 280:3920-3927.

Song, M.S., S.J. Song, N.G. Ayad, J.S. Chang, J.H. Lee, H.K. Hong, H. Lee, N. Choi, J. Kim, H. Kim, J.W. Kim, E.J. Choi, M.W. Kirschner, and D.S. Lim. 2004. The tumour suppressor RASSF1A regulates mitosis by inhibiting the APC-Cdc20 complex. *Nat Cell Biol*. 6:129-137.

Song, M.S., S.J. Song, S.J. Kim, K. Nakayama, K.I. Nakayama, and D.S. Lim. 2008a. Skp2 regulates the antiproliferative function of the tumor suppressor RASSF1A via ubiquitin-mediated degradation at the G1-S transition. *Oncogene*. 27:3176-3185.

Song, M.S., S.J. Song, S.Y. Kim, H.J. Oh, and D.S. Lim. 2008b. The tumour suppressor RASSF1A promotes MDM2 self-ubiquitination by disrupting the MDM2-DAXX-HAUSP complex. *Embo J*. 27:1863-1874.

Song, S.J., S.J. Kim, M.S. Song, and D.S. Lim. 2009a. Aurora B-mediated phosphorylation of RASSF1A maintains proper cytokinesis by recruiting Syntaxin16 to the midzone and midbody. *Cancer Res*. 69:8540-8544.

Song, S.J., M.S. Song, S.J. Kim, S.Y. Kim, S.H. Kwon, J.G. Kim, D.F. Calvisi, D. Kang, and D.S. Lim. 2009b. Aurora A regulates prometaphase progression by inhibiting the ability of RASSF1A to suppress APC-Cdc20 activity. *Cancer Res*. 69:2314-2323.

Sorlie, T., C.M. Perou, R. Tibshirani, T. Aas, S. Geisler, H. Johnsen, T. Hastie, M.B. Eisen, M. van de Rijn, S.S. Jeffrey, T. Thorsen, H. Quist, J.C. Matese, P.O. Brown, D. Botstein, P.E. Lonning, and A.L. Borresen-Dale. 2001. Gene expression patterns of breast carcinomas distinguish tumor subclasses with clinical implications. *Proc Natl Acad Sci U S A*. 98:10869-10874.

Stehelin, D., H.E. Varmus, J.M. Bishop, and P.K. Vogt. 1976. DNA related to the transforming gene(s) of avian sarcoma viruses is present in normal avian DNA. *Nature*. 260:170-173.

Stephens, P.J., P.S. Tarpey, H. Davies, P. Van Loo, C. Greenman, D.C. Wedge, S. Nik-Zainal, S. Martin, I. Varela, G.R. Bignell, L.R. Yates, E. Papaemmanuil, D. Beare, A. Butler, A. Cheverton, J. Gamble, J. Hinton, M. Jia, A. Jayakumar, D. Jones, C. Latimer, K.W. Lau, S. McLaren, D.J. McBride, A. Menzies, L. Mudie, K. Raine, R. Rad, M.S. Chapman, J. Teague, D. Easton, A. Langerod, M.T. Lee, C.Y. Shen, B.T. Tee, B.W. Huimin, A. Broeks, A.C. Vargas, G. Turashvili, J. Martens, A. Fatima, P. Miron, S.F. Chin, G. Thomas, S. Boyault, O. Mariani, S.R. Lakhani, M. van de Vijver, L. van 't Veer, J. Foekens, C. Desmedt, C. Sotiriou, A. Tutt, C. Caldas, J.S. Reis-Filho, S.A. Aparicio, A.V. Salomon, A.L. Borresen-Dale, A.L. Richardson, P.J. Campbell, P.A. Futreal, and M.R. Stratton. 2012. The landscape of cancer genes and mutational processes in breast cancer. *Nature*. 486:400-404.

Stewart, J.M., P.A. Shaw, C. Gedye, M.Q. Bernardini, B.G. Neel, and L.E. Ailles. 2011. Phenotypic heterogeneity and instability of human ovarian tumor-initiating cells. *Proc Natl Acad Sci U S A*. 108:6468-6473.

Stieglitz, B., C. Bee, D. Schwarz, O. Yildiz, A. Moshnikova, A. Khokhlatchev, and C. Herrmann. 2008. Novel type of Ras effector interaction established between tumour suppressor NORE1A and Ras switch II. *Embo J*. 27:1995-2005.

Stockinger, A., A. Eger, J. Wolf, H. Beug, and R. Foisner. 2001. E-cadherin regulates cell growth by modulating proliferation-dependent beta-catenin transcriptional activity. *J Cell Biol*. 154:1185-1196.

Strano, S., O. Monti, N. Pediconi, A. Baccarini, G. Fontemaggi, E. Lapi, F. Mantovani, A. Damalas, G. Citro, A. Sacchi, G. Del Sal, M. Levrero, and G. Blandino. 2005. The transcriptional coactivator Yes-associated protein drives p73 gene-target specificity in response to DNA Damage. *Molecular cell*. 18:447-459.

Strumane, K., G. Berx, and F. Van Roy. 2004. Cadherins in cancer. *Handb Exp Pharmacol*:69-103.

Stuffers, S., C. Sem Wegner, H. Stenmark, and A. Brech. 2009. Multivesicular endosome biogenesis in the absence of ESCRTs. *Traffic*. 10:925-937.

Stutterheim, J., F.A. Ichou, E. den Ouden, R. Versteeg, H.N. Caron, M. Tytgat Ga, and C.E. van der Schoot. 2012. Methylated RASSF1a is the first specific DNA marker for minimal residual disease testing in neuroblastoma. *Clin Cancer Res*. 18:808-814.

Sudakin, V., G.K. Chan, and T.J. Yen. 2001. Checkpoint inhibition of the APC/C in HeLa cells is mediated by a complex of BUBR1, BUB3, CDC20, and MAD2. *J Cell Biol*. 154:925-936.

Sudol, M., H.I. Chen, C. Bougeret, A. Einbond, and P. Bork. 1995. Characterization of a novel protein-binding module--the WW domain. *FEBS Lett*. 369:67-71.

Sundaresan, V., P. Ganly, P. Hasleton, R. Rudd, G. Sinha, N.M. Bleehen, and P. Rabbitts. 1992. p53 and chromosome 3 abnormalities, characteristic of malignant lung tumours, are detectable in preinvasive lesions of the bronchus. *Oncogene*. 7:1989-1997.

Swaminathan, G., and C.A. Cartwright. 2012. Rack1 promotes epithelial cell-cell adhesion by regulating E-cadherin endocytosis. *Oncogene*. 31:376-389.

Takahashi, K., and S. Yamanaka. 2006. Induction of pluripotent stem cells from mouse embryonic and adult fibroblast cultures by defined factors. *Cell*. 126:663-676.

Takahashi, Y., Y. Miyoshi, C. Takahata, N. Irahara, T. Taguchi, Y. Tamaki, and S. Noguchi. 2005. Down-regulation of LATS1 and LATS2 mRNA expression by promoter hypermethylation and its association with biologically aggressive phenotype in human breast cancers. *Clin Cancer Res*. 11:1380-1385.

Takai, D., and P.A. Jones. 2002. Comprehensive analysis of CpG islands in human chromosomes 21 and 22. *Proc Natl Acad Sci U S A*. 99:3740-3745.

Takeda, H., A. Nagafuchi, S. Yonemura, S. Tsukita, J. Behrens, and W. Birchmeier. 1995. V-src kinase shifts the cadherin-based cell adhesion from the strong to the weak state and beta catenin is not required for the shift. *J Cell Biol*. 131:1839-1847.

Takeichi, M. 1977. Functional correlation between cell adhesive properties and some cell surface proteins. *J Cell Biol*. 75:464-474.

Talmadge, J.E., and I.J. Fidler. 2010. AACR centennial series: the biology of cancer metastasis: historical perspective. *Cancer Res*. 70:5649-5669.

Tamm, C., N. Bower, and C. Anneren. 2011. Regulation of mouse embryonic stem cell self-renewal by a Yes-YAP-TEAD2 signaling pathway downstream of LIF. *J Cell Sci*. 124:1136-1144.

Tanemura, A., A. Terando, M. Sim, A. van Hoesel, M. de Maat, D. Morton, and D. Hoon. 2009. CpG island methylator phenotype predicts progression of malignant melanoma. *Clin Cancer Res*. 15:1801-1807.

Tang, Z., H. Shu, D. Oncel, S. Chen, and H. Yu. 2004. Phosphorylation of Cdc20 by Bub1 provides a catalytic mechanism for APC/C inhibition by the spindle checkpoint. *Molecular cell*. 16:387-397.

Taniguchi, K., L.W. Wu, S.I. Grivennikov, P.R. de Jong, I. Lian, F.X. Yu, K. Wang, S.B. Ho, B.S. Boland, J.T. Chang, W.J. Sandborn, G. Hardiman, E. Raz, Y. Maehara, A. Yoshimura, J. Zucman-Rossi, K.L. Guan, and M. Karin. 2015. A gp130-Src-YAP module links inflammation to epithelial regeneration. *Nature*. 519:57-62.

Tauro, B.J., D.W. Greening, R.A. Mathias, S. Mathivanan, H. Ji, and R.J. Simpson. 2013. Two distinct populations of exosomes are released from LIM1863 colon carcinoma cell-derived organoids. *Mol Cell Proteomics*. 12:587-598.

Tay, Y., J. Zhang, A.M. Thomson, B. Lim, and I. Rigoutsos. 2008. MicroRNAs to Nanog, Oct4 and Sox2 coding regions modulate embryonic stem cell differentiation. *Nature*. 455:1124-1128.

Taylor, D.D., and C. Gercel-Taylor. 2008. MicroRNA signatures of tumor-derived exosomes as diagnostic biomarkers of ovarian cancer. *Gynecol Oncol*. 110:13-21.

Taylor, D.D., C. Gercel-Taylor, K.S. Lyons, J. Stanson, and T.L. Whiteside. 2003. T-cell apoptosis and suppression of T-cell receptor/CD3-zeta by Fas ligand-containing membrane vesicles shed from ovarian tumors. *Clin Cancer Res*. 9:5113-5119.

Taylor, D.D., H.D. Homesley, and G.J. Doellgast. 1983. "Membrane-associated" immunoglobulins in cyst and ascites fluids of ovarian cancer patients. *Am J Reprod Immunol*. 3:7-11.

`

Tejera, E., V. Rocha-Perugini, S. Lopez-Martin, D. Perez-Hernandez, A.I. Bachir, A.R. Horwitz, J. Vazquez, F. Sanchez-Madrid, and M. Yanez-Mo. 2013. CD81 regulates cell migration through its association with Rac GTPase. *Mol Biol Cell*. 24:261-273.

ten Klooster, J.P., Z.M. Jaffer, J. Chernoff, and P.L. Hordijk. 2006. Targeting and activation of Rac1 are mediated by the exchange factor beta-Pix. *J Cell Biol*. 172:759-769.

Tepass, U., K. Truong, D. Godt, M. Ikura, and M. Peifer. 2000. Cadherins in embryonic and neural morphogenesis. *Nat Rev Mol Cell Biol*. 1:91-100.

Teuliere, J., M.M. Faraldo, M.A. Deugnier, M. Shtutman, A. Ben-Ze'ev, J.P. Thiery, and M.A. Glukhova. 2005. Targeted activation of beta-catenin signaling in basal mammary epithelial cells affects mammary development and leads to hyperplasia. *Development*. 132:267-277.

Thaler, S., P.S. Hahnel, A. Schad, R. Dammann, and M. Schuler. 2009. RASSF1A mediates p21Cip1/Waf1-dependent cell cycle arrest and senescence through modulation of the Raf-MEK-ERK pathway and inhibition of Akt. *Cancer Res*. 69:1748-1757.

Thery, C., S. Amigorena, G. Raposo, and A. Clayton. 2006. Isolation and characterization of exosomes from cell culture supernatants and biological fluids. *Curr Protoc Cell Biol*. Chapter 3:Unit 3 22.

Thiery, J.P. 2002. Epithelial-mesenchymal transitions in tumour progression. *Nat Rev Cancer*. 2:442-454.

Thiery, J.P., H. Acloque, R.Y. Huang, and M.A. Nieto. 2009. Epithelial-mesenchymal transitions in development and disease. *Cell*. 139:871-890.

Thomas, S.M., and J.S. Brugge. 1997. Cellular functions regulated by Src family kinases. *Annu Rev Cell Dev Biol*. 13:513-609.

Tian, Y., Y. Hou, X. Zhou, H. Cheng, and R. Zhou. 2011. Tumor Suppressor RASSF1A Promoter: p53 Binding and Methylation. *PLoS One*. 6:e17017.

Timpson, P., G.E. Jones, M.C. Frame, and V.G. Brunton. 2001. Coordination of cell polarization and migration by the Rho family GTPases requires Src tyrosine kinase activity. *Curr Biol*. 11:1836-1846.

Toma, J.G., M. Akhavan, K.J. Fernandes, F. Barnabe-Heider, A. Sadikot, D.R. Kaplan, and F.D. Miller. 2001. Isolation of multipotent adult stem cells from the dermis of mammalian skin. *Nat Cell Biol*. 3:778-784.

Tomizawa, Y., T. Kohno, H. Kondo, A. Otsuka, M. Nishioka, T. Niki, T. Yamada, A. Maeshima, K. Yoshimura, R. Saito, J. Minna, and J. Yokota. 2002. Clinicopathological significance of epigenetic inactivation of RASSF1A at 3p21.3 in stage I lung adenocarcinoma. *Clin Cancer*. 8:2362-2368.

Tommasi, S., A. Besaratinia, S.P. Wilczynski, and G.P. Pfeifer. 2011a. Loss of Rassf1a enhances p53-mediated tumor predisposition and accelerates progression to aneuploidy. *Oncogene*. 30:690-700.

Tommasi, S., R. Dammann, Z. Zhang, Y. Wang, L. Liu, W.M. Tsark, S.P. Wilczynski, J. Li, M. You, and G.P. Pfeifer. 2005. Tumor susceptibility of Rassf1a knockout mice. *Cancer Res*. 65:92-98.

Tommasi, S., R. Pinto, D. Petriella, B. Pilato, R. Lacalamita, D. Santini, F. Zito, G. Colucci, A. Paradiso, and N. Silvestris. 2011b. Oncosuppressor methylation: a possible key role in colon metastatic progression. *J Cell Physiol*. 226:1934-1939.

Tozluoglu, M., A.L. Tournier, R.P. Jenkins, S. Hooper, P.A. Bates, and E. Sahai. 2013. Matrix geometry determines optimal cancer cell migration strategy and modulates response to interventions. *Nat Cell Biol*. 15:751-762.

Trams, E.G., C.J. Lauter, N. Salem, Jr., and U. Heine. 1981. Exfoliation of membrane ecto-enzymes in the form of micro-vesicles. *Biochim Biophys Acta*. 645:63-70.

Tsai, J.H., J.L. Donaher, D.A. Murphy, S. Chau, and J. Yang. 2012. Spatiotemporal regulation of epithelial-mesenchymal transition is essential for squamous cell carcinoma metastasis. *Cancer Cell*. 22:725-736.

Tsai, J.H., and J. Yang. 2013. Epithelial-mesenchymal plasticity in carcinoma metastasis. *Genes Dev*. 27:2192-2206.

Tu, C., C.F. Ortega-Cava, P. Winograd, M.J. Stanton, A.L. Reddi, I. Dodge, R. Arya, M. Dimri, R.J. Clubb, M. Naramura, K.U. Wagner, V. Band, and H. Band. 2010. Endosomal-sorting complexes required for transport (ESCRT) pathway-dependent endosomal traffic regulates the localization of active Src at focal adhesions. *Proc Natl Acad Sci U S A*. 107:16107-16112.

Twiss, F., and J. de Rooij. 2013. Cadherin mechanotransduction in tissue remodeling. *Cell. Mol. Life Sci.*

Ullrich, O., S. Reinsch, S. Urbe, M. Zerial, and R.G. Parton. 1996. Rab11 regulates recycling through the pericentriolar recycling endosome. *The Journal of cell biology*. 135:913-924.

Valadi, H., K. Ekstrom, A. Bossios, M. Sjostrand, J.J. Lee, and J.O. Lotvall. 2007. Exosome-mediated transfer of mRNAs and microRNAs is a novel mechanism of genetic exchange between cells. *Nat Cell Biol*. 9:654-659.

Valenta, T., G. Hausmann, and K. Basler. 2012. The many faces and functions of beta-catenin. *Embo J*. 31:2714-2736.

van der Weyden, L., and D.J. Adams. 2007. The Ras-association domain family (RASSF) members and their role in human tumourigenesis. *Biochim Biophys Acta*. 1776:58-85.

van der Weyden, L., M.J. Arends, O.M. Dovey, H.L. Harrison, G. Lefebvre, N. Conte, F.V. Gergely, A. Bradley, and D.J. Adams. 2008. Loss of Rassf1a cooperates with Apc(Min) to accelerate intestinal tumourigenesis. *Oncogene*. 27:4503-4508.

van der Weyden, L., A. Papaspyropoulos, G. Poulogiannis, A.G. Rust, M. Rashid, D.J. Adams, M.J. Arends, and E. O'Neill. 2012. Loss of Rassf1a Synergizes with Deregulated Runx2 Signaling in Tumorigenesis. *Cancer Res*.

van der Weyden, L., K.K. Tachibana, M.A. Gonzalez, D.J. Adams, B.L. Ng, R. Petty, A.R. Venkitaraman, M.J. Arends, and A. Bradley. 2005. The RASSF1A isoform of RASSF1 promotes microtubule stability and suppresses tumorigenesis. *Mol Cell Biol*. 25:8356-8367.

van Niel, G., S. Charrin, S. Simoes, M. Romao, L. Rochin, P. Saftig, M.S. Marks, E. Rubinstein, and G. Raposo. 2011. The tetraspanin CD63 regulates ESCRT-independent and -dependent endosomal sorting during melanogenesis. *Dev Cell*. 21:708-721.

Van Slambrouck, S., A.R. Jenkins, A.E. Romero, and W.F. Steelant. 2009. Reorganization of the integrin alpha2 subunit controls cell adhesion and cancer cell invasion in prostate cancer. *International journal of oncology*. 34:1717-1726.

Varelas, X. 2010. The Crumbs complex couples cell density sensing to Hippo-dependent control of the TGF-[beta]-SMAD pathway. *Dev. Cell*. 19:831-844.

Vassilev, A., K.J. Kaneko, H. Shu, Y. Zhao, and M.L. DePamphilis. 2001. TEAD/TEF transcription factors utilize the activation domain of YAP65, a Src/Yes-associated protein localized in the cytoplasm. *Genes Dev.* 15:1229-1241.

Vavvas, D., X. Li, J. Avruch, and X.F. Zhang. 1998. Identification of Nore1 as a potential Ras effector. *J Biol Chem*. 273:5439-5442.

Velho, S., G. Corso, C. Oliveira, and R. Seruca. 2010. KRAS signaling pathway alterations in microsatellite unstable gastrointestinal cancers. *Adv Cancer Res*. 109:123-143.

Verbeek, B.S., T.M. Vroom, S.S. Adriaansen-Slot, A.E. Ottenhoff-Kalff, J.G. Geertzema, A. Hennipman, and G. Rijksen. 1996. c-Src protein expression is increased in human breast cancer. An immunohistochemical and biochemical analysis. *The Journal of pathology*. 180:383-388.

Vermeulen, L., E.M.F. De Sousa, M. van der Heijden, K. Cameron, J.H. de Jong, T. Borovski, J.B. Tuynman, M. Todaro, C. Merz, H. Rodermond, M.R. Sprick, K. Kemper, D.J. Richel, G. Stassi, and J.P. Medema. 2010. Wnt activity defines colon cancer stem cells and is regulated by the microenvironment. *Nat Cell Biol*. 12:468-476.

Vermeulen, L., M. Todaro, F. de Sousa Mello, M.R. Sprick, K. Kemper, M. Perez Alea, D.J. Richel, G. Stassi, and J.P. Medema. 2008. Single-cell cloning of colon cancer stem cells reveals a multi-lineage differentiation capacity. *Proc Natl Acad Sci U S A*. 105:13427-13432.

Viale, A., F. De Franco, A. Orleth, V. Cambiaghi, V. Giuliani, D. Bossi, C. Ronchini, S. Ronzoni, I. Muradore, S. Monestiroli, A. Gobbi, M. Alcalay, S. Minucci, and P.G. Pelicci. 2009. Cell-cycle

restriction limits DNA damage and maintains self-renewal of leukaemia stem cells. *Nature*. 457:51-56.

Vigil, D., J. Cherfils, K.L. Rossman, and C.J. Der. 2010. Ras superfamily GEFs and GAPs: validated and tractable targets for cancer therapy? *Nat Rev Cancer*. 10:842-857.

Vivo, C., W. Liu, and V.C. Broaddus. 2003. c-Jun N-terminal kinase contributes to apoptotic synergy induced by tumor necrosis factor-related apoptosis-inducing ligand plus DNA damage in chemoresistant, p53 inactive mesothelioma cells. *J Biol Chem*. 278:25461-25467.

Vlahov, N., S. Scrace, M.S. Soto, A.M. Grawenda, L. Bradley, D. Pankova, A. Papaspyropoulos, K.S. Yee, F. Buffa, C.R. Goding, P. Timpson, N. Sibson, and E. O'Neill. 2015. Alternate RASSF1 Transcripts Control SRC Activity, E-Cadherin Contacts, and YAP-Mediated Invasion. *Curr Biol*. 25:3019-3034.

Vleminckx, K., L. Vakaet, Jr., M. Mareel, W. Fiers, and F. van Roy. 1991. Genetic manipulation of E-cadherin expression by epithelial tumor cells reveals an invasion suppressor role. *Cell*. 66:107-119.

Vlug, E.J., R.A. van de Ven, J.F. Vermeulen, P. Bult, P.J. van Diest, and P.W. Derksen. 2013. Nuclear localization of the transcriptional coactivator YAP is associated with invasive lobular breast cancer. *Cell Oncol (Dordr)*. 36:375-384.

Vogelstein, B., D. Lane, and A.J. Levine. 2000. Surfing the p53 network. *Nature*. 408:307-310.

Volodko, N., M. Gordon, M. Salla, H.A. Ghazaleh, and S. Baksh. 2014. RASSF tumor suppressor gene family: biological functions and regulation. *FEBS Lett*. 588:2671-2684.

Vos, M.D., C.A. Ellis, A. Bell, M.J. Birrer, and G.J. Clark. 2000. Ras uses the novel tumor suppressor RASSF1 as an effector to mediate apoptosis. *J Biol Chem*. 275:35669-35672.

Vos, M.D., A. Martinez, C. Elam, A. Dallol, B.J. Taylor, F. Latif, and G.J. Clark. 2004. A role for the RASSF1A tumor suppressor in the regulation of tubulin polymerization and genomic stability. *Cancer Res*. 64:4244-4250.

Vousden, K.H., and X. Lu. 2002. Live or let die: the cell's response to p53. *Nat Rev Cancer*. 2:594-604.

Wada, K., K. Itoga, T. Okano, S. Yonemura, and H. Sasaki. 2011. Hippo pathway regulation by cell morphology and stress fibers. *Development*. 138:3907-3914.

Wang, D., P. Lu, H. Zhang, M. Luo, X. Zhang, X. Wei, J. Gao, Z. Zhao, and C. Liu. 2014a. Oct-4 and Nanog promote the epithelial-mesenchymal transition of breast cancer stem cells and are associated with poor prognosis in breast cancer patients. *Oncotarget*. 5:10803-10815.

Wang, H., M. Yang, J. Xu, B. Zou, Q. Zhou, J. Bian, and X. Wang. 2015. Survivin mRNA-circulating tumor cells are associated with prostate cancer metastasis. *Tumour Biol*.

Wang, H.L., Y. Zhang, P. Liu, and P.Y. Zhou. 2014b. Aberrant promoter methylation of RASSF1A gene may be correlated with colorectal carcinogenesis: a meta-analysis. *Molecular biology reports*. 41:3991-3999.

Wang, J., S. Rao, J. Chu, X. Shen, D.N. Levasseur, T.W. Theunissen, and S.H. Orkin. 2006. A protein interaction network for pluripotency of embryonic stem cells. *Nature*. 444:364-368.

Wang, J., B. Wang, X. Chen, and J. Bi. 2011a. The prognostic value of RASSF1A promoter hypermethylation in non-small cell lung carcinoma: a systematic review and meta-analysis. *Carcinogenesis*. 32:411-416.

Wang, K., C. Degerny, M. Xu, and X.J. Yang. 2009. YAP, TAZ, and Yorkie: a conserved family of signal-responsive transcriptional coregulators in animal development and human disease. *Biochem Cell Biol*. 87:77-91.

Wang, W., J. Huang, and J. Chen. 2011b. Angiomotin-like proteins associate with and negatively regulate YAP1. *J. Biol. Chem.* 286:4364-4370.

Wang, X., K. Di, X. Zhang, H.Y. Han, Y.C. Wong, S.C. Leung, and M.T. Ling. 2008. Id-1 promotes chromosomal instability through modification of APC/C activity during mitosis in response to microtubule disruption. *Oncogene*. 27:4456-4466.

Wang, Y., Z. Yu, T. Wang, J. Zhang, L. Hong, and L. Chen. 2007. Identification of epigenetic aberrant promoter methylation of RASSF1A in serum DNA and its clinicopathological significance in lung cancer. *Lung Cancer*. 56:289-294.

Webb, D.J., K. Donais, L.A. Whitmore, S.M. Thomas, C.E. Turner, J.T. Parsons, and A.F. Horwitz. 2004. FAK-Src signalling through paxillin, ERK and MLCK regulates adhesion disassembly. *Nat Cell Biol*. 6:154-161.

Webber, J., R. Steadman, M.D. Mason, Z. Tabi, and A. Clayton. 2010. Cancer exosomes trigger fibroblast to myofibroblast differentiation. *Cancer Res*. 70:9621-9630.

Wei, J., M. Wunderlich, C. Fox, S. Alvarez, J.C. Cigudosa, J.S. Wilhelm, Y. Zheng, J.A. Cancelas, Y. Gu, M. Jansen, J.F. Dimartino, and J.C. Mulloy. 2008. Microenvironment determines lineage fate in a human model of MLL-AF9 leukemia. *Cancer Cell*. 13:483-495.

Wei, X., T. Shimizu, and Z.C. Lai. 2007. Mob as tumor suppressor is activated by Hippo kinase for growth inhibition in Drosophila. *EMBO J.* 26:1772-1781.

Welham, M.J., and J.A. Wyke. 1988. A single point mutation has pleiotropic effects on pp60v-src function. *J Virol*. 62:1898-1906.

Welte, Y., J. Adjaye, H.R. Lehrach, and C.R. Regenbrecht. 2010. Cancer stem cells in solid tumors: elusive or illusive? *Cell Commun Signal*. 8:6.

Wen, W., F. Zhu, J. Zhang, Y.S. Keum, T. Zykova, K. Yao, C. Peng, D. Zheng, Y.Y. Cho, W.Y. Ma, A.M. Bode, and Z. Dong. 2010. MST1 promotes apoptosis through phosphorylation of histone H2AX. *J Biol Chem*. 285:39108-39116.

Wennerberg, K., K.L. Rossman, and C.J. Der. 2005. The Ras superfamily at a glance. *J Cell Sci*. 118:843-846.

Whang, Y.M., Y.H. Kim, J.S. Kim, and Y.D. Yoo. 2005. RASSF1A suppresses the c-Jun-NH2-kinase pathway and inhibits cell cycle progression. *Cancer Res*. 65:3682-3690.

Whitehurst, A.W., R. Ram, L. Shivakumar, B. Gao, J.D. Minna, and M.A. White. 2008. The RASSF1A tumor suppressor restrains anaphase-promoting complex/cyclosome activity during the G1/S phase transition to promote cell cycle progression in human epithelial cells. *Mol Cell Biol*. 28:3190-3197.

Wiseman, D.H., B.F. Greystoke, and T.C. Somervaille. 2014. The variety of leukemic stem cells in myeloid malignancy. *Oncogene*. 33:3091-3098.

Wistuba, II, C. Behrens, S. Milchgrub, D. Bryant, J. Hung, J.D. Minna, and A.F. Gazdar. 1999. Sequential molecular abnormalities are involved in the multistage development of squamous cell lung carcinoma. *Oncogene*. 18:643-650.

Wistuba, II, C. Behrens, A.K. Virmani, G. Mele, S. Milchgrub, L. Girard, J.W. Fondon, 3rd, H.R. Garner, B. McKay, F. Latif, M.I. Lerman, S. Lam, A.F. Gazdar, and J.D. Minna. 2000. High resolution chromosome 3p allelotyping of human lung cancer and preneoplastic/preinvasive bronchial epithelium reveals multiple, discontinuous sites of 3p allele loss and three regions of frequent breakpoints. *Cancer Res*. 60:1949-1960.

Wohlgemuth, S., C. Kiel, A. Kramer, L. Serrano, F. Wittinghofer, and C. Herrmann. 2005. Recognizing and defining true Ras binding domains I: biochemical analysis. *J Mol Biol*. 348:741-758.

Wolfer, A., and S. Ramaswamy. 2011. MYC and metastasis. *Cancer Res*. 71:2034-2037.

Wolfers, J., A. Lozier, G. Raposo, A. Regnault, C. Thery, C. Masurier, C. Flament, S. Pouzieux, F. Faure, T. Tursz, E. Angevin, S. Amigorena, and L. Zitvogel. 2001. Tumor-derived exosomes are a source of shared tumor rejection antigens for CTL cross-priming. *Nature medicine*. 7:297-303.

Woodcock, S.A., C. Rooney, M. Liontos, Y. Connolly, V. Zoumpourlis, A.D. Whetton, V.G. Gorgoulis, and A. Malliri. 2009. SRC-induced disassembly of adherens junctions requires localized phosphorylation and degradation of the rac activator tiam1. *Mol Cell*. 33:639-653.

Wu, S., J. Huang, J. Dong, and D. Pan. 2003. Hippo encodes a Ste-20 family protein kinase that restricts cell proliferation and promotes apoptosis in conjunction with salvador and warts. *Cell*. 114:445-456.

Wu, S., Y. Liu, Y. Zheng, J. Dong, and D. Pan. 2008a. The TEAD/TEF family protein Scalloped mediates transcriptional output of the Hippo growth-regulatory pathway. *Dev. Cell*. 14:388-398.

Wu, X., X. Tu, K.S. Joeng, M.J. Hilton, D.A. Williams, and F. Long. 2008b. Rac1 activation controls nuclear localization of beta-catenin during canonical Wnt signaling. *Cell*. 133:340-353.

Xiao, L., D. Chen, P. Hu, J. Wu, W. Liu, Y. Zhao, M. Cao, Y. Fang, W. Bi, Z. Zheng, J. Ren, G. Ji, Y. Wang, and Z. Yuan. 2011. The c-Abl-MST1 signaling pathway mediates oxidative stress-induced neuronal cell death. *J Neurosci*. 31:9611-9619.

Xu, W., S.C. Harrison, and M.J. Eck. 1997. Three-dimensional structure of the tyrosine kinase c-Src. *Nature*. 385:595-602.

Yamamoto, T., S. Taya, and K. Kaibuchi. 1999. Ras-induced transformation and signaling pathway. *J Biochem*. 126:799-803.

Yang, C., and P.D. Robbins. 2011. The roles of tumor-derived exosomes in cancer pathogenesis. *Clin Dev Immunol*. 2011:842849.

Yang, X., W. Dai, D.-W. Kwong, C.Y.Y. Szeto, E.-W. Wong, W.T. Ng, A.W.M. Lee, R.K.C. Ngan, C.C. Yau, S.Y. Tung, and M.L. Lung. 2014. Epigenetic markers for noninvasive early detection of nasopharyngeal carcinoma by methylation-sensitive high resolution melting. *Int J Cancer*. 136:E127-E135.

Yang, X., R. Khosravi-Far, H.Y. Chang, and D. Baltimore. 1997. Daxx, a novel Fas-binding protein that activates JNK and apoptosis. *Cell*. 89:1067-1076.

Yap, A.S., C.M. Niessen, and B.M. Gumbiner. 1998. The juxtamembrane region of the cadherin cytoplasmic tail supports lateral clustering, adhesive strengthening, and interaction with p120ctn. *J Cell Biol*. 141:779-789.

Yaqub, S., H. Abrahamsen, B. Zimmerman, N. Kholod, K.M. Torgersen, T. Mustelin, F.W. Herberg, K. Tasken, and T. Vang. 2003. Activation of C-terminal Src kinase (Csk) by phosphorylation at serine-364 depends on the Csk-Src homology 3 domain. *Biochem J*. 372:271-278.

Yee, K.S., L. Grochola, G. Hamilton, A. Grawenda, E.E. Bond, H. Taubert, P. Wurl, G.L. Bond, and E. O'Neill. 2012. A RASSF1A polymorphism restricts p53/p73 activation and associates with poor survival and accelerated age of onset of soft tissue sarcoma. *Cancer Res*. 72:2206-2217.

Yee, K.S., and E. O'Neill. 2010. YAP1: Friend and foe. *Cell Cycle*. 9.

Yi, C. 2011. A tight junction-associated Merlin-angiomotin complex mediates Merlin's regulation of mitogenic signaling and tumor suppressive functions. *Cancer Cell*. 19:527-540.

Yi, C. 2013. The p130 isoform of angiomotin is required for Yap-mediated hepatic epithelial cell proliferation and tumorigenesis. *Sci. Signal.* 6:ra77.

Yip, S.C., M. El-Sibai, S.J. Coniglio, G. Mouneimne, R.J. Eddy, B.E. Drees, P.O. Neilsen, S. Goswami, M. Symons, J.S. Condeelis, and J.M. Backer. 2007. The distinct roles of Ras and Rac in PI 3-kinase-dependent protrusion during EGF-stimulated cell migration. *J Cell Sci*. 120:3138-3146.

Yoon, J.H., R. Dammann, and G.P. Pfeifer. 2001. Hypermethylation of the CpG island of the RASSF1A gene in ovarian and renal cell carcinomas. *Int J Cancer*. 94:212-217.

Yoshida, M., A. Ichikawa, H. Miyoshi, J. Kiyasu, Y. Kimura, F. Arakawa, D. Niino, and K. Ohshima. 2015a. Clinicopathological features of double-hit B-cell lymphomas with MYC and BCL2, BCL6 or CCND1 rearrangements. *Pathol Int*.

Yoshida, M., A. Ichikawa, H. Miyoshi, J. Kiyasu, Y. Kimura, D. Niino, and K. Ohshima. 2015b. Low incidence of MYC/BCL2 double-hit in Burkitt lymphoma. *Pathol Int*.

Yoshiura, K., Y. Kanai, A. Ochiai, Y. Shimoyama, T. Sugimura, and S. Hirohashi. 1995. Silencing of the E-cadherin invasion-suppressor gene by CpG methylation in human carcinomas. *Proc Natl Acad Sci U S A*. 92:7416-7419.

Youle, R.J., and A. Strasser. 2008. The BCL-2 protein family: opposing activities that mediate cell death. *Nat Rev Mol Cell Biol*. 9:47-59.

Yu, F., H. Yao, P. Zhu, X. Zhang, Q. Pan, C. Gong, Y. Huang, X. Hu, F. Su, J. Lieberman, and E. Song. 2007. let-7 regulates self renewal and tumorigenicity of breast cancer cells. *Cell*. 131:1109-1123.

Yu, F.X. 2012. Regulation of the Hippo-YAP pathway by G-protein-coupled receptor signaling. *Cell*. 150:780-791.

Yu, J. 2010. Kibra functions as a tumor suppressor protein that regulates Hippo signaling in conjunction with Merlin and Expanded. *Dev. Cell*. 18:288-299.

Zaidi, S.K., A.J. Sullivan, R. Medina, Y. Ito, A.J. van Wijnen, J.L. Stein, J.B. Lian, and G.S. Stein. 2004. Tyrosine phosphorylation controls Runx2-mediated subnuclear targeting of YAP to repress transcription. *Embo J*. 23:790-799.

Zanconato, F., M. Forcato, G. Battilana, L. Azzolin, E. Quaranta, B. Bodega, A. Rosato, S. Bicciato, M. Cordenonsi, and S. Piccolo. 2015. Genome-wide association between YAP/TAZ/TEAD and AP-1 at enhancers drives oncogenic growth. *Nat Cell Biol*.

Zhang, C.Y., Y.X. Zhao, R.H. Xia, J. Han, B.S. Wang, Z. Tian, L.Z. Wang, Y.H. Hu, and J. Li. 2014a. RASSF1A promoter hypermethylation is a strong biomarker of poor survival in patients with salivary adenoid cystic carcinoma in a Chinese population. *PLoS One*. 9:e110159.

Zhang, H., C.Y. Liu, Z.Y. Zha, B. Zhao, J. Yao, S. Zhao, Y. Xiong, Q.Y. Lei, and K.L. Guan. 2009. TEAD transcription factors mediate the function of TAZ in cell growth and epithelial-mesenchymal transition. *J Biol Chem*. 284:13355-13362.

Zhang, H., A. von Gise, Q. Liu, T. Hu, X. Tian, L. He, W. Pu, X. Huang, L. He, C.L. Cai, F.D. Camargo, W.T. Pu, and B. Zhou. 2014b. Yap1 is required for endothelial to mesenchymal transition of the atrioventricular cushion. *J Biol Chem*. 289:18681-18692.

Zhang, L. 2008. The TEAD/TEF family of transcription factor Scalloped mediates Hippo signaling in organ size control. *Dev. Cell*. 14:377-387.

Zhang, P., R. Andrianakos, Y. Yang, C. Liu, and W. Lu. 2010. Kruppel-like factor 4 (Klf4) prevents embryonic stem (ES) cell differentiation by regulating Nanog gene expression. *J Biol Chem*. 285:9180-9189.

Zhang, W., N. Nandakumar, Y. Shi, M. Manzano, A. Smith, G. Graham, S. Gupta, E.E. Vietsch, S.Z. Laughlin, M. Wadhwa, M. Chetram, M. Joshi, F. Wang, B. Kallakury, J. Toretsky, A. Wellstein, and C. Yi. 2014c. Downstream of mutant KRAS, the transcription regulator YAP is essential for neoplastic progression to pancreatic ductal adenocarcinoma. *Sci Signal*. 7:ra42.

Zhang, W.C., N. Shyh-Chang, H. Yang, A. Rai, S. Umashankar, S. Ma, B.S. Soh, L.L. Sun, B.C. Tai, M.E. Nga, K.K. Bhakoo, S.R. Jayapal, M. Nichane, Q. Yu, D.A. Ahmed, C. Tan, W.P. Sing, J. Tam, A. Thirugananam, M.S. Noghabi, Y.H. Pang, H.S. Ang, W. Mitchell, P. Robson, P. Kaldis, R.A. Soo, S. Swarup, E.H. Lim, and B. Lim. 2012. Glycine decarboxylase activity drives non-small cell lung cancer tumor-initiating cells and tumorigenesis. *Cell*. 148:259-272.

Zhang, Y.L., L.Q. Pang, Y. Wu, X.Y. Wang, C.Q. Wang, and Y. Fan. 2008. Significance of Bcl-xL in human colon carcinoma. *World J Gastroenterol*. 14:3069-3073.

Zhao, B. 2008. TEAD mediates YAP-dependent gene induction and growth control. *Genes Dev.* 22:1962-1971.

Zhao, B. 2011. Angiomotin is a novel Hippo pathway component that inhibits YAP oncoprotein. *Genes Dev.* 25:51-63.

Zhao, B., L. Li, K. Tumaneng, C.Y. Wang, and K.L. Guan. 2010. A coordinated phosphorylation by Lats and CK1 regulates YAP stability through SCF[beta]-TRCP. *Genes Dev.* 24:72-85.

Zhao, B., L. Li, L. Wang, C.Y. Wang, J. Yu, and K.L. Guan. 2012. Cell detachment activates the Hippo pathway via cytoskeleton reorganization to induce anoikis. *Genes Dev*. 26:54-68.

Zhao, B., X. Wei, W. Li, R.S. Udan, Q. Yang, J. Kim, J. Xie, T. Ikenoue, J. Yu, L. Li, P. Zheng, K. Ye, A. Chinnaiyan, G. Halder, Z.C. Lai, and K.L. Guan. 2007. Inactivation of YAP oncoprotein by the Hippo pathway is involved in cell contact inhibition and tissue growth control. *Genes Dev*. 21:2747-2761.

Zhao, B., X. Ye, J. Yu, L. Li, W. Li, S. Li, J.D. Lin, C.Y. Wang, A.M. Chinnaiyan, Z.C. Lai, and K.L. Guan. 2008. TEAD mediates YAP-dependent gene induction and growth control. *Genes Dev*. 22:1962-1971.

Zhao, Q.Z., and K.F. Dou. 2007. Methylation of Ras association domain family protein 1, isoform A correlated with proliferation and drug resistance in hepatocellular carcinoma cell line SMMC-7721. *J Gastroenterol Hepatol*. 22:683-689.

Zheng, X.M., Y. Wang, and C.J. Pallen. 1992. Cell transformation and activation of pp60c-src by overexpression of a protein tyrosine phosphatase. *Nature*. 359:336-339.

`

Zhou, X., T. Li, X. Feng, E. Hsiang, Y. Xiong, K.L. Guan, and Q. Lei. 2011. Targeted polyubiquitylation of RASSF1C by the Mule and SCFbeta-TrCP ligases in response to DNA damage. *Biochem J*.

Zhou, X., Y. Liu, J. You, H. Zhang, X. Zhang, and L. Ye. 2008. Myosin light-chain kinase contributes to the proliferation and migration of breast cancer cells through cross-talk with activated ERK1/2. *Cancer Lett*. 270:312-327.

Zhuang, G., X. Wu, Z. Jiang, I. Kasman, J. Yao, Y. Guan, J. Oeh, Z. Modrusan, C. Bais, D. Sampath, and N. Ferrara. 2012. Tumour-secreted miR-9 promotes endothelial cell migration and angiogenesis by activating the JAK-STAT pathway. *Embo J*. 31:3513-3523.

Zomer, A., C. Maynard, F.J. Verweij, A. Kamermans, R. Schafer, E. Beerling, R.M. Schiffelers, E. de Wit, J. Berenguer, S.I. Ellenbroek, T. Wurdinger, D.M. Pegtel, and J. van Rheenen. 2015. In Vivo imaging reveals extracellular vesicle-mediated phenocopying of metastatic behavior. *Cell*. 161:1046-1057.

Zylbersztejn, K., and T. Galli. 2011. Vesicular traffic in cell navigation. *Febs J*. 278:4497-4505.